Earthquakes in Switzerland and surrounding regions 1996-2012

Introduction

The present report constitutes a synthesis of the yearly reports about earthquakes in Switzerland and surroundings from 1996 until 2012 published by the Swiss Seismological Service (SED) in the *Eclogae Geologicae Helvetiae - Swiss Journal of Geosciences* (Baer et al. 1997; 1999; 2001; 2003; 2005; 2007; Deichmann et al. 1998; 2000a; 2002; 2004; 2006; 2008; 2009; 2010; 2011; 2012; Diehl et al. 2013). In its present form, the report consists of

- an introduction, including an overview of procedures of data acquisition and analysis,

- for each year a report about the seismic activity and significant earthquakes,

- a comprehensive bibliography for the references cited in the introduction and the yearly reports.

In contrast to the journal versions of the annual reports, the yearly documentation of the configuration of the monitoring network is not part of this document. Moreover, for an overview of focal depths in Switzerland, which used to be part of this documentation before 2010, the reader is referred to the annual report of 1999 (Deichmann et al. 2000a).

In some instances, the information presented in this report is updated with new results that were not available at the time of the original publication or in previous versions.

Version 2014.1 includes the annual report for 2012, as well as an updated bibliography and introduction.

Version 2012.2 includes the annual report for 2011, as well as an updated bibliography and introduction.

Version 2012.1 for the years 2005 and 2009 changed an earthquake in Val Formazza to quarry blast; added the focal mechanisms of Cima di Jazzi (2002) as well as of Brail and La Stretta (2008); updated the bibliography and introduction;

Version 2011.1 includes the annual report for 2010, as well as an updated bibliography and introduction; corrected magnitude (M_L 3.5 to 3.6) and focal mechanism of the 2009 Bivio event; changed one event from explosion to earthquake in 1997 and changed an explosion to a probable landslide in 2000 and 2005;

Version 2010.1 includes the yearly report for 2009 and an updated bibliography; in earlier versions, the introduction, bibliography and each annual

report consisted of separate documents; starting with this version and in conjunction with the new website of the SED, the individual parts are included in a single document; for the year 2005, the section on the M_L 4.9 Vallorcine earthquake has been updated with the results of a detailed analysis published in 2010 (Fréchet et al. 2010).

Version 2009.2 includes the yearly report for 2008 and an updated bibliography.

Version 2009.1 a review of potential quarry blasts revealed some unrecognized explosions (in particular the quarry of Chiesa Val Malenco in northern Italy); as a result the number of earthquakes and explosions has been corrected in all reports between 1996 and 2007; the quarry of Chiesa Val Malenco has been removed from the corresponding epicenter maps; the following additional changes have been made: 1996, corrected location and magnitude of the Valpelline event; 1999, 2000 and 2001, set focal depths of all Bormio events to 5 km (based on preliminary results of a still ongoing reanalysis of these events); 2001 added the relative location analysis of the Martigny sequence, which used to be a separate document in earlier versions; 2005, corrected location of the Piz Quattervals event.

Version 2008.1 includes the yearly report for 2007 as well as the updated introduction, station documentation and bibliography; for the year 2006, the number of earthquakes has been corrected (an additional small event in the Valais and an additional induced event in Basel) and the focal mechanism parameters of the Basel mainshock have been changed (± 2 degrees) to be consistent with the results published in Deichmann & Ernst (2009).

Version 2007.1 includes the yearly report for 2006 as well as the updated introduction, station documentation and bibliography; in addition, for the year 1999, new results regarding the focal depth and mechanism of the Fribourg event have been added.

Version 2006.1 includes the yearly report for 2005 as well as the updated introduction, station documentation and bibliography.

Version 2005.2 is an updated version of the previous one with the following modifications: 2004, the focal mechanism of the Derborence main shock has been added; 2000, a discussion of the earthquake sequence of Samoëns has been added, including the focal mechanism and relative locations; 1996, the focal mechanism of the Annecy event has been added as well as a minor modification to the text concerning the Leukerbad events.

Version 2005.1 includes the yearly report for 2004 as well as the updated introduction, station documentation and bibliography.

Version 2004.1 includes the yearly report for 2003 as well as the updated introduction, station documentation and bibliography.

Version 2003.1 includes the yearly reports 1996 – 2002 as well as the review of focal depths and the documentation of the Martigny sequence of 2001. With respect to the original publication (Baer et al. 1997), the report for 1996 has been revised significantly and updated to include focal mechanisms and related information for three additional events.

Previous publications

Past earthquake activity in and around Switzerland has been documented in an uninterrupted series of annual reports from 1879 until 1963 (*Jahresberichte des Schweizerischen Erdbebendienstes*). Three additional annual reports have been published for the years 1972-1974. These reports together with historical records of earthquakes dating back to the 13th century have been summarized by Pavoni (1977) and provided the basis for the first seismic hazard map of Switzerland (Sägesser & Mayer-Rosa, 1978). With the advent of routine data processing by computer, the wealth of data acquired by the nationwide seismograph network has been regularly documented in bulletins with detailed lists of all recorded events (*Monthly Bulletin of the Swiss Seismological Service*). Since 1996, annual reports summarizing the seismic activity in Switzerland and surrounding regions have been published in the second or third issue of the *Eclogae Geologicae Helvetiae - Swiss Journal of Geosciences* of the following year. In the course of reassessing the seismic hazard in Switzerland, a uniform earthquake catalog covering both the historical and instrumental periods was compiled in 2002 (Fäh et al. 2003). The official seismic hazard map of Switzerland based on this catalog was released in 2004 (Giardini et al. 2004; Wiemer et al. 2009). In 2009, the Earthquake Catalog of Switzerland was revised (ECOS-09) and is now available on line (http://www.seismo.ethz.ch/prod/catalog/index). In addition, numerous studies covering different aspects of the recent seismicity of Switzerland have been published in the scientific literature (for an overview and additional references see, e.g. Pavoni, 1984; 1987; Deichmann, 1990; Deichmann & Baer, 1990; Pavoni & Roth, 1990; Deichmann, 1992; Rüttener, 1995; Rüttener at al., 1996; Pavoni et al., 1997; Deichmann et al., 2000b, Kastrup et al., 2004; 2007; Marschall et al. 2013).

Data acquisition

Seismic monitoring networks in Switzerland

The Swiss Seismological Service operates two separate nationwide seismic networks, a high-gain seismometer network and a low-gain accelerograph network. The former is designed to continuously monitor the ongoing earthquake activity down to magnitudes well below the human perception threshold (Baer, 1990), whereas the latter is principally aimed at engineering concerns and thus only records so-called strong motions (Smit, 1998a). The data that has been collected by the strong-motion network is documented separately (Smit, 1997; 1998b; Spühler, 1999; Mattle, 2000; Wyss, 2002; 2003; 2004; 2005). Beginning in 2003, efforts are underway to merge these two networks, primarily by upgrading the accelerograph network, primarily by upgrading the accelerograph network with modern strong-motion sensors and digitisers featuring realtime continuous communication, higher dynamic range, broader frequency bandwidth and higher sensitivity. Twelve stations of the high-gain broad-band network include an additional accelerometer. In 2009, the Swiss Federal Council approved a project to renew the National Strong Motion Network; thirty high quality stations are to be installed within four years.

The observations presented here are based mainly on the high-sensitivity monitoring network. Beginning in 1998, the configuration of the national high-gain network has undergone a transformation from a short-period analog telemetry system to a digital high-dynamic-range network equipped almost entirely

with broad-band STS-2 sensors. For a detailed description of the new data acquisition system, see Baer et al. (2001). By the end of 2001, the installation of the new network was almost completed and the two systems were operating in parallel. After the new system had demonstrated its reliability, the old network, except for two stations, was decommissioned in February 2002.

Moreover, to monitor potential induced seismicity in conjunction with the construction of the new Gotthard railway tunnel and with several projects aimed at exploiting deep geothermal energy (Basel, Zürich and Brigerbad), specialized local monitoring networks have been installed and operated in recent years. Details of these networks as well as of the evolution of the nationwide networks are documented in the published annual reports.

Data from foreign networks

For detailed studies of selected earthquakes and for constraining the location and the focal mechanisms of earthquakes situated on the periphery or outside the Swiss station networks, we use additional data obtained from the Erdbebendienst des Landesamtes für Geologie, Rohstoffe und Bergbau Baden Württemberg in Freiburg, from the Zentralanstalt für Meteorologie und Geodynamik in Vienna, from the SISMALP array operated by the Laboratoire de Géophysique Interne et Tectonophysique, Observatoire de Grenoble, from the Laboratoire de Détection et Géophysique in Bruyères-le-Châtel, from the RENASS array operated by the Ecole et Observatoire des Sciences de la Terre in Strasbourg, from the Istituto Nazionale di Geofisica e Vulcanologìa in Rome and from the Istituto di Geofisica, Università di Genova.

To improve the reliability of locations for events at the periphery or outside of Switzerland, we are engaged in an ongoing cross-frontier cooperative effort to exchange seismic data in realtime. Since 2005 we continuously record and archive signals from stations in Austria operated by the Zentralanstalt für Meteorologie und Geodynamik in Vienna (ZAMG), in southern Germany operated by the Erdbebendienst des Landesamtes für Geologie, Rohstoffe und Bergbau Baden Württemberg in Freiburg, and in Italy operated by the Istituto Nazionale di Geofisica e Vulcanologìa in Rome (INGV), by the Istituto di Geofisica, Università di Genova, by the Zivilschutz der Autonomen Provinz Bozen-Südtirol and by the Istituto Nazionale di Oceanografia e di Geofisica Sperimentale (OGS) in Trieste. In 2011, we began receiving data in realtime also from the Reseau Sismologique et Godsique Franais (RESIF) in France (including, for the first time, a foreign strong-motion station). A total of 29 foreign stations were monitored at the SED in 2011, and the number continues to increases as new high-quality stations come on-line in the border region.

Data analysis

Hypocentral locations and faultplane solutions

Preliminary hypocenter locations are determined on the basis of an automatic arrival time picker (Baer & Kradolfer, 1987), but final arrival times and locations are subsequently reviewed by a seismologist. Before the year 2005, locations were calculated either with a modified version of the widely used HYPO-71 algorithm originally developed by Lee & Lahr (1972) or with a grid search algorithm based on direct foreward modeling of travel times. The seismic velocity models consist of three horizontal crustal layers with constant velocities

overlying a mantle half-space. The models account for differences between the near-surface geology in the Alps and foreland as well as, in a simplified way, for the large depth variation of the crust-mantle boundary. In addition, calculated travel times are corrected for differences in station elevation. As an added feature, these two algorithms include the possibility to use secondary arrivals, such as the reflection at the Moho, PmP, or the direct wave, Pg, at distances were the Moho refraction, Pn, is the first arrival.

With the year 2005, hypocenters of most of the local earthquakes have been calculated using the software package NonLinLoc (Lomax et al. 2000). This procedure is based on a combination of probabilistic earthquake location and non-linear, global search algorithms using nested grids or the Oct-Tree Importance sampling algorithm (Lomax and Curtis, 2001). The probabilistic, non-linear formulation of the earthquake location problem contains a complete description of location uncertainties. In this approach, a priori known errors such as measurement errors or travel time calculation errors are explicitly incorporated in terms of probability density functions. These methods not only provide a complete description of uncertainty estimates, but can also be used with any available velocity model and method of travel time calculation. The P-wave velocity model used in this context was derived from a 3D tomographic inversion of local earthquake data with constraints from controlled source seismics (Husen et al. 2003). A 3D S-wave velocity model is not available yet, so that the S-velocities are calculated from the P-velocity using a V_p/V_s ratio of 1.71. In regions where it is well-constrained, the 3D velocity model gives more accurate ray paths, in particular at larger distances and for arrivals refracted at the Moho. This permits more reliable focal depth determinations, even for events where the minimal epicentral distance is large relative to the focal depth.

In the case of selected events, in particular those for which we constructed focal mechanisms, focal depths were checked by 2-D ray-trace modeling of the travel-time differences between the direct ray (Pg) and the reflection from the Moho (PmP) or between the Pg and the ray refracted in the upper mantle (Pn) (e.g. Garcia-Fernandez & Mayer-Rosa, 1986; Deichmann, 1987; Deichmann & Rybach, 1989). The crustal velocities used for the ray-trace models are obtained from tomographic and seismic refraction studies (e.g. Maurer & Ansorge, 1992; Maurer & Kradolfer, 1996; Pfister, 1990; Yan & Mechie, 1989; Ye et al., 1995) and the Moho topography is based on the results of Waldhauser (1996) and Waldhauser et al. (1998), thus accounting realistically for the crustal heterogeneity. The same ray-tracing technique is also employed to correctly identify first arrivals and to estimate take-off angles of the rays at the source, which are used for constructing the focal mechanisms based on first-motion polarities (e.g. Eva et al., 1998; Deichmann et al., 2000b).

In the earthquake lists for each year, the estimated reliability of the given locations has been classified with letters A, B, C and D based on the criteria listed in Table 1.1.

Moment tensor inversions

The newly installed broadband stations allow the use of state-of-the-art waveform modeling techniques to study the source parameters of some larger earthquakes in Switzerland. We invert complete three-component waveforms recorded at local to regional distances for the seismic moment tensor by minimizing the least squares misfit between observed and synthetic seismograms. Strike, dip, rake, and seismic moment follow directly from the moment tensor

Rating	Criteria		Uncertainty	
Q	GAP	DM	H	Z
	(degrees)	(km)	(km)	(km)
A	≤ 180	$\leq 1.5{\times}Z$	≤ 2	≤ 3
B	≤ 200	≤ 25	≤ 5	≤ 10
C	≤ 270	≤ 60	≤ 10	> 10
D	> 270	> 60	> 10	> 10

Table 1.1: Criteria and location uncertainty corresponding to the quality rating (Q) of the hypocentral parameters in the following epicenter lists. GAP = largest angle between epicenter and two adjacent stations; DM = minimum epicentral distance; H = horizontal location; Z = focal depth.

formulation. Earthquake depth is found by repeating the inversion for several trial depths. The inversion is performed at relatively low frequencies; thus, a simple one-dimensional velocity-depth model is sufficient to calculate synthetic discrete wavenumber seismograms (Bouchon, 1982) for all stations. The model consists of a 35 km thick continental crust with an average ratio between the P- and S-wave velocities of 1.73. Using three-component data and low-frequency waveforms provides robust and stable source parameter estimates; moderate changes in the crustal model affect the moment tensor solutions only slightly. We refer to Nabelek and Xia (1995) and Braunmiller et al. (1995) for a more detailed description of the method and to Deichmann et al., (2000a) for an illustration of the application to a local earthquake in Switzerland. The complete set of moment tensors calculated by the Swiss Seismological Service, including plots of all waveform fits, is available on line (`http://www.seismo.ethz.ch/mt/`).

In an effort to automate the procedure, a new automated moment tensor inversion scheme, which estimates the double couple and compensated linear vector dipole (CLVD) components was implemented at the Swiss Seismological Service in 2006. Similarly to the method described above, the solution, based on the time domain inversion scheme developed by Dreger (2003), also provides a moment magnitude, M_w, the best fitting double couple, and an optimal depth estimate based on the given location. Synthetic seismograms created using 1-D Green's functions from various simple velocity profiles (Saikia, 1994) are matched with the observed 3-component long period waveforms to minimise the least squares time domain waveform misfit. The range of signal periods used in the inversion are determined from the routinely determined M_L magnitude, and range from 8-20 s for $M_L < 3.8$ to 50-100 s for $M_L > 5.3$. In this fully automated implementation, data from all stations out to 500 km distance which pass quality control criteria are initially individually inverted to rank the stations in terms of waveform quality, and then an iterative search is performed to find the best solution for up to 6 stations. Additional information on the method can be found in Clinton (2006), which describes a similar implementation for the Southern California Seismic Network, USA.

Magnitudes

From the records of the short-period stations, magnitudes are determined from the maximum amplitudes of the vertical components of ground velocity. In order to obtain the local magnitude (M_L), these amplitude values and the corresponding period are converted to what they would be if the signals had been recorded

by a standard Wood-Anderson seismograph. The broad-band signals, on the other hand, are digitally filtered to simulate the response of a Wood-Anderson seismograph, and M_L is then determined directly from the maximum amplitudes of the resulting horizontal seismograms. The attenuation with epicentral distance is accounted for by an empirically determined relation (Kradolfer & Mayer-Rosa, 1988). The final magnitude corresponds to the median value of all individual station magnitudes. During the transition time from the short-period to the broad-band network, magnitudes were determined from the records of both systems. However, since February 2002, magnitude calculations are based almost entirely on seismograms from the new stations.

Assuming a Wood-Anderson gain of 2800 and adding a correction of 0.1 to each station magnitude results in values for M_L that are consistent with M_L determined previously from the vertical component short-period stations.

For the events for which we could derive a moment tensor from a full-waveform inversion, we list the moment magnitude (M_w) in addition to the local magnitude (M_L). Moment magnitude is calculated from the seismic moment M_0 obtained from the moment tensor using the relation $M_w = (2/3) \log M_0 - 6$, where M_0 is given in N-m (Hanks & Kanamori 1979). For the compilation of a unified earthquake catalog of Switzerland, that includes both historical and instrumental data (ECOS), it was decided to adopt moment magnitude M_w as a uniform estimate of earthquake size (Fäh et al., 2003). An analysis performed in this context showed that on average the M_L determined routinely by the Swiss Seismological Service is 0.2 magnitude units higher than M_w (Braunmiller et al. 2005).

Recently an additional procedure has been implemented that routinely and automatically provides estimates of M_w also for earthquakes of lower magnitudes. Mw values are computed using a spectral fitting technique following the method of Edwards et al. (2010). The far-field signal moments are obtained by simultaneously fitting the spectrum of a theoretical source model (Brune 1970, 1971) along with path variable attenuation and event stress-drop to observed Fourier velocity spectra. The seismic moment is derived from the far-field signal moments assuming a simple geometrical spreading model that accounts for body and surface wave propagation. Site amplification is derived for the whole network following the approach detailed in Edwards et al. (2013). Using this information all data are corrected to a reference hard-rock recording site (Poggi et al. 2011) before computing M_w.

Public alert procedures

To meet the increasing demands of both the public and the media for rapid information, in May 2003 the Swiss Seismological Service started to automatically update its web-page with information about earthquakes in Switzerland whose magnitude exceeds M_L 3.0 (http://www.seismo.ethz.ch). In addition, location and magnitude together with a preliminary assessment of possible damage are disseminated automatically to authorities and media within minutes after a strong seismic event.
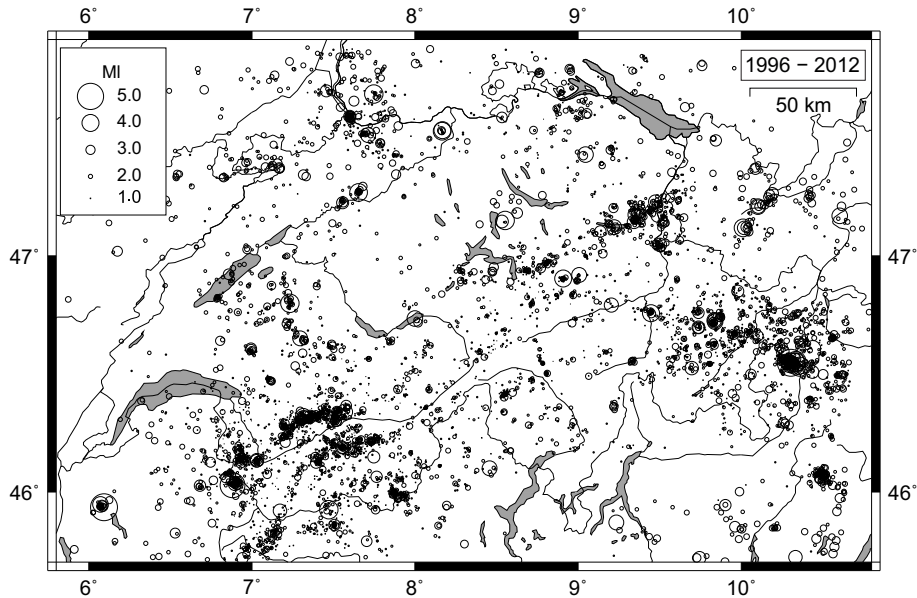
Overview of the seismic activity 1996 - 2012

Figure 1.1: Epicenters of earthquakes with Magnitudes $M_L > 0$, during the period 1996 – 2012.

As an overview of the period covered by this report, Figure 1.1 shows the epicenters of the earthquakes with $M_L > 0$, which have been recorded and located by the Swiss Seismological Service in Switzerland and surrounding regions since 1996. The change from the analog short-period to the digital broad-band network in the Fall of 2001 was followed by a pronounced change in the detection threshold. This is clearly seen in the plots of the magnitude of each earthquake and of the cumulative number of events as a function of time shown in Figure 1.2. Thus, also the apparent increase in the yearly seismicity rate for $M_L > 0$ beginning in 2002, seen in Figure 1.2c, is mainly an artifact of changes in the data acquisition system.

However, the fluctuations in number of events per year for earthquakes with $M_L \geq 2$ shown in Figure 1.2d are real and are not due to changes in the magnitude of completeness, which is certainly below M_L 2.0 for the entire time period. The peak in 1996 is due mainly to the aftershocks of the M_L 5.1 Annecy earthquake and to a concentration of seismicity in the region between Lac de Salanfe and Val d'Illiez (VS). The latter was most likely a consequence of the renewed impoundment of the hydro-electric reservoir of Salanfe in 1994 and 1995 (CRE-ALP, 1998). The increased seismicity in 1999 corresponds to the earthquake sequence of Fribourg, a concentration of seismic activity in the Toggenburg, NE of Walensee, and the beginning of the long-lasting earthquake sequence of Bormio, at the border between Graubünden and northern Italy. The latter as well as a sequence in Val Baone, south of Bormio, were the main cause for the increased activity in the years 2000-2003, together with the seismic sequences of Martigny, VS, (2001), Cima di Jazzi, VS, (2002-2003), Sertig, GR, (2003) and Glarey, VS, (2003). For further details regarding these earthquake sequences, see the corresponding annual reports that follow this introduction. In contrast,
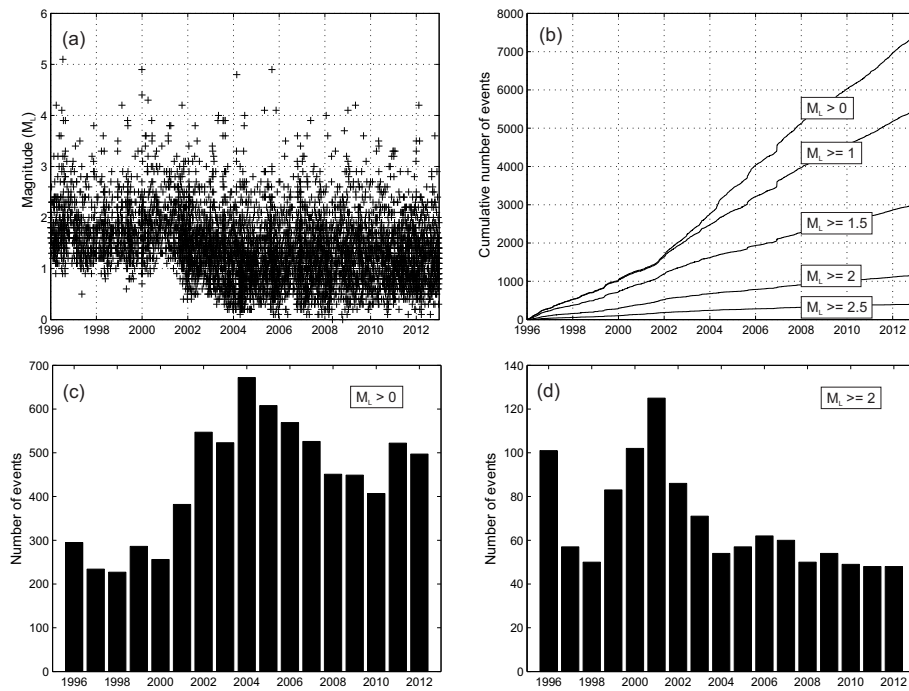
Figure 1.2: Local magnitude (a), cumulative number of earthquakes (b), and histograms of events/year for $M_L > 0$ (c) and for $M_L \geq 2$ (d) recorded in Switzerland and surroundings in the period 1996 - 2012. The change in slope of the two uppermost curves in (b) at the end of 2001 is due to the change of the event detection from the analog short-period to the digital broad-band network. The pronounced step at the end of 2006, most clearly visible for $M_L > 0$, corresponds to the seismicity induced by the geothermal project in Basel.

the seismic activity over the years 1997, 1998 and 2004-2012 has been remarkably constant at 50-60 events with $M_L \geq 2$ per year.

Seismic activity during 1996

Overview

During 1996, the Swiss Seismological Service detected and located 339 seismic events in the region shown in Figure 1996.1. Based on such criteria as the time of occurrence, the location, the signal character or direct information, 39 of these events were identified as quarry blasts. In some cases, we applied other detection methods for identifying explosions, which are based on signal cross-correlation, multivariate statistical analysis or on full waveform inversion (Campus and Fäh, 1997), but which are not yet implemented as a routine procedure. As discussed in more detail below, 5 events were landslides. Magnitude values of the 295 earthquakes recorded in 1996 range between M_L 0.9 and 5.1 (Fig. 1996.2). The events with $M_L \geq 2.5$ are listed in Table 1996.1. Overall, the seismic activity in 1996 was representative of what has been observed over a longer time span. In particular, the highest earthquake activity, both in terms of number of events and in terms of their size, occurred once again in the Valais. The only note-worthy exception to this overall agreement is the almost total lack of activity during 1996 along the easternmost border of Switzerland, where there has been a striking concentration of events over the previous 21 years.

Focal depths range between 0 and 31 km, but only 11 hypocenters are located at depths greater than 15 km. Clearly, the depths of many of the shallow events are poorly constrained. With increasing depth, however, focal depth determinations become more reliable. Indeed, a critical review of the location of each of these 11 events as well as ray-trace modelling of three of them show that their focal depths are well constrained. Moreover, because of the greater reliability of larger focal depths, it is unlikely that many of those events that have been located in the upper crust actually occurred at significantly greater depths. Thus, the results indicate that most of the seismic activity in 1996 was restricted to the upper part of the crust and that less than 5 % of all earthquakes occurred below about 15 km. Moreover, all of these deeper hypocenters are located below the Jura Mountains and Molasse Basin of northern Switzerland.

The regional variation of maximum focal depths, exemplified by the Kirchberg event in the lower crust below the Molasse Basin and by the complete lack of earthquakes below about 15 km in the Alps, is representative of the long-term focal depth distribution (Deichmann & Baer, 1990; Deichmann, 1992).

Macroseismic observations are available for 4 events and are displayed in Figure 1996.3. The fault-plane solutions with first-motion directions are shown in Figure 1996.4 and the corresponding parameters are listed in Table 1996.2.
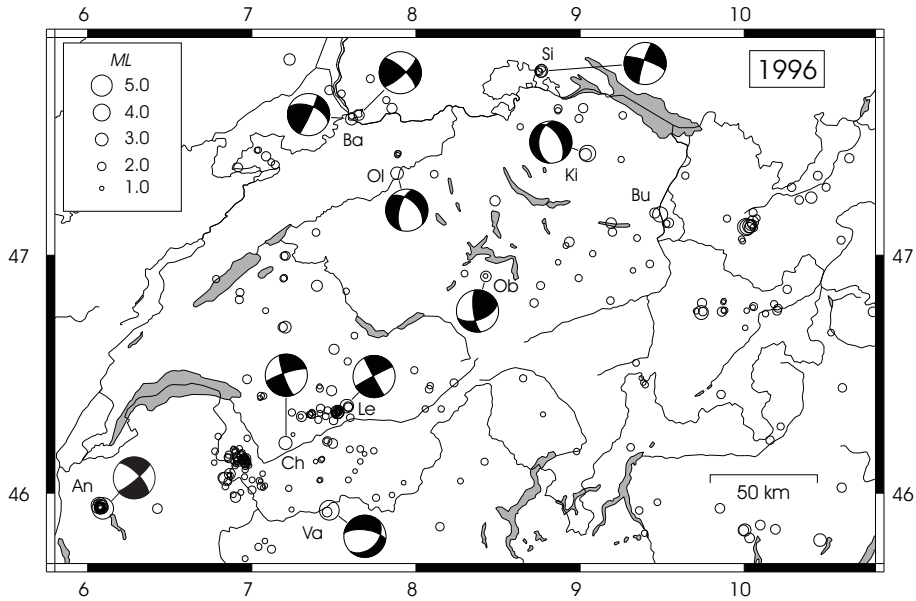
Figure 1996.1: Epicenters and focal mechanisms of earthquakes recorded by the Swiss Seismological Service during 1996. Epicenters of earthquakes mentioned in the text are labeled: An = Annecy, Ba = Basel, Bu = Buchs, Ch = Chamoson, Ki = Kirchberg, Le = Leukerbad, Ob = Oberrickenbach, Ol = Olten, Si = Singen, Va = Valpelline. The focal mechanism of the Annecy event is from Thouvenot et al. (1998)
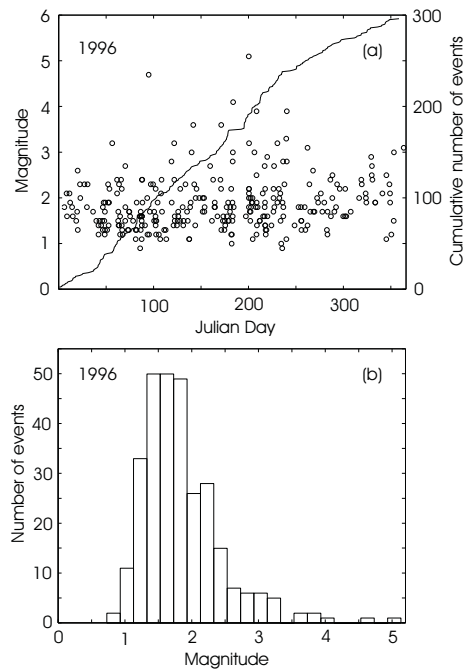

Figure 1996.2: Earthquake activity during 1996: magnitude of each event and cumulative number of events (a); histogram of magnitudes (b).

Date & Time UTC	Lat. [°N]	Lon. [°E]	X / Y [km]	Depth [km]	Mag. [M_L]	Q	Location
1996.01.16 07:00:20	46.873	7.397	597/191	19	2.6	B	Niederscherli, BE
1996.02.21 18:57:28	46.368	7.579	611/135	5	3.2	A	Leukerbad, VS
1996.03.06 14:16:28	46.144	6.960	563/110	6	2.7	B	Le Luison, VS
1996.03.31 06:08:01	45.938	7.460	602/ 87	4	4.2	A	Valpelline, I
1996.04.24 09:36:57	47.565	7.607	613/268	12	2.8	A	Basel, BS
1996.04.27 06:59:59	47.121	10.032	797/222	10	3.2	C	Arlberg, A
1996.05.15 15:05:51	45.800	10.462	835/ 76	10	3.0	D	Bagolino, I
1996.05.17 09:30:59	47.170	9.488	755/226	1	3.6	B	Buchs, SG
1996.06.04 05:05:23	47.810	7.230	584/295	10	2.7	C	Mulhouse, F
1996.06.15 21:40:09	47.118	10.019	796/222	10	3.6	C	Arlberg, A
1996.06.27 22:40:00	46.700	7.204	582/172	10	2.8	B	La Berra, FR
1996.06.28 03:43:10	47.763	8.764	699/291	9	3.0	A	Singen, D
1996.06.28 09:57:48	47.118	10.012	795/222	10	4.1	C	Arlberg, A
1996.07.15 00:13:30	45.935	6.092	495/ 88	3	5.1	A	Annecy, F
1996.07.15 05:46:13	45.940	6.084	495/ 88	3	3.2	A	Annecy, F
1996.07.20 22:04:34	45.946	6.080	495/ 89	3	3.0	A	Annecy, F
1996.07.23 02:50:31	45.937	6.090	495/ 88	3	2.5	A	Annecy, F
1996.07.23 04:08:41	45.947	6.071	494/ 89	2	3.9	A	Annecy, F
1996.07.31 16:26:43	46.341	7.525	607/132	4	2.7	A	Crans, VS
1996.08.03 10:48:28	46.341	7.522	606/132	4	2.9	A	Crans, VS
1996.08.10 13:57:45	47.760	8.760	699/291	9	2.7	A	Singen, D
1996.08.14 04:37:45	46.343	7.522	606/132	4	3.2	A	Crans, VS
1996.08.20 04:59:56	47.139	10.051	798/224	10	2.8	C	Arlberg, A
1996.08.23 13:27:46	46.761	9.739	776/181	1	3.3	B	Arosa, GR
1996.08.24 02:38:22	47.423	9.045	721/254	29	3.9	A	Kirchberg, SG
1996.08.24 02:42:25	47.419	9.033	720/253	29	2.8	A	Kirchberg, SG
1996.09.14 22:54:52	46.061	6.839	554/101	10	3.1	C	Le Buet, F
1996.09.20 17:37:27	46.081	6.866	556/103	5	2.6	C	Le Buet, F
1996.10.11 07:43:24	47.134	9.189	733/222	1	2.5	A	Walensee, SG
1996.11.21 05:30:24	45.843	10.004	799/ 80	10	2.9	D	Lago d'Iseo, I
1996.11.21 18:56:56	45.842	9.995	798/ 80	10	2.5	D	Lago d'Iseo, I
1996.11.21 23:08:13	47.240	10.408	825/236	10	2.7	C	Stockach, A
1996.12.07 05:34:28	46.912	8.426	675/196	2	2.5	A	Oberrickenbach, NW
1996.12.15 04:49:08	47.341	7.885	634/243	20	3.0	A	Olten, SO
1996.12.25 12:39:25	46.212	7.205	582/118	7	3.1	A	Chamoson, VS

Table 1996.1: Earthquakes during 1996 with $M_L \geq 2.5$. The hypocentral coordinates of the Annecy events are from the Observatoire de Grenoble. The locations of the events of Leukerbad, Valpelline, Basel, Singen, Kirchberg, Oberrickenbach, Olten and Chamoson are based on additional data from foreign institutions and focal depths are constrained by 2-D ray-tracing.
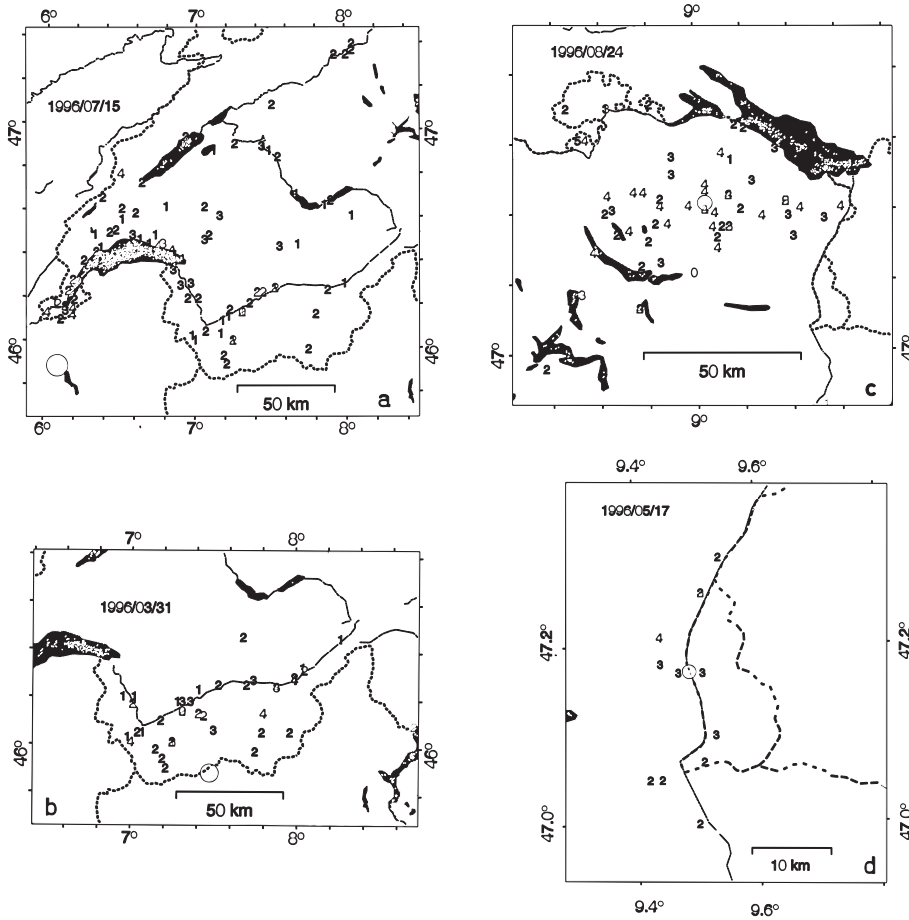
Figure 1996.3: Macroseismic observations of 4 earthquakes (a = Annecy, b = Valpelline, c = Kirchberg, d = Buchs).

Location	Date & Time [UTC]	Depth [km]	Mag.	Plane 1 Plane 2 Strike/Dip/Rake		P-Axis T-Axis Az/Dip	
Leukerbad	1996.02.21 18:57	5	$M_L 3.2$	242/87/-178	152/88/-003	107/04	197/01
Valpelline	1996.03.31 06:08	4	$M_L 4.2$	44/38/-137	278/65/-060	231/59	347/15
Basel	1996.04.24 09:36	12	$M_L 2.8$	292/55/ 174	25/85/ 035	153/20	254/28
Basel	1996.06.15 01:05	21	$M_L 2.4$	314/73/ 165	48/76/ 017	180/02	271/23
Singen	1996.06.28 03:43	9	$M_L 3.0$	289/78/-172	197/82/-012	153/14	244/03
Annecy	1996.07.15 00:13	3	$M_L 5.1$	316/70/-010	49/81/-160	274/21	181/07
Kirchberg	1996.08.24 02:38	29	$M_L 3.9$	184/42/-063	330/53/-112	183/72	75/06
Oberrickenbach	1996.12.07 05:34	2	$M_L 2.5$	172/74/ 036	70/56/ 160	297/11	36/37
Olten	1996.12.15 04:49	20	$M_L 3.0$	313/50/-141	195/61/-047	158/53	256/06
Chamoson	1996.12.25 12:39	7	$M_L 3.1$	252/80/-170	160/80/-010	116/14	206/00

Table 1996.2: Focal mechanism parameters 1996. Parameters of the Annecy event are from Thouvenot et al. (1998).
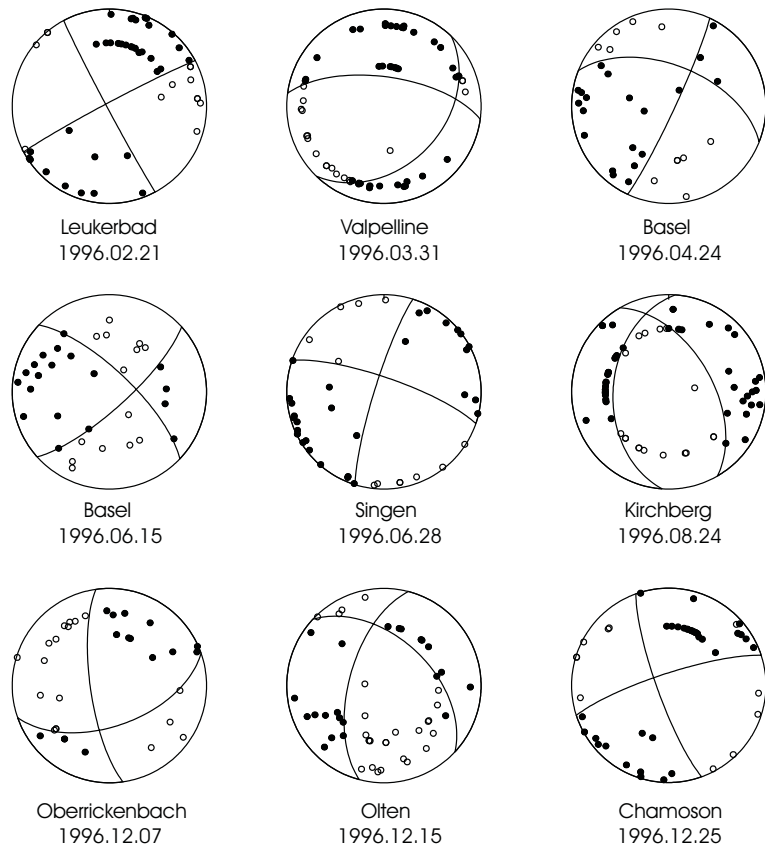
Figure 1996.4: Fault-plane solutions (lower hemisphere, equal area projection). Solid circles, compressive first motion (up) and empty circles, dilatational first motion (down).
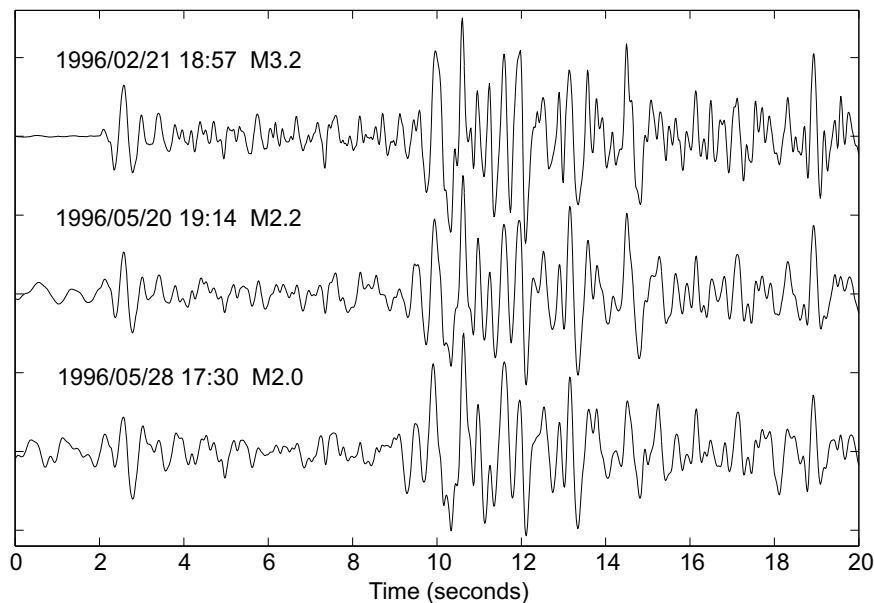
Figure 1996.5: Vertical-component seismograms of the Leukerbad mainshock and two aftershocks recorded at station BRI, bandpass filtered 1-4 Hz.

Significant seismic events in 1996

Leukerbad

At 19:57 local time on February 21st, a magnitude 3.2 event occurred 4 km SW of Leukerbad. Its epicenter coincides with the eastern end of the prominent ENE-WSW striking epicenter alignment, which has been identified north of the Rhone Valley by previous studies (Maurer & Deichmann, 1995; Maurer & Kradolfer, 1996; Pavoni et al., 1997). Thanks to the onscale recording of both P- and S-waves at station LKBD, which is situated only 4 km from the epicenter, the focal depth of 5 km is well constrained.

The fault plane solution corresponds to a strike-slip mechanism (Fig. 1996.4 and Table 1996.2), which is typical for the predominant focal mechanism type observed in the northern Valais (Maurer et al., 1997). The two nodal planes strike NNW-SSE with left-lateral slip and ENE-WSW with right-lateral slip. The February 21st event was followed by two smaller aftershocks on May 20th and 28th. The signals of these two aftershocks are almost identical to those of the mainshock (Fig. 1996.5), which means that all three events must have occurred close to each other on the same fault and with the same mechanism. Precise relative locations, using a master event location procedure based on cross-correlation of the waveforms (Console & DiGiovambattista, 1987; Deichmann & Garcia-Fernandez, 1992), show that the three hypocenters lie on a plane that matches closely one of the nodal planes of the focal mechanism. Therefore, contrary to what was hypothesized in an earlier version of this report (Baer et al., 1997), the rupture of the Luekerbad event and its aftershocks occurred as right-lateral slip on an almost vertically dipping, ENE-WSW striking fault. The orientation of this faultplane is close to the general trend of the epicenter alignment in the Helvetic domain of the northern Valais.
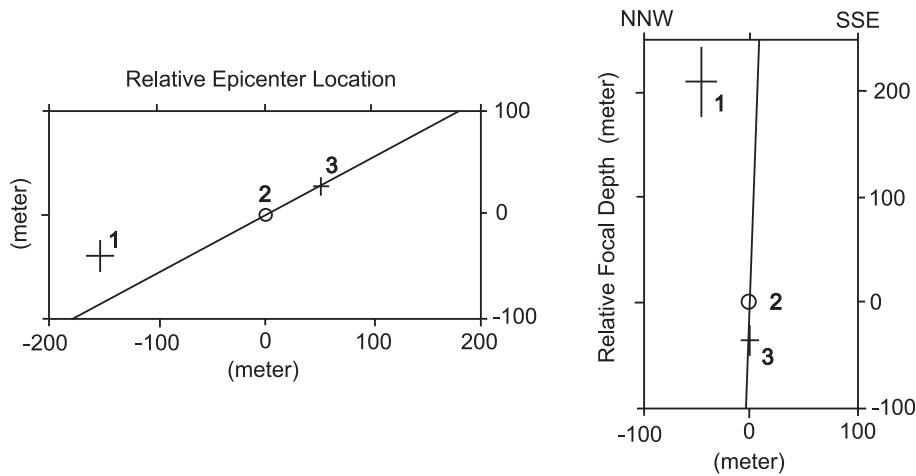
Figure 1996.6: Relative locations of the Leukerbad mainshock (1) and its two aftershocks (2 and 3). Aftershock number 2 was used as master event. The size of the crosses corresponds to one standard deviation of the locations. The stright lines across each plot show the strike and dip of the ENE-WSW striking nodal plane of the focal mechanism.

Valpelline

At 08:08 local time of March 31st, a moderate earthquake occurred in a relatively remote area of the Valais near the border with the Aosta Valley, Italy. Ray-trace modelling indicates that its focal depth hardly exceeded 5 km. It was felt throughout the Valais. The strength was sufficient to trigger the accelerograph arrays in the Mauvoisin and Grande Dixence dams, as well as several other accelerographs out to a distance of 40 km (Smit, 1997). The peak ground acceleration measured by the free-field station at Grande Dixence, situated at an epicentral distance of 18 km, reached 6 cm/s^2. Most of the high-gain stations of the Swiss national network were clipped, so the magnitude is uncertain: first estimates suggested a value of M_L 4.6-4.7, but a revision showed that a value of M_L 4.2 is more likely. However, surprisingly for an earthquake of that strength, most of the recorded seismograms are characterized by relatively weak and emergent onsets. Detailed analysis of the observed signals shows that the source process actually consisted of two subevents 0.6 s apart, and that the first subevent was smaller by about one magnitude unit (Fig. 1996.7).

The focal mechanism determined from the first-motion polarities of the first subevent corresponds to a normal fault with a N-S trending T-axis (Fig. 1996.4 and Table 1996.2). The resulting extensional deformation oriented at a high angle to the strike of the Alpine mountain range is consistent with other focal mechanisms observed in that area and is a typical feature of the tectonic regime of the southern Valais (Eva et al., 1997; Maurer et al., 1997).

Basel

On April 24th and June 15th, two small earthquakes (M_L = 2.8 and 2.4), for which fault plane solutions could be constructed, occurred in the vicinity of Basel. Though their focal depths differ significantly (12 and 21 km), both events have strike-slip mechanisms with N-S to NNW-SSW oriented P-Axes
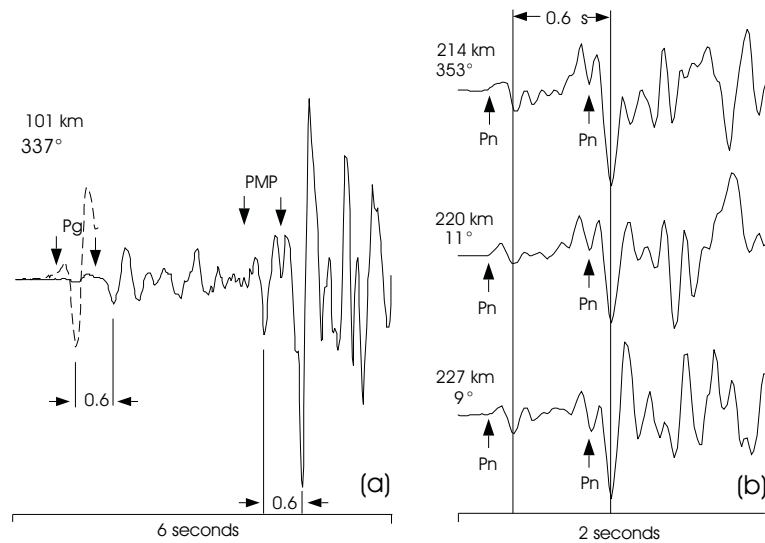
Figure 1996.7: Seismogram examples which show that the Valpelline quake consisted of two subevents 0.6 seconds apart. Epicentral distance and azimuth are indicated for each signal. (a) Pg and PMP recorded by the low-gain channel of station ROM (continuous trace) and the onset of the first subevent as recorded by the high-gain channel (dashed trace, magnified 20 times). (b) Pn arrivals recorded by three stations in the Vosges Mountains, France, and Black Forest, Germany.

(Fig. 1996.4 and Table 1996.2).

Singen

The magnitude 3 event of June 28th is part of a sequence of 7 events with epicenter near Singen, southern Germany, and magnitudes between 1.6 and 3.3, that were recorded between March 1995 and August 1996. The focal depth of 9 km is constrained by 2-D ray-trace modelling of PmP-Pg and Pg-Pn travel-time differences. The similarity of the recorded waveforms demonstrate that these 7 earthquakes form a sequence of events that ruptured the same fault. the faultplane solution corresponds to a strike-slip mechanism with a NNW-SSE oriented P-axis (Fig. 1996.4 and Table 1996.2). Results of high-precision relative hypocenter locations based on waveform crosscorrelations show that rupture occurred as right-lateral slip on the WNW-ESE striking faultplane (Deichmann et al., 2000b).

Annecy

The most significant earthquake to have occurred in Switzerland or the surrounding areas in 1996 struck the town of Annecy, France, at 02:13 local time of July 15th. Its epicenter was located near Epagny, 4 km NW of Annecy. With a magnitude of 5.1 (the Observatoire de Grenoble reports a value of 5.3) and with a focal depth of about 3 km, the epicentral intensity reached a value of VII to VIII on the MSK scale (Bisch, 1996). The shaking toppled chimneys and caused significant damage to several buildings in and around Annecy. A four-

story apartment building in Meythet suffered such severe structural damage that it had to be evacuated (Davidovici, 1996).

Immediately after the main shock, the Observatoire de Grenoble installed a temporary seismograph network to monitor the aftershock activity. Close to a thousand aftershocks were detected (Thouvenot et al., 1998). Twenty of these aftershocks, ranging in magnitude between 1.7 and 4.0 were also recorded by the national network of the Swiss Seismological Service. However, in Table 1996.1 we report the locations determined by the Observatoire de Grenoble (J. Fréchet, personal communication), which are also plotted in Figure 1996.1.

Based on the fault plane solution, on the distribution of aftershocks and on the tectonic setting, it is clear that the Annecy earthquake was caused by left-lateral slip on the steeply dipping, NW-SE striking Vuache fault, which has been seismically active in the past (Thouvenot, 1996; Thouvenot et al., 1998; Courboulex et al., 1999).

The Annecy earthquake with a magnitude of 5.1 or 5.3 was only slightly stronger than the Grand-Bornand earthquake, which occurred only about 40 km ENE of Annecy on December 14h, 1994, (Fréchet et al., 1996) and the November 21st, 1991, earthquake of Vaz, Graubünden. In fact, earthquakes of this size are not uncommon in the Alps and larger ones must be expected as well (Sägesser & Mayer-Rosa, 1978; Rüttener, 1995). Although the individual damages caused by the Annecy earthquake were not overwhelming, the total financial loss has been estimated at 300 million French Francs (Davidovici, 1996). This shows once again that even moderate earthquakes, when they occur in densely populated industrialized areas, can have significant economic impact.

Kirchberg (SG)

The magnitude 3.9 event, which occurred in the early morning hours of August 24th, was located at a depth of 29 km below the town of Kirchberg, in the Untertoggenburg. The unusually large focal depth for an earthquake of this size in Switzerland is well constrained both by the nearby recording of station WIL and by 2-D ray-tracing. Because of its large focal depth, it was felt throughout all of northeastern Switzerland, even though the epicentral intensity was not more than IV (MSK) (Fig. 1996.3). Several strong-motion stations were triggered: in Buchs (SG), at an epicentral distance of 44 km, peak ground acceleration reached a value of 6 cm/s^2 (Smit, 1997).

The faultplane solution corresponds to an almost pure normal faulting mechanism (Fig. 1996.4 and Table 1996.2). The orientation of the T-axis is typical for the ENE-WSW oriented extension of the northern Swiss Molasse Basin as derived from earlier focal mechanism studies (e.g. Pavoni, 1987; Deichmann, 1992).

The mainshock was followed 4 minutes later by a magnitude 2.8 aftershock, which, judging from the high degree of similarity between the seismograms of the two events, must have occurred nearby and on the same fault.

Oberrickenbach

Despite its small magnitude ($M_L = 2.5$) the event of Oberrickenbach of December 7th is of particular interest, because of its location in the vicinity of the considered site for a nuclear waste repository below the Wellenberg, Niedwalden. The focal depth in the range of 1-5 km is constrained by 2-D ray-tracing, which indicates that the hypocenter is located in the near-surface sedimentary cover.

Date	Time [UT]	Time (local)	Mag. $[M_L]$	Energy ratio	Location
96.01.24	08:00	09:00	2.6	1/2	Zuetribistock
96.03.03	18:30	19:30	2.8	1/1	Zuetribistock
96.05.19	19:35	21:35	1.6	1/700	unknown
96.09.04	02:42	04:42	1.9	1/46	Zuetribistock
96.10.05	04:39	06:39	1.6	1/43	Ochsenstock

Table 1996.3: Landslides detected south of Linthal, Canton Glarus. The energy ratios were calculated from the integral of the square of the recorded ground velocities.

The conclusion that the source must have been shallow is supported both by the fact that, based on the observed first-motion polarities and on take-off angles for a source in the crystalline basement, it is not possible to construct a consistent faultplane solution and by the fact that this small-magnitude event was actually felt by the local population (Deichmann et al. 2000b). The focal mechanism and the relative location of a smaller event with identical waveforms, that occured about one hour earlier, show that the rupture occurred as left-lateral slip with a slight thrust component on a steeply dipping nearly N-S striking fault (Deichmann et al. 2000b).

Olten

The hypocenter of the magnitude 3.0 event, which occurred in the early morning of December 15th, was located at a depth of 20 km below the town of Olten, at the southern margin of the Jura Mountains. Both the focal depth and the faultplane solution are well constrained by the high station density in northern Switzerland and southern Germany. Although the focal mechanism has a much stronger strike-slip component than that of the Kirchberg event, the ENE-WSW trend of the nearly horizontal T-axis is practically the same for both events (Fig. 1996.4 and Table 1996.2).

Chamoson

Relative to the Leukerbad event of February 21st, the epicenter of the quake, that occurred on the afternoon of Christmas Day near Chamoson, is located at the opposite end of the prominent WSW-ENE striking epicenter alignment that characterizes the seismicity in the Helvetic domain of the Valais. The strike-slip focal mechanism agrees with that of the Leukerbad event within $< 10°$ (Table 1996.2), but we have no means of identifying the active faultplane in this case. The focal depth of about 7 km, which is constrained by 2-D ray-tracing, is typical of the upper-crustal seismicity in this region (Maurer & Kradolfer, 1996).

Landslides

Based on their signal character, five events detected by the national network during 1996 were judged to correspond to large landslides in the vicinity of station LLS, situated at the Linth-Limmern hydroelectric dam, Canton Glarus. In fact, as listed in Table 1996.3, four of these events can be associated with landslides that fell onto Sandalp, south of Linthal, Canton Glarus (K. Stüssi,

Kraftwerke Linth-Limmern, AG, personal communication). The nature of the event which occurred on May 19th and which was considerably smaller than the others has not been confirmed. However, the similarity of the signals with those of the other landslides strongly suggests that this event was due to the same cause.

For landslides occurring in the same place, the equivalent earthquake magnitudes, calculated from the maximum amplitudes of the recorded signals, give a rough indication of the relative size of the individual events. A more reliable estimate of the combined effect of the total rock mass and the corresponding impact velocity can be obtained from the cumulative seismic energy radiated by each event. Thus, the ratios between the time integrals of the square of the ground velocity recorded at various stations suggest that the landslide of March 3rd on the flanks of Zuetribistock was about twice as energetic as the one of January 24th and 40 to 50 times more energetic than the one that occurred on September 4th (Table 1996.3).

Seismic activity during 1997

Overview

During 1997, the Swiss Seismological Service detected and located 234 earthquakes in the region shown in Figure 1997.1. Based on such criteria as the time of occurrence, the location, the signal character or direct information, 57 additional seismic events were identified as quarry blasts. As discussed in more detail below, the network also recorded 5 landslides or rock avalanches.

Routinely calculated focal depths range between 0 and 31 km, but only 7 hypocenters are located at depths greater than 15 km. One of these deeper events ($M_L = 2.0$) is located 16 km below the Chablais, south of Lake Geneva, but its location is poorly constrained. Another deeper one is the M_L 3.1 event of Nov. 17th, located north of Basel at a depth of 17 km. The other 5 deep events are all located at depths greater than 20 km in the lower crust beneath the Jura Mountains and Molasse Basin of northern Switzerland.

Magnitude values of the events recorded in 1997 range between M_L 0.5 and 3.8 (Fig. 1997.2). The events with $M_L \geq 2.5$ are listed in Table 1997.1. Where available, the epicentral coordinates and focal depths given in Table 1997.1 are based on the results that include additional data from foreign networks and on 2-D ray-tracing.

Averaged over the past 23 years, the seismic activity is equivalent to 24 events with $M_L \geq 2.5$ per year. Thus, with 22 earthquakes having an $M_L \geq 2.5$, the seismic activity in 1997 was close to normal in terms of number of events. However, without a single event with $M_L > 4$ and only one having an $M_L > 3.5$, the seismicity was below average in terms of magnitudes.

In agreement with longterm observations, most of the earthquakes occurred in the Valais and in Graubünden. Particularly noteworthy is the concentration of earthquakes, including two $M_L > 3$ events, in the area between the Ofenpass, GR, and the upper part of the Valtellina, Italy, which was unusually quiet during 1996 (Baer et al., 1997). Unfortunately, due to the unavailability of data from stations south of the border, the epicentral locations are poorly constrained and the focal mechanisms in that region are unknown.

Both the lower-crustal seismicity below the northern Alpine foreland as well as the lack of seismicity deeper than about 15 km below the Alpine mountain chain confirm the focal depth distribution documented in previous studies (Deichmann & Baer, 1990; Deichmann, 1992a).

The fault-plane solutions are shown in Figures 1997.3 and 1997.7, and the corresponding parameters are listed in Table 1997.2. The Lötschental earthquake provides, at present, the only known focal mechanism in the Aar Massif. Thus, it is not yet possible to draw any general conclusions about the style of deformation in that region. However, the three focal mechanisms in northern Switzerland presented in this report, are typical of the ENE-WSW oriented ex-
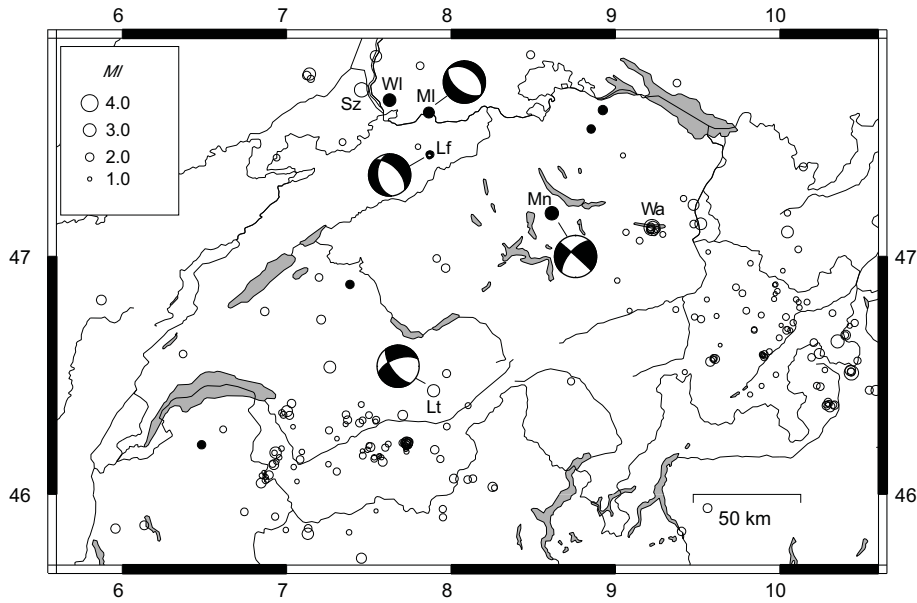
Figure 1997.1: Epicenters and focal mechanisms of earthquakes recorded by the Swiss Seismological Service during 1997. The black symbols correspond to events with focal depths > 15 km. Epicenters of earthquakes mentioned in the text are labeled: Lf = Läufelfingen, Lt = Lötschental, Ml = Möhlin, Mn = Menzingen, Sz = Sierentz, Wa = Walensee, Wl = Weil.
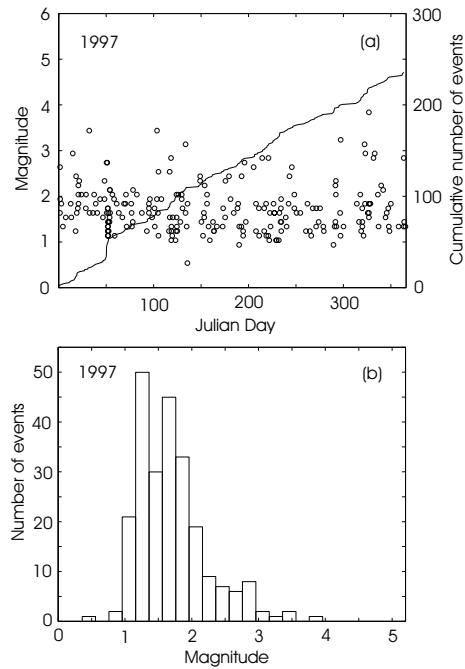

Figure 1997.2: Earthquake activity during 1997: magnitude of each event and cumulative number of events (a); histogram of magnitudes (b).

Date & Time UTC	Lat. [°N]	Lon. [°E]	X / Y [km]	Depth [km]	Mag. [M_L]	Q	Location
1997.01.01 19:56:42	47.214	9.475	754/231	1	2.6	B	Gams, SG
1997.01.15 05:35:10	47.753	7.139	577/289	10	2.9	C	Rhinegraben, F
1997.02.01 14:01:58	47.688	7.456	601/282	10	3.4	C	Sierentz, F
1997.02.19 18:41:56	46.217	7.731	622/118	2	2.7	B	Turtmanntal, VS
1997.02.20 15:39:34	47.826	7.543	608/297	10	2.7	D	Rhinegraben, D
1997.04.12 23:00:00	46.513	10.435	830/156	10	3.4	D	Bormio, I
1997.04.14 13:13:13	46.523	10.429	829/157	10	2.5	D	Bormio, I
1997.04.26 08:24:12	46.214	7.733	623/118	2	2.5	B	Turtmanntal, VS
1997.04.27 17:01:13	46.218	7.729	622/118	1	2.8	B	Turtmanntal, VS
1997.05.13 02:58:42	46.645	10.351	823/170	10	3.1	D	Ofenpass, GR
1997.07.14 02:57:56	45.833	7.129	576/ 76	10	2.7	C	G.S.Bernard, I
1997.07.23 18:15:56	46.352	7.002	566/133	5	2.6	B	Leysin, VD
1997.08.01 20:58:35	46.544	7.269	586/154	10	2.8	B	Gstaadt, BE
1997.08.08 10:54:45	47.135	9.519	758/222	1	2.8	B	Buchs, SG
1997.09.02 00:30:53	47.606	7.861	632/272	23	2.6	A	Möhlin, AG
1997.10.23 12:07:01	47.181	8.624	689/226	30	3.2	A	Menzingen, ZG
1997.11.17 17:09:22	47.639	7.626	614/277	17	3.1	A	Weil, D
1997.11.18 12:23:47	47.134	9.189	733/222	1	2.9	A	Walensee, SG
1997.11.22 04:56:10	47.134	9.189	733/222	1	3.8	A	Walensee, SG
1997.11.27 04:03:47	46.177	6.933	561/114	4	2.7	B	Dents du Midi, VS
1997.11.28 08:30:20	46.437	7.898	635/143	12	2.9	A	Lötschental, VS
1997.12.28 22:52:27	47.101	10.046	798/220	10	2.8	C	Arlberg, A

Table 1997.1: Earthquakes during 1997 with $M_L \geq 2.5$. Locations of the Gstaadt, Möhlin, Menzingen, Weil and Lötschental events are based on 2-D ray-tracing or on additional foreign data. The coordinates of the Walensee events were fixed based on comparisons with the quarry blasts near Quinten (see text).

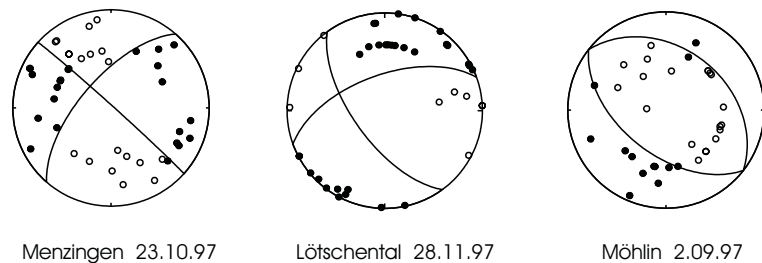Menzingen 23.10.97   Lötschental 28.11.97   Möhlin 2.09.97

Figure 1997.3: Fault-plane solutions (lower hemisphere, equal area projection). Solid circles, compressive first motion (up) and empty circles, dilatational first motion (down).

Location	Date & Time [UTC]	Depth [km]	Mag.	Plane 1 Strike/Dip/Rake	Plane 2	P-Axis Az/Dip	T-Axis
Läufelfingen	1997.02.21 05:04	8	M_L1.8	316/55/-114	174/42/-060	171/69	63/07
Möhlin	1997.09.02 00:30	23	M_L2.6	128/53/-090	308/37/-090	38/82	218/08
Menzingen	1997.10.23 12:07	30	M_L3.2	221/65/-002	312/88/-155	179/19	84/16
Lötschental	1997.11.28 08:30	12	M_L2.9	250/60/-150	144/64/-034	105/41	198/03

Table 1997.2: Focal mechanism parameters 1997.
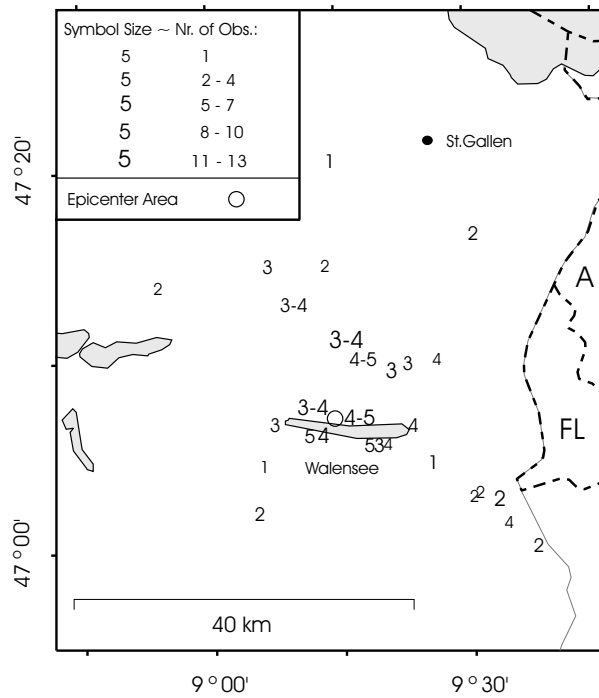
Figure 1997.4: Macroseismic observations of the M_L 3.8 Walensee event of Nov. 22. 1997.

tension common to all earthquakes observed below the northern Alpine foreland (Pavoni, 1987; Deichmann, 1990; Deichmann, 1992b; Baer et al., 1997).

Significant earthquakes of 1997

Walensee

With a magnitude M_L of 3.8, the earthquake which occurred on November 22 at 05:56 local time beneath the north shore of the Walensee, was the strongest event in Switzerland during 1997. It was clearly felt by the residents of Quinten, but the observed intensities decrease rapidly with distance (Fig. 1997.4), which suggests that the source was shallow. This event is actually part of a swarm that has been active intermittently for some time and of which the national network recorded 10 events in 1997 (Table 1997.3). Judging from the similarity of the observed signals (Fig. 1997.5), the hypocenters of all these events must be tightly clustered and the focal mechanisms must be similar. Moreover, also

Date & Time [UT]	Mag. [M_L]
1997.04.10 07:24	1.7
1997.11.18 03:57	1.8
1997.11.18 12:24	2.9
1997.11.22 04:56	3.8
1997.11.22 05:32	1.8
1997.11.22 06:09	1.5
1997.11.22 06:26	1.6
1997.11.22 23:04	1.8
1997.11.23 20:27	1.8
1997.12.29 11:40	1.4

Table 1997.3: Earthquakes near Quinten (Walensee) recorded by the national seismograph network in 1997.

the M_L 2.5 event of October 11, 1996 (Baer et al., 1997, Table 2) is part of this cluster. Whether additional events recorded in previous years also belong to the same cluster remains to be investigated. A temporary three-component digital seismograph was installed a few hundred meters east of Quinten one day after the mainshock. During the week in which this temporary station was in operation, it recorded the aftershock of Nov. 23, which was detected by the national network, as well as numerous weaker events.

Due to the fact that the true seismic velocities associated with the complex 6 km thick sedimentary structure in the Walensee region deviate strongly from the simple regional velocity model adopted in the routine location procedure, it is difficult to obtain a stable and reliable location. Even the temporay station at Quinten did not improve the location accuracy significantly. However, the travel time differences between the P- and S-waves of all the aftershocks observed at this station are less than 0.5 s, so that the radial distance to the source must be less than about 3 km. The three-dimensional particle motion of the P-waves at the temporary station suggest that the source was situated NW of Quinten. However, due to the steep topography all along the E-W trending northern shore of the Walensee, it is very likely that the rays arriving at the temporary station are deviated by a lateral velocity gradient. Consequently, based on the particle motion alone, the source could be located anywhere inside a NW-SW sector from Quinten.

The strongest constraint on the locations, however, is given by a comparison of the earthquake records with the signals recorded from several explosions in a quarry situated just 2.5 km W of Quinten. Despite the fact that neither the focal mechanisms nor the depths of the earthquakes and the explosions are the same, there is a striking similarity among the corresponding signals (Fig. 1997.6). This similarity together with the fact that the S-wave arrival-time differences seem to be almost the same for all azimuths suggests that the epicenter of the earthquakes must be in the immediate vicinity of the quarry. In an attempt to relocate the earthquakes relative to the quarry, the large timing uncertainties of the weak and emergent arrivals of the explosion signals could be reduced by performing a cross-correlation in the time domain between the signals of one of the explosions and the first foreshock. Then, with the relative arrival times obtained from the cross-correlation the relocation was performed using a linearized master event location procedure (Console and DiGiovambattista, 1987) and a realistic velocity structure that accounts for the sedimentary layers
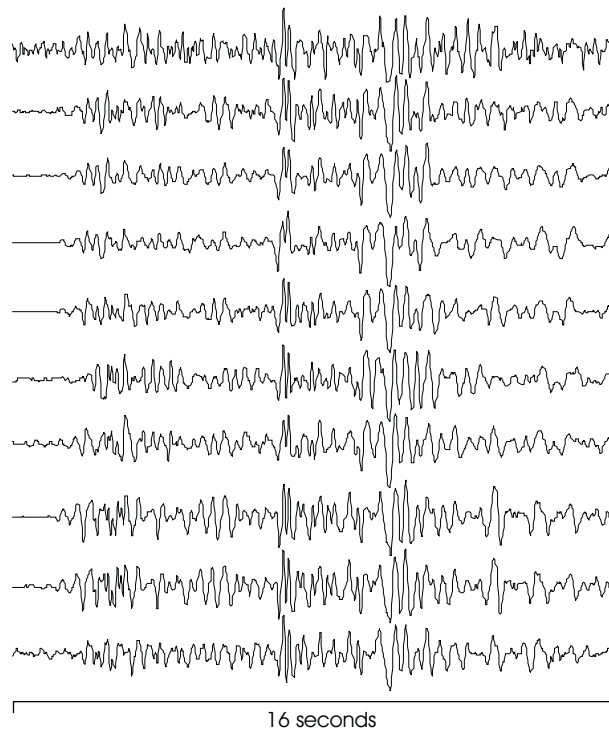
16 seconds

Figure 1997.5: Seismograms of the 1997 Walensee events recorded at station WIL (vertical component), as listed in Table 3 (from top to bottom).

overlying the crystalline basement. Even allowing for the remaining timing uncertainties due to ambiguities in the correlation, the earthquake hypocenters seem be located 1 - 2 km below and within about 0.5 km horizontally from the quarry.

Because of the shallow hypocenter and the complex geologic structure in the source region, the polarity of the P-arrivals beyond an epicentral distance of about 100 km can not be determined with sufficient confidence to construct a reliable fault-plane solution. Further efforts to correctly model the take-off angles at the source might at least constrain the focal mechanism type. This would then allow one to address the question of whether the location of the Walensee earthquakes so close to the quarry of Quinten is merely fortuitous or whether the events actually may have been triggered by the mining activity.

Menzingen

With a focal depth of 30 km, the M_L 3.2 earthquake of Menzingen (ZG), which occurred at 14:07 local time on October 23, belongs to a previously known group of lower-crustal events in the area between the lakes of Zürich and Zug. The well-constrained fault-plane solution corresponds to a strike-slip mechanism with a N-S trending P-axis (Fig. 1997.3), in agreement with the other known focal mechanisms in this region (Deichmann, 1992b).
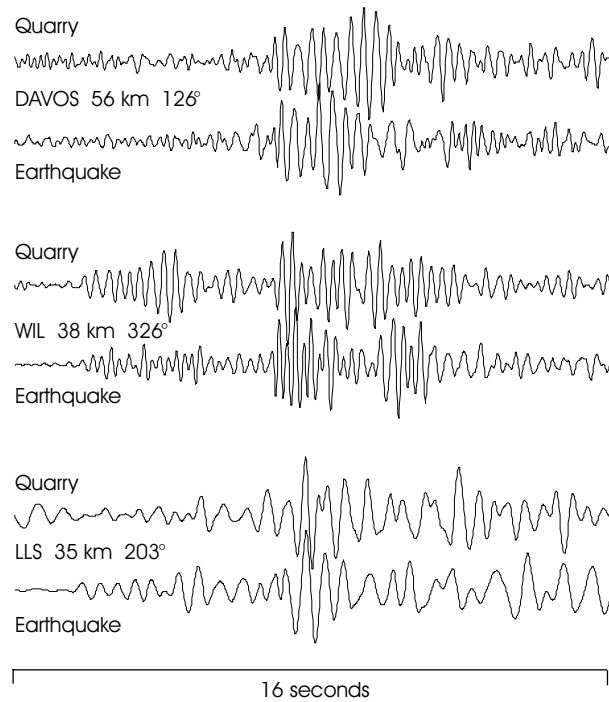
Figure 1997.6: Pairs of seismograms of the explosion of 1997.02.24 in the quarry of Quinten (upper trace) and the M_L 1.8 earthquake of 1997.11.18 recorded at stations DAVOS, WIL and LLS (with epicentral distance and azimuth from the quarry to each station). The signals of DAVOS and WIL are horizontal component records, whereas LLS is a vertical component record. The large amplitude phases in the middle of each trace correspond to the shear and surface waves. The signals of the explosion and the earthquake are plotted with the the same time difference for all three stations. The close match shows that the earthquake source must be located in the immediate vicinity of the quarry.

Lötschental

The hypocenter of the M_L 2.9 earthquake that occurred on November 28 at 09:30 local time, about 3 km east of Fafleralp in the Lötschental, was located at a depth of about 12 km below the southern margin of the Aar Massif. Unfortunately, the first arrivals at the more distant stations to the southwest are unclear and inconsistent, so that the fault-plane solution is not well constrained. Thus the range of focal mechanisms compatible with the available first-motion polarities alone ranges from almost pure strike-slip to a normal fault with a transcurrent component. However, the chosen solution (Fig. 1997.3 and Table 1997.2), which exhibits a strong normal-faulting component with a NNE-SSW trending T-axis, is also in agreement, at least in a qualitative way, with the relative P- and S-wave amplitudes of the observed seismograms. An M_L 3.5 earthquake occurred at almost the same location in 1986, but the focal mechanism of this earlier event still remains to be evaluated.

Möhlin

On September 2 at 02:30 local time, a magnitude M_L 2.6 earthquake occurred just north of the Rhine near the town of Möhlin. Despite its low magnitude and a relatively large focal depth (23km), it is, together with the events of Sierentz and Weil (Table 1997.1), one of three earthquakes that were felt in the Basel area during 1997. The focal mechanism of this event is well constrained and corresponds to a pure normal fault (Fig. 1997.3).

Läufelfingen Cluster

The seismic activity below the Jura Mountains southeast of Basel is known to occur in a swarm-like fashion: a significant fraction of the earthquakes tend to occur tightly clustered in space and time. The signals of the individual events in such earthquake clusters usually show a high degree of similarity, which is an indication of a common focal mechanism, and the hypocenters tend to lie on a plane which coincides with one of the nodal planes of the fault-plane solution (Deichmann, 1990). The 14 events, ranging in magnitude between 1.1 and 1.8, which occurred on February 21 at a depth of 7 - 8 km below Läufelfingen, (Table 1997.4) are a typical example of this behaviour.

Because of the low magnitude of these events, the number of usable signals is insufficient for the construction of a unique fault-plane solution based on first-motion polarities alone. However, the relative amplitudes of the P- and S-waves in the observed seismograms show large variations, depending on how close the corresponding take-off angles of the rays at the source are to a nodal plane. Thus, of all the possible fault-plane solutions, the one shown in Figure 1997.7 is the only one which is consistent, at least in a qualitative way, with the character of the observed signals. Based on the results of a high-precision master-event location technique using waveform cross-correlations (Deichmann and Garcia-Fernandez, 1992), the individual hypocenters of this cluster lie on a NNW-SSE striking plane that is almost coincident with the NW-SE striking nodal plane of the focal mechanism (Fig. 1997.7).

The routinely calculated location of this earthquake cluster practically coincides with the location of a larger swarm that occurred in April 1987 (Deichmann and Garcia-Fernandez, 1992). Indeed, applying the above mentioned relative location technique to the master events of the two clusters shows that the 1997 cluster was located about 250 m below and 300 m north of the 1987

Date & Time [UT]	Mag. [M_L]	
1997.02.21 00:50	1.7	M
1997.02.21 02:29	1.1	R
1997.02.21 02:55	1.2	R
1997.02.21 03:28	1.3	R
1997.02.21 05:04	1.8	R
1997.02.21 05:48	1.4	R
1997.02.21 07:02	1.1	R
1997.02.21 08:17	1.3	
1997.02.21 09:05	1.2	R
1997.02.21 09:38	1.2	
1997.02.21 10:58	1.2	
1997.02.21 11:56	1.4	
1997.02.21 13:36	1.1	R
1997.02.21 18:43	1.6	

Table 1997.4: The 1997 earthquake sequence of Läufelfingen. M = master event for relative location; R = relocated events.
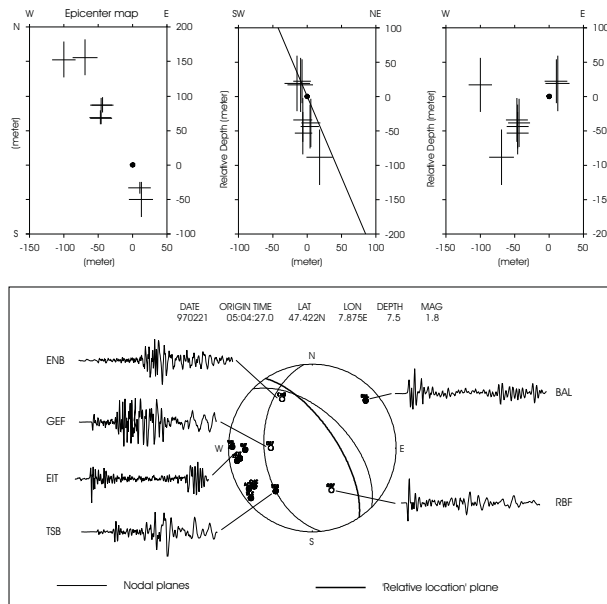
Figure 1997.7: The Läufelfingen swarm of February 21, 1997. Bottom: fault-plane solution of the best recorded event with selected seismograms illustrating the dependence of the signal character on the proximity to the nodal planes. Top: locations of the individual events (crosses) relative to the master event (black dot). Left: epicenter map; middle: SW-NE cross-section with trace of the inferred fault plane (bold curve in the fault-plane solution shown below); right: W-E cross-section. The size of each cross corresponds to one standard deviation of the location.

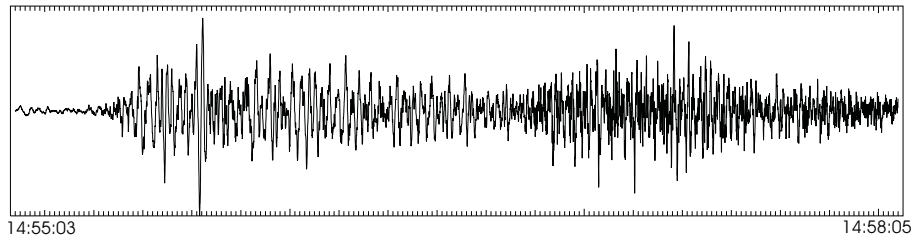14:55:03   14:58:05

Figure 1997.8: Vertical component of ground velocity caused by the rock and ice avalanche off the E face of Montblanc, recorded at station Vieux Emosson (EMV) on January 18, 1997.

cluster. However, it is interesting to note that, whereas in 1997 slip occurred on a normal fault striking roughly NW-SE with a dip of about 60°, the main part of the 1987 cluster occurred as left-lateral slip on an almost vertical and more or less N-S striking fault.

Landslides and rock avalanches

Montblanc

At 14:55 local time on January 18th, a rock mass of roughly 1.5 Mio m^3 broke off from the Brenva face of the Montblanc and fell onto the underlying Brenva Glacier. There it entrained large quantities of snow, thus triggering a massive avalanche of snow and ice mixed with rock fragments, that swept across the lower parts of a ski run of Courmayeur, killing two skiers (Keusen, 1997). The seismic signals associated with this event were recorded by almost the entire seismograph network of Switzerland. The amplitudes of the signals correspond to an M_L 2.2 earthquake and the total signal duration is about 3 minutes. On the records observed at the stations located at Emosson, VS, at a distance of about 25 km (Fig. 1997.8), one can clearly identify a first low-frequency phase, followed 1.5 minutes later by a second phase with higher frequencies. These two distinct phases in the signals are presumably associated with the avalanche first hitting the relatively flat part of the Brenva Glacier at the foot of the mountain and then later continuing down the steeper lower part of the glacier towards the valley floor.

Aiguille du Petit Dru

In the middle of the night at 01:23 local time of Sept. 18th, another rock avalanche in the Montblanc massif broke loose from the west face of the Aguille du Petit Dru. Again the seismic signals associated with this event were recorded by the entire Swiss seismograph network and correspond to an M_L 2.4 earthquake. Ten days later, on Sept. 28th, 17:52 local time, a second smaller rock avalanche occurred in the same location and generated signals corresponding to an M_L 1.6 event.

Zuetribistock

Already in 1996, several massive Landslides broke loose from the southeast face of the Zuetribistock, south of Linthal, GL, and buried part of the Sandalp under

tens of meters of debris. The largest of these events produced seismic signals equivalent to a magnitude M_L 2.8 (Baer et al., 1997). In 1997, the mountain continued to discharge rock avalanches of various sizes. The seismic signals of two of these rock avalanches (1997.09.24 16:49 and 1997.09.27 10:00 local time) were recorded by the seismographs installed near the Linth-Limmern dam 3 km away. However, at all other stations, the signals were two weak to emerge significantly above the background noise, indicating that these events were much smaller than those of the previous year.

Seismic activity during 1998

Overview

During 1998, the Swiss Seismological Service detected and located 227 earthquakes in the region shown in Figure 1998.1. Based on such criteria as the time of occurrence, the location, the signal character or direct information, 55 additional seismic events were identified as quarry blasts. As discussed in more detail below, the network also recorded several landslides or rock avalanches.

Routinely calculated focal depths range between 0 and 31 km, but only 11 hypocenters are located at depths greater than 14 km. One of these deeper events (1998.04.26 12.43, $M_L = 1.8$) is located 20 km below the Klöntal at the northern edge of the Helveticum, but its location is poorly constrained. The other 10 deep events are all located at depths of at least 20 km in the lower crust beneath the Jura Mountains and Molasse Basin of northern Switzerland. The hypocentral locations of the earthquakes observed in 1998 thus confirm once again the focal depth distribution documented in previous studies (Deichmann & Baer, 1990; Deichmann, 1992a).

Magnitude values of the events recorded in 1998 range between $M_L = 0.8$ and 3.6 (Fig. 1998.2). The events with $M_L \geq 2.5$ are listed in Table 1998.1. Where available, the epicentral coordinates and focal depths given in Table 1998.1 are based on the results that include additional data from foreign networks and on 2-D ray-tracing.

Averaged over the last 24 years, the seismic activity is equivalent to 24 events with $M_L \geq 2.5$ and at least one event with $M_L \geq 4$ per year. The strongest events in this time span are the two magnitude 5 events of 1990 near Vaz, Graubünden, and of 1996 near Annecy, France. Thus, with only 18 earthquakes having an $M_L \geq 2.5$ and without a single event with $M_L > 3.6$, the seismic activity in 1998 was below average both in terms of number of events and in terms of magnitude.

In agreement with longterm observations, most of the earthquakes occurred in the Valais and in Graubünden. In addition, however, the year 1998 saw a remarkable concentration of activity in the area of the Walensee and in the Rhine Valley bordering on Liechtenstein. It is also noteworthy that 20 % of the seismic events recorded in 1998 occurred in the two swarmlike earthquake clusters of Walenstadt and Grimentz.

The fault-plane solutions with first-motion directions are shown in Figure 1998.3 and the corresponding parameters are listed in Table 1998.2.
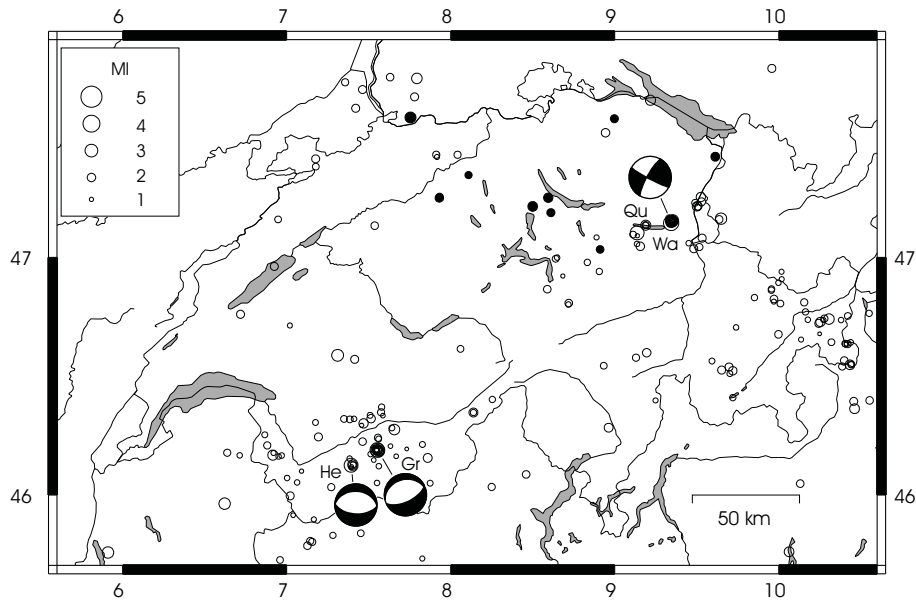
Figure 1998.1: Epicenters and focal mechanisms of earthquakes recorded by the Swiss Seismological Service during 1998. The black symbols correspond to events with focal depths ≥ 20 km. The focal depths of all other events are < 15 km. Epicenters of earthquakes mentioned in the text are labeled: He = Val d'Hérémence, Gr = Grimentz, Qu = Quinten, Wa = Walenstadt.
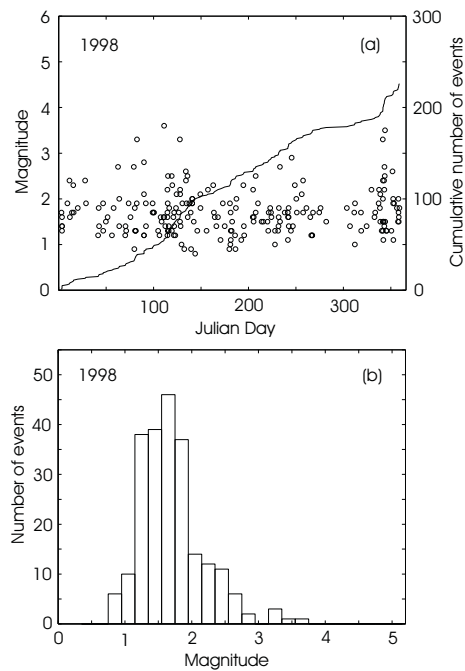

Figure 1998.2: Earthquake activity during 1998: magnitude of each event and cumulative number of events (a); histogram of magnitudes (b).

Date & Time UTC	Lat. [°N]	Lon. [°E]	X / Y [km]	Depth [km]	Mag. [M_L]	Q	Location
1998.03.03 13:52:35	45.755	5.911	481/ 68	10	2.7	D	Haute Savoye, F
1998.03.20 03:11:42	47.161	9.648	767/226	4	2.7	B	Vorarlberg, A
1998.03.23 13:07:18	47.102	9.137	729/218	5	3.3	B	Kerenzerberg, GL
1998.03.30 20:48:59	46.590	7.311	590/160	12	2.8	B	Jaunpass, FR
1998.04.21 02:30:56	47.143	9.344	744/223	10	3.6	A	Walenstadt, SG
1998.04.25 04:17:20	47.741	7.794	627/288	10	2.5	C	Dinkelberg, D
1998.04.29 03:40:18	46.742	10.306	819/181	10	2.5	C	S-charl, GR
1998.05.07 17:16:43	46.126	7.393	596/108	6	3.3	A	Val d'Heremence, VS
1998.05.14 00:25:19	47.150	9.347	745/224	10	2.6	A	Walenstadt, SG
1998.05.15 17:33:35	46.277	7.657	617/125	3	2.5	B	Oberems, VS
1998.07.26 12:46:39	47.152	9.351	745/224	10	2.5	A	Walenstadt, SG
1998.08.21 04:19:56	47.154	9.354	745/224	10	2.7	A	Walenstadt, SG
1998.09.02 12:51:33	47.150	9.347	745/224	10	2.9	A	Walenstadt, SG
1998.12.07 13:46:25	46.189	7.556	609/115	4	3.3	A	Grimentz, VS
1998.12.09 08:56:02	45.963	6.622	537/ 90	5	2.7	C	Col de Balme, F
1998.12.09 13:49:47	46.187	7.559	609/115	4	2.5	A	Grimentz, VS
1998.12.09 22:08:14	46.191	7.552	609/115	4	3.4	A	Grimentz, VS
1998.12.17 19:36:23	47.580	7.755	624/270	25	2.6	A	Rheinfelden, D

Table 1998.1: Earthquakes with $M_L \geq 2.5$ during 1998. The focal depths of the earthquakes of Walenstadt, Val d'Hérémence and Grimentz are based on 2-D ray-tracing. The depth of the Rheinfelden event is well constrained by stations close to the epicenter. All other focal depths are poorly constrained.

Location	Date & Time [UTC]	Depth [km]	Mag.	Plane 1 Strike/Dip/Rake	Plane 2 Strike/Dip/Rake	P-Axis Az/Dip	T-Axis Az/Dip
Walenstadt	1998.04.21 02:30	10	$M_L 3.6$	209/78/ 006	118/84/ 168	164/04	73/13
Val d'Hérémence	1998.05.07 17:16	6	$M_L 3.3$	92/55/-090	272/35/-090	2/80	182/10
Grimentz	1998.12.09 22:08	4	$M_L 3.4$	256/28/-080	65/62/-095	323/72	159/17

Table 1998.2: Focal mechanism parameters 1998.

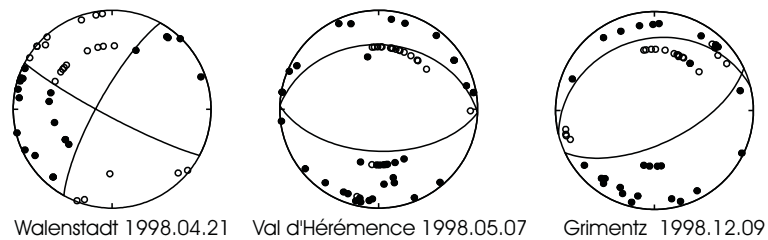Walenstadt 1998.04.21   Val d'Hérémence 1998.05.07   Grimentz 1998.12.09

Figure 1998.3: Fault-plane solutions (lower hemisphere, equal area projection). Solid circles, compressive first motion (up) and empty circles, dilatational first motion (down).
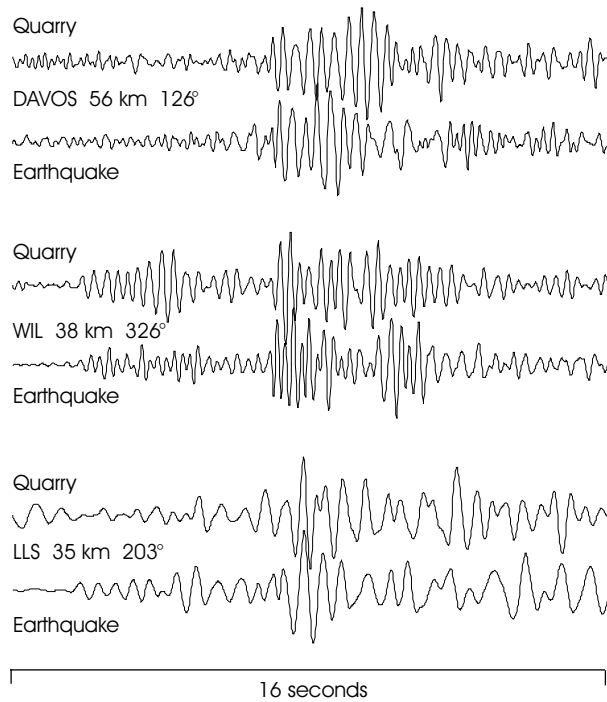
Figure 1998.4: Pairs of seismograms of the explosion of 1997.02.24 in the quarry of Quinten (upper trace) and the M_L 1.8 earthquake of 1997.11.18 recorded at stations DAVOS, WIL and LLS (with epicentral distance and azimuth from the quarry to each station). The signals of DAVOS and WIL are horizontal component records, whereas LLS is a vertical component record. The large amplitude phases in the middle of each trace correspond to the shear and surface waves. The signals of the explosion and the earthquake are plotted with the the same time difference for all three stations. The close match shows that the earthquake source must be located in the immediate vicinity of the quarry.
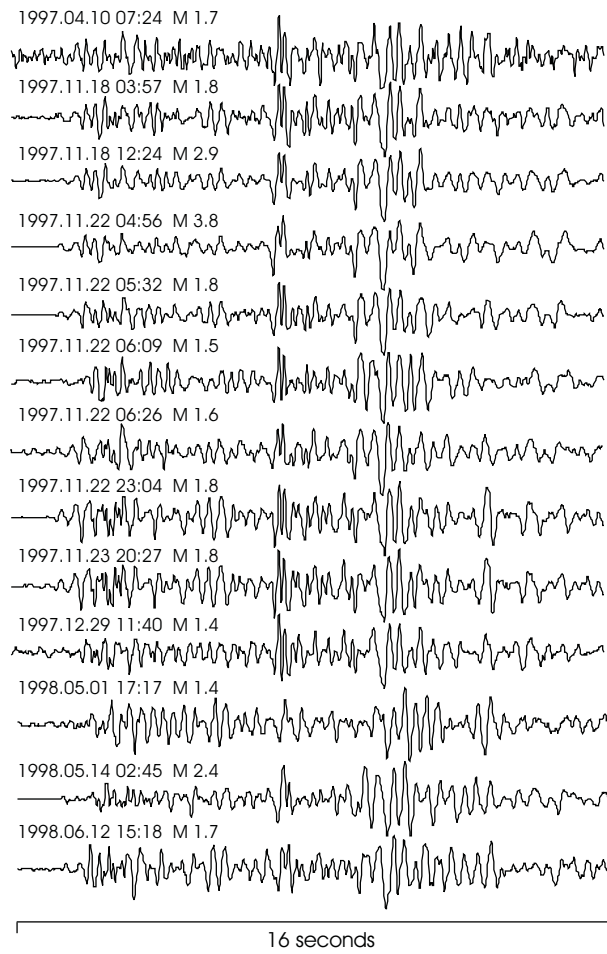
Figure 1998.5: Seismograms of the 1997 and 1998 Walensee events recorded at station WIL (vertical component).
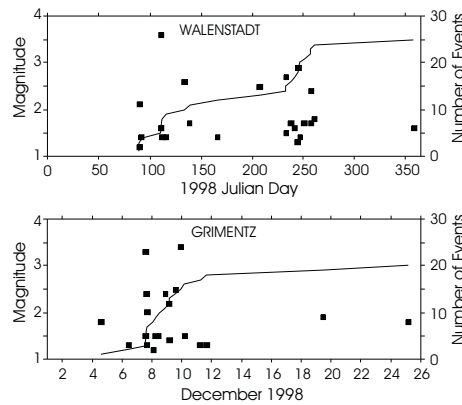

Figure 1998.6: Magnitude (black squares) and cumulative number of events (continuous line) as a function of time for the Walenstadt and Grimentz earthquake swarms.

Significant earthquakes of 1998

Walensee

Already in 1997, the Walensee region was the site of enhanced seismic activity with a series of events that included an $M_L = 3.8$ earthquake. As illustrated in Figure 1998.4, these earthquakes must have been located at a shallow depth below the quarry of Quinten (Deichmann et al. 1998). Of all the earthquakes that occurred in the area of the Walensee in 1998, three produced signals that are sufficiently similar to those observed in 1997 (Fig. 1998.5) to conclude that the same source continues to remain active.

However, in 1998, the two strongest events occurred in the Kerenzerberg area, at the SW end of the lake (1998.03.23 14:07, local time, with $M_L = 3.3$) and near Walenstadt, at the NE end (1998.04.21 04:30, local time, with $M_L = 3.6$). While the Kerenzerberg event was followed three months later by two possible aftershocks, the Walenstadt earthquake was part of a series of 25 events lasting from the end of March to the end of December. The irregular distribution in time of both the number of events and their magnitudes shown in Figure 1998.6 is typical of swarm-like behaviour as opposed to a classical mainshock-aftershock sequence. Moreover, judging from the routinely computed locations as well as from the high degree of signal similarity between the individual events, the Walenstadt series must form a tight cluster of nearly colocated hypocenters. With the closest station at an epicentral distance of 12 km and clear PmP and Pn arrivals at several stations, the focal depth of 10 km is sufficiently well constrained to conclude that these earthquakes occurred in the basement rather than in the thick sedimentary cover in this region. The fault-plane solution corresponds to a nearly pure strike-slip mechanism with a NNW-SSE striking P-axis (Fig. 1998.3). The orientation of the P- and T-axes of the strike-slip focal mechanism of the Walenstadt series is in general agreement with other known focal mechanisms in this area (Roth et al. 1992).

Val d'Hérémence

The epicenter of the Val d'Hérémence earthquake, which occurred on May 7 at 19:17 local time, was located 5 km N of the Grande Dixence Dam. With a magnitude $M_L = 3.4$ and a focal depth of only 5-6 km, it triggered both the accelerometers in the dam and the free-field accelerometers in Sion. It was followed by five aftershocks with magnitudes decreasing from $M_L = 2.2$ to $M_L = 0.9$. The first three aftershocks occurred within a day after the mainshock, while the last two occurred five and twelve days later. The focal mechanism corresponds to a pure normal fault with a N-S trending T-Axis (Fig. 1998.3).

Grimentz

In December, a similar swarm-like activity to the one observed north of Walenstadt occurred also near the village of Grimentz, at the southern end of Val d'Anniviers. With a total of 20 events and maximum magnitudes reaching 3.3 and 3.4, the activity in the Grimentz series is comparable to that of the Walenstadt swarm (Fig. 1998.6). However, practically the whole Grimentz sequence took place within a single week, while the one near Walenstadt continued for more than half a year. Again, both the routinely computed locations and the similarity of the observed signals are evidence for a tightly clustered hypocentral distribution. The focal depth obtained from 2-D ray-tracing is 4 km. Such a

relatively shallow focal depth is also suggested by the fact that the two main events were clearly felt by the population (epicentral intensity = IV), despite their moderate magnitudes. The focal mechanism of the strongest event and probably also of the most of the other events in this earthquake sequence corresponds to an almost pure normal fault with a NNW-SSE oriented T-axis (Fig. 1998.3). The normal faulting mechanisms of the Val d'Hérémence and Grimentz earthquakes are typical for the extensional deformation observed in the Penninic domain of the western Swiss Alps (Maurer et al. 1997; Eva et al. 1998).

Landslides

Zuetribistock

Several massive Landslides broke loose from the southeast face of Zuetribistock, south of Linthal, GL, in 1996 and buried part of Sandalp under tens of meters of debris. In the following year, the mountain continued to discharge rock avalanches of various sizes. This activity continued in 1998 with several landslides and numerous smaller rock avalanches. As in the past, some of these events produced seismic signals comparable to small earthquakes: the landslides of March 31st at 09:43 and 11:58 local time were equivalent to earthquakes of magnitude M_L 1.7 and 1.8, whereas the event of May 10th at 06:43 attained M_L 1.5. Additional rock avalanches on May 10th (one at 06:39 and three between 13:46 and 13:49 local time) were recorded mainly by the seismographs installed at the Linth-Limmern dam 3 km away. Thus all of these events were significantly smaller than the main landslide from Zuetribistock in 1996, which was equivalent to a magnitude M_L 2.8 earthquake (Baer et al. 1997).

Seismic activity during 1999

Overview

During 1999, the Swiss Seismological Service detected and located 286 earthquakes in the region shown in Figure 1999.1. Based on such criteria as the time of occurrence, the location, the signal character or direct information, 46 additional seismic events were identified as quarry blasts.

Magnitude values of the events recorded in 1999 range between $M_L = 0.7$ and 4.9 (Fig. 1999.2). The events with $M_L \geq 2.5$ are listed in Tables 1999.1. For several events, epicentral coordinates and focal depths in Table 1999.1 were recalculated using additional data from foreign networks and were checked with 2-D ray-tracing.

Averaged over the last 25 years, the seismic activity is equivalent to 24 events with $M_L \geq 2.5$ and about one event with $M_L \geq 4$ per year. With 27 events with $M_L \geq 2.5$ and with 3 events reaching $M_L > 4$, the seismic activity in 1999 was thus above the average over the last 25 years. The strongest events in this time span are the two magnitude 5 events of 1990 near Vaz, Graubünden, and of 1996 near Annecy, France, as well as the M_L 4.9 earthquake, which occurred near Bormio in 1999.

In agreement with longterm observations, most of the earthquakes during 1999 occurred in the Valais and in Graubünden. A concentration of activity can also be noted in northeastern Switzerland, between the Walensee and the Rhine Valley of Sankt Gallen (Fig. 1999.1). The two M_L 2.5 and 2.7 Fulfirst earthquakes of May 23rd and 24th (Table 1999.1) are part of this activity, most of which occurred between mid May and mid July, 1999 (Fig 1999.2). The magnitudes of the majority of these events are in the range between 1 and 2. Consequently, their signal quality is poor and they are difficult to locate properly. It is thus very likely that in reality they cluster much more tightly than the scatter in Figure 1999.1 implies.

Routinely calculated focal depths range between 0 and 30 km, but, of the 283 earthquakes recorded in 1999, only 6 hypocenters are deeper than 15 km. As in the past, these deep sources are located in the lower crust beneath the Jura Mountains and Molasse Basin of northern Switzerland.

The fault-plane solutions with first-motion directions are shown in Figure 1999.3 and the corresponding parameters are listed in Table 1999.2 together with the results of the moment tensor inversions. In what follows, we present the highlights of the seismic activity observed during 1999.
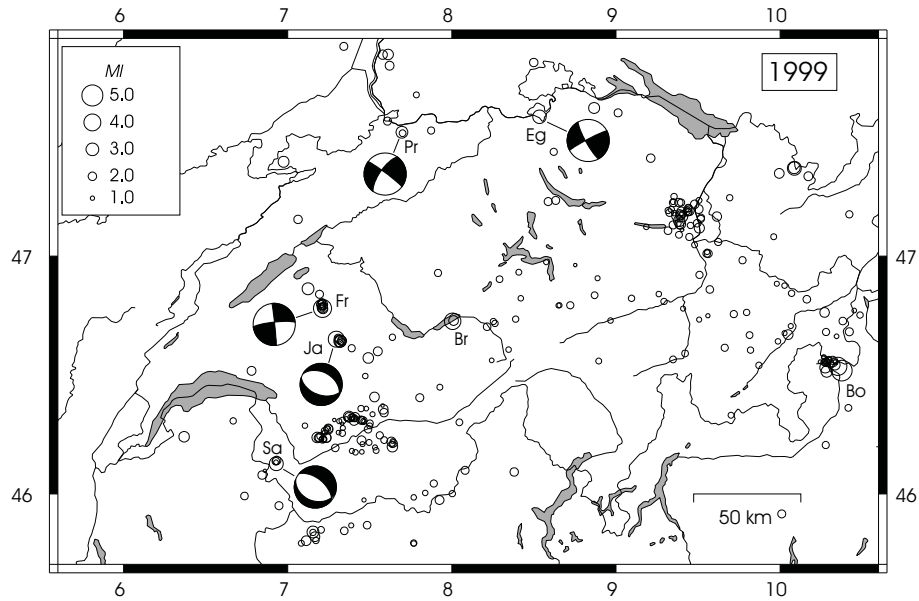
Figure 1999.1: Epicenters and focal mechanisms of earthquakes (based on first-motion polarities) recorded by the Swiss Seismological Service during 1999. Epicenters of earthquakes mentioned in the text are Bormio, Dec. 29 and 31 (Bo), Brienz, May 14 (Br), Eglisau, Sep. 12 (Eg), Fribourg, Feb. 14 (Fr), Jaun, May 20 (Ja), Pratteln, July 13 (Pr) and Lac de Salanfe, Dec. 29 (Sa).
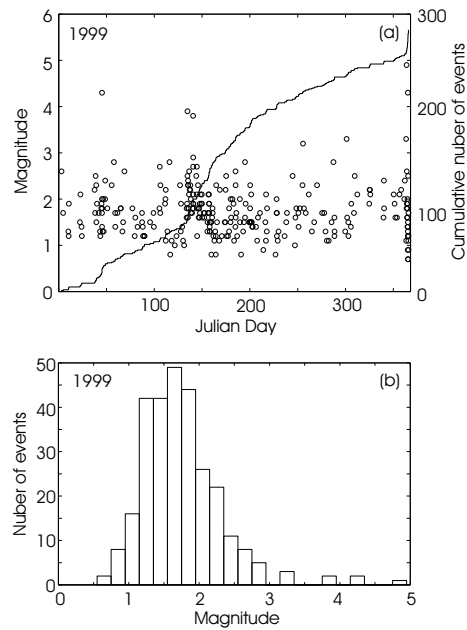

Figure 1999.2: Earthquake activity during 1999: magnitude of each event and cumulative number of events (a); histogram of magnitudes (b).

Date & Time UTC	Lat. [°N]	Lon. [°E]	X / Y [km]	Depth [km]	Mag. [M_L]	Q	Location
1999.01.02 21:01:54	47.392	6.975	565/249	13	2.6	C	Chevenez, JU
1999.02.07 14:51:33	47.834	7.612	613/298	12	2.5	C	Muellheim, D
1999.02.14 05:57:54	46.793	7.215	583/182	2	4.3	A	Fribourg, FR
1999.02.26 19:30:19	46.864	7.124	576/190	10	2.8	B	Courtepin, FR
1999.03.09 18:01:08	47.614	8.867	707/275	25	2.6	B	Huettwilen, TG
1999.04.15 17:19:52	46.517	10.253	816/156	6	2.7	A	Bormio, I
1999.04.25 20:36:47	45.838	7.154	578/ 76	12	2.8	C	G.S.Bernard, I
1999.05.14 15:21:29	46.574	7.491	604/158	6	2.5	B	Zwischenflueh, BE
1999.05.14 18:25:28	46.728	8.005	643/175	7	3.9	B	Brienz, BE
1999.05.16 10:24:06	47.473	10.649	842/263	10	2.6	D	Lechtal, A
1999.05.20 13:11:35	46.655	7.320	591/167	7	3.8	A	Jaun, FR
1999.05.20 15:48:09	46.655	7.320	591/167	7	2.7	A	Jaun, FR
1999.05.20 17:56:41	46.655	7.320	591/167	7	2.9	A	Jaun, FR
1999.05.23 20:53:03	47.134	9.392	748/222	2	2.5	B	Fulfirst, SG
1999.05.24 13:39:49	47.147	9.386	748/223	2	2.7	B	Fulfirst, SG
1999.06.24 03:20:47	46.242	6.369	517/122	12	2.5	C	Chablais, F
1999.07.03 22:40:04	46.327	7.373	595/130	6	2.6	A	Arbaz, VS
1999.07.13 20:47:01	47.514	7.696	619/262	19	2.8	A	Pratteln, BL
1999.09.01 15:54:47	46.239	7.180	580/121	7	2.5	B	Chamoson, VS
1999.09.12 13:25:22	47.578	8.534	682/270	2	3.2	A	Eglisau, ZH
1999.10.14 09:33:41	47.367	10.086	800/249	3	2.8	C	Bregenzerwald, A
1999.10.28 04:54:22	47.365	10.087	800/249	3	3.3	C	Bregenzerwald, A
1999.11.05 14:30:31	46.200	7.638	615/116	6	2.5	B	Zinal, VS
1999.12.29 09:29:29	46.129	6.923	561/109	4	3.3	A	Lac Salanfe, VS
1999.12.29 20:42:33	46.553	10.305	820/160	5	4.9	B	Bormio, I
1999.12.30 03:21:42	46.530	10.306	820/157	5	2.6	B	Bormio, I
1999.12.31 04:55:53	46.554	10.321	821/160	5	4.3	B	Bormio, I
1999.12.31 15:01:55	46.559	10.320	821/160	5	2.5	B	Bormio, I

Table 1999.1: Earthquakes with $M_L \geq 2.5$ during 1999. The focal depths of the earthquakes of Fribourg, Jaun, Pratteln, Eglisau, Lac de Salanfe and Bormio are based on 2-D ray-tracing or on additional data from foreign networks.

Location	Date & Time [UTC]	Depth [km]	Mag.	Plane 1 Strike/Dip/Rake	Plane 2	P-Axis Az/Dip	T-Axis
Fribourg	1999.02.14 05:58	2	M_L4.3	354/88/ 009	264/81/ 178	129/05	219/08
		4	M_w4.0	180/81/-005	270/85/-171	135/10	45/03
Jaun	1999.05.20 13:11	7	M_L3.8	300/42/-082	109/49/-097	326/84	204/03
		4	M_w3.5	325/40/-064	113/55/-110	333/72	217/08
Pratteln	1999.07.13 20:47	19	M_L2.7	215/70/-005	307/85/-160	173/17	79/11
Eglisau	1999.09.12 13:25	2	M_L3.1	151/80/ 175	242/85/ 010	16/03	107/11
Lac de Salanfe	1999.12.29 09:29	4	M_L3.3	111/34/-105	309/57/-080	249/76	32/11
		4	M_w3.0	117/34/-103	312/57/-081	248/76	36/12

Table 1999.2: Focal mechanism parameters based on first-motion polarities (first line with M_L) and full-waveform inversion (second line with M_w, where available).

Fribourg 1999.02.14   Jaun 1999.05.20   Pratteln 1999.07.13   Eglisau 1999.09.12   Salanfe 1999.12.29
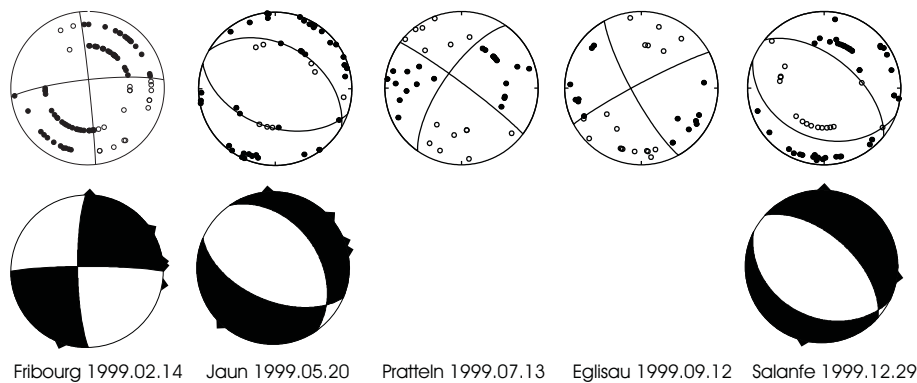
Figure 1999.3: Fault-plane solutions based on first-motion polarities and moment tensors based on full-waveform inversions (lower hemisphere, equal area projection). In the fault-plane solutions (above), solid circles correspond to compressive first motion (up) and empty circles to dilatational first motion (down); on the moment tensors (below), triangles show the station locations.

Significant earthquakes of 1999

Fribourg

Early Sunday morning, February 14th, many inhabitants of northern Switzerland were awakened by an earthquake with epicenter near the town of Marly, 5 km southeast of the city of Fribourg. Although the magnitude, M_L, did not exceed 4.3, the macroseismic intensity in the epicentral area reached $I_0 = V$ (Fig. 1999.4), causing objects to fall off shelves and tables and causing plaster to crack and come off walls. The peak horizontal ground acceleration (PGA) measured by an accelerometer at a station 13 km from the epicenter (SLAE in Laupen, BE) reached 4% g (Spühler, 1999). The routinely calculated focal depth (≈ 15 km) based on a 1D velocity model is not reliable. A first two-dimensional ray-trace modeling of PmP-Pg and Pg-Pn arrival-time differences gave a hypocentral depth of 10 km (Deichmann et al. 2000a). A revision of the ray-trace modeling, using revised crustal velocities and Moho depths suggested a focal depth of 7 ± 3 km, which agrees relatively well with the value of 6 ± 3 km obtained from applying a probabilistic location procedure based on a 3D velocity model (Kastrup et al. 2007). However, the remaining uncertainty did not allow to decide whether this earthquake occurred in the basement or in the overlying sediments. Moreover, the long-period waveforms modelled by the moment-tensor inversion are matched best for a focal depth of 4 km, and the rapid intensity decay with epicentral distance (Fig. 1999.4) would also suggest a shallow source. Synthetic seismogram calculations then showed that travel-time differences between sPmP and PmP observed at some stations in northern Switzerland can only be matched by a much shallower focal depth around 2 km (Kastrup et al. 2007). Since the sPmP - PmP travel-time difference for a given focal depth depends only on the S-wave velocity between the source and the earth's surface, for shallow earthquakes this method constitutes a very strong constraint. Ths result together with the observation that the strong surface waves seen in several seismograms can not be reproduced by synthetic seismograms calculated for a source in the basement constrain the hypocenter of the
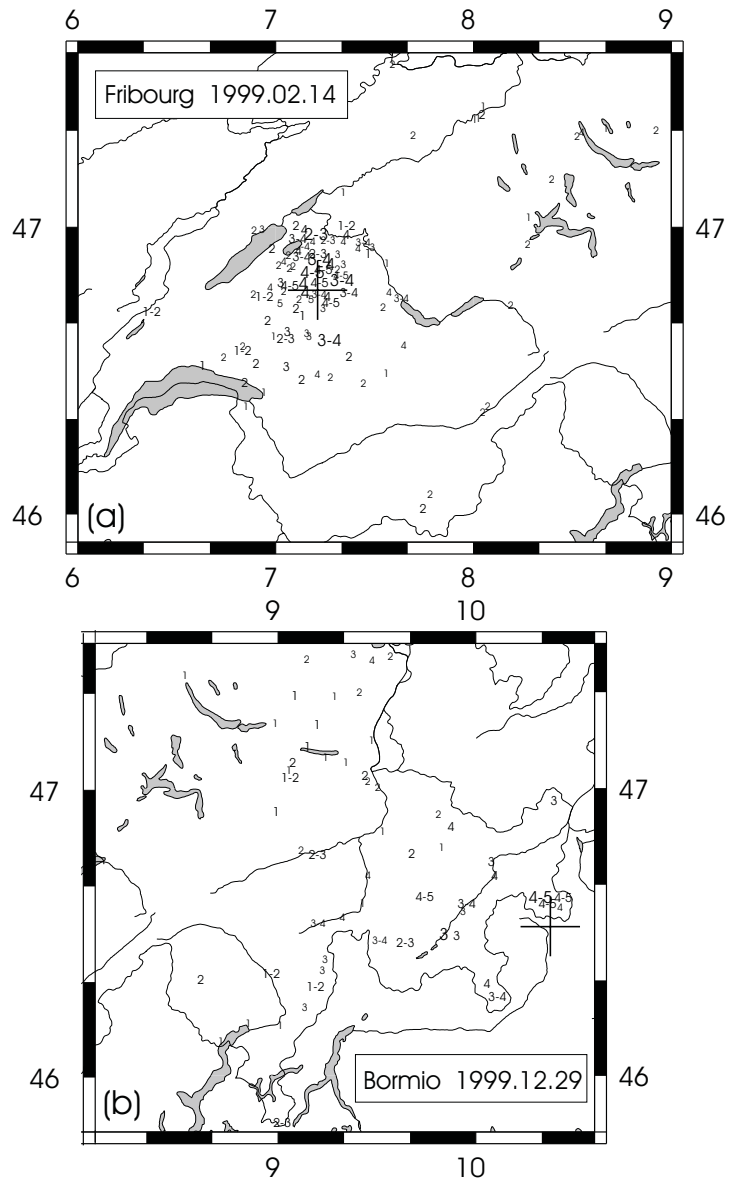
Figure 1999.4: Observed macroseismic intensities (EMS98) for the Feb. 14th, 1999, Fribourg (a) and the Dec. 29th, 1999, Bormio (b) earthquakes.

Fribourg earthquake to lie in the sediments (Kastrup et al. 2007).

The focal mechanisms deduced from first motion polarities and from the full waveform inversion agree very well with each other. Both results show that the earthquake occurred as a strike slip rupture on a roughly N-S or E-W oriented fault plane. The main event was followed by a classical aftershock sequence: four events occurred within two hours of the mainshock and three more over the following 10 days; another small spurt of activity occurred in April with three events and in November with a single one. The magnitudes of these 11 aftershocks range from 1.4 to 2.4.

The 1999 events near Marly are the latest manifestation of an ongoing seismic activity that appears as a N-S trending alignment of epicenters in the region south of Fribourg. This activity includes two earthquakes with M_L of 3.7 and 3.5, that occurred in the Fall of 1995 at practically the same location as the 1999 events, and an M_L 3.9 event in 1987, 3 km further to the South (Kastrup et al. 2007).

Brienz

In the evening of May 14th, the region around Brienz, in the Bernese Oberland, experienced an earthquake with $M_L = 3.9$. The epicenter was located below the Lake of Brienz. The routinely calculated focal depth is 7 km, but the fact that it was felt only in the immediate vicinity of the epicenter suggests that it probably was considerably shallower. A shallow source would be compatible also with the character of the observed seismograms, which feature emergent first arrivals and large surface waves even at short distances.

Jaun

The M_L 3.8 earthquake that occurred on May 20th near Jaun, FR, is the third and strongest of a swarm-like sequence of 9 events recorded between the 15th and 26th of May. Seven of these events actually occurred within a period of only 9 hours on May 20th and included two events with M_L 2.7 and 2.9 in addition to the main event. The magnitudes of the other events range from 1.6 to 2.2. The closest station is located at an epicentral distance of 31 km, so that the routinely calculated focal depths (15 - 19 km) are not reliable. However, in 1987, in the context of a seismic refraction study of the crustal structure below the Helvetic nappes, an explosion was set off at the Jaunpass, located about 5 km south of the epicenter of the 1999 earthquake sequence (Maurer & Ansorge, 1992). Using Pg and PmP arrivals at stations that recorded the 1987 explosion as well as the 1999 earthquakes, it was possible to calibrate the location algorithm and the crustal model for the 2-D ray-tracing and thus to obtain reliable hypocentral parameters (Table 1999.1). With reference to the crustal model of Maurer and Ansorge (1992), the focal depth of 7 km puts the source of this earthquake sequence in the crystalline basement. The fault-plane solution based on first-motion polarities and the moment tensor inversion based on waveform fitting result in a normal-faulting mechanism with a NNE-SSW or NE-SW trending T-axis (Fig. 1999.3 and Table 1999.2).

Pratteln

In the evening of July 13th, Pratteln, near Basel, was the site of an earthquake doublet consisting of an M_L 2.8 event followed 7 minutes later by an M_L 1.6 event with almost identical signal character. The significance of this doublet

lies in the fact that its epicenter coincides with the location of a cluster of earthquakes that has been intermittently active over the years between 1987 and 1993 (Deichmann et al., 2000). Contrary to the earlier earthquakes, which were located at depths of 10 and 12 km, the most recent doublet occurred at a depth of 19 km. The focal depth is well constrained by observations close to the epicenter (minimum epicentral distance 11 km) and by 2-D ray-tracing. There is thus no direct relation between the 1999 doublet and the earlier earthquake cluster. The focal mechanism corresponds to strike-slip motion on either a NW-SE or a NE-SW striking fault plane (Fig. 1999.3). This mechanism is similar to that of two earlier events at 10 and 12 km depth ($M_L = 2.4$ and $M_L = 1.2$). It is, however, rotated by almost 45° relative to the mechanism of the majority of the 10 km deep events, which occurred as left-lateral motion on a vertical N-S striking fault (Faber et al., 1994).

Eglisau

On Sunday afternoon, September 12th, the region north of Zürich was jolted by an earthquake with an M_L of 3.1 and an epicentral intensity, I_0, of IV. The calculated epicenter is situated between Eglisau and Buchberg. This area has seen repeated earthquake activity in the past: between 1705 and 1878, there have been 9 events with $I_0 \geq$ V and, since 1879, 7 events reached an intensity of at least IV (e.g. Rüttener, 1995); in addition, between 1984 and 1991, the Swiss Seismological Service detected 6 events with M_L between 1.0 and 2.1 (Deichmann et al., 2000). At stations in central Switzerland, PmP arrival times of this most recent earthquake are matched best for a focal depth of 4-5 km. On the other hand, the fact that it was felt only out to a distance of about 10 km as well as the observation that many signals are dominated by strong surface waves and that the apparent velocity of the direct Pg wave over the first 80 km is clearly less than 6.0 km/s suggest that the source was shallower. The conclusion that the source is probably close to the surface is also supported by the fact that one of the events with very similar signal character recorded in 1984 was felt in the epicentral area, although the magnitude of that event was only 1.4 (Deichmann et al., 2000). We have therefore fixed the focal depth at 2 km (Table 1999.1). This puts the hypocenter just below the sediment/basement transition; it is, however, equally possible that it was situated in the sedimentary rocks above. The fault-plane solution corresponds to a strike-slip mechanism (Fig. 1999.3 and Table 1999.2). Whereas the data leave room for variation in the dip of the nodal planes, the strike is well constrained. It is important to note that the P- and T-axes are oriented NNE-SSW and WNW-ESE, thus deviating significantly from the NNW-SSE and ENE-WSW directions usually observed in the Alpine foreland and Jura Mountains of northern Switzerland (Deichmann et al., 2000).

Lac de Salanfe

The M_L 3.3 event, which occurred in the morning of Dec. 29th near Lac de Salanfe, is particularly interesting, because its epicenter is located in the SW corner of the Valais, where seismic activity has been observed before but reliable focal mechanisms have not been available previously. The epicentral location and focal depth (4 km) are well constrained by the P- and S-arrivals observed at the accelerographs of the Emosson hydroelectric dam situated at a distance of only 7 km. The focal mechanisms based on first-motion polarities and on the full-waveform inversion are practically identical and correspond to a normal

faulting mechanism with a T-axis oriented in a direction between NNE-SSW and NE-SW. Although the T-Axis is rotated somewhat compared to the usually observed N-S orientation, the normal faulting mechanism constitutes a confirmation of the presently predominant extensional deformation in the Penninic nappes of the southern Valais (Maurer et al., 1997; Eva et al., 1998).

Bormio

The strongest earthquake of the year 1999 in and around Switzerland occurred at 21:42 local time on Dec. 29th just accross the border between Val Müstair and Bormio, Italy. With $M_L = 4.9$, it reached an epicentral intensity of IV-V and was felt throughout eastern Switzerland as well as in adjacent regions of Italy and Austria (Fig. 1999.4). Peak free-field accelerations on hard rock at a distance of 11 km near the Punt dal Gall hydroelectric dam reached 1 % g, while 9 % g was measured at one site close to the crest of the dam. In Zernez and Scuol, on soft soil 22 and 27 km away, peak accelerations were about 2 % g. This earthquake was preceded by two smaller events on April 15th ($M_L = 2.6$) and on Dec. 28th ($M_L = 2.4$) and subsequently was followed by vigorous aftershock activity, that continued for several months, with sporadic events still occurring more than half a year later. The strongest aftershock was an M_L 4.3 event in the early morning of Dec. 31st. Due this sequence's location at the perifery of the Swiss network, routinely determined epicenters and in particular focal depths are poorly constrained. Integration of the Swiss data with those of the Italian Istituto Nazionale di Geofisica, which operates a short period station (BR9) about 10 km SW of the epicentral area, is still underway. The hypocentral parameters in Table 1999.1 include the available arrival times from station BR9 and from the accelerographs at the Punt Dal Gall dam, but are preliminary, pending a complete analysis of all data. First results of moment tensor inversions and of first-motion fault-plane solutions indicate that this earthquake sequence occurred on a NNW-SSE striking normal fault.

Seismic activity during 2000

Overview

During 2000, the Swiss Seismological Service detected and located 256 earthquakes in the region shown in Figure 2000.1. Based on such criteria as the time of occurrence, the location, the signal character or direct information, 49 additional seismic events were identified as quarry blasts. Magnitude values of the events recorded in 2000 range between $M_L = 0.8$ and 4.2. The events with $M_L \geq 2.5$ are listed in Tables 2000.1. Where available, the epicentral coordinates and focal depths given in Table 2000.1 are based on the results that include additional data from foreign networks and on 2-D ray-tracing.

Averaged over the last 26 years, the number of earthquakes amount to about 24 events with $M_L \geq 2.5$ and about 7 events with $M_L \geq 3$ per year. With 37 events with $M_L \geq 2.5$ and 17 events reaching $M_L \geq 3$, the seismic activity in 2000 was thus above the average over the last 26 years for earthquakes in these magnitude ranges. However, it is important to note that one third of the total number of events and one fourth of the events with $M_L \geq 2.5$ must be attributed to the aftershock sequence of Bormio (Fig. 2000.2).

In addition to the Bormio aftershocks, seismic activity in the year 2000 has been particularly high in the eastern parts Switzerland. As in the past, the Valais was active as well, giving rise to a suggestive rectilinear alignment of epicenters that extends the well-known seismicity of the northern Valais (Maurer et al., 1997) towards the southwest across the Rhone Valley and into France.

Routinely calculated focal depths for the 256 earthquakes recorded in 2000 range between 1 and 23 km, but only 7 of these hypocenters are deeper than 15 km. As in the past (e.g. Deichmann et al. 2000a), these deep sources are located in the lower crust beneath the Jura Mountains and Molasse Basin of northern Switzerland.

The fault-plane solutions with first-motion directions are shown in Figure 2000.3, and the corresponding parameters are listed in Table 2000.2 together with the results of the moment tensor inversions. The focal mechanisms, that could be determined for five events with magnitudes around 3.5 in eastern Switzerland and the adjacent area of Austria, complement the existing focal mechanism data in a region where previously reliable observations had been scarce.

Significant earthquakes of 2000

Bormio

More than one third of all the earthquakes recorded in Switzerland and surroundings during the year 2000 are aftershocks of the $M_L 4.9$ earthquake that occurred on Dec. 29th 1999 on the Swiss-Italian Border between Val Müstair

Date & Time [UTC]	Lat. [°N]	Lon. [°E]	X / Y [km]	Depth [km]	Mag. [M_L]	Q	Location
2000.01.10 05:30:09	46.149	7.389	596/111	9	3.1	A	Euseigne, VS
2000.02.09 16:01:17	46.581	10.318	821/163	5	2.7	B	Bormio, I
2000.02.22 22:45:33	46.851	9.975	793/192	4	3.3	B	Klosters, GR
2000.02.23 04:07:07	47.044	9.501	757/212	7	3.6	A	Bad Ragaz, SG
2000.03.04 15:43:20	47.221	9.480	755/232	3	3.6	B	Buchs, SG
2000.03.26 05:13:30	46.322	7.393	596/130	10	2.9	A	Anzere, VS
2000.03.28 03:09:39	47.385	7.141	578/248	1	2.8	A	Saint Ursanne, JU
2000.03.28 05:29:50	47.386	7.157	579/248	1	3.0	A	Saint Ursanne, JU
2000.03.28 05:33:02	47.366	7.168	580/246	1	3.0	A	Saint Ursanne, JU
2000.04.03 00:28:05	46.551	10.320	821/159	5	2.9	B	Bormio, I
2000.04.06 00:43:18	47.367	7.168	580/246	1	3.2	A	Saint Ursanne, JU
2000.04.06 17:40:37	46.539	10.333	822/158	5	4.2	B	Bormio, I
2000.04.11 12:09:53	46.541	10.313	820/158	5	2.5	B	Bormio, I
2000.04.19 21:06:43	47.333	7.478	603/242	21	2.5	A	Vermes, JU
2000.05.03 19:04:11	45.833	7.160	578/ 76	10	2.5	C	Gr.S.Bernard, I
2000.05.17 05:40:38	46.537	10.323	821/158	5	2.6	B	Bormio, I
2000.05.28 11:22:20	46.534	10.348	823/158	5	3.0	B	Bormio, I
2000.06.03 15:14:10	47.202	10.122	803/231	3	3.8	B	Lech, A
2000.06.03 19:41:35	47.207	10.107	802/232	3	2.7	B	Lech, A
2000.06.09 05:06:06	46.539	10.304	820/158	5	3.2	B	Bormio, I
2000.06.10 05:51:02	47.202	10.114	803/231	3	3.6	B	Lech, A
2000.06.20 06:18:49	47.469	7.786	626/258	18	2.9	A	Sissach, BL
2000.06.20 06:25:33	47.472	7.788	626/258	18	2.6	A	Sissach, BL
2000.06.24 00:24:08	46.541	10.282	818/158	5	2.5	B	Bormio, I
2000.07.10 02:48:47	47.222	7.561	609/230	10	2.9	A	Solothurn, SO
2000.07.29 07:14:19	45.852	9.961	796/ 81	14	3.2	D	Lovere, I
2000.08.13 01:07:03	47.772	8.951	713/292	10	2.5	C	Radolfzell, D
2000.08.17 07:14:08	46.952	8.484	680/201	10	3.0	A	Beckenried, NW
2000.08.19 08:37:25	46.027	6.682	541/ 97	5	3.3	A	Samoëns, F
2000.08.24 04:58:57	47.775	8.957	714/293	10	3.0	C	Radolfzell, D
2000.09.09 02:02:07	47.211	10.121	803/232	3	2.9	B	Lech, A
2000.10.08 22:38:44	46.539	10.341	823/158	5	2.9	B	Bormio, I
2000.10.31 19:10:24	46.759	10.344	822/183	10	2.6	C	S'Charl, GR
2000.11.13 16:30:40	47.218	7.565	610/230	10	3.4	A	Solothurn, SO
2000.11.30 08:34:22	46.574	8.424	676/158	14	2.5	B	Furkapass, UR
2000.12.21 06:30:00	47.134	9.189	733/222	1	2.9	B	Walensee, SG
2000.12.25 10:18:02	46.717	8.963	717/175	9	2.7	B	Trun, GR

Table 2000.1: Earthquakes with $M_L \geq 2.5$ during 2000. The focal depths of the earthquakes for which focal mechanisms have been calculated are based on 2-D ray-tracing or on additional data from foreign networks.
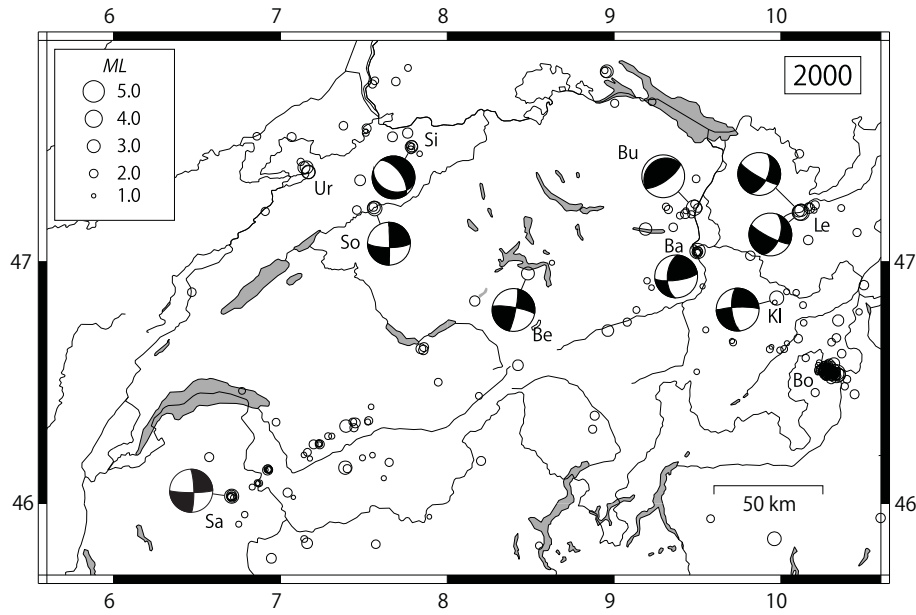
Figure 2000.1: Epicenters and focal mechanisms of earthquakes recorded by the Swiss Seismological Service during 2000. Epicenters of earthquakes mentioned in the text are Bad Ragaz, Feb. 22 (Ba), Beckenried, Jul. 17 (Be), Bormio, all year (Bo), Buchs, Mar. 4 (Bu), Klosters, Feb. 22 (Kl), Lech, Jun. 6 and 10 (Le), Samoëns, Aug. 19 (Sa), Sissach, Jun. 20 (Si), Solothurn, Jul. 10 and Nov. 13 (So), and Saint Ursanne, Mar. 28 and Apr. 6 (Ur). The focal mechanism of the Samoëns main shock is from Delacou et al. (2005).

Location	Date & Time [UTC]	Depth [km]	Mag.	Plane 1 Strike/Dip/Rake	Plane 2	P-Axis Az/Dip	T-Axis
Klosters	2000.02.22 22:46	4	M_L3.3	174/68/-010	268/81/-158	133/22	039/09
		6	M_w3.1	171/89/-009	261/81/-179	126/07	217/06
Bad Ragaz	2000.02.23 04:07	7	M_L3.6	183/56/ 018	083/75/ 145	137/12	038/35
		6	M_w3.1	190/65/ 020	092/72/ 154	142/05	049/31
Buchs	2000.03.04 15:43	3	M_L3.6	235/20/ 090	055/70/ 090	145/25	325/65
		2	M_w3.6	234/17/ 090	054/73/ 090	144/28	324/62
Lech	2000.06.03 15:14	3	M_L3.8	023/57/-012	120/80/-146	347/31	247/15
		6	M_w3.6	019/77/ 007	287/83/ 167	334/04	243/14
Lech	2000.06.10 05:51	3	M_L3.6	019/53/-013	117/80/-142	345/33	243/18
		6	M_w3.4	010/71/ 007	278/83/ 161	326/08	233/18
Sissach	2000.06.20 06:19	18	M_L2.9	111/35/-118	324/60/-072	273/70	041/13
Beckenried	2000.08.17 07:14	10	M_L3.0	280/80/ 172	011/82/ 010	145/01	235/13
		10	M_w2.9	107/86/-172	017/82/-004	332/09	242/03
Samoëns	2000.08.19 08:37	5	M_L3.3	090/83/-170	359/80/-007	315/12	224/02
Solothurn	2000.11.13 16:31	10	M_L3.4	090/75/-178	359/88/-015	313/12	045/09
		10	M_w3.2	275/85/ 164	007/74/ 006	322/07	230/15

Table 2000.2: Focal mechanism parameters based on first-motion polarities (first line with M_L) and full-waveform inversion (second line with M_w, where available). The parameters of the Samoëns main shock are from Delacou et al. (2005).
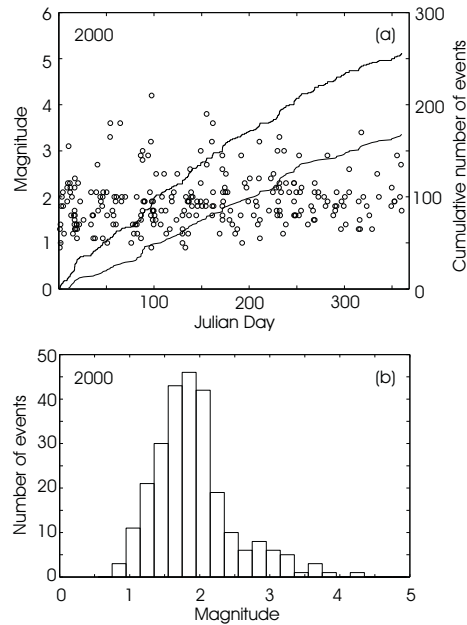
Figure 2000.2: Earthquake activity during 2000: magnitude of each event and cumulative number of events (a); histogram of magnitudes (b). In (a) the upper curve shows the cumulative number of all events, whereas the lower curve corresponds to the number of events without the Bormio aftershocks.

and Bormio. Routine locations of these 88 events cluster in an area of 12×10 km. Being situated at the perifery of the seismic network, the locations are poorly constrained, so that the apparent scatter is certainly larger than the area actually occupied by these events. Among these aftershocks is also an event with $M_L = 4.2$, that occurred on April 6th and that is the strongest event recorded in the year 2000 in Switzerland, as well as 8 other events with magnitudes between $M_L = 2.5$ and 3.2 (Table 2000.1). A comprehensive analysis of the 1999 mainshock and this aftershock sequence is still underway.

Klosters

The February 22nd Klosters earthquake was the first of three events with a magnitude around 3.5 to occur within a period of only 10 days at the beginning of the year in eastern Switzerland. Its epicenter was located about 8 km east of Klosters and the earthquake reached a magnitude M_L of 3.3. The routinely calculated focal depth is 6 km, but the closest station (DAVOS) is 14 km away, so that this value is not well constrained. Travel time differences of PmP-Pg at stations in central Switzerland are matched best for a depth of 4 km. The agreement between the focal mechanism resulting from the first-motion analysis and that from the waveform inversion is not perfect. In addition, neither result is free from internal inconsistencies: three polarities near the nodal planes are mismatched in the faultplane solution and only the transverse components of the seismograms are well modeled by the theoretical waveforms. Nevertheless, a significantly different result from the strike-slip mechanism shown in Figure 2000.3 is not compatible with the observations. Moreover, the NW-SE and NE-SW
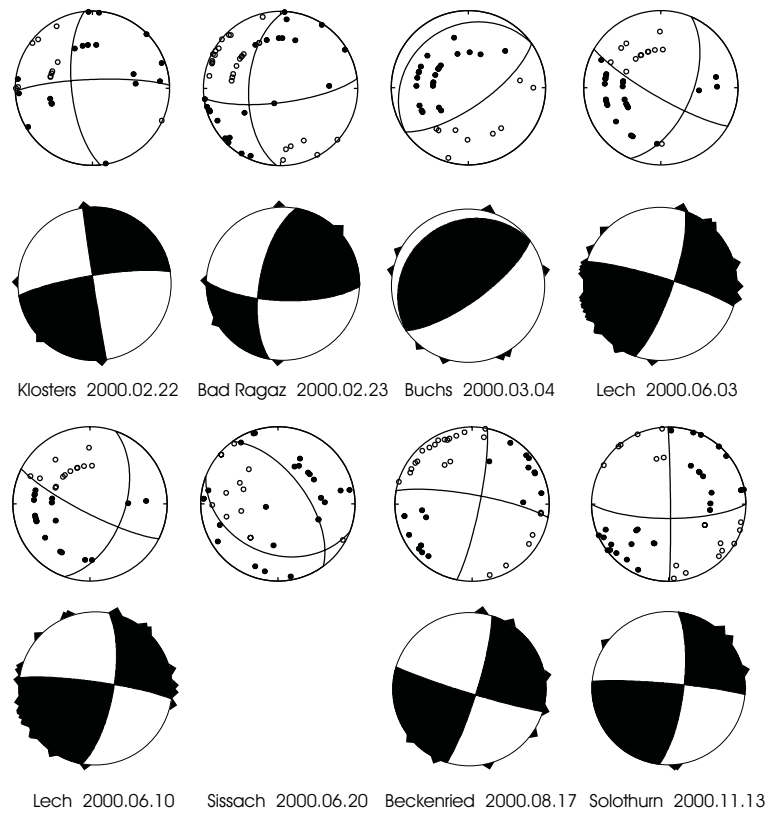
Figure 2000.3: Faultplane solutions based on first-motion polarities and moment tensors based on full-waveform inversions (lower hemisphere, equal area projection). In the fault-plane solutions (above), solid circles correspond to compressive first motion (up) and empty circles to dilatational first motion (down); on the moment tensors (below), triangles show the station locations.

orientation of the P- and T-axes is typical for this region (Roth et al., 1992; Pavoni et al., 1997).

Bad Ragaz

Only 5 hours after the Klosters event, a magnitude M_L 3.6 earthquake occurred below the Fläscherberg, 4 km north of Bad Ragaz. It was well recorded by high-gain stations out to distances of more than 300 km and by six of the local strong-motion stations. This event was associated with one foreshock ($M_L = 2.0$) on January 13th and with five aftershocks ($1.2 \leq M_L \leq 2.2$) distributed over the following eight months. With station MELS at only 9 km from the epicenter, a dense azimuthal station coverage and a good match of the theoretical Pn travel times with the observed arrivals at stations in northern Switzerland, the focal depth of 7 km is well constrained. The impulsive signal character of both P- and S-waves and the clear records even at large distances are an additional qualitative indication that the hypocenter must be located in the crystalline basement below the thick and complex sedimentary sequence known to exist in this region (e.g. Stäuble & Pfiffner 1991). The basically strike-slip mechanism is documented by both the first-motion analysis and by the waveform inversion (Fig. 2000.3). Its orientation is similar to that of the Klosters event.

Buchs

The last of the three earthquakes to jolt eastern Switzerland within 10 days occurred on March 4th. Its epicenter was located about 7 km north of Buchs in the Rhine Valley of Sankt Gallen and its magnitude was 3.6. Although it was possible to improve the azimuthal station coverage by using data from stations DAVA in Austria and UBR in southern Germany, the location is not optimally resolved. At most stations, S-wave travel-time residuals remain very high, so that S-arrivals were not used for the location. Thus also the focal depth is poorly constrained by the routine location procedure. However, the poor match of observed and calculated S-wave travel times suggests that the hypocenter is located in the near-surface sedimentary layers, which are laterally highly heterogeneous in this area and for which the V_p/V_s ratio differs significantly from the standard velocity model used in the location procedure. This conclusion is supported also by the surface-wave dominated signal character observed at several stations, by 2-D ray tracing and by the waveform inversions. In addition, assuming that the hypocenter was located in the crystalline basement requires take-off angles of the rays at the source which lead to an inconsistent distribution of P-wave polarities in the faultplane solution. An assumed focal depth of 2-3 km places the source more or less at mid-depth within the sedimentary sequences in the epicentral region and is consistent with all observations. The resulting focal mechanism corresponds to almost pure thrust faulting (Fig. 2000.3). From the first-motion analysis the strike and dip of the steep nodal plane is well constrained, whereas the strike of the flat nodal plane is not. The preferred solution corresponds to an intermediate result, which also matches the waveform inversion almost perfectly. Although well-constrained thrust-fault mechanisms are rare in Switzerland, some have been found in the uppermost crust of the Helvetic domain in the region of Sarnen (Deichmann et al., 2000b) and in the Walensee area (Roth et al., 1992; Pavoni et al., 1997). The orientation of the P-axis of the Buchs mechanism agrees well with the NW-SE direction of maximum crustal shortening observed in the other focal mechanisms in Figure 2000.3 and deduced from earlier studies (Roth et al., 1992; Pavoni et al., 1997).

Saint Ursanne

During the early morning hours of March 28th, the population of Saint Ursanne were jolted by a series of four earthquakes with magnitudes as high as 3.0. Ten days later, a fifth earthquake with $M_L = 3.2$ occurred at practically the same location. That all five events have almost identical hypocentral locations and focal mechanisms is evidenced by the high similarity of the observed signals. The routine location procedure results in a focal depth of 6-7 km, which corresponds to a source in the upper crystalline crust. However, the seismograms recorded at most stations in northern Switzerland and adjacent regions of France feature exceptionally strong and long-lasting surface wave codas, that are usually only observed from quarry blasts at the Earth's surface. Thus a shallow source within the Mezozoic sedimentary cover of the Jura Mountains is much more likely. Based on this argument, the focal depth given in Table 2000.1 has been fixed to 1 km, but this needs to be verified by a more thorough analysis that is not yet completed.

Lech

Another remarkable series comprising eight earthquakes occurred between the beginning of June and the end of October near the town of Lech, north of the Arlberg Pass in Austria. The two strongest events attained magnitudes M_L of 3.6 and 3.8. Routinely calculated focal depths are poorly constrained. However, based on the same observations and arguments as cited for the Buchs event, all evidence suggests that the hypocenters must be situated in the near-surface sedimentary sequences. The strike-slip focal mechanisms of the two strongest events differ only little from each other (Fig. 2000.3). Both the first-motion analysis and the waveform inversion give subhorizontal, ENE-WSW oriented T-axes, whereas the NNW-SSE oriented P-axes obtained from the first-motion analysis are slightly more inclined than those from the waveform inversion.

Sissach

The two Sissach earthquakes listed in Table 2000.1 are part of a sequence of five events with magnitudes M_L between 1.5 and 2.9, which occurred on June 20th within less than four hours. The focal depth of 18 km obtained from 2-D ray-tracing differs only slightly from the 16 km determined routinely and falls within the depth range of numerous other hypocenters in northwestern Switzerland.

A focal mechanism solution for the strongest event is available only from first-motion analysis and the result is not entirely free of inconsistencies: two mismatched polarities are from observations close to a nodal plane and could be due to mispicks or errors in take-off angle. The third mismatch concerns the positive first-motion polarity in the middle of the dilatational quadrant, observed at station RBF. This station is situated practically at the epicenter and the signals are completely saturated starting right at the first break. The P-onset observed at station RBF for the second event starts with a very slight downward motion before rising as impulsively as for the first event. Considering that the signals recorded at all other stations are practically identical for these two events, it is likely that the mismatched polarity at RBF is a result of instrument malfunction due to severe signal saturation. Despite these inconsistencies, the resulting normal-faulting mechanism is well constrained and the NE-SW orientation of the T-axis is typical for the focal mechanisms observed in northwestern Switzerland (e.g. Deichmann et al., 2000b).
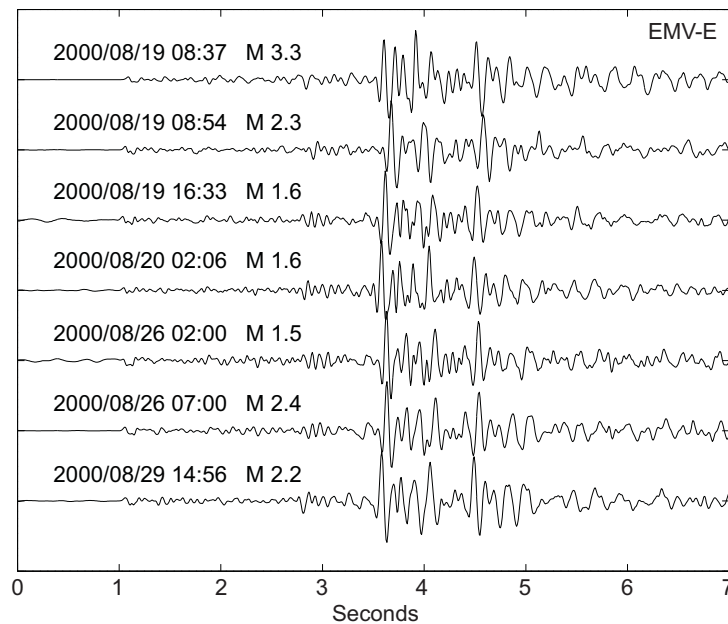
Figure 2000.4: Seismograms of the earthquake sequence of Samoëns recorded at station EMV (E-W component).

The signals are similar enough to determine high-precision relative locations of the hypocenters based on signal cross-correlations only for the first two events. The resulting locations suggest that the SW dipping nodal plane could correspond to the active fault plane, but the results are not entirely unambiguous.

Beckenried

The hypocenter of the M_L 3.0 earthquake, which ocurred on August 17th near Beckenried on the south shore of the Vierwaldstättersee, was located at a depth of about 10-12 km. With three azimuthally well distributed stations at epicentral distances of 10-17 km and with impulsive S-wave arrivals, the location is well constrained. This focal depth places the Beckenried quake with certainty in the crystalline basement, in contrast to most other well-constrained earthquakes in central Switzerland, which are located in the overlying Helvetic Nappes (Deichmann et al., 2000b). However, the orientation of the focal mechanism (strike-slip with NW-SE oriented P-axis, Fig. 2000.3 matches the general deformation direction deduced for central Switzerland from the shallower events (Deichmann et al., 2000b).

Samoëns

The mainshock of the earthquake sequence of Samoëns occurred on August 19th at 08:37 (UTC) with magnitude M_L 3.3. Six additional events with magnitudes between 1.5 and 2.4 and with almost identical signals were recorded during the following 10 days by both the SISMALP network of the University of Grenoble and by the network of the Swiss Seismological Service (Fig. 2000.4). Routine location procedures give a focal depth of 5 km. Given a good azimuthal coverage

and a station at an epicentral distance of only 5 km (OG03), the uncertainty of the calculated focal depth is on the order of ± 2 km.

The faultplane solution of the mainshock (Fig. 2000.1 and Table 2000.2) was constructed using take-off angles calculated by 2-D ray tracing. Given 34 identifiable first-motion polarities with an even azimuthal distribution, the result is a well-constrained strike-slip mechanism with N-S and E-W striking nodal planes and a NW-SE oriented P-axis (Delacou et al. 2005).

The striking waveform similarity of the different events shown in Figure 2000.4 for station EMV and visible also at the other stations demonstrates that the earthquakes in this sequence must all have similar source locations and the same focal mechanism. High-precision relative locations based on signal cross-correlations demonstrate that the hypocenters of the Samoëns cluster define a plane with an orientation that differs only slightly from the E-W striking nodal plane of the faultplane solution (Delacou et al. 2005). Thus, the seismic sequence of Samoëns occurred as dextral slip on a steeply dipping more or less E-W striking fault at a depth of about 5 km. However, according to Delacou et al. (2005), given the remaining hypocentral uncertainty of ± 2 km and the 1.2 km vertical extent of the whole cluster, it is not possible to determine whether the fault is located in the crystalline basement or in the Helvetic cover or whether it intersects the sediment-basement transition.

Solothurn

The magnitude M_L 3.4 earthquake of November 13th occurred 2.5 km north of Solothurn and was clearly felt by the local population. This event was the second one of almost two identical events. The first occurred 4 months earlier on July 10th and had a magnitude of 2.9. A smaller aftershock (M_L 2.0), which occurred on November 15th at the same location, produced slightly different waveforms from those of the other two. The focal depth of about 10 km is constrained by a good azimuthal station coverage and a minimal epicentral distance of only 9 km and by two-dimensional raytracing of the travel-time differences between Pg and PmP at several stations, as well as full waveform modeling. The results of the analysis of the first motion distribution and of the full waveform inversion are practically identical, giving a focal mechanism that is almost pure strike-slip with N-S and E-W oriented nodal planes and with P- and T-axes that reflect the known orientation of the stress field in northern Switzerland (Deichmann et al., 2000b). Attempts to identify the active fault plane by waveform correlations and precise relative locations failed: the hypocenters of the first two events were located practically below each other with a separation of only 50 m, so that within the remaining location uncertainties they could lie on either of the two nodal planes, and the waveforms of the third event did not match those of the previous events closely enough to obtain a sufficient number of usable correlation results.

Non-seismic events

Airplane crash near Zürich Airport

On January 10th, an airplane crashed shortly after take-off from the airport of Zürich. The impact was sufficiently violent to produce a seismic signal that was recorded clearly at station ZLA, 6.37 km away (Fig. 2000.5). As an application of forensic seismology on behalf of the authorities investigating the cause of the
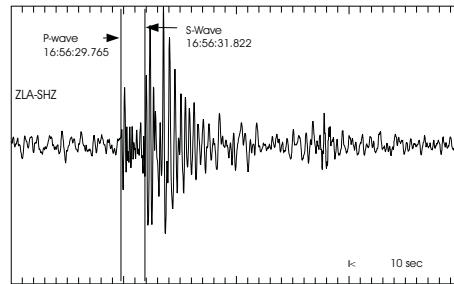
Figure 2000.5: Signal of the airplane crash of January 10th near Zürich airport recorded at station ZLA. Time is UTC.
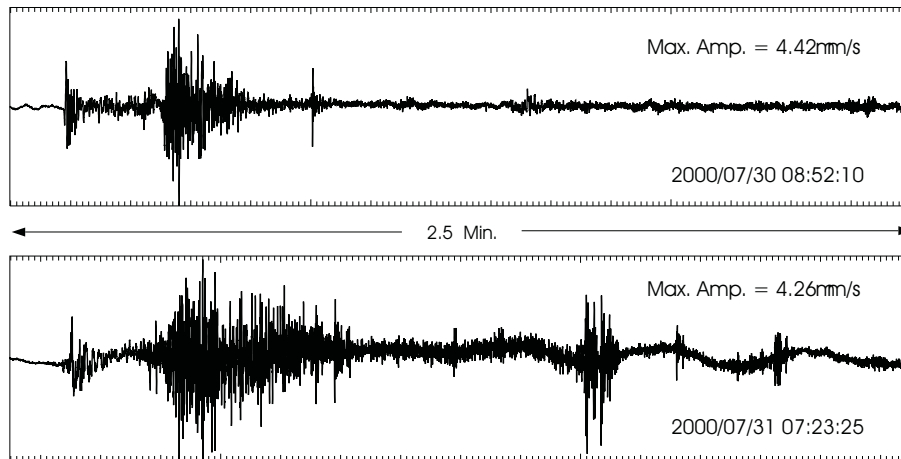

Figure 2000.6: Signals of the two ice avalanches from Allalin Glacier recorded by the E-W component of the broad-band sensor installed in the east buttress of the Mattmark dam (station MMK). Time is local summer time.

accident, the exact time of the impact was determined from the arrival times of the P- and S-waves at ZLA.

Ice avalanches of Allalin Glacier

On July 30th at 8:52 local time, a massive ice avalanche broke loose from the tongue of Allalin Glacier, in the Valais. The next morning at 7:23, an even larger ice mass broke off, the debris of which reached the valley floor close to the west buttress of the Mattmark hydroelectric dam. The total volume of the two ice avalanches was estimated at more than $10^6 \mathrm{m}^3$ (Funk & Bösch, 2001). The vibrations caused by the two avalanches saturated the short-period instruments of station MMK and MMK2, installed at either side of the Mattmark dam, and were clearly recorded by the broad-band sensors located in the east buttress of the dam. These broad-band records provided useful information regarding the exact time and duration of the two events (Fig. 2000.6).
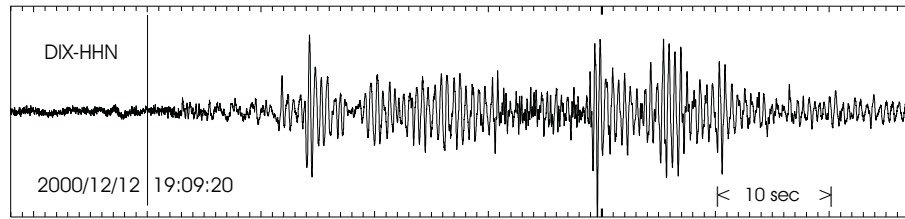
Figure 2000.7: Signal associated with the rupture of the Cleuson-Dixence pressure shaft on December 12th, recorded by the NS component of the broad-band seismometer installed in the east buttress of the Grand Dixence dam (station DIX). Time is UTC.

Rupture of the pressure shaft at Cleuson-Dixence

On December 12th, shortly after shutdown of the turbines at the hydroelectric powerplant of Bieudron, the pressure shaft coming from Lac des Dix ruptured. The volume of water that escaped from the leak was sufficient to trigger a massive landslide, which demolished several cottages and killed three people near the town of Nendaz. Seismic signals associated with this accident were recorded by the seismometers installed at Grande Dixence dam. As can be seen in the seismogram recorded by the N-S component of the broad-band sensor installed in the west buttress of the dam (Fig. 2000.7), the signals lasted for more than a minute and are highly monochromatic, with a dominant frequency of 2 Hz. Given this signal character and a distance of about 15 km from the location of the rupture, the signals recorded at the Grande Dixence dam most likely correspond to the response either of the dam itself or of the hydrodynamic system to a protracted source of vibrations, rather than to the rupture itself or to the ensuing landslide.

Seismic activity during 2001

Overview

During 2001, the Swiss Seismological Service detected and located 382 earthquakes in the region shown in Figure 2001.1. Based on such criteria as the time of occurrence, the location, the signal character or on direct information, 52 additional seismic events were identified as quarry blasts.

Magnitude values of the events recorded in 2001 range between $M_L = 0.4$ and 4.1. The events with $M_L \geq 2.5$ are listed in Table 2001.1. Where available, the epicentral coordinates and focal depths given in Table 2001.1 are based on the results that include additional data from foreign networks and on 2-D ray-tracing.

Averaged over the last 27 years, the number of earthquakes amount to about 25 events with $M_L \geq 2.5$ and about 8 events with $M_L \geq 3$ per year. With 44 events with $M_L \geq 2.5$ and 11 events reaching $M_L \geq 3$, the seismic activity in 2001 was thus above the average over the last 27 years for earthquakes in these magnitude ranges. However, 17 of the 44 events with $M_L \geq 2.5$ are part of the three sequences of Martigny, Val Baone and Bormio.

Figure 2001.2 shows the temporal evolution of seismicity. Even after subtracting the events of the Bormio and Val Baone sequences, activity seems to increase towards the end of the year. This is due to the fact that, as of August 27th 2001, the event detection algorithms operate on the broad-band signals instead of on the old short-period data. With this change, the frequency band is extended to higher frequencies, with the result that the network has become more sensitive to low-magnitude events.

In addition to the Bormio aftershocks, seismic activity in the year 2001 has been particularly high in Canton Graubünden. As in the past, the Valais was active as well, in particular with the sequence of Martigny.

Routinely calculated focal depths for the 382 earthquakes recorded in 2001 range between 1 and 30 km, but only 7 of these hypocenters are deeper than 15 km. As in the past (e.g. Deichmann et al. 2000a), almost all these deep sources are located in the lower crust beneath the Jura Mountains and Molasse Basin of northern Switzerland. The only exception is the source of the Erba event at a depth of more than 20 km beneath the southern margin of the Alps.

The fault-plane solutions with first-motion directions are shown in Figure 2001.3, and the corresponding parameters are listed in Table 2001.2 together with the results of the moment tensor inversions. In what follows, we present the highlights of the seismic activity observed during 2001.

Date & Time UTC	Lat. [°N]	Lon. [°E]	X / Y [km]	Depth [km]	Mag. [M_L]	Q	Location
2001.01.20 15:49:10	45.856	8.142	655/ 78	13	2.6	C	Val Sesia, I
2001.01.25 02:17:15	46.050	6.764	548/100	7	2.9	B	Sixt, F
2001.01.30 03:24:21	47.035	9.506	757/211	9	2.9	A	Bad Ragaz, SG
2001.02.23 22:19:41	46.136	7.031	568/109	6	3.6	A	Martigny, VS
2001.02.25 01:22:30	46.133	7.028	568/109	6	3.5	A	Martigny, VS
2001.02.25 02:07:57	46.136	7.038	568/109	6	2.7	A	Martigny, VS
2001.02.28 09:26:27	46.126	7.021	568/109	6	2.6	A	Martigny, VS
2001.03.14 10:37:18	47.350	9.576	761/246	30	2.9	A	Oberriet, SG
2001.03.16 05:40:36	47.214	10.145	805/233	5	2.8	C	Lech, A
2001.03.17 00:29:59	46.920	9.006	719/198	3	3.8	A	Linthal, GL
2001.03.19 00:31:17	47.308	6.087	498/240	7	2.8	D	Besancon, F
2001.03.19 14:12:13	46.402	9.965	794/142	8	2.6	A	Lago Bianco, GR
2001.03.28 03:42:27	46.333	7.447	601/131	10	2.7	A	Tseuzier, VS
2001.04.06 02:22:52	45.870	9.234	739/ 81	22	3.8	C	Erba, I
2001.04.07 08:11:44	46.142	6.929	561/110	6	2.7	A	Lac Salanfe, VS
2001.04.12 07:06:43	47.620	7.543	608/274	8	2.9	A	Basel-St.Louis, F
2001.05.30 22:43:50	45.825	6.530	529/ 75	10	3.1	C	Haute Savoie, F
2001.06.02 08:12:04	46.892	8.586	687/194	6	2.6	A	Seedorf, UR
2001.06.12 14:54:25	46.364	9.220	737/136	12	2.8	B	San Bernardino, GR
2001.06.12 14:58:31	46.366	9.216	737/136	9	2.6	B	San Bernardino, GR
2001.07.09 22:50:02	46.172	7.626	614/113	6	3.2	B	Ayer, VS
2001.07.17 22:30:16	47.328	6.821	553/242	1	2.6	A	St. Hippolyte, F
2001.07.17 23:20:03	47.328	6.827	554/242	1	2.9	A	St. Hippolyte, F
2001.07.30 17:49:34	46.584	9.796	781/162	9	2.6	B	Albulapass, GR
2001.08.03 03:05:00	46.543	10.318	821/159	5	2.6	B	Bormio, I
2001.08.05 06:04:54	46.078	10.521	838/107	10	2.5	C	Val Baone, I
2001.08.07 21:55:40	47.254	10.432	826/238	10	2.6	C	Lechtal, A
2001.08.15 16:26:24	46.051	10.512	838/104	10	2.8	C	Val Baone, I
2001.08.24 14:37:59	46.056	10.479	835/105	10	3.0	C	Val Baone, I
2001.08.30 02:44:48	46.054	10.475	835/105	10	2.5	C	Val Baone, I
2001.09.04 14:30:05	46.029	10.560	842/102	11	2.8	C	Val Baone, I
2001.09.07 20:57:31	47.246	10.421	826/237	8	2.7	C	Lechtal, A
2001.09.07 21:52:18	47.256	10.416	825/238	10	2.7	C	Lechtal, A
2001.09.22 10:57:04	46.041	10.492	836/103	10	2.6	C	Val Baone, I
2001.10.01 06:36:22	46.547	10.327	821/159	5	4.1	B	Bormio, I
2001.10.01 06:41:22	46.561	10.306	820/161	5	2.8	B	Bormio, I
2001.10.01 07:27:01	46.559	10.309	820/160	5	2.9	B	Bormio, I
2001.10.11 22:47:46	46.699	7.216	583/172	13	2.5	B	Montevraz, FR
2001.10.28 00:09:29	45.765	10.571	844/ 73	10	3.0	D	Lago d'Idro, I
2001.10.30 17:30:22	47.256	10.174	807/237	10	3.1	C	Lech, A
2001.10.30 17:31:32	47.246	10.164	806/236	10	2.9	C	Lech, A
2001.11.05 22:01:26	46.563	10.312	820/161	5	2.5	B	Bormio, I
2001.11.24 18:05:49	46.561	10.255	816/160	5	3.0	B	Bormio, I
2001.12.14 09:52:41	46.530	10.313	820/157	5	2.5	B	Bormio, I

Table 2001.1: Earthquakes with $M_L \geq 2.5$. The focal depths of the earthquakes for which focal mechanisms have been calculated are based on 2-D ray-tracing or on additional data from foreign networks.
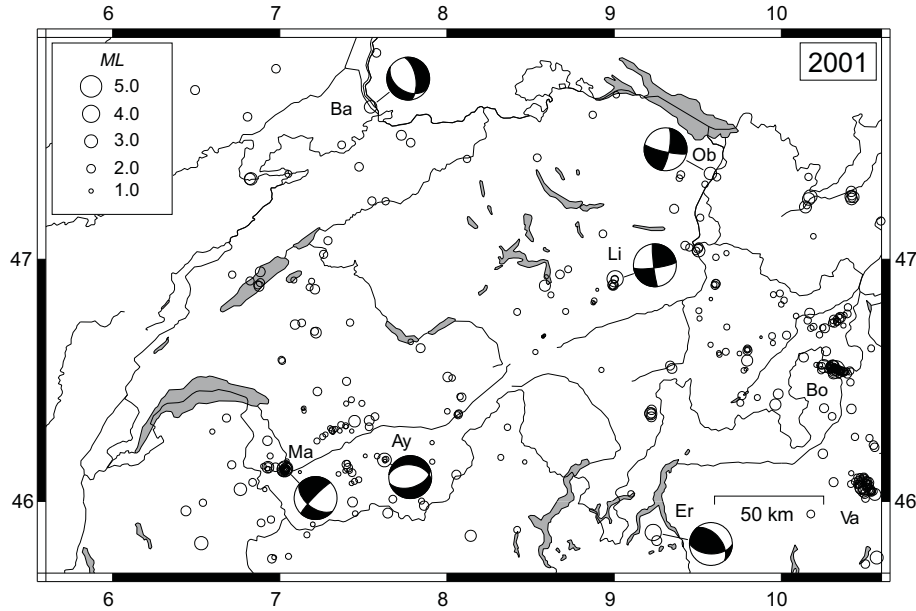
Figure 2001.1: Epicenters and focal mechanisms of earthquakes recorded by the Swiss Seismological Service during 2001. Epicenters of earthquakes mentioned in the text are Ayer (Ay), Basel-St.Louis (Ba), Bormio (Bo), Erba (Er), Linthal (Li), Martigny (Ma), Oberriet (Ob), Val Baone (Va). In the case of Martigny, only one of the two focal mechanisms is shown.

Location	Date & Time [UTC]	Depth [km]	Mag.	Plane 1 Plane 2 Strike/Dip/Rake		P-Axis T-Axis Az/Dip	
Martigny	2001.02.23 22:20	6	M_L 3.6	129/52/-009	224/83/-142	093/31	350/20
		6	M_w 3.6	123/48/-026	231/71/-136	096/44	352/14
Martigny	2001.02.25 01:23	6	M_L 3.5	138/56/-011	234/81/-146	101/30	002/16
		9	M_w 3.3	132/51/-009	228/83/-141	098/32	354/21
Oberriet	2001.03.14 10:37	30	M_L 2.9	010/76/-010	102/80/-166	327/17	236/03
Linthal	2001.03.17 00:30	3	M_L 3.8	082/80/ 175	173/85/ 010	307/03	038/11
		4	M_w 3.4	261/88/ 174	352/84/ 002	307/03	216/06
Erba	2001.04.06 02:23	22	M_L 3.8	320/50/ 126	091/52/ 055	205/01	297/63
		24	M_w 3.5	319/65/ 126	079/43/ 039	024/13	275/55
Basel-S.Louis	2001.04.12 07:07	8	M_L 2.9	123/40/-130	351/61/-062	308/63	061/11
Ayer	2001.07.09 22:50	6	M_L 3.2	276/42/-072	072/50/-106	283/77	173/04
		6	M_w 3.1	283/42/-059	064/55/-115	279/69	171/07

Table 2001.2: Focal mechanism parameters based on first-motion polarities (first line with M_L) and full-waveform inversion (second line with M_w, where available).
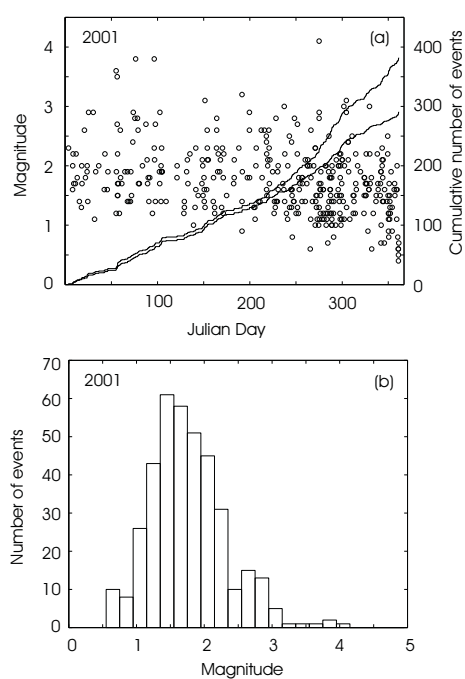
Figure 2001.2: Earthquake activity during 2001: magnitude of each event and cumulative number of events (a); histogram of magnitudes (b). In (a) the upper curve shows the cumulative number of all events, whereas the lower curve corresponds to the number of events without the Bormio aftershocks and the Val Baone events.
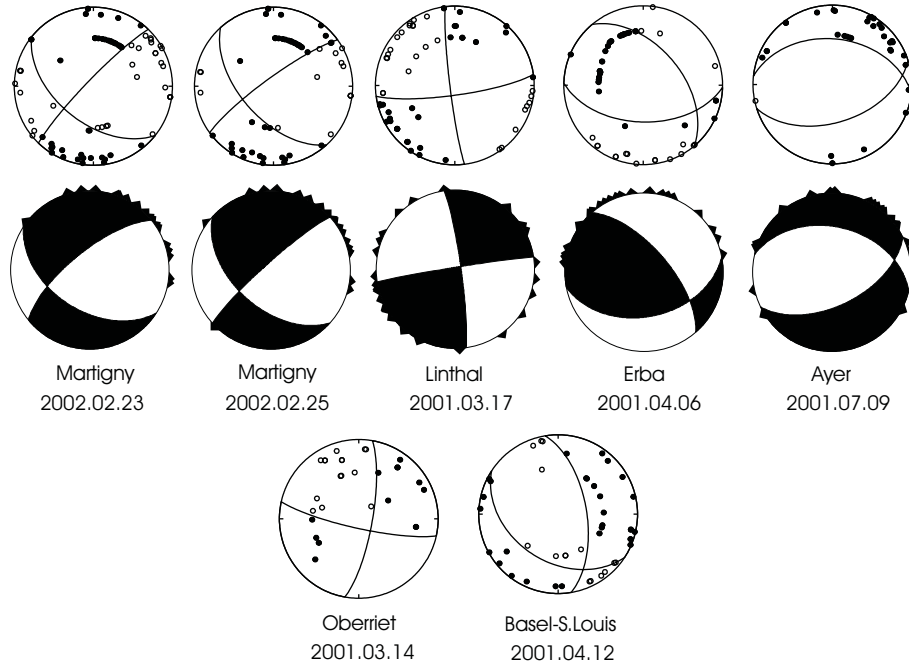
Figure 2001.3: Fault-plane solutions based on first-motion polarities and moment tensors based on full-waveform inversions (lower hemisphere, equal area projection). In the fault-plane solutions (above), solid circles correspond to compressive first motion (up) and empty circles to dilatational first motion (down); on the moment tensors (below), triangles show the station locations.
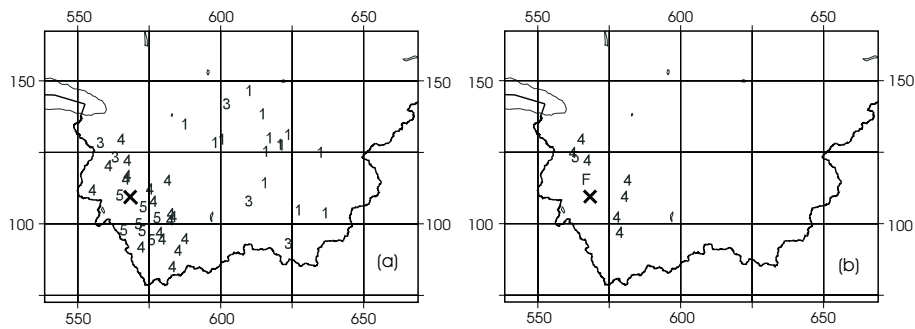
Figure 2001.4: Macroseismic observations of the two strongest Martigny events: (a) 2001/02/23 23:19 local time and (b) 2001/02/25 02:22 local time. Each value represents the macroseismic intensity (EMS-98) assigned to a single postal code zone. The X corresponds to the instrumental epicenter. The Swiss cartesian coordinate grid is labeled in km.

Nr.	Date & Time (UTC)	M_L
1	2001.01.08 09:29:02	2.2
2	2001.01.15 04:14:14	1.4
3	2001.02.23 22:19:42	3.6
4	2001.02.23 23:45:56	1.2
5	2001.02.24 06:17:49	1.9
6	2001.02.25 01:22:31	3.5
7	2001.02.25 02:07:57	2.7
8	2001.02.25 09:01:19	1.5
9	2001.02.25 16:06:43	1.5
10	2001.02.26 09:14:42	1.7
11	2001.02.27 10:36:45	1.2
12	2001.02.28 09:26:28	2.6
13	2001.03.02 01:56:39	1.7
14	2001.03.05 09:41:58	1.9
15	2001.03.09 16:39:08	1.4
16	2001.03.12 13:24:51	1.5
17	2001.03.13 22:20:17	2.4
18	2001.03.31 07:41:43	1.4
19	2001.05.28 19:55:05	1.5
20	2001.05.30 03:57:23	1.4
21	2001.05.30 23:17:51	1.3
22	2001.06.30 23:14:41	1.7
23	2001.09.16 07:43:01	1.4
24	2001.09.16 07:49:51	2.1
25	2001.09.22 04:07:58	1.1
26	2001.10.13 03:03:57	1.2
27	2001.10.24 14:59:50	2.2

Table 2001.3: List of events belonging to the cluster of Martigny.

Significant earthquakes of 2001

Martigny

At 23:20 local time on February 23rd and at 02:22 on February 25th, 2001, the lower Valais was shaken by two earthquakes that reached maximum intensity values of V (EMS-98) and that caused some concern among the local population. The macroseismic observations shown in Figure 2001.4 seem to indicate that the first event was stronger then the second one. However, the macroseismic field of the second event is not complete: this event occurred later in the night and thus was not felt as consciously by as many people as the first one, and in addition, many of those who responded to the requests for information referred only to the first event. In fact, with M_L 3.6 and 3.5 their magnitudes do not differ by much. Moreover, peak horizontal ground accelerations of the two events recorded by the free-field strong-motion stations in the epicentral area differ by less than 10% (Wyss, 2002).

Both events were part of a sequence of 27 events that occurred between January 8th and October 24th, 2001 (Table 2001.3). The seismograms of all events are very similar to each other (Figure 2001.5), implying that their hypocenters must be located close together and that their focal mechanisms must be practically identical. The event with the best-constrained absolute location occurred on September 16th at 7:49 UTC. Although it only reached M_L 2.1, it triggered the strong-motion station at Martigny and in addition, was also recorded by
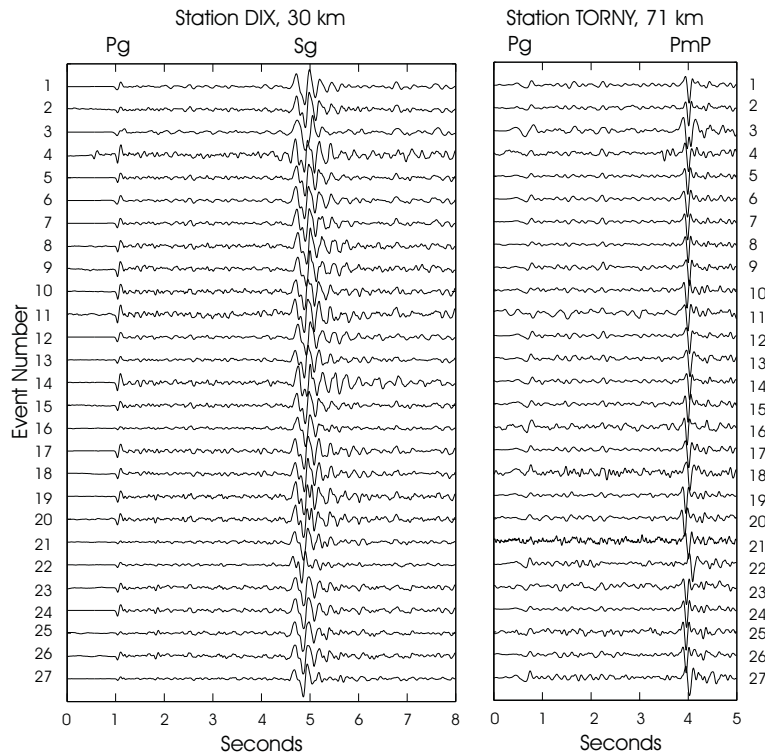
Figure 2001.5: Seismograms of the Martigny events recorded at stations DIX and TORNY. The signals at DIX are aligned on the Pg arrivals and bandpass filtered between 0.5 and 16 Hz; the signals at TORNY are bandpass filtered between 1 and 10 Hz and aligned on the Pg arrivals at station AIGLE, which features more impulsive onsets and which is located in practically the same direction as TORNY. The clearly visible shift between the PmP of events 20 and 22 implies that event 20 must be deeper and event 22 shallower.

the newly installed high-gain station at Lac de Salanfe, situated only 4.3 km from the epicenter. To reduce errors due to unmodelled lateral velocity hetorogeneities, we located the event using only stations within a distance radius of 50 km; despite this restriction, the azimuthal station gap amounted to only 94°. The resulting location places the epicenter 6 km NW of Martigny, at the SE side of the Rhone Valley, and gives a focal depth of 6 km. The location uncertainty is estimated to be ±1 km horizontally and ±2 km in depth.

Focal mechanisms for the two strongest events, based both on first-motion fault-plane solutions and on full-waveform inversion, are shown in Figure 2001.3 and the corresponding parameters are listed in Table 2001.2. The results of both techniques are well constrained by the data and are largely consistent with each other. The mechanisms of the two events correspond to strike-slip faulting with only small differences in the orientation of the nodal planes.

To resolve the source geometry and to identify the active fault plane of such an earthquake cluster, it is necessary to determine high-precision relative hypocenter locations of the individual events, and thus to determine relative arrival times at sub-sample precision. Such a high timing precision was obtained by exploiting the similarity among the signals and applying a time-domain cross-
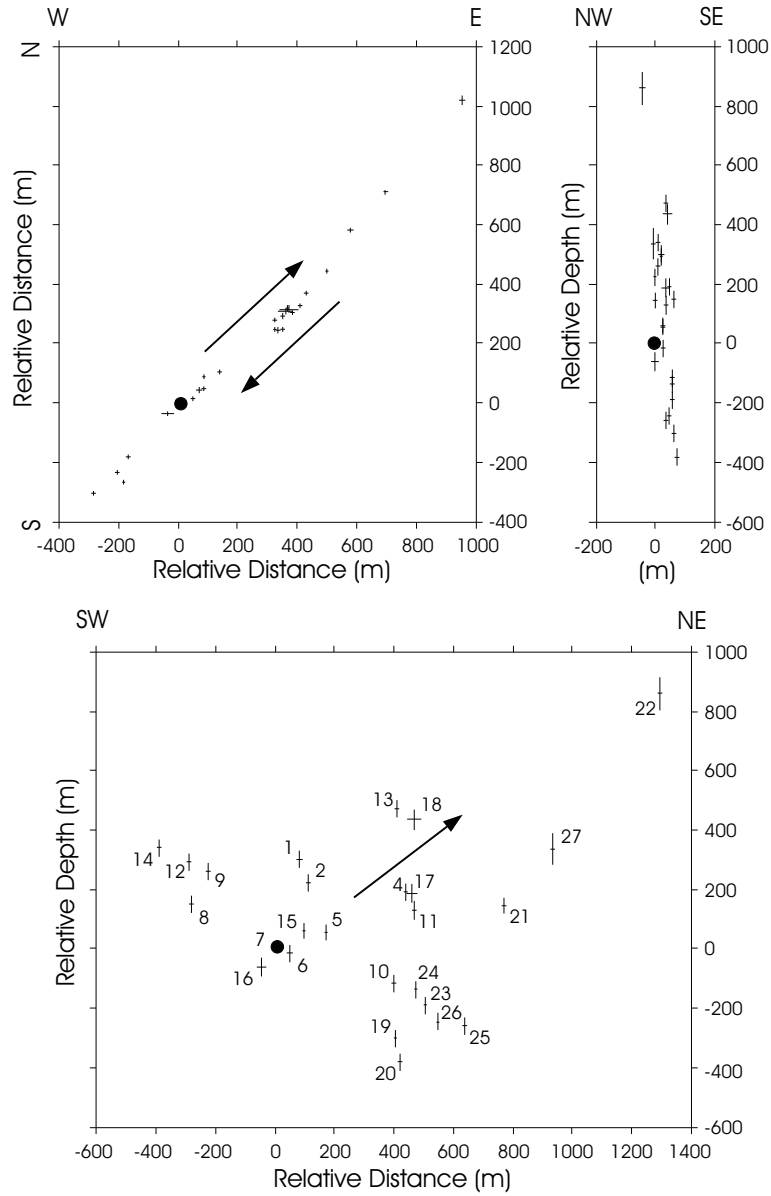
Figure 2001.6: Relative locations of the Martigny events: epicenter map (a) and depth section perpendicular (b) and parallel (c) to the inferred fault plane. The numbers in (c) refer to Table 5. The black dot shows the location of event Nr. 7, which we chose as master event. Event Nr. 3 is missing, because its signals could not be correlated with the others (see text). The size of the crosses corresponds to the computed relative location uncertainty (1σ) of each event. The pair of arrows in (a) shows the sense of dislocation along the inferred fault and the arrow in (c) corresponds to the slip vector of the hanging wall.

correlation technique (Deichmann & Garcia-Fernandez 1992). With the high-precision relative arrival times we then made use of a master-event location algorithm proposed by Console & DiGiovambattista (1987) to obtain relative

location uncertainties on the order of a few tens of meters. Of the 27 events only event number 3, the strongest one, could not be included in the relative location procedure because of insufficient signal similarity. The difference in signal character of this event relative to the others is due to a longer source-time function, that consists of two distinct subevents. This can be seen best by comparing the PmP waveforms at station TORNY, shown in Figure 2001.5: instead of the simple wavelet with a single strong downward swing seen in all other seismograms, the downward pulse of event number 3 is two-pronged, corresponding to two subevents within a time interval of less than 0.1 s.

Event number 4 is also a doublet, but in this case, the seismograms correspond to two separate events that occurred 0.4 s apart. Thus effectively, the total number of events in the Martigny sequence detected by the high-gain network is 28. However, since the hypocenter of the first and weaker event of this doublet can not be located, we have not included it in our analysis.

For the cross-correlation and subsequently as input for the relative location algorithm we used the Pg and Sg arrivals at stations EMV, DIX and AIGLE as well as the PmP phase at station TORNY. These stations are well distributed around the epicenter (gap = 129°), therefore the three P and the three S arrivals together with the downgoing raypath of the PmP at TORNY provide excellent constraints on both the horizontal and vertical coordinates of the relative locations. The hypocenters define an almost vertical SW-NE striking plane, that extends roughly 2 km horizontally and more than 1 km vertically (Figure 2001.6). A comparison with the focal mechanisms (Fig. 2001.3) shows that this plane closely matches one of the nodal planes and thus constitutes the active fault of the Martigny sequence. The dislocation on this fault corresponds to dextral strike-slip motion with a significant vertical component.

At the 2σ level of the location uncertainty, it is possible to fit a single fault plane through almost all hypocenters. However, in addition to the finite width of the hypocenter distribution suggested by Figure 2001.6, two additional observations favour the view of a fault zone consisting of several individual subfaults, rather than of a single planar fault: (1) the structure imaged by the relative hypocenter locations dips slightly to the SE, whereas in the focal mechanisms of both of the strongest events (Fig. 2001.3), the active fault planes dip slightly towards the NW; (2) variations in the amplitude ratios of P- to S-phases seen in the seismograms recorded at station DIX (Fig. 2001.5) together with the observation that P-wave polarities at station EMS, situated exactly SW of the epicenters, are opposite to each other for about 50% of the events are evidence for differences in the strike of individual fault planes.

Figure 2001.7 shows the location of the Martigny cluster superimposed on a digital elevation model. The epicenters are aligned parallel to the strike of the main geomorphic features of the region and to the strike of pre-Alpine internal structures of the Aiguilles Rouges Massif, such as the Miéville mylonite zone and the Carboniferous Salvan-Dorénaz graben. The location of the earthquakes coincides exactly with the center of this graben structure, which extends from the area of Vallorcine in the SW to below the Dents de Morcles NE of the Rhone Valley (Steck et al., 1999). Although it is unlikely that the sedimentary graben fill extends down to a depth of 6 km (Pilloud, 1991), it is probable that the earthquakes reactivated a boundary fault of this late hercynian structure (M. Burkhard, personal communication): late Alpine, post Morcles nappe emplacement reactivation and inversion of this graben has been shown to be responsible for the "synformal" shape and internal folding (Pilloud, 1991; Badertscher & Burkhard, 1998). Considering that both the mylonites of Miéville and the Car-
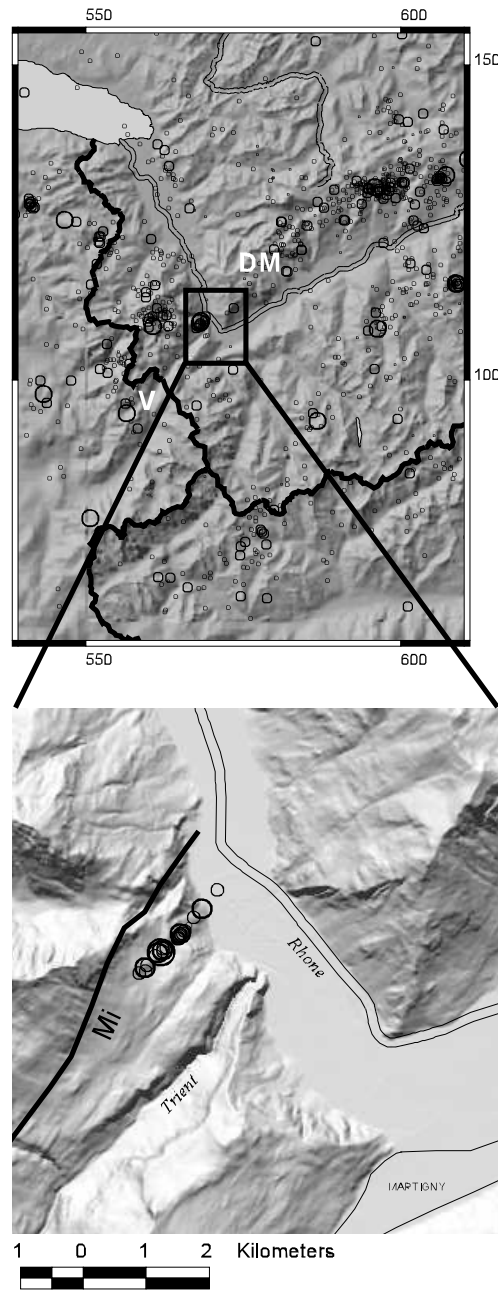
Figure 2001.7: Top: epicenters of all events with $M_L \geq 1$ over the period 1984-2001 (DM = Dent de Morcles, V = Vallorcine). Some of the events along the Rhone Valley might correspond to unidentified quarry blasts. Bottom: the Martigny cluster, fixed to the absolute location of event Nr. 24 (Mi = mylonite zone of Miéville). The SW-NE striking Carboniferous wedge of Salvan-Dorénaz lies between the Trient valley and the mylonites of Miéville. Digital elevation models RIMINI and DHM25 reproduced with permission from the Swiss Federal Office of Topography (BA024517).

boniferous wedge extend over more than 20 km with practically the same strike as that of the fault patch imaged at depth by the earthquake sequence of 2001, it is conceivable that at some time a single earthquake could rupture a significantly larger portion of this fault zone. Note, however, that the strike of the fault delineated by the Martigny cluster differs by about 15° from the strike of the suggestive rectilinear alignment of epicenters that extends from the northern Valais towards the southwest across the Rhone Valley into France (Fig. 2001.7 and Baer et al., 2001, Fig. 3).

Oberriet

This M_L 2.9 event, which occurred on March 14th near the northern end of the Rhine Valley of St. Gallen, is of particular interest, because of its focal depth of 30 km. The location is well constrained by a station distribution with a maximum azimuthal gap of 108° and by three stations at epicentral distances closer than 25 km. The Moho at this location is at a depth of 36 km (Waldhauser et al. 1998). Thus this earthquake provides evidence for the eastward continuation of the well-known lower-crustal seismicity of the northern Alpine foreland of Switzerland (e.g. Deichmann et al. 2000a). Although we do not have any observations in the SE quadrant, the fault-plane solution is constrained to within less than ±10° and corresponds to a strike-slip mechanism with an orientation typical for the earthquakes in this region (Deichmann et al. 2000b).

Linthal

This event, which occurred at 1:30 in the morning (local time) of March 17th below the town of Linthal, Canton Glarus, is remarkable: although its magnitude is moderate ($M_L = 3.8$ and $M_w = 3.4$), the free-field strong-motion station in Linthal, at an epicentral distance of 1 km, recorded a peak horizontal acceleration of 20% g (Wyss, 2002). The reasons for such a high acceleration are probably the shallow focal depth (3 km maximum, constrained by an S-P time of less than 0.5 s at the strong-motion station) and the amplifying effect of the soft alluvial fill of the valley floor. The effect of the shallow source can also be seen in the macroseismic observations shown in Figure 2001.8: several intensity values of V are concentrated in the epicentral area and the intensity fall-off with distance is rapid. In the subsequent four days, this earthquake was followed by two small aftershocks with $M_L < 2$, and in the first half of August four additional events with M_L between 1.4 and 2.4 occurred about 3 km further south. The strike-slip focal mechanism with N-S and E-W striking nodal planes is optimally constrained by both the first-motion fault-plane solution and the full-waveform inversion.

In November of 1990, the area just south of Linthal was already the site of a sequence of earthquakes that included a M_L 3.6 event. This earlier event also features a strike-slip mechanism, but its nodal planes strike NNW-SSE and ENE-WSW (Kastrup, 2002). The rough N-S alignment of the routine epicenter locations in this region would suggest that the N-S and NNW-SSE trending nodal plane constitute parts of an active fault in this area. However this needs to be confirmed by a more detailed analysis.
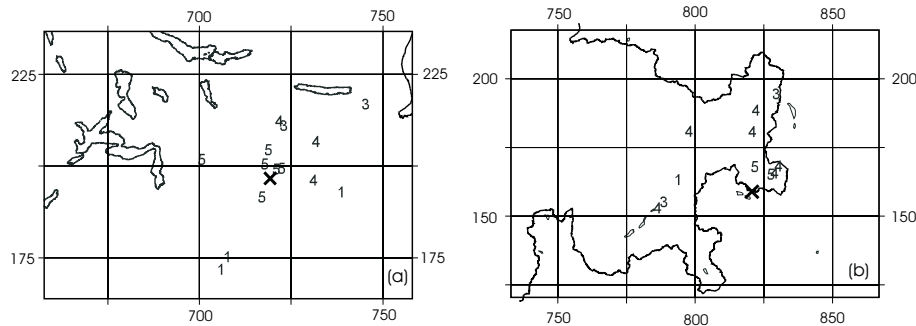
Figure 2001.8: Macroseismic observations of the Linthal event of 2001/03/17 (a) and of the Bormio event of 2001/10/01 (b). Each value represents the macroseismic intensity (EMS-98) assigned to a single postal code zone. The X corresponds to the instrumental epicenter. The Swiss cartesian coordinate grid is labeled in km.

Erba

The epicenter of this event (M_L 3.8 and M_w 3.5), that occurred on April 6th, is located between Como and Lecco at the southern margin of the Alps. The full-waveform inversion for this event results in a thrust faulting mechanism at a depth of 24 km. Within the limits imposed by our imperfect model of the complex crustal structure in this region, the focal depth can be matched by 2-D ray tracing and the moment tensor is in good agreement with the fault-plane solution derived from the first-motion polarities (Table 2001.2 and Fig. 2001.3). This event is particularly interesting for two reasons: firstly, it confirms earlier reports about the existence of lower-crustal earthquakes beneath the southern margin of the Alps (e.g. Deichmann & Baer, 1990) and secondly, it provides a focal mechanism in a region where well-constrained mechanisms are sparse.

Basel-St.Louis

The epicenter of this M_L 2.9 event was located near the airport of Mulhouse, NW of Basel. Based on a station distribution with an azimuthal gap of only 87° and a minimum epicentral distance of 9 km, the routinely determined focal depth lies between 7 and 10 km, and two-dimensional ray-tracing gives a best fit for a depth of 8 km. The normal faulting mechanism is well constrained with a ENE-WSW striking T-axis (Fig. 2001.3 and Table 2001.2).

Ayer

This event with $M_L = 3.2$ and $M_w = 3.1$ occurred on July 9th near the town of Ayer, in the southern Valais. With a minimum epicentral distance of about 20 km, routine locations do not constrain the focal depth. The full-waveform inversion exhibits a best fit for a focal depth of 6 km; raytracing suggests a depth closer to 9 km, but, because the modelling results are not entirely satisfactory, we have retained the result of the moment tensor inversion. By itself the fault-plane solution based on first-motion polarities is not optimally constrained, but together with the moment tensor inversion the result is reliable. The normal-faulting mechanism with a practically N-S trending T-axis is similar to mechanisms of past earthquakes in this region: Vissoie 1986 (Eva et al.,

1998), Vissoie 1990 (Maurer et al., 1997) and Grimentz 1998 (Baer et al., 1999). These earthquakes are evidence of the typical extensional deformation presently active in the Penninic Nappes of the southern Valais (e.g. Maurer et al., 1997).

Val Baone

In the second half of 2001, an earthquake swarm with epicenter in Val Baone near the Tonale Pass in northern Italy became active (Fig. 2001.1). The Swiss high-gain network detected 42 events that are associated with this cluster; the strongest event reached M_L 3.0.

Bormio

The strongest earthquake during 2001 in Switzerland and its immediate surroundings was the M_L 4.1 event of October 1st with epicenter between Bormio and Val Müstair. In the epicentral region this quake produced shaking of intensity V (Fig. 2001.8). This event, together with 48 other weaker ones, represents continuing activity in the epicentral region of the M_L 4.9 Bormio earthquake of Dec. 29th, 1999.

Seismic activity during 2002

Overview

During 2002, the Swiss Seismological Service detected and located 547 earthquakes in the region shown in Figure 2002.1. Based on such criteria as the time of occurrence, the location, the signal character or on direct information, 142 additional seismic events were identified as quarry blasts.

Magnitude values of the events recorded in 2002 range between $M_L = 0.4$ and 3.8. The events with $M_L \geq 2.5$ are listed in Table 2002.1. Where available, the epicentral coordinates and focal depths given in Table 2002.1 are based on the results that include additional data from foreign networks and on 2-D ray-tracing.

Compared to the period 1996-2001, when the number of recorded earthquakes ranged between 226 and 382 events/year, the year 2002 seems at first sight to have witnessed an unusually high seismic activity. However, averaged over the last 28 years, the number of earthquakes in Switzerland and surrounding regions amount to about 25 events with $M_L \geq 2.5$ and about 8 events with $M_L \geq 3$ per year. With 27 events with $M_L \geq 2.5$ and 8 events reaching $M_L \geq 3$ (Table 2002.1 and Fig. 2002.2), the seismic activity in 2002 was thus about equal to the average over the last 28 years for earthquakes in these magnitude ranges. Consequently the observed activity increase is due only to the lower-magnitude events. This is caused by the lower detection threshold following the completion of the new broad-band network (Deichmann et al. 2002), and by the occurrence of an unusual number of earthquake swarms during 2002. In fact, 39 % of the total number of events were associated with the six earthquake sequences of Bormio, Val Baone, Anzère, Cima di Jazzi, Samedan and Monte Cevedale. Thus, the enhanced activity visible in the plot of the temporal evolution of seismicity (Fig. 2002.2) at the beginning of the year is due to the Bormio and Val Baone events, while the sharp increase during the last days of the year reflects the sudden occurrence of the swarms of Samedan and Monte Cevedale.

Routinely calculated focal depths for the 547 earthquakes recorded in 2002 range between 1 and 30 km, but only 25 of these hypocenters are deeper than 15 km. As in the past (e.g. Deichmann et al. 2000a), almost all these deep sources are located in the lower crust beneath the Jura Mountains and Molasse Basin of northern Switzerland. Notable exceptions are the hypocenters of the Santa Maria Maggiore event at a depth of more than 20 km in the Ivrea Zone and of the Monte Cevedale sequence. However, the focal depths of the latter (15-20 km), determined from routine analysis only, are questionable and need to be confirmed by additional evidence.

Overall, as in previous years, most of the seismic activity during 2002 was concentrated in the Valais, the southeastern part of Graubünden and in the adjacent regions of northern Italy (Fig. 2002.1).
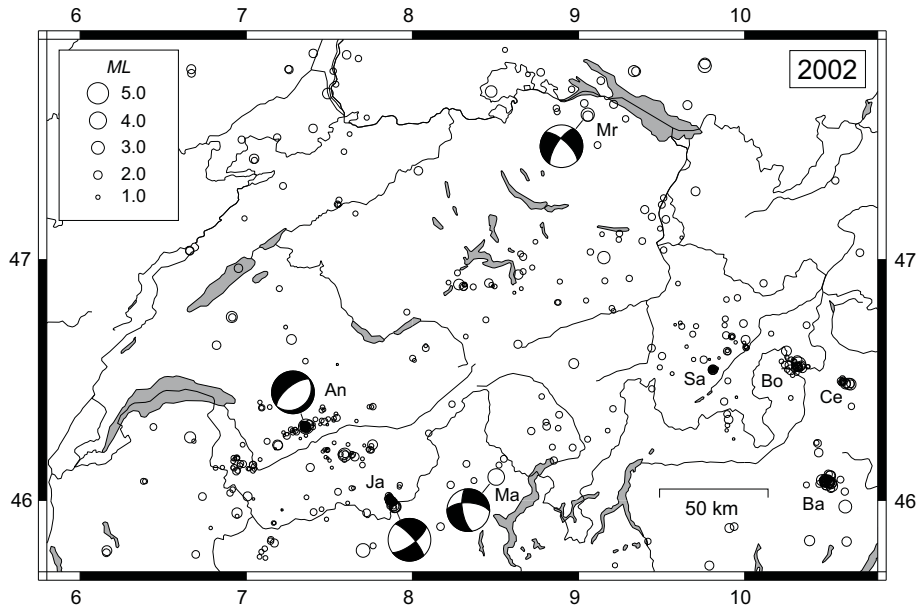
Figure 2002.1: Epicenters and focal mechanisms of earthquakes recorded by the Swiss Seismological Service during 2002. Epicenters of earthquakes mentioned in the text are Anzère (An), Val Baone (Ba), Bormio (Bo), M. Cevedale (Ce), Cima di Jazzi (Ja), Märstetten (Mr), Samedan (Sa), S. Maria Maggiore (Ma).
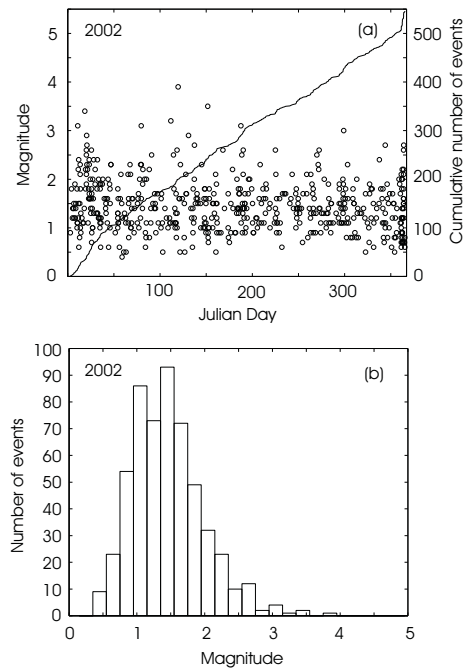

Figure 2002.2: Earthquake activity during 2002: magnitude of each event and cumulative number of events (a); histogram of magnitudes (b).

Date & Time UTC	Lat. [°N]	Lon. [°E]	X / Y [km]	Depth [km]	Mag. [M_L]	Q	Location
2002.01.10 19:27:25	47.594	9.055	721/273	25	3.1	A	Märstetten, TG
2002.01.18 11:14:54	46.563	10.316	820/161	7	3.4	B	Bormio, I
2002.01.20 03:56:40	46.071	10.518	838/107	10	2.5	C	Val Baone, I
2002.01.20 04:09:49	46.074	10.520	838/107	10	2.6	C	Val Baone, I
2002.01.20 11:17:04	46.069	10.495	836/106	10	2.9	C	Val Baone, I
2002.01.20 17:24:13	46.061	10.524	839/106	10	2.7	C	Val Baone, I
2002.01.25 16:19:39	46.085	10.465	834/108	10	2.6	C	Val Baone, I
2002.03.20 14:44:13	46.191	7.592	612/115	7	3.1	B	Zinal, VS
2002.03.31 19:39:27	46.898	8.280	664/194	3	2.5	A	Kerns, OW
2002.04.21 17:57:15	45.790	7.703	620/ 71	4	3.2	C	Val d'Ayas, I
2002.04.24 13:03:31	46.308	7.357	594/128	3	2.5	B	Anzère, VS
2002.04.28 09:06:45	46.264	6.662	540/124	3	2.6	B	Le Biot, F
2002.04.29 15:14:09	46.102	8.457	679/106	21	3.8	B	S.Maria Magg., I
2002.05.10 19:55:02	47.009	9.152	730/208	5	2.9	B	Engi, GL
2002.05.17 07:19:39	47.688	8.474	678/282	24	2.7	A	Hallau, SH
2002.05.31 16:50:33	46.322	7.359	594/130	5	3.5	A	Anzère, VS
2002.06.17 01:50:31	46.764	6.913	560/179	6	2.6	A	Granges, VD
2002.07.06 14:09:55	47.792	9.759	774/296	27	3.1	C	Waldburg, D
2002.07.07 12:27:25	47.802	9.760	774/297	25	2.5	C	Waldburg, D
2002.07.09 03:21:21	47.771	9.333	742/293	20	2.6	C	Markdorf, D
2002.08.12 22:07:25	45.976	7.930	638/ 92	7	2.6	A	Cima di Jazzi, I
2002.09.26 21:01:39	47.680	7.491	604/281	11	2.5	C	Rheingraben, F
2002.09.29 08:10:45	45.973	7.930	638/ 91	7	2.6	A	Cima di Jazzi, I
2002.10.25 23:34:48	45.974	10.605	845/ 96	12	3.0	D	V.Giudicarie, I
2002.12.09 22:41:55	45.975	7.932	638/ 92	8	2.7	A	Cima di Jazzi, I
2002.12.29 18:21:14	46.499	10.621	844/155	18	2.6	B	M.Cevedale, I
2002.12.29 22:54:51	46.500	10.621	844/155	18	2.7	B	M.Cevedale, I

Table 2002.1: Earthquakes with $M_L \geq 2.5$. The focal depths of the earthquakes for which focal mechanisms have been calculated are based on 2-D ray-tracing or on additional data from foreign networks.

Location	Date & Time [UTC]	Depth [km]	Mag.	Plane 1 Strike/Dip/Rake	Plane 2	P-Axis Az/Dip	T-Axis
Märstetten	2002.01.10 19:27	25	M_L 3.1	312/68/-158	213/70/-024	172/31	263/01
S.Maria Magg.	2002.04.29 15:14	21	M_w 3.5	170/68/-031	273/61/-154	129/37	223/04
Anzère	2002.05.31 16:50	5	M_L 3.5	046/24/-094	231/66/-088	145/69	319/21
		4	M_w 3.3	061/19/-073	223/72/-096	124/63	318/27
Cima di Jazzi	2002.12.09 22:41	8	M_L 2.7	318/76/-020	053/71/-165	275/24	006/04

Table 2002.2: Focal mechanism parameters based on first-motion polarities (lines with M_L) and full-waveform inversion (lines with M_w).
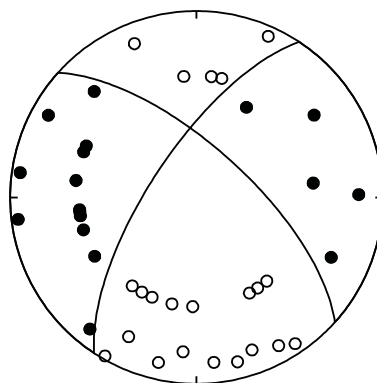
Märstetten
2002.01.10

Figure 2002.3: Fault-plane solution based on first-motion polarities (lower hemisphere, equal area projection) for the Märstetten event. Solid circles correspond to compressive first motion (up) and empty circles to dilatational first motion (down).

In what follows, we present the highlights of the seismic activity observed during 2002.

Significant earthquakes of 2002

Märstetten

The source of the earthquake, which occurred on Jan. 10th with magnitude M_L 3.1 and epicenter near the village of Märstetten, TG, was located in the lower crust at a depth of 25 km. It was followed a day later by an aftershock with M_L 2.4. The focal depth determination is based on records from stations in northern Switzerland and southern Germany ($gap = 109°$ and $D_{min} = 23$ km) and is confirmed by ray-trace modelling of Pn phases. Earthquakes in the lower crust below the Molasse basin of northern Switzerland and southern Germany are not uncommon (e.g. Deichmann et al., 2000b). The well constrained fault plane solution based on first-motion polarities (Fig. 2002.3) corresponds to a strike-slip mechanism with orientations of the P- and T-axes (Table 2002.2) that are typical for earthquakes in northeastern Switzerland (Deichmann et al.,
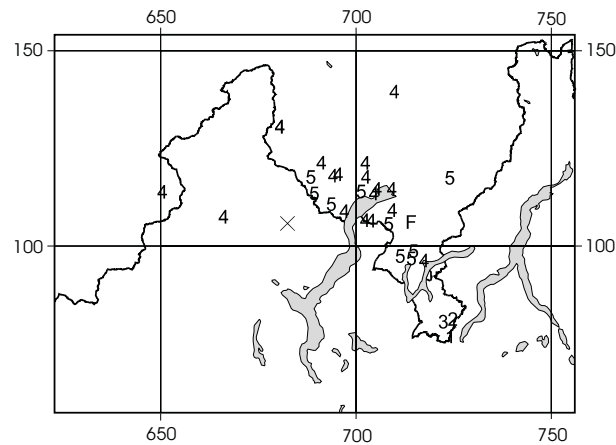
Figure 2002.4: Macroseismic observations of the S. Maria Maggiore event of 2002/04/29. Each value represents the macroseismic intensity (EMS-98) assigned to a single postal code zone. The X corresponds to the instrumental epicenter. The Swiss cartesian coordinate grid is labeled in km.

2000b; Kastrup, 2002).

Bormio

The M_L 3.4 event of Jan. 18th, together with 31 other weaker ones, represents continuing activity in the epicentral region of the M_L 4.9 Bormio earthquake of Dec. 29th, 1999. During 2002, most of this aftershock activity occurred in January and February. It gradually decreased over the subsequent months with the last event having occurred at the end of September. Thus the entire aftershock sequence of the 1999 Bormio event seems to have lasted for nearly 3 years.

Val Baone

In the second half of 2001, an earthquake swarm with epicenter in Val Baone near the Tonale Pass in northern Italy became active. During 2001, the Swiss high-gain network detected 42 events that are associated with this cluster; the strongest event reached M_L 3.0. This activity persisted at a high rate during January and February 2002 with an additional 36 events (Fig. 2002.1). The strongest of these events with M_L 2.9 occurred on Jan. 20th (Table 2002.1). After four more events with $M_L \leq 2.2$, that occurred between end of June and end of October, the activity in this cluster seems to have ceased. Given a minimum epicentral distance from the Swiss network of around 50 km and an azimuthal gap of about 300°, the epicentral locations shown in Figure 2002.1 are poorly constrained. Judging from the similarity of the observed waveforms, the true epicenters are certainly more concentrated than the apparent scatter in Figure 2002.1 would suggest.

Santa Maria Maggiore

With M_L 3.8 and M_w 3.5, this event, which occurred on April 29th in the border region between Ticino and northern Italy, was the strongest event to
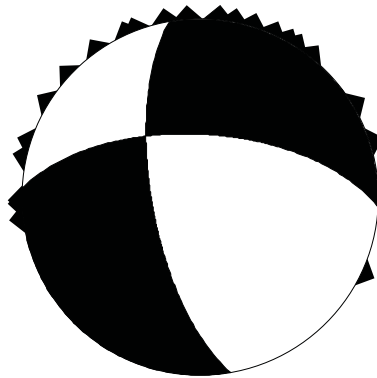
Santa Maria Maggiore
2002.04.29

Figure 2002.5: Focal mechanism (lower hemisphere, equal area projection) for the event of S. Maria Maggiore, based on full-waveform moment tensor inversion. Triangles on the periphery of the stereo plots show the station locations.

have been recorded in 2002 in Switzerland and surrounding regions. It reached a maximum intensity of V and was felt all over southern Switzerland and the adjoining regions of northern Italy (Fig. 2002.4). The epicenter was located about 5 km south of Santa Maria Maggiore between Val Vigezzo and Valgrande, Italy. This location situates the epicenter in the middle of the Ivrea Zone, which is characterized by outcropping mantle rocks with P-wave velocities in the range of 7-8 km/s. The 1-D velocity model used routinely for location is thus only a poor approximation of the real crustal structure in this region. To minimize the possible effects of lateral velocity variations on the location, we used stations out to an epicentral distance of only 50 km. Including also data from several Italian stations, this gave 5 P- and 4 S-arrivals with which to calculate the location. Despite a good azimuthal station distribution ($gap = 120°$), the remaining epicentral uncertainty is probably on the order of 5 km. Since the nearest station is about 35 km from the epicenter the focal depth is even more poorly constrained and very sensitive to the assumed V_p/V_s velocity ratio. Thus we chose to fix the focal depth to 21 km, which gives the best wave-form fit in the moment tensor inversion. The moment tensor corresponds to a strike-slip mechanism with a strong normal faulting component and with P- and T-axes directed NW-SE and NE-SW (Fig. 2002.5). Due to the difficulty of calculating correct take-off angles from a source located in such a complex geological structure as the Ivrea Zone, we did not attempt to construct a self-consistent fault plane solution from first motion polarities. However, within the uncertainties of the routinely calculated take-off angles, the moment tensor result matches the first motion polarities reasonably well.

Anzère

The M_L 3.5 earthquake that occurred on May 31st with epicenter 4 km NW of Anzère, VS, was the strongest event of an earthquake sequence that lasted for several months. Of the 35 detected and locatable events that were associated with this swarm, 3 occurred in January and February, 2 in October, and the
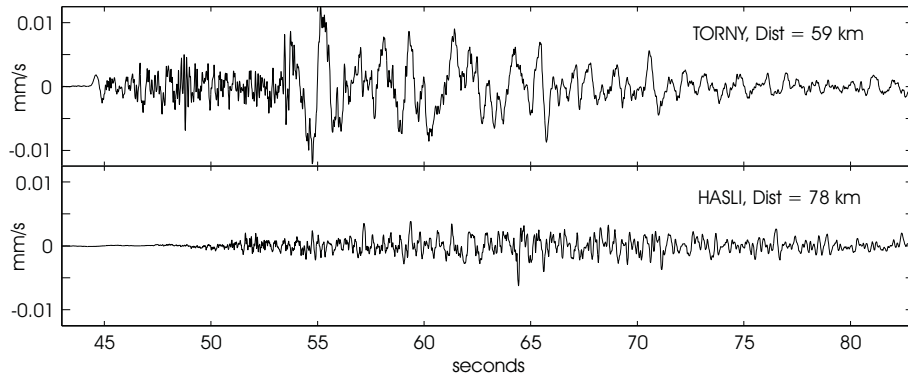
Figure 2002.6: Vertical component broad-band signals of the Anzère event recorded at stations TORNY and HASLI. Amplitudes at HASLI have been scaled to match the epicentral distance of TORNY by assuming a geometrical spreading dependence equal to 1/distance. Note the impulsive P- and S-arrivals as well as the pronounced surface wave train beyond 55 seconds at TORNY and, in contrast to this, the largely featureless low-amplitude signal consisting only of scattered waves at HASLI.
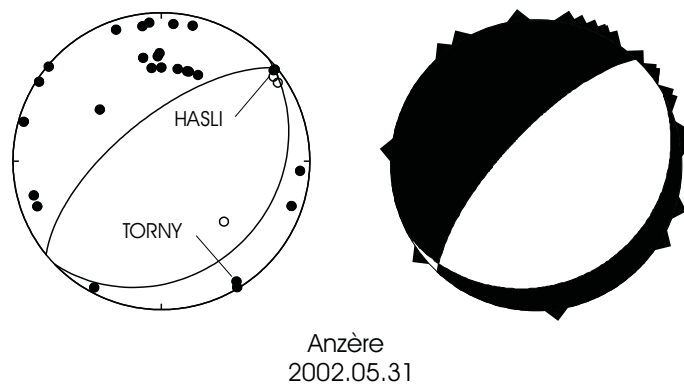

Figure 2002.7: Focal mechanism for the Anzère event, based on first-motion polarities and on full-waveform inversion. The labeled data points correspond to the two stations mentioned in the text.

remaining events occurred all between Apr. 24th and June 14th. Except for the main shock and three others with M_L between 2.1 and 2.5, magnitudes of the locatable events were all between M_L 0.5 and 1.8.

At several stations, the signals of the main shock are dominated by pronounced surface wave trains (e.g. station TORNY in Fig. 2002.6, which at first sight would suggest that the source is located at a depth of only 1 or 2 km within the near-surface sedimentary cover. However, such a shallow source is at odds with the travel-time data. In fact, the hypocentral location is well constrained by station SENIN, at an epicentral distance of only 6 km, and by the P- and S-arrival times at two additional strong-motion stations (SAYF and SIOV) at distances of 5 and 9 km (Wyss 2003). The resulting focal depth of 4 to 6 km is corroborated by ray-trace modelling of PmP-Pg arrival-time differences at stations in northern Switzerland (5 km) and by the results of the moment tensor calculations (4 km).

The orientation of focal the mechanism of this event differs radically from anything observed so far in the northern Valais. It corresponds to a normal faulting mechanism on either a steeply dipping or a flat lying fault plane that strikes in a NE-SW direction. The NW-SE trending extensional (T) axis is rotated by about 90° relative to the T-axes of most of the neighboring focal mechanisms (Maurer et al., 1997; Pavoni et al., 1997; Kastrup, 2002). The mechanisms derived from the fault-plane solution based on first motion polarities and from the full wave-form moment tensor inversion are well constrained by data (Fig. 2002.7), and the corresponding parameters agree with each other to within 10° (Table 2002.2). In particular, the null (B) axis and thus the strike of the nodal planes in the first-motion fault-plane solution are well constrained by the take-off direction of the ray to station HASLI. As shown in Figure 2002.6, the signal recorded at this station lacks any recognizable onset of either a P- or S-wave. Such featureless signals consist only of scattered energy from waves leaving the source in directions other than the direct ray to the observer, which is consistent with the fact that a double-couple source does not radiate any energy in the direction of the null axis. When available, such signals are powerful constraints on the orientation of the focal mechanism.

The apparently discrepant orientation of the focal mechanism relative to the prevailing stress field (Kastrup, 2002) can not be explained by questioning the reliability of the observations or by invoking possible near-surface stress heterogeneities affecting an unusually shallow source (i.e. the Anzère event occurring within a mechanically decoupled sedimentary layer and thus possibly responding to a different stress field). Given that the most robust feature of stress inversions performed on the basis of the hitherto observed focal mechanisms in the northern Valais is the NE-SW orientation and the nearly horizontal plunge of the least principal stress σ_3 (Kastrup, 2002), a local perturbation of the stress field that would lead to a horizontal rotation of σ_3 of as much as 90° at a depth of 5 km within the Earth's crust is also highly unlikely. A possible explanation consistent with previous stress inversions (Kastrup, 2002) can however be found by observing that the orientation of the null axis matches almost exactly the orientation of σ_3 and that the possible orientations of σ_1 and σ_2 can take on any value within a vertical plane perpendicular to σ_3. In this case, slip on a pre-existing fault with an orientation as that of the Anzère event is possible and will be triggered not by the difference $\sigma_1 - \sigma_3$ but by $\sigma_1 - \sigma_2$. The permutability of the directions of σ_1 and σ_2 is favoured if their magnitudes are similar, implying that the fault, which was active during the earthquake sequence of Anzère, must have been particularly weak. Temporarily elevated fluid pressures on the fault
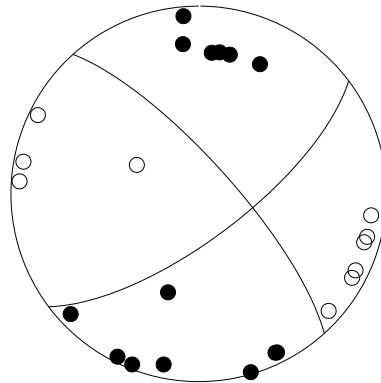
Cima di Jazzi
2002.12.09

Figure 2002.8: Fault-plane solution based on first-motion polarities (lower hemi-sphere, equal area projection) for the Cima di Jazzi event. Solid circles correspond to compressive first motion (up) and empty circles to dilatational first motion (down).

would not only have the necessary weakening effect, but would also function as a trigger mechanism for the observed swarm-like occurrence of these events.

Cima di Jazzi

A particularly active earthquake sequence manifested itself during 2002 on the Swiss-Italian border between the valleys of Zermatt and Macugnaga. After 3 preliminary events ($M_L \leq 1.5$) in January and February, activity suddenly picked up again at the beginning of July, with 24 events detected during that month alone. It continued at a somewhat slower pace over subsequent months, reaching a total of 73 detected events by the end of the year. Three earthquakes reached magnitudes, M_L, of 2.6 and 2.7 (Table 2002.1). The magnitudes of all other events were between 0.9 and 2.2. Preliminary locations scattered over a distance of more than 10 km, with an apparent distribution into two subclusters separated by an aseismic gap of about 3 km. It turned out that this was entirely an artifact of the location procedure and of the complicated crustal structure in this region. Rays leaving the hypocenters of these events towards the east and northeast are strongly affected by the Ivrea Body, with its high lateral velocity contrast relative to the surrounding crust. For this situation the one-dimensional velocity model originally used in our routine location procedure constitutes an inadequate simplification. In addition, the epicentral area lies at the periphery of the Swiss station network ($gap > 180°$). As a consequence, locations that include arrivals at stations FUSIO and MUGIO are systematically shifted to the SE by about 6 km relative to the locations of the generally weaker events based only on the three closest stations MMK, DIX and LKBD in the Valais. For four of the stronger events, we obtained data from the Italian stations Macugnaga (MCGN), Oropa (ORO) and Varese (VAI). The most stable and reliable locations, which are listed in Table 2002.1, are based only on arrivals at stations MCGN, ORO, MMK, DIX and LKBD and have been recomputed using

the 3D velocity model of Husen et al. (2003). The parameters that characterize these locations are: number of arrivals used, $N_{obs} = 8$ - 10, Minimum epicentral distance, $D_{min} = 5$ km, $gap = 111°$ and the root-mean-square of the travel-time residuals, $rms = 0.10$ - 0.12 s. Compared to the original locations in Baer et al. (2003), the epicenters are shifted by about 3 km to the East and focal depths increase from about 6 km to 7 - 8 km. The resulting travel-time residuals at the Italian station VAI (Varese) and at stations FUSIO and MUGIO, which were not used for calculating the locations, range between -0.82 and -1.37 s using the 1D velocity model, which is at least qualitatively consistent with the expected effect of the high-velocity Ivrea Body. Using the 3D velocity model, the median value of these travel-time residuals is -0.36 s, which is a considerable imrovement.

Based on these revised locations and the take-off angles calculated by the location algorithm for the 3D model, we obtain a reasonably well-constrained fault-plane solution, that corresponds to a strike-slip mechanism with a slight extensional component (Figure 2002.8).

Samedan

Beginning on December 27th, a sequence of microearthquakes ($M_L = 0.6$ - 2.2) became active north of Samedan in the Upper Engadine. By December 31st, the total number of detected earthquakes belonging to this cluster had reached 21, but most of the events occurred in two spurts of activity lasting one hour each in the early morning of December 27th (8 events) and 28th (7 events).

Monte Cevedale

The last earthquake sequence recorded in 2002 occurred over a time period of only five hours on the evening of Dec. 29th. Its epicenter was situated in northern Italy, 30 km SE of station FUORN, in the area of Monte Cevedale. A total of 12 detected events with $M_L = 1.2$ - 2.6 were associated with this cluster.

Seismic activity during 2003

Overview

During 2003, the Swiss Seismological Service detected and located 523 earthquakes in the region shown in Figure 2003.1. Based on such criteria as the time of occurrence, the location, the signal character or on direct information, 128 additional seismic events were identified as quarry blasts.

Magnitude values of the events recorded in 2003 range between $M_L = 0.2$ and 4.0. The events with $M_L \geq 2.5$ are listed in Tables 2003.1. Where available, the epicentral coordinates and focal depths given in Table 2003.1 are based on the results that include additional data from foreign networks and on 2-D ray-tracing.

Averaged over the last 29 years, we observe about 25 events with $M_L \geq 2.5$ and 8 events with $M_L \geq 3$ per year. With 30 $M_L \geq 2.5$ events and 11 events reaching $M_L \geq 3$ in 2003 (Table 2003.1 and Fig. 2003.2), the seismic activity in these magnitude ranges was thus slightly higher than the 29 year average.

The enhanced activity between mid July and end of August, visible in the plot of the temporal evolution of seismicity (Julian days 185-240 in Fig. 2003.2), corresponds to the earthquake sequences of Sertig and Glarey, which together contribute 16 % to the total number of recorded earthquakes in 2003. Two additional small earthquake sequences with about a dozen events each occurred near Grosio, south of Graubünden in Valtellina, and near Cheyres, at the southern end of Lake Neuchâtel (Fig. 2003.1). The seismic activity below Cima di Jazzi, between Zermatt and Macugnaga, which started in 2002 (Baer et al. 2003), continued with an additional 24 events over the first half of 2003 and with 4 more between September and December.

As in previous years, most of the earthquakes occurred in the Valais and in Graubünden. However, the events of Urnerboden, Nesslau and Lech are evidence for continuing seismic activity also along the northern Alpine front (Fig. 2003.1).

Routinely calculated focal depths for the 523 earthquakes recorded in 2003 range between 1 and 32 km, but only 23 of these hypocenters are deeper than 15 km. As in the past (e.g. Deichmann et al. 2000a), almost all these deep sources are located in the lower crust beneath the Jura Mountains and the Molasse Basin of northern Switzerland.

In what follows, we present the highlights of the seismic activity observed during 2003.

Date & Time UTC	Lat. [°N]	Lon. [°E]	X / Y [km]	Depth [km]	Mag. [M_L]	Q	Location
2003.01.27 16:17:25	45.917	10.587	844/ 90	14	2.8	D	V. Giudicarie, I
2003.01.29 08:00:04	47.261	10.191	808/238	7	3.4	B	Lech, A
2003.01.29 15:18:14	47.241	10.172	807/236	4	2.5	B	Lech, A
2003.02.03 13:11:43	47.027	6.971	564/208	3	2.9	A	Neuchâtel, NE
2003.02.04 20:49:41	46.065	7.765	625/101	6	3.3	B	Täsch, VS
2003.02.09 08:22:46	46.289	10.266	818/130	12	2.8	C	Grosio, I
2003.02.09 16:55:52	46.303	10.249	816/132	14	2.9	C	Grosio, I
2003.02.18 07:42:44	47.246	10.198	809/236	4	2.5	B	Lech, A
2003.02.19 11:30:17	46.297	10.254	817/131	13	3.2	C	Grosio, I
2003.02.24 21:21:21	47.020	6.175	504/208	1	3.1	C	Reugney, F
2003.03.24 07:54:22	47.692	6.707	545/283	18	2.9	C	Belfort, F
2003.04.29 04:55:09	46.341	7.570	610/132	10	3.9	A	Salgesch, VS
2003.05.06 21:59:43	46.905	8.908	712/196	3	4.0	A	Urnerboden, UR
2003.07.16 22:00:33	46.723	9.827	783/177	7	2.8	A	Sertig, GR
2003.07.17 02:27:17	46.729	9.838	783/178	7	3.6	A	Sertig, GR
2003.07.18 10:40:40	46.719	9.832	783/177	7	2.7	A	Sertig, GR
2003.07.18 11:01:36	46.723	9.840	783/177	7	3.9	A	Sertig, GR
2003.07.21 05:45:58	46.823	6.789	550/186	11	2.6	A	Cheyres, FR
2003.08.01 03:20:23	46.729	9.837	783/178	7	3.9	A	Sertig, GR
2003.08.02 08:07:57	46.637	9.838	784/168	7	2.5	B	Piz Kesch, GR
2003.08.12 00:38:54	46.723	9.829	783/177	7	2.9	A	Sertig, GR
2003.08.22 09:21:32	46.323	7.316	590/130	6	3.9	A	Glarey, VS
2003.08.22 09:30:09	46.318	7.315	590/130	6	3.6	A	Glarey, VS
2003.08.24 12:43:41	47.801	8.003	642/295	27	2.9	C	Todtnau, D
2003.08.26 08:58:03	46.420	9.950	793/144	8	2.9	B	Diavolezza, GR
2003.08.31 05:06:35	46.002	9.989	797/ 98	12	2.9	C	Valbondione, I
2003.08.31 05:38:58	47.542	7.898	635/266	17	2.9	A	Zeiningen, AG
2003.10.01 07:31:06	47.200	9.216	735/229	8	3.0	A	Nesslau, SG
2003.11.18 02:44:36	46.493	9.066	725/150	7	2.5	B	Rheinquellhorn, GR
2003.12.02 10:10:26	45.745	10.508	839/ 71	10	2.5	D	Lago d'Idro, I

Table 2003.1: Earthquakes with $M_L \geq 2.5$. The focal depths of the earthquakes for which focal mechanisms have been calculated are based on 2-D ray-tracing or on additional data from foreign networks.
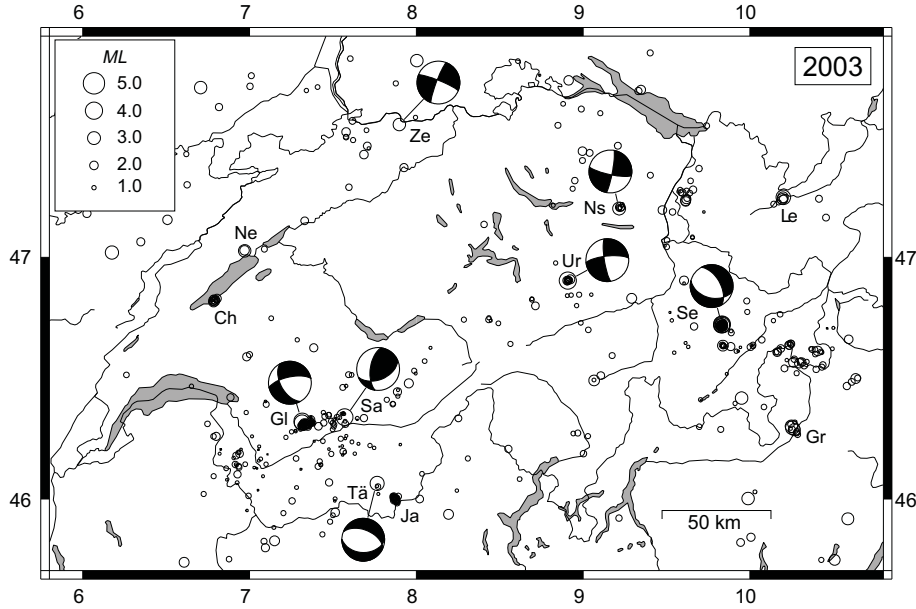
Figure 2003.1: Epicenters and focal mechanisms of earthquakes recorded by the Swiss Seismological Service during 2003. Epicenters of earthquakes mentioned in the text are Cheyres (Ch), Glarey (Gl), Grosio (Gr), Cima di Jazzi (Ja), Lech (Le), Neuchâtel (Ne), Nesslau (Ns), Salgesch (Sa), Sertig (Se), Täsch (Tä), Urnerboden (Ur), Zeiningen (Ze).

Location	Date & Time [UTC]	Depth [km]	Mag.	Plane 1	Plane 2	P-Axis	T-Axis
				Strike/Dip/Rake		Az/Dip	
Täsch	2003/02/04 20:50	6	M_L 3.3	091/40/-106	292/52/-077	252/78	013/06
		9	M_w 3.2	105/47/-102	303/44/-077	303/81	204/01
Salgesch	2003/04/29 04:55	10	M_L 3.9	067/48/ 138	188/60/ 050	305/07	045/55
		12	M_w 3.5	080/68/ 139	188/53/ 028	137/09	038/44
Urnerboden	2003/05/06 22:00	3	M_L 4.0	264/74/-169	171/79/-016	127/19	218/03
		4	M_w 3.7	256/81/-170	164/80/-009	120/13	030/00
Sertig	2003/07/18 11:02	7	M_L 3.9	105/44/-127	331/56/-060	296/64	040/07
		6	M_w 3.6	109/43/-133	341/60/-057	301/60	048/09
Glarey	2003/08/22 09:22	6	M_L 3.9	151/54/-027	258/68/-141	120/43	022/08
		6	M_w 3.7	153/55/-016	252/77/-144	119/34	018/15
Zeiningen	2003/08/31 05:39	17	M_L 2.9	292/82/-172	201/82/-008	156/11	246/00
Nesslau	2003/10/01 07:31	8	M_L 3.0	102/78/-172	010/82/-012	326/14	057/03

Table 2003.2: Focal mechanism parameters based on first-motion polarities (lines with M_L) and full-waveform inversion (lines with M_w).
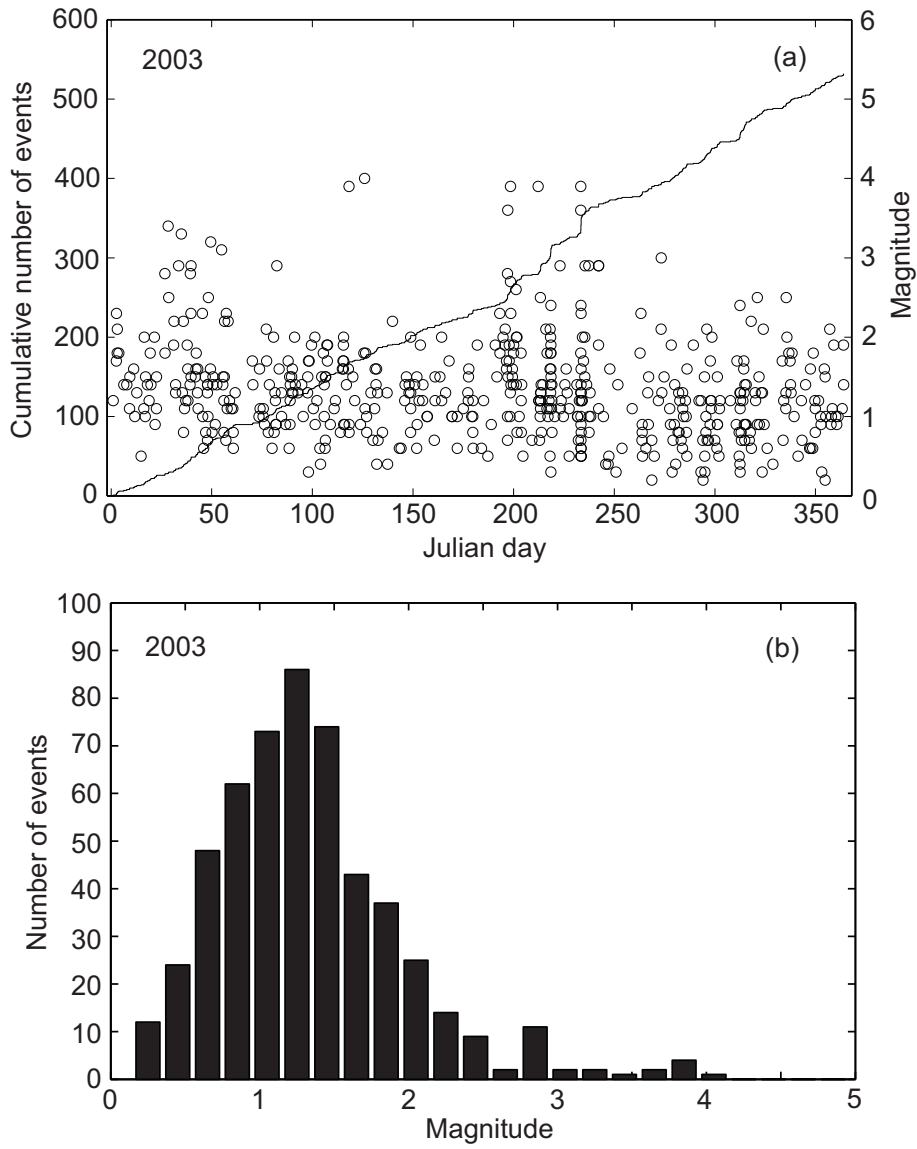
Figure 2003.2: Earthquake activity during 2003: magnitude of each event and cumulative number of events (a); histogram of magnitudes (b).
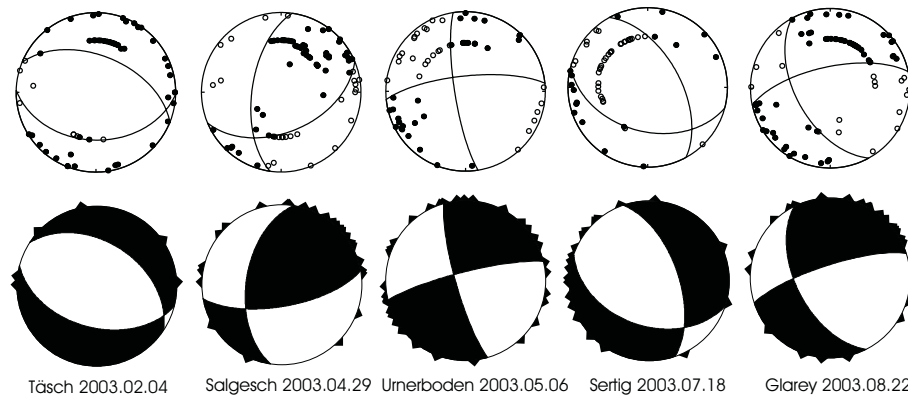
Figure 2003.3: Faultplane solutions (above) based on first-motion polarities and moment tensors (below) based on full-waveform inversion (lower hemisphere, equal area projection). In the faultplane solutions, solid circles correspond to compressive first motion (up) and empty circles to dilatational first motion (down); on the moment tensors, triangles show the station locations.

Significant earthquakes of 2003

Neuchâtel

Although the magnitude of this event, that occurred on February 3rd, reached only a value of M_L 2.9, it was felt quite strongly by the population in the city of Neuchâtel and surroundings. The E-W component of the instrument of the Swiss Strong Motion Network in Neuchâtel, located at an epicentral distance of about 2 km, recorded a peak ground acceleration of 3 % g (Wyss 2004). It was followed by a single aftershock with M_L 2.2 on February 5th. Based on the travel-time difference of only 0.44 seconds between the S- and P-waves recorded by the accelerograph in Neuchâtel, and allowing for uncertainties in epicentral location and seismic velocities, the focal depth must lie between 1.8 and 2.5 km. The sediment thickness in the epicentral area is estimated to be about 2.3 km (Sommaruga 1997). Thus within the remaining hypocentral uncertainty it is not possible to determine whether the source of this event was located in the basement or the overlying mesozoic sediments. The fact that the signals recorded at several seismic stations in the Swiss and French Jura show very strong and long-lasting surface waves, similar to those usually observed from strong quarry blasts at the Earth's surface, suggests that the source was located in the sediments rather than in the basement. However, this hypothesis needs to be tested with synthetic seismograms. Given the focal depth uncertainty and the relatively low magnitude of this event, it was not possible to determine a unique focal mechanism either from first-motion polarities or from a full-waveform inversion. Based on first-motion polarities, both a strike-slip and a thrust-fault mechanism are possible solutions. In both cases, the P-axis is oriented in a NW-SE direction.

Täsch

This event occurred on February 4th in the southern Valais between Randa and Täsch and had a magnitude M_L 3.3 and M_w 3.2. Although it was also recorded
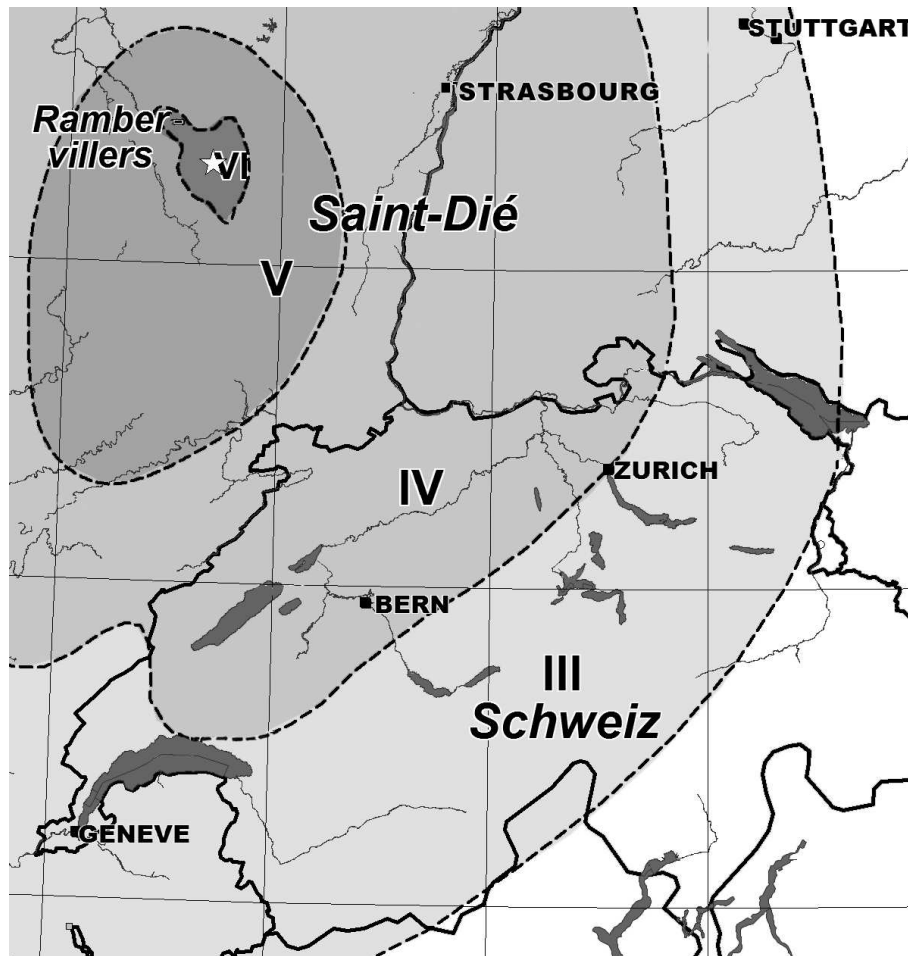
Figure 2003.4: Isoseismal map of the M_L 5.4 Rambervillers event of 2003/02/22 (after Cara et al. 2005).

by temporary instruments deployed above the landslide of Randa at an epicentral distance of about 6 km, and arrival times were modelled by 2D ray-tracing, the focal depth can not be constrained to better than 6 ± 3 km. Nevertheless, the focal mechanism is well constrained by both first-motion polarities and a full-waveform moment tensor inversion: both solutions correspond to normal fault mechanisms whose T-axes agree within $< 10°$. Both the style of faulting and the NNE-SSW orientation of the T-axis is typical of events in the Penninic domain of the southern Valais (Eva et al. 1998, Maurer et. al. 1997, Kastrup et al. 2004).

Rambervillers – Saint Dié

The epicenter of this earthquake, which occurred on February 22nd at 20:41 UTC, was located between the towns of Rambervillers and Saint Dié, in the Vosges mountains of France. It is consequently outside the map in Figure 2003.1 and is therefore not included in Table 2003.1. Nevertheless, this earthquake caused shaking of intensity IV (EMS-98) across all of northwestern Switzerland

	Z	R	T
BUG 8/349			
BSEG 21/675			
RGN 31/834			
RUE 45/688			
MOX 53/446			
BRG 59/603			
GRFO 64/372			
DPC 68/749			
STU 75/199			
KRUC 80/727			
BFO 89/130			
ARSA 96/681			
KBA 102/527			
OBKA 105/635			
DAVA 114/274			
WILA 119/203			
DAVOX 123/303			
BERNI 128/337			
VDL 132/300			
TUE 138/302			
HASLI 145/212			
WIMIS 156/202			
SENIN 165/226			
EMV 174/254			
BNI 178/366			
BRAN 182/156			
GIMEL 186/202			
ARBF 190/547			
EMUR 211/1327			
ATE 226/813			
MTE 237/1426			
ESK 322/1026			
WLF 348/150			

Maximum amplitude: 4.57 μm   500 sec

Figure 2003.5: Moment tensor and waveform fit of the Rambervillers event of 2003/02/22. The best fit is obtained for $M_w = 4.8$ and for a focal depth of 12 km. Strike/dip/rake of the two nodal planes are 304/56/-124 and 174/47/-50; azimuth/plunge of the P- and T-exis are 156/62 and 57/05. Uncertainties estimated from the misfit function are $\pm 5°$ for strike, dip and rake and +1/-3 km for depth.

(Fig. 2003.4) and certainly was the seismic event in 2003, which the public was most aware of. In the area of Basel at an epicentral distance of about 140 km, a strong-motion instrument recorded a peak horizontal ground acceleration of 1 % g (Wyss 2004).

The local magnitude M_L calculated from the Swiss broad-band records with the hypocenter fixed at 48.37°N/6.64°E and 10 km depth, the location calculated by RéNass in Strasbourg from the French and German networks, gives a value of 5.4 (http://eost.u-strasbg.fr/bcsf/). This is the same value as given by RéNass and matches the value of 5.9 given by LDG (http://eost.u-strasbg.fr/bcsf/), for which magnitudes are on average 0.5 units higher than those calculated by the Swiss network (Braunmiller et al. 2005). On the other hand, the moment magnitude M_w from moment tensor inversion of waveforms recorded by Swiss, German and French broad-band stations is only 4.8. The moment tensor itself corresponds to a normal faulting mechanism with a small strike-slip component and a NE-SW oriented T-axis (Fig. 2003.5). The relatively large discrepancy of 0.6 magnitude units between M_L and M_w, compared to the average difference of 0.2, suggests that the source of this event radiated more high-frequency energy than usual.

Salgesch

The M_L 3.9 event that occurred shortly before 7 in the morning on April 29th (local time) caused shaking of intensity IV and V (EMS98) throughout the central Valais (Fig. 2003.6). It was followed 43 minutes later by an aftershock of M_L 1.2. It is also possible that some of the other events detected during the following months in the vicinity of this earthquake constitute additional aftershocks, but this could not be determined with certainty.

The source was located at a depth of 10 km below the town of Salgesch. With four stations (including two strong-motion instruments) within an epicentral distance of only 10 km, the routinely calculated focal depth is reliable. The value of 10 km is confirmed, moreover, by 2D ray-tracing and by the full-waveform inversion, which gives a best fit at 12 km (Table 2003.2).

The focal mechanism, which is well-constrained by numerous first-motion polarities, corresponds to a thrust fault with a strike-slip component and NW-SE oriented P-axis. The moment tensor derived from the full-waveform inversion corresponds to a thrust fault as well, but with a somewhat stronger strike-slip component (Fig. 2003.3). However, strike and dip of one of its nodal planes violate the first-motion data. In the Valais, where normal faulting mechanisms predominate in the Penninic domain south of the Rhone valley and strike-slip mechanisms are the rule in the Helvetic domain to the north, (Maurer et al. 1997; Eva at al. 1998; Kastrup et al. 2004), such thrust fault mechanisms are rare. Nevertheless, the NW-SE orientation of the P-axis matches the direction of maximum horizontal compression derived previously for the northern Valais (Kastrup et al. 2004).

Urnerboden

Shortly before midnight (local time) on May 6th, the population in the region between the cantons Glarus and Uri experienced a moderate earthquake with intensities up to V. The strong-motion station in Linthal, 8 km from the epicenter located in the area of Urnerboden, recorded a peak horizontal acceleration of 7 % g (Wyss 2004). The magnitudes calculated for this event are M_L 4.0 and M_w 3.7.
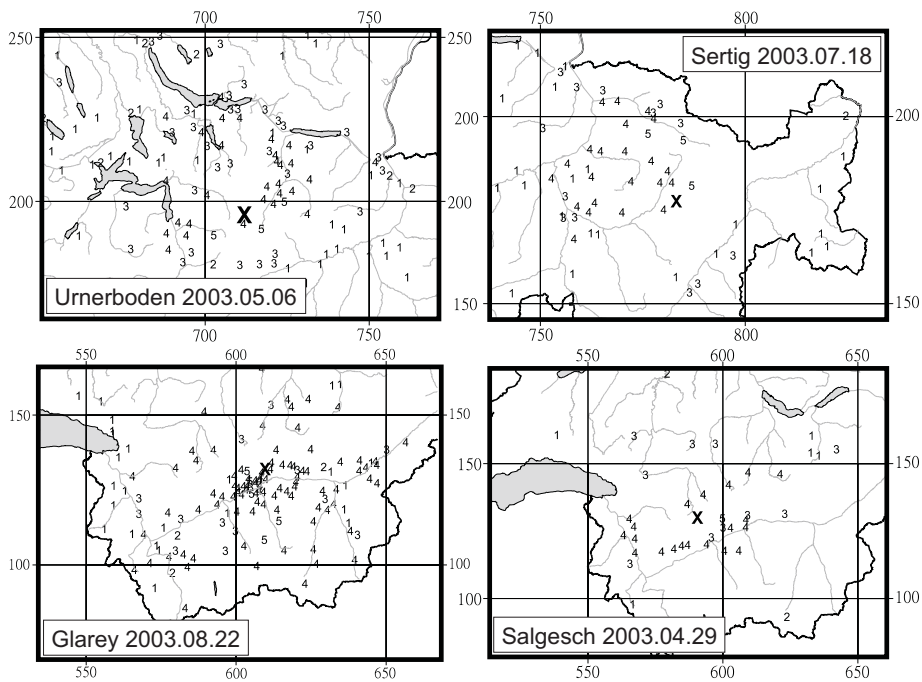
Figure 2003.6: Macroseismic observations for the events of Urnerboden (2003/05/06, 21:59), Sertig (2003/07/18, 11:01)), Salgesch (2003/04/29, 04:55) and Glarey (2003/08/22, 09:21). Each value represents the macroseismic intensity (EMS-98) assigned to a single postal code zone. The X corresponds to the instrumental epicenter. The Swiss cartesian coordinate grid is labeled in km.
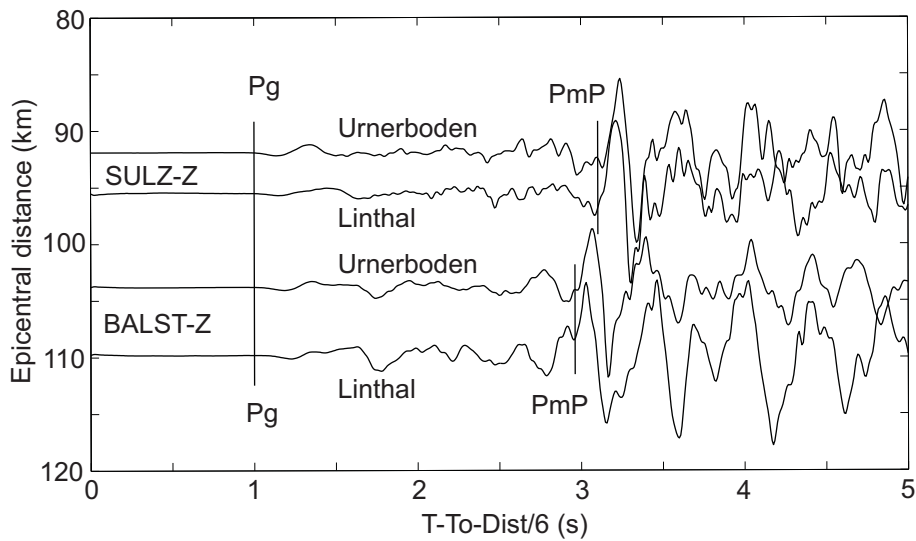
Figure 2003.7: Pairs of signals of the 2003 Urnerboden and the 2001 Linthal events recorded at stations SULZ and BALST. Note the almost identical travel-time differences between PmP and Pg for the two events, which implies that focal depths must be practically the same.

With a minimum epicentral distance of 8 km, the focal depth obtained from routine location procedures is not well constrained. However, the epicenter of this earthquake is located only 7-8 km west of the epicenter of an earthquake that occurred on March 17th 2001 near the town of Linthal. The focal depth of the latter was determined to be 3 km, based on the S-P arrival-time difference observed at the strong-motion station in the immediate vicinity of the epicenter (Deichmann et al. 2002). A comparison of selected seismograms of these two earthquakes shows that focal depths must be practically identical. As shown in Figure 2003.7, travel-time differences between the wave reflected at the Moho (PmP) and the direct wave through the upper crust (Pg) at stations SULZ and BALST, situated at comparable distance and azimuths from the two epicenters, differ by less than 0.1 seconds for the two events. A similar agreement is observed for the travel-time differences between the Pg at SLE and the wave refracted at the Moho (Pn) at station LANF situated on the western border of the Rhinegraben. Thus we fix the focal depth at 3 km for the Urnerboden event as well. This realtively shallow focal depth agrees also with the value of 4 km obtained from the moment tensor inversion.

The strike-slip focal mechanism ist well-constrained by both the first-motion polarities and the full-waveform inversion (Fig. 2003.3). The NW-SE orientation of the P-axis is similar to that observed for the two Linthal events of 1990 and 2001 (Deichmann et al. 2002; Kastrup et al. 2004).

Sertig

July 16th marked the beginning of a swarm-like earthquake sequence of 51 events located about 10 km south of Davos near the village of Sertig Dörfli. As illustrated in Figure 2003.8, the sequence occurred over two distinct time intervals: the first, consisting of 23 events, lasted for one week and included an
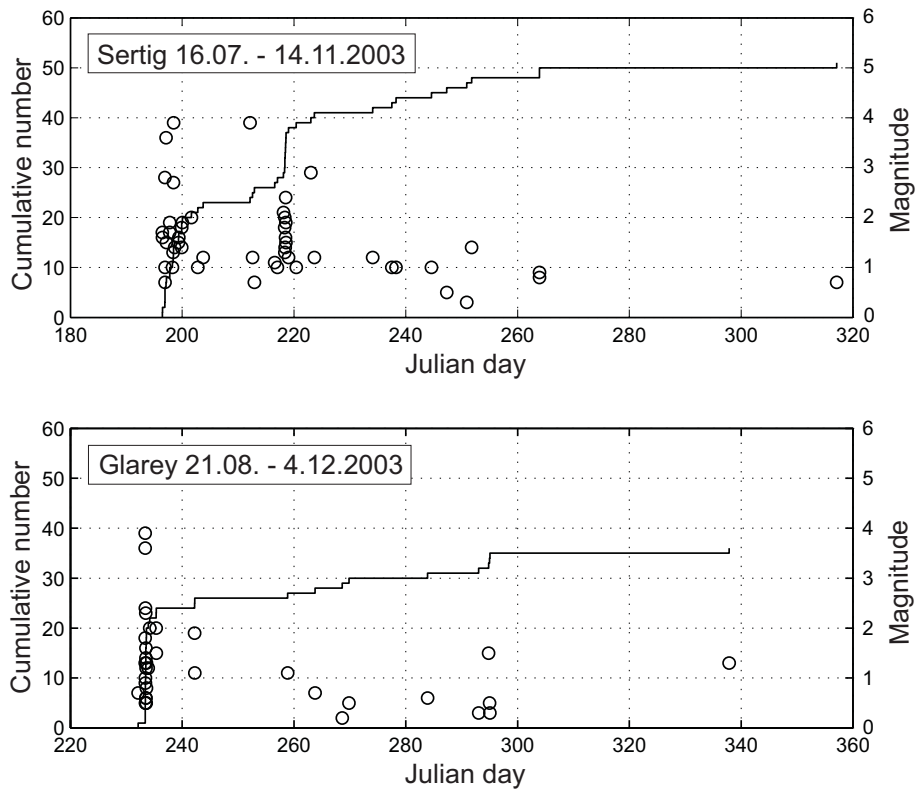
Figure 2003.8: Magnitudes and cumulative number of events for the Sertig and the Glarey earthquake sequences. The concentration of the largest magnitudes and the peak activity at the beginning of the Glarey sequence is typical for a classical mainshock-aftershock pattern; the Sertig sequence, on the other hand, exhibits a more swarm-like behaviour: there are several stronger events and their occurrence does not necessarily coincide with the periods of peak activity.

M_L 3.6 and an M_L 3.9 event (Table 2003.1); after a pause of one week, activity resumed with another M_L 3.9 event on August 1st, and a peak rate of 9 events in less than 12 hours on August 7th. The last event in the sequence was recorded on Nov. 14th.

After the second stronger event on July 18th, a temporary seismograph was deployed 2 km from the epicenter. This instrument recorded 7 events with magnitudes M_L between 1.0 and 2.0. Based on the P- and S-onsets observed at this site, the source of these events must be at a depth of 6-8 km. From a comparison of the arrival times of the reflection from the Moho observed at station MUO, it is evident that the focal depth of all 51 events in the sequence does not vary significantly. We have therefore fixed the focal depth of the $M_L \geq 2.5$ events in Table 2003.1 at 7 km.

Faultplane solutions of the three strongest events are exceptionally well constrained by numerous first-motion polarities. Since all three mechanisms are identical, we include only the focal mechanism of the July 18th event in Table 2003.2 and in Figures 2003.1 and 2003.3. The parameters of the focal mechanisms derived from the full-waveform inversion agree with the fault-plane solutions to within less than 10° for the first two events, and the corresponding focal depth is 6 km in both cases. For the third event, the full-waveform inversion gives a best fit for a focal depth of 9 km and some of the focal mechanism parameters deviate by more than 20° from the other two events. However, a 6 km deep source does not give a significantly larger misfit than the one at 9 km, and in that case the focal mechanism is again within about 10° of the first-motion solution. All solutions correspond to a normal faulting mechanism and the orientations of the T-axis differ by less than 10°. Extensional mechanisms with NE-SW orientation of the T-axis are typical for earthquakes in the eastern Swiss Alps (Kastrup et al. 2004).

Attempts to identify the active faultplane from high-precision relative relocations of the individual hypocenters in this earthquake swarm failed. Most of the rays to the stations at short epicentral distances have take-off angles that are close to one of the nodal planes. As a consequence, the P-waves are weak, and even small focal mechanism variations degrade the signal similarity to the extent that accurate arrival-time determinations based on signal correlations are not possible.

Glarey

In contrast to the swarm-like behaviour of the Sertig sequence, the earthquake sequence of Glarey, Valais, followed a classical foreshock-mainshock-aftershock pattern (Fig 2003.8). After a single small foreshock the day before (M_L 0.7), the sequence started August 22nd at 11:21 (local time) with the M_L 3.9 (M_w 3.7) mainshock. Over the following 4 months an additional 34 events were detected within a 2 by 2 km large epicentral area that includes the mainshock. The peak activity, however, was concentrated at the beginning of the sequence, with the occurrence of 18 events in the first 5 hours, including an M_L 3.6 (M_w 3.5) event less than 8 minutes after the mainshock.

In addition to station SENIN at an epicentral distance of 5 km, six strong-motion stations recorded the mainshock within a radius of 8-12 km. Thus both the epicenter and the focal depth are well constrained. The epicenter is located 3-4 km SE of the Sanetsch Pass. Shaking intensities as high as V (EMS-98) were reported in the area of Ayent, which coincides with a peak horizontal acceleration of close to 6 % g recorded by an accelerograph in Ayent-Fortunoz,
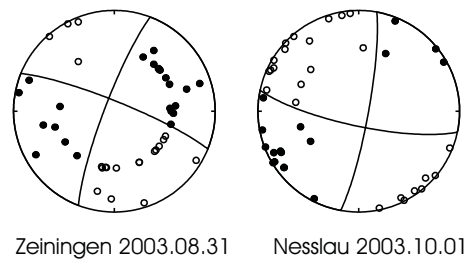
Zeiningen 2003.08.31   Nesslau 2003.10.01

Figure 2003.9: Faultplane solutions based on first-motion polarities for the Zeiningen and Nesslau events.

about 7 km from the epicenter (Wyss 2004). Intensities of IV were observed out to epicentral distances of about 30 km. The focal depth of 6 km determined routinely matches the value obtained from the full-waveform inversion.

The focal mechanism of the mainshock from both the first-motion analysis and the moment tensor inversion corresponds to a normal fault with a strong strike-slip component (Table 2003.2 and Fig. 2003.3). The moment tensor solution for the strongest aftershock does not differ significantly from that of the mainshock and is thus not included separately. The resulting NNE-SSW orientation of the T-axis lies within the range of T-axis orientations observed previously in the northern Valais (Kastrup 2004).

Zeiningen

Both the focal depth and the faultplane solution (Fig. 2003.9) of this M_L 2.9 event, which occurred August 31st near the town of Zeiningen, Aargau, are well-constrained by numerous observations and by 2D ray-tracing. This event is typical for the lower-crustal earthquakes below the Tabular Jura mountains of northern Switzerland (Deichmann et al. 2000b; Kastrup et al. 2004). In fact, the focal depth of 17 km as well as the strike-slip mechanism with NNW-SSE oriented P-axis are almost identical to those of the event that occurred in 1999 about 15 km further west near the town of Pratteln (Deichmann et al. 2000a).

Nesslau

The M_L 3.0 earthquake that occurred on October 1st north of the Walensee near Nesslau was the second and strongest event of a sequence of 8 events: the first 4 occurred between October 1st and 2nd, while the second four occurred between November 10th and 12th. Magnitudes of the other events are between M_L 0.7 and 2.1.

Routine location procedures give a focal depth of 12 km. However, with a minimum epicentral distance of 21 km, this value is unreliable. The focal depth of 8 km, which results from a non-linear location procedure based on a 3-D velocity model (Husen at al. 2003) and which is supported by 2-D ray tracing, is the more likely value. Given the thickness of the sedimentary cover in this region (Stäuble & Pfiffner 1991) and the remaining focal depth uncertainty, it is not possible to decide whether the source is located in the crystalline basement or above.

The strike-slip focal mechanism (Fig. 2003.9) is well constrained and is very similar to that of the M_L 3.6 Walenstadt event of April 21st, 1998 (Baer et al.

1999). The latter was located 11 km east of the Nessalu event at a depth of about 10 km and its P- and T-axes are rotated 20° clockwise with respect to the Nesslau event. The mechanisms of both events agree with the predominant NW-SE oriented compression in this region (Roth et al. 1992; Kastrup et al. 2004).

Seismic activity during 2004

Overview

On a global level, the seismicity of the year 2004 will undoubtedly be remembered for the enormous earthquake on December 26th off the west coast of Sumatra, which was one of the two or three largest earthquakes of the past century and which caused one of the most disastrous tsunamies in known history. Although the direct seismological consequences of this earthquake were comparably insignificant for Switzerland, it is noteworthy that the broad-band seismometers of the Swiss Seismological Service recorded a vertical displacement of more than 2 cm as the long-period surface waves propagated across the country.

On a local scale in 2004, five earthquakes produced ground shaking of intensity IV over large regions of the country. This is somewhat unusual and serves to remind the public that seismic hazard is a concern also for Switzerland. Nevertheless, in terms of numbers of recorded earthquakes, the year 2004 in Switzerland and immediate surroundings was not out of the ordinary. During 2004, the Swiss Seismological Service detected and located 672 earthquakes in the region shown in Figure 2004.1. Based on such criteria as the time of occurrence, the location, the signal character or on direct information, 101 additional seismic events were identified as quarry blasts. Magnitude values of the events recorded in 2004 range between $M_L = 0.1$ and 4.8. The events with $M_L \geq 2.5$ are listed in Table 2004.1. Where available, the epicentral coordinates and focal depths given in Table 2004.1 are based on the results that include additional data from foreign networks and on 2-D ray-tracing.

Averaged over the last 30 years, we observe about 25 events with $M_L \geq 2.5$ and 8 events with $M_L \geq 3$ per year. With 22 $M_L \geq 2.5$ events and 7 events reaching $M_L \geq 3$ in 2004 (Table 2004.1 and Fig. 2004.2), the seismic activity in these magnitude ranges was thus close to the 30 year average.

The enhanced activity in April and May, visible in the plot of the temporal evolution of seismicity (Julian days 100-150 in Fig. 2004.2), corresponds to the earthquake sequence of Derborence (Valais), which alone contributes 25 % to the total number of recorded earthquakes in 2004. The seismic activity in the region of Cima di Jazzi, between Zermatt and Macugnaga, which started in 2002 (Baer et al. 2003, Deichmann et al. 2004), flared up again in March 2004 and continued throughout the whole year with an additional 31 events ranging in magnitude between 0.9 and 2.3. Moreover, in autumn a small cluster of a dozen events with magnitudes between 0.4 and 1.9 appeared near Sierre. Thus the large total number of detected earthquakes (672) in 2004, compared to previous years, is due in part to these earthquake sequences and in part to an increase in sensitivity of the high-gain network since switching the event detection from the old analog data acqusition system to the new broad-band

Date & Time UTC	Lat. [°N]	Lon. [°E]	X / Y [km]	Depth [km]	Mag. [M_L]	Q	Location
2004.02.17 03:53:44	46.721	10.642	845/179	21	2.5	B	Val Venosta, I
2004.02.18 14:26:01	46.607	6.995	566/162	9	3.1	A	Bulle, FR
2004.02.18 14:31:58	46.609	6.995	566/162	9	3.3	A	Bulle, FR
2004.02.18 15:29:36	46.604	6.999	566/161	9	2.6	A	Bulle, FR
2004.02.23 17:31:21	47.278	6.270	512/237	15	4.8	B	Besançon, F
2004.04.15 15:14:58	47.525	8.726	697/264	13	2.7	A	Winterthur, ZH
2004.04.18 03:21:05	47.621	9.655	767/277	31	3.0	A	Lindau, D
2004.04.18 08:23:35	47.692	8.892	709/283	22	2.6	A	Stein am Rhein, SH
2004.05.17 08:35:06	45.735	6.966	563/ 65	12	2.6	B	Pré St.-Didier, I
2004.05.30 07:20:15	46.284	7.191	581/126	9	2.7	A	Derborence, VS
2004.05.30 09:46:17	46.284	7.193	581/126	9	2.9	A	Derborence, VS
2004.06.12 04:44:33	45.717	6.947	562/ 63	12	3.3	B	Pré St.-Didier, I
2004.06.12 16:47:24	46.276	7.197	581/125	8	2.6	A	Derborence, VS
2004.06.21 23:10:02	47.505	7.713	621/261	22	3.8	A	Liestal, BL
2004.06.28 23:42:30	47.525	8.169	655/264	20	4.0	A	Brugg, AG
2004.06.29 00:02:12	47.523	8.163	654/264	20	2.7	A	Brugg, AG
2004.06.29 22:43:04	47.520	8.165	655/263	20	2.6	A	Brugg, AG
2004.07.27 23:05:24	47.342	6.543	532/244	1	2.7	C	Col de Ferriere, F
2004.07.28 16:25:17	47.342	6.555	533/244	1	2.5	C	Col de Ferriere, F
2004.10.09 22:19:35	46.430	10.545	839/147	13	2.5	C	M. Cevedale, I
2004.11.08 11:52:40	47.715	8.519	681/285	23	2.8	A	Siblingen, SH
2004.12.06 01:52:17	47.426	7.885	634/253	11	2.5	B	Gelterkinden, BL

Table 2004.1: Earthquakes with $M_L \geq 2.5$. The focal depths of the earthquakes for which focal mechanisms have been calculated are based on 2-D ray-tracing or on additional data from foreign networks.
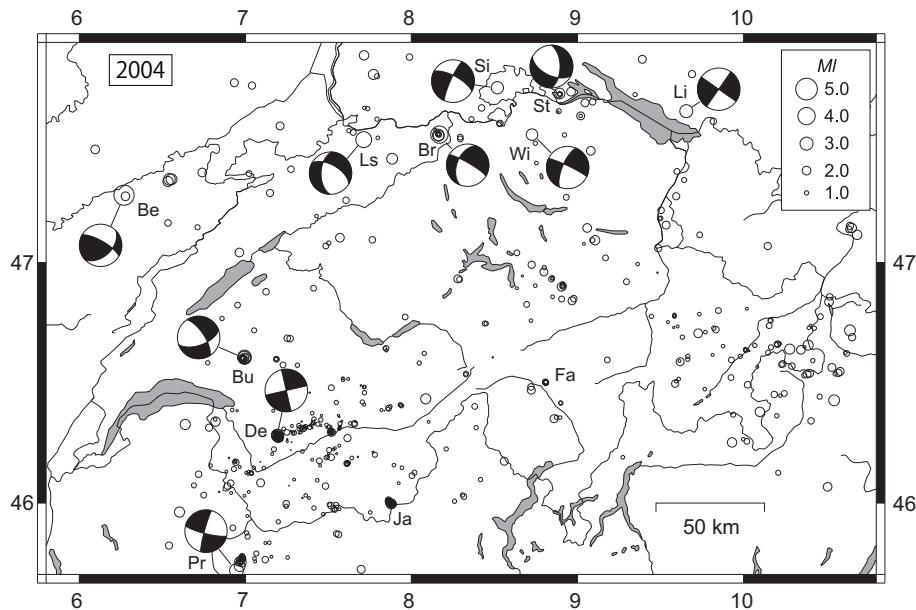
Figure 2004.1: Epicenters and focal mechanisms of earthquakes recorded by the Swiss Seismological Service during 2004. Epicenters of earthquakes mentioned in the text are Besançon (Be), Brugg (Br), Bulle (Bu), Derborance (De), Faido (Fa), Cima di Jazzi (Ja), Liestal (Ls), Lindau (Ld), Pré St.-Didier, Siblingen (Si), Stein am Rhein (St), Winterthur (Wi).

digital instrumentation at the end of August 2001 (Deichmann et al. 2002).

As in previous years, most of the earthquakes occurred in the Valais and in Graubünden. However, the strongest events (Besançon, Brugg and Liestal) occurred below the northern Alpine foreland. Routinely calculated focal depths for the 672 earthquakes recorded in 2004 range between 0 and 31 km, but only 39 of these hypocenters are deeper than 15 km. As in the past (e.g. Deichmann et al. 2000a), almost all these deep sources, and in particular the magnitude M_L 4.0 event of Brugg with its 7 aftershocks, are located in the lower crust beneath the Jura Mountains or the Molasse Basin of northern Switzerland.

In what follows, we present the highlights of the seismic activity observed during 2004. For the stronger events, the traditional determination of focal mechanisms from the azimuthal distribution of first-motion polarities (fault-plane solutions) has been complemented by a moment tensor based on full-waveform inversion. For these events we list in Table 2004.2 the moment magnitude (M_w) in addition to the local magnitude (M_L). Moment magnitude is calculated from the seismic moment M_0 obtained from the moment tensor inversion using the relation $M_w = (2/3) \log M_0 - 6$, where M_0 is given in N-m (Hanks & Kanamori 1979). The complete set of moment tensors calculated by the Swiss Seismological Service, including plots of all waveform fits, is available on line (http://www.seismo.ethz.ch/mt/). More comprehensive and detailed explanations of the data analysis procedures are given in previous annual reports (e.g Deichmann et al. 2004) and can be downloaded from our website (*Introduction.pdf* under *Reports* at http://www.seismo.ethz.ch).

Figure 2004.2: Earthquake activity during 2004: magnitude of each event and cumulative number of events (above); histogram of magnitudes (below).

Location	Date & Time [UTC]	Depth [km]	Mag.	Plane 1 Strike/Dip/Rake	Plane 2	P-Axis Az/Dip	T-Axis
Bulle	2004/02/18 14:32	9	M_L 3.3	327/69/-032	070/60/-155	286/38	020/05
		9	M_w 3.2	336/80/-019	070/71/-020	292/20	024/06
Besançon	2004/02/23 17:31	15	M_L 4.8	300/73/ 134	047/47/ 024	359/16	253/44
		12	M_w 4.5	296/74/ 119	053/32/ 031	004/24	240/53
Winterthur	2004/04/15 15:15	13	M_L 2.7	203/70/-007	295/83/-160	161/19	068/09
Lindau	2004/04/18 03:21	31	M_L 3.0	215/90/ 000	125/90/ 180	170/00	080/00
Stein am Rhein	2004/04/18 08:23	22	M_L 2.6	116/56/-139	360/57/-042	327/51	058/01
Derborence	2004/05/30 09:46	9	M_L 2.9	347/90/ 000	077/90/-180	302/00	212/00
Pré St.-Didier	2004/06/12 04:44	12	M_L 3.3	104/80/-006	195/84/-170	060/11	329/03
		12	M_w 3.3	099/86/-013	190/77/-176	054/12	145/06
Liestal	2004/06/21 23:10	22	M_L 3.8	182/53/-041	300/58/-135	154/53	060/03
		21	M_w 3.4	199/66/-043	309/51/-149	158/47	257/09
Brugg	2004/06/28 23:42	20	M_L 4.0	202/48/-012	300/81/-137	170/36	064/21
		21	M_w 3.5	202/44/-004	295/88/-134	169/33	059/28
Siblingen	2004/11/08 11:53	23	M_L 2.8	298/70/-170	205/81/-020	160/21	253/07
Lago di Garda	2004/11/24 22:59	9	M_w 5.0	068/60/ 103	223/32/ 069	148/14	008/72
Waldkirch	2004/12/05 01:52	12	M_w 4.6	014/75/-016	109/74/-165	331/22	062/01

Table 2004.2: Focal mechanism parameters based on first-motion polarities (lines with M_L) and full-waveform inversion (lines with M_w).

Significant earthquakes of 2004

The sequence of Bulle

On February 18th at 15:26 local time, the region between Lausanne and Fribourg was jolted by a first earthquake of magnitude M_L 3.0. It was followed six minutes later by a second slightly stronger event (M_L 3.3) and an hour later by a third one with M_L 2.6. All three were felt by the public. These three stronger events were part of a small sequence of 12 recorded events during the time between January 2nd and October 9th. The epicenters were located about 5 km west of the town of Bulle. Routine hypocenter location gives a focal depth of around 10 km for the strongest and best recorded event. However, with an epicentral distance to the closest station of 20 km, this value is poorly constrained. Using a 3D velocity model (Husen et al. 2003) and Pn arrivals out to distances of more than 200 km gives a focal depth of 9 km. This value is the most likely focal depth and is confirmed by 2D ray tracing along a profile trending NE from the epicenter and by the result of the full-waveform moment tensor inversion. For the strongest of theses events, both the moment tensor and the faultplane solution based on first motion polarities result in a strike-slip focal mechanism with a slight normal-faulting component (Figure 2004.3 and Table 2004.2). Based on the strong waveform similarity and the almost identical P to S amplitude ratios, it is evident that the three strongest events occurred almost at the same location and with the same focal mechanism. The moment magnitude, M_w, is 3.0 for the first and 3.2 for the second of the two strongest events. The WNW-ESE orientation of the P-axis and the corresponding NNE-SSW orientation of the T-axis are what one would expect from the stress field deduced from previous earthquakes in the Alpine foreland of western Switzerland (Kastrup et al. 2004).

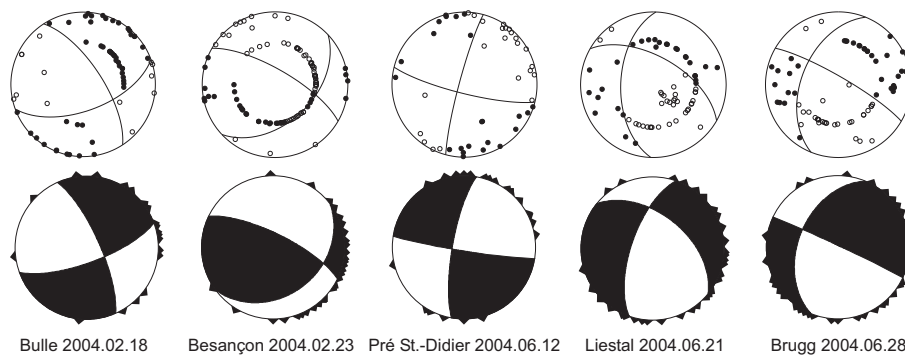| Bulle 2004.02.18 | Besançon 2004.02.23 | Pré St.-Didier 2004.06.12 | Liestal 2004.06.21 | Brugg 2004.06.28 |

Figure 2004.3: Faultplane solutions (above) based on first-motion polarities and moment tensors (below) based on full-waveform inversion (lower hemisphere, equal area projection). In the faultplane solutions, solid circles correspond to compressive first motion (up) and empty circles to dilatational first motion (down); on the moment tensors, triangles show the station locations.

Besançon – Roulans

The strongest event of 2004 in the region covered by the map in Figure 2004.1 occurred on February 23rd at 18:31 local time. Its epicenter was located in the French Jura, near the town of Roulans, approximately 20 km NE of Besançon. According to a compilation of the Bureau Central Sismologique Français, this earthquake caused some light damage in the epicentral area, so that the epicentral intensity I_0 was estimated to be V-VI on the European Macroseismic Scale (BCSF 2004). As shown in Figure 2004.4, it was clearly felt (intensity IV) across most of western and northern Switzerland. Magnitudes calculated by the Swiss Seismological Service are M_L 4.8 and M_w 4.5. Local magnitudes reported by other institutions are in part significantly higher: 5.0 (LED *Jahresbulletin 2004*), 5.1 (RéNaSS) and 5.9 (LDG) (BCSF, 2004). One aftershock, on Feb. 26th at 01:58 local time, was strong enough (M_L 2.1) to trigger the Swiss network. Locations based both on 1D and 3D crustal models give focal depths in the range between 11 and 17 km. Given that the closest epicentral distance is over 40 km, these depth values are unreliable. The best fit of the full-waveform inversion is obtained for 12 km and a good match between observed and calculated travel-time differences for 2D raytrace profiles trending SE and E is obtained for 15 and 16 km. In Table 2004.1 and for calculating take-off angles for the faultplane solution, the focal depth was fixed at 15 km. Both the moment tensor and the faultplane solution correspond to an oblique thrust (Table 2004.2 and Figure 2004.3). The strike and dip of the NW-SE trending nodal plane is very well constrained by the observed first motion polarities and differ by less than 5 degrees from the moment tensor solution. For some stations, later arrivals with impulsive onsets, which could be identified unequivocally as direct waves based on 2D ray tracing, were also used in the faultplane solution. The orientation of the other nodal plane and thus the degree of thrusting depend strongly on the take-off angles of the negative onsets observed in the SE quadrant of the faultplane solution. Whereas the strike of this nodal plane differs by only 5 degrees between faultplane solution and moment tensor, the dip differs by 14 degrees. Nevertheless, both the style of faulting and the orientation of the P-axis are well constrained and are rather unusual. Earthquakes with a strong
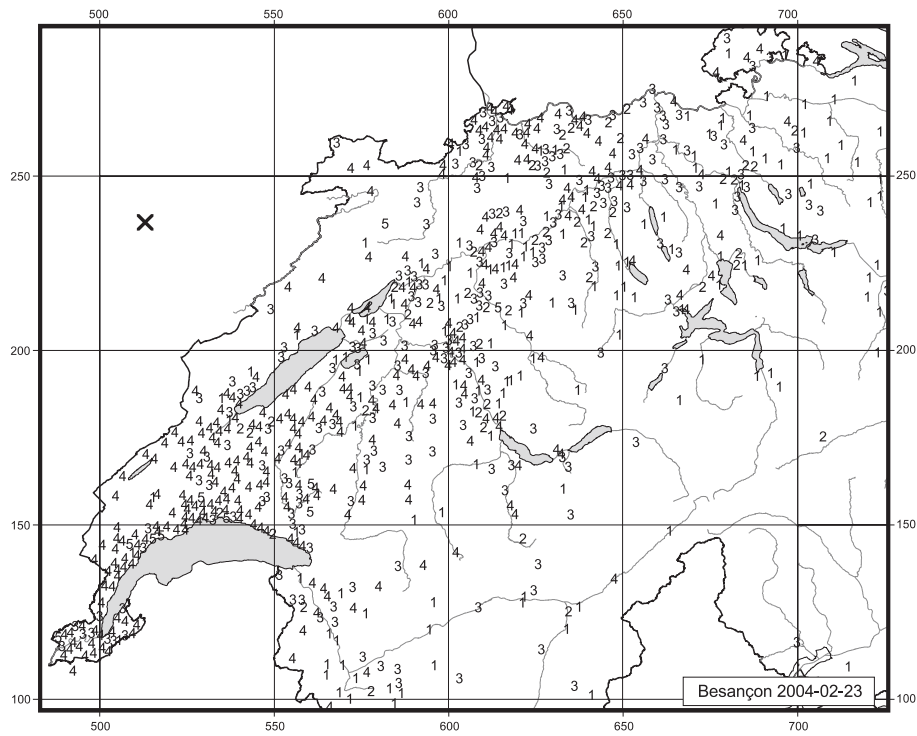
Figure 2004.4:   Macroseismic   observations   for   the   event   of   Besançon (2004/02/23, 18:31 local time).   Each value represents the macroseismic intensity (EMS-98) assigned to a single postal code zone. The X corresponds to the instrumental epicenter. The Swiss cartesian coordinate grid is labeled in km.
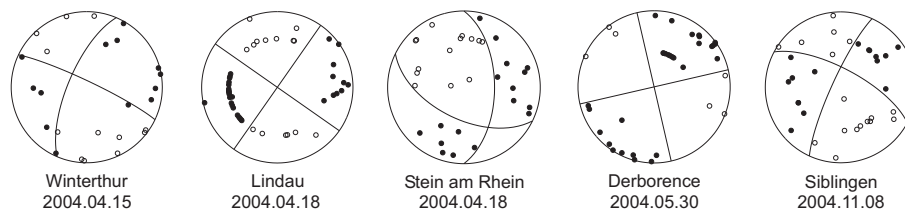
Figure 2004.5: Faultplane solutions based on first-motion polarities for four small earthquakes in northeastern Switzerland.

thrust component are rare in the crystalline basement of the northern Alpine foreland, and from an extrapolation of regional stress inversions one would expect a NW-SE oriented P-axis rather than the observed N-S orientation (Müller et al. 1992; Delouis et al., 1993; Plenefisch & Bonjer 1997; Kastrup et al. 2004).

Seismic events and rockbursts in the new Gotthard tunnel

Between March 26th and April 16th, 2004, a small earthquake sequence of five events with magnitudes M_L between 0.9 and 1.4 occurred near Faido, TI. This sequence was not recognised as being anything unusual, until it became known that both the time of occurrence and the epicentral location of these events correlate with some rather violent rockbursts in a section of the new Gotthard railroad tunnel, that is still under construction. Given that the seismic activity has flared up again in 2005, the causal relation between the earthquakes, rockbursts and observed deformation of the tunnel cross-section is the object of further studies, that include the deployment of an additional temporary network of seismometers in the epicentral area.

Winterthur

Despite its small magnitude (M_L 2.7), this earthquake, that occurred on April 15th at 17:15 local time near Winterthur, was felt by a few people. With good azimuthal station coverage and with two stations at epicentral distances close to the focal depth, both the epicenter location and the focal depth of 13 km are well constrained. The strike-slip focal mechanism with NNE-SSW and ENE-WSW oriented P- and T-axes (Figure 2004.5) is typical for midcrustal earthquakes in northeastern Switzerland (Deichmann et al. 2000b; Kastrup et al. 2004).

Lindau

The earthquake with M_L 3.0 that occurred at 05:21 local time on April 18th NE of Lake Constance near the town of Lindau was the deepest event recorded in 2004 in and around Switzerland. Focal depths for this event determined routinely with a 1D velocity model range between 29 and 33 km. The location based on the 3D model of Husen et al. (2003) also gives a focal depth of 33 km. Modelling of travel-time differences between the direct arrival (Pg) and the refracted at the Moho (Pn) shows that the source must be one or two km above the Moho, which according to Waldhauser et al. (1998) is at a depth of 32 km. In Table 2004.1 and for calculating take-off angles for the faultplane solution, the focal depth was thus fixed at 31 km. Although the available first-motion data allow for some variability in strike and dip of the nodal planes, the style of

faulting (strike-slip) is unambiguous (Figure 2004.5). Both the orientation of the P- and T-axes and the focal depth are not unusual for northeastern Switzerland and the neighboring parts of southern Germany. In 2001 an earthquake with M_L 2.9, a focal depth of 30 km and a similar strike-slip mechanism occurred near Oberriet, SG, just 30 km to the south of the Lindau event (Deichmann et al. 2002).

Stein am Rhein

This small earthquake (M_L 2.6), which occurred only 5 hours after the Lindau event, was located at a depth of 22 km just north of Stein am Rhein. The high station density provided by the newly installed instruments in northeastern Switzerland in 2003 and by the stations in southern Germany provide an excellent azimuthal coverage and thus a reliable location and a well-determined faultplane solution (Figure 2004.5). With four stations within an epicentral distance of less than 20 km, the focal depth is also well constrained. The oblique normal faulting mechanism with a ENE-WSW striking T-axis is similar to that of the M_L 4.2 event that occurred near Steckborn in 1986 (Deichmann et al. 2000b; Kastrup et al. 2004).

The sequence of Pré St.-Didier

Between April 15th and November 9th the Swiss seismograph network recorded a sequence of 17 events near Pré St.-Didier, east of Courmayeur, Italy. The magnitudes range between M_L 0.9 and 3.3. Five of these events, including one with M_L 2.6, occurred on May 17th and four, including the strongest event, on June 12th (Table 2004.1). Because of their location outside of the Swiss network, the quality of the routine epicenter determination is poor and the focal depth can not be determined. For the strongest event, we merged the Swiss data with the waveforms obtained from the universities of Genova and of Grenoble. To ensure a sufficiently good azimuthal coverage and to minimize the effects of crustal heterogeneity, for the final location we used 16 P and 5 S readings at stations out to 70 km. Despite this measure, some traveltime residuals, in particular for the S-readings, remain high, indicating that the crustal model used is probably unsuitable for this region. Thus, given also that the epicentral distance to the closest station is 19 km, the resulting focal depth of 7 km is not reliable. The optimal depth obtained from matching the waveforms in the inversion for the moment tensor as well as the travel-time differences between the direct waves (Pg) and the waves refracted at the Moho (Pn) along a 2D raytrace profile across the Alps and northern Alpine foreland is 12 km. This is the depth that was used to calculate the take-off angles of the rays at the source for the faultplane solution. However it was not possible to construct a completely self-consistent faultplane solution. The result shown in Figure 2004.3 and listed in Table 2004.2 is the one with a minimum number of inconsistent polarities (3) that most closely matches the moment tensor solution. While the exact orientation of the nodal planes, because of the remaining inconsistencies, is still slightly ambiguous, the style of faulting (strike-slip) is well constrained by both the faultplane solution and the moment tensor. The orientation of the T-axis at a high angle to the strike of the Alpine chain in this area is typical for the extensional regime observed in many zones of high elevations in the Alps (e.g. Maurer et al. 1997; Eva et al. 1998; Kastrup et al. 2004).
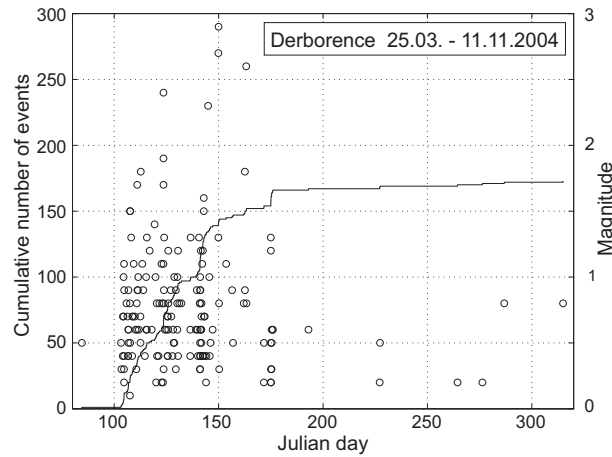
Figure 2004.6: Magnitudes and cumulative number of events for the Derborence earthquake sequence.

The sequence of Derborence

In Table 2004.1, we list three events with magnitudes M_L 2.7, 2.9 and 2.6 at location Derborence. The two strongest ones occurred within a few hours of each other on May 30th. All three are part of an earthquake sequence comprising 173 detected events in the magnitude range between 0.2 and 2.9. As shown in Figure 2004.6, the first event was recorded on March 25th and the last one on November 11th. However, the main activity (165 events) was concentrated between April 13th and June 25th, with the peaks, in terms of number of events per 24 hours, on May 21st-22nd (17 events) and on June 24th-25th (12 events). It is noteworthy that after this last activity spurt the event frequency dropped very abruptly and that the three strongest events occurred during a period of relative quiescence. Routine locations put the epicenters of this cluster near Pas de Cheville, located 2 km south of the summit of Les Diablerets, and epicenters of 90% of the events are scattered within a radius of 1 km about the mean location. Based on the high degree of signal similarity, the epicenters of these events are probably clustered even more tightly in reality, but this would need to be verified by signal correlation and relative location procedures. Routinely calculated focal depths range between 6 and 9 km. Modelling of travel-time differences between Pn and Pg at stations in northern Switzerland and southern Germany suggests a depth of 9 km. The faultplane solution for the strongest event based on the available first-motion data is compatible with a pure strike-slip focal mechanism (Table 2004.2 and Fig. 2004.5), with one of the nodal planes striking in the same direction as the general trend of the epicenter alignment in the northern Valais (Fig. 2004.1). Whereas this nodal plane is well constrained by the data, the orientation of the other nodal plane is poorly determined. It is thus possible that the actual direction of slip was more oblique than suggested by Figure 2004.5, but this would not change the NW-SE and NE-SW orientation of the P- and T-axes significantly.
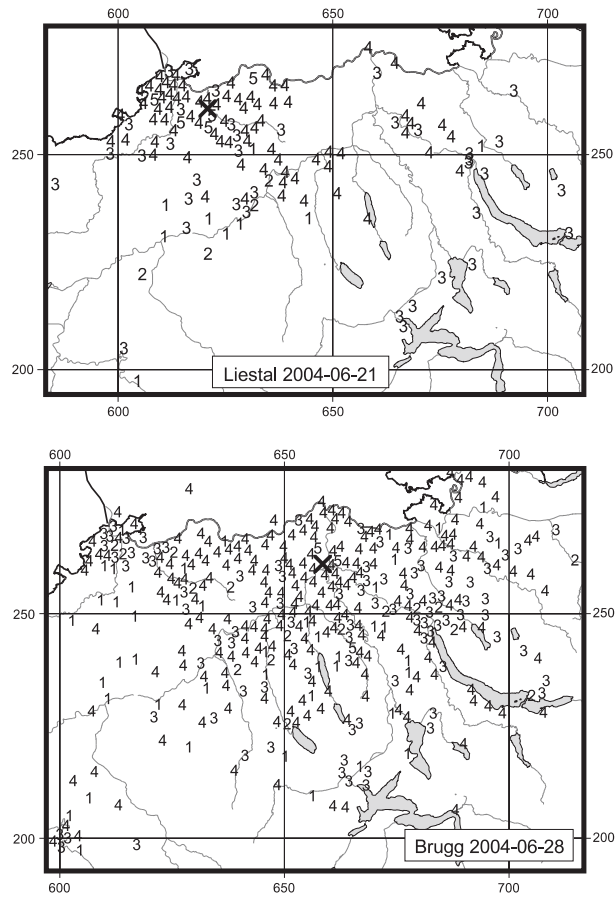
Figure 2004.7: Macroseismic observations for the events of Liestal (2004/06/22 01:10 local time) and Brugg (2004/06/29, 01:42 local time). Otherwise as in Figure 4.

Liestal

The earthquake, which occurred during the night of June 21st to 22nd near Liestal, BL, woke up many people in northwestern Switzerland. The epicentral intensity reached IV and magnitudes are M_L 3.8 and M_w 3.4 (Figure 2004.7). Given a large number of strong-motion stations in the Basel area, the focal depth of 22 km is well constrained by 14 records within an epicentral distance of less than 20 km. Thanks to the excellent azimuthal distribution of records from seismic stations in southern Germany as well as in Switzerland, the normal faulting focal mechanism with an ENE-WSW oriented T-axis obtained from the faultplane solution is also very well determined (Figure 2004.3). The moment tensor has a slightly stronger strike-slip component and its T-axis is rotated clockwise by 17 degrees with respect to the faultplane solution (Table 2004.2). No aftershocks were detected for this earthquake.

Brugg

Almost exactly one week after the Liestal event, during the night of June 28th to 29th, another moderate earthquake produced shaking of intensity IV over most of northern Switzerland (Figure 2004.7). Magnitude values computed for this event are M_L 4.0 and M_w 3.5. The focal depth, constrained by clear S- and P-arrivals at stations SULZ and ACB, located at epicentral distances of 4 and 9 km, is 20 km. The faultplane solution and the moment tensor are well determined and almost identical (Figure 2004.3 and Table 2004.2). The resulting focal mechanism is rather unusual: it corresponds either to lateral motion on a flatly dipping NNE-SSW striking faultplane or to oblique normal faulting on an almost vertical NW-SE striking faultplane. However, the ENE-WSW orientation of the T-axis agrees with the regional deformation pattern and stress regime of the region (Deichmann et al. 2000b; Kastrup et al. 2004). This earthquake was followed by seven aftershocks with M_L between 0.7 and 2.7. The first four occurred within 24 hours of the mainshock, the next two followed on July 2nd and 10th, and the last one occurred almost six months later, on October 10th. The earthquake of Brugg and its aftershocks occurred in a previously aseismic area of northern Switzerland. Practically no other earthquake had been detected in this area since the beginning of modern instrumental monitoring in 1975, and at most one single comparable event is likely to have occurred here since the foundation of the Swiss Earthquake Commission in 1878 (Deichmann et al. 2000b). It is noteworthy that, judging from Figure 2004.7, the event of Brugg seems to have been felt much more widely than the Liestal event, although their magnitudes M_L differ by only 0.2 units and they both occurred at the same time of day, at almost the same focal depth and in the same general region.

Siblingen

The small event (M_L 2.8) that occurred on November 8th near Siblingen, NW of Schaffhausen, is another one of those lower-crustal earthquakes commonly observed below the northern Alpine foreland. Its location and focal depth of 23 km are well constrained by a uniform azimuthal station distribution and by three stations within an epicentral distance of 20 km. The well-determined strike-slip mechanism with an ENE-WSW oriented T-axis (Figure 2004.5) is typical for northeastern Switzerland (Deichmann et al. 2000b; Kastrup et al. 2004).
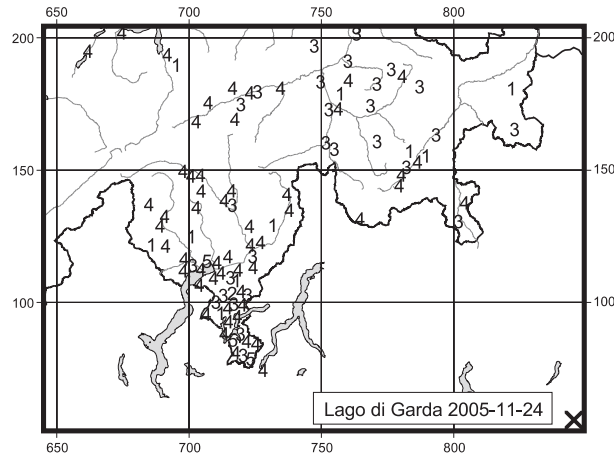
Figure 2004.8: Macroseismic observations for the event of Lago di Garda (2004/11/24, 23:59 local time). Otherwise as in Figure 4.
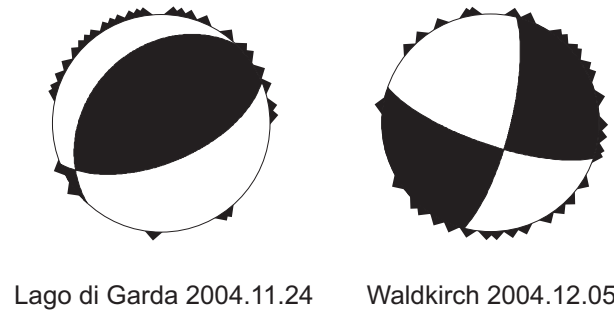

Lago di Garda 2004.11.24   Waldkirch 2004.12.05

Figure 2004.9: Moment tensors of the Lago di Garda and Waldkirch events.

Lago di Garda, northern Italy

One minute before midnight, local time, on November 24th, a moderately strong earthquake in northern Italy caused ground shaking that woke up many people in southern and southeastern Switzerland (Figure 2004.8). The epicenter was located near the town of Saló, W of Lake Garda. In the epicentral region the shaking was severe, causing the collapse of several poorly built houses and forcing people to abandon some heavily damaged buildings. This corresponds to an epicentral intensity I_0 of VII-VIII. Although the epicenter of this event was located outside the area covered by the map in Figure 2004.1, we mention it here, because it was the strongest earthquake in 2004 that produced significant ground shaking in Switzerland. In fact in canton Ticino it caused the most intense shaking in many years and intensities of IV were observed as far north as Lucerne. Magnitudes calculated by the Swiss Seismological Service are M_L 5.3 and M_w 5.0, which agree well with the values of M_L 5.2 and M_w 5.0 published by INGV (2004). The focal mechanism derived from the moment tensor inversion is a thrust fault with a NW-SE oriented P-axis at a depth of 9 km (Figure 2004.9 and Table 2004.2), which also differs only little from results obtained by INGV (INGV 2004).
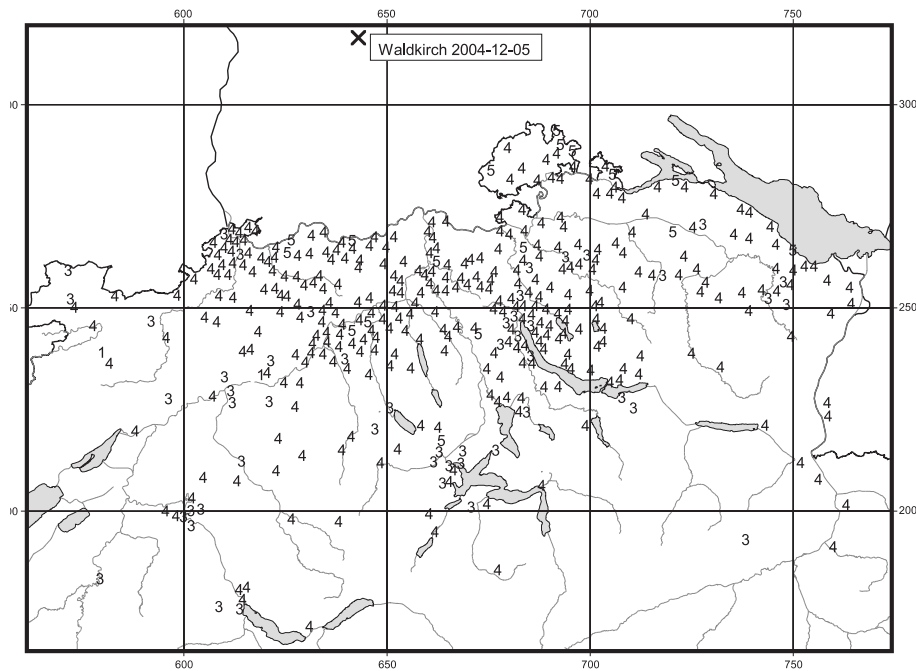
Figure 2004.10: Macroseismic observations for the event of Waldkirch (2004/12/05, 02:52 local time). Otherwise as in Figure 4.

Waldkirch, southern Germany

Another earthquake in 2004, which caused significant shaking in Switzerland and was located outside the map in Figure 2004.1, occurred on December 5th at 02:52 local time. The epicenter was in southern Germany near the town of Waldkirch, about 17 km north of Freiburg im Breisgau. Magnitude values computed by the Swiss Seismological Service are M_L 5.1 and M_w 4.6, and the focal depth corresponding to the best fit of the moment tensor inversion is 12 km. Despite the relatively small difference in M_L with respect to the event of Lago di Garda, structural damage was only slight, being limited to minor cracks in walls and chimneys and some fallen roof shingles (LED 2004). Thus the epicentral intensity was not greater than VI, but it was nevertheless clearly felt over most of northern Switzerland and some people were awakened as far south as Chur and Interlaken (Figure 2004.10). The moment tensor corresponds to a strike-slip focal mechanism with sinistral slip on a NNE-SSW striking fault or dextral slip on a WNW-ESE striking fault (Figure 2004.9 and Table 2004.2). The orientation of the NW-SE and NE-SW orientation of the P- and T-axes matches the stress field derived from other earthquakes in the crystalline basement of the Black Forest (Plenefisch & Bonjer 1997).

Seismic activity during 2005

Overview

During 2005, the Swiss Seismological Service detected and located 608 earthquakes in the region shown in Figure 2005.1. Based on such criteria as the time of occurrence, the location, the signal character or on direct information, 98 additional seismic events were identified as quarry blasts and two as landslides.

Magnitude values of the events recorded in 2005 range between M_L 0.1 and 4.9. The events with $M_L \geq 2.5$ are listed in Tables 2005.1. Where available, the epicentral coordinates and focal depths given in Table 2005.1 are based on the results that include additional data from foreign networks and on 2-D ray-tracing.

The total number of 19 events with $M_L \geq 2.5$ that occurred in 2005 is below the 30-year average of 25 events in this magnitude category per year. However, this apparent activity deficit is compensated for by three earthquakes with M_L between 4.1 and 4.9 and by the surge in microseismic activity associated with the intense precipitation at the end of August (Figure 2005.2). The main event of the year is certainly the M_L 4.9 earthquake of Vallorcine on September 8th and its large number of aftershocks.

Overall, as in previous years, most of the earthquakes occurred in the Valais and in Graubünden. However, two of the strongest events (Rumisberg and Brugg) were located below the northern Alpine foreland. Routinely calculated focal depths for the 608 earthquakes recorded in 2005 range between close to the surface and 30 km, but only 44 of these hypocenters are deeper than 15 km. As in the past (e.g. Deichmann et al. 2000a), all of those deep sources with reasonably well-constrained focal depths, and in particular the magnitude M_L 4.1 hypocenters of Rumisberg and Brugg, are located in the lower crust beneath the Jura Mountains or the Molasse Basin of northern Switzerland.

In what follows, we present the highlights of the seismic activity observed during 2005. For the stronger events, the traditional determination of focal mechanisms from the azimuthal distribution of first-motion polarities (fault-plane solutions) has been complemented by a moment tensor based on full-waveform inversion. For these events we list in Table 2005.2 the moment magnitude (M_w) in addition to the local magnitude (M_L). Moment magnitude is calculated from the seismic moment M_0 obtained from the moment tensor inversion using the relation $M_w = (2/3) \log M_0 - 6$, where M_0 is given in N-m (Hanks & Kanamori 1979). The complete set of moment tensors calculated by the Swiss Seismological Service, including plots of all waveform fits, is available on line (http://www.seismo.ethz.ch/mt/). More comprehensive and detailed explanations of the data analysis procedures are given in previous annual reports (e.g Deichmann et al. 2004) and can be downloaded from our website (*Introduction.pdf* under *Reports* at http://www.seismo.ethz.ch).

Date & Time UTC	Lat. [°N]	Lon. [°E]	X / Y [km]	Depth [km]	Mag. [M_L]	Q	Location
2005.01.19 14:46:51	47.365	7.174	580/246	3	2.6	B	Saint Ursanne, JU
2005.02.27 08:20:15	47.345	9.828	780/246	1	2.5	B	Mellau, A
2005.03.16 03:41:31	47.389	6.962	564/249	8	2.7	A	Chevenez, JU
2005.05.08 14:29:40	47.291	7.681	618/238	25	2.9	A	Klus, SO
2005.05.12 01:38:05	47.267	7.657	616/235	25	4.1	A	Rumisberg, BE
2005.05.19 14:56:54	46.152	7.450	601/111	2	2.5	B	Saint-Martin, VS
2005.05.19 17:16:28	45.943	8.195	659/ 88	10	2.9	B	Cima Capezzone, I
2005.05.27 17:22:44	47.034	9.509	757/211	8	2.9	A	Bad Ragaz, SG
2005.06.24 16:20:58	46.623	10.132	806/167	4	2.6	A	Piz Quattervals, GR
2005.07.04 23:02:35	47.221	10.432	827/234	6	2.7	D	Arlberg, A
2005.07.10 18:44:21	46.835	8.969	717/188	1	2.6	A	Selbsanft, GL
2005.07.21 03:20:33	47.269	7.657	616/235	25	2.6	A	Rumisberg, BE
2005.09.01 05:28:20	46.388	6.320	514/138	1	2.6	B	Nyon, VD
2005.09.08 11:27:17	46.032	6.897	558/ 98	4	4.9	A	Vallorcine, F
2005.09.08 11:53:10	46.031	6.905	559/ 98	4	3.0	A	Vallorcine, F
2005.09.08 14:10:02	46.033	6.897	558/ 98	4	2.9	A	Vallorcine, F
2005.11.12 19:31:16	47.523	8.166	655/264	20	4.1	A	Brugg, AG
2005.12.03 03:31:41	46.651	9.998	796/170	4	2.5	B	Brail, GR
2005.12.30 16:50:01	46.623	9.835	783/166	4	2.7	B	Albulapass, GR

Table 2005.1: Earthquakes with $M_L \geq 2.5$. The focal depths of the earthquakes for which focal mechanisms have been calculated are based on 2-D ray-tracing or on additional data from foreign networks. Focal depth of the Vallorcine events is taken from Fréchet et al. (2010)

Location	Date & Time [UTC]	Depth [km]	Mag.	Plane 1 Strike/Dip/Rake	Plane 2	P-Axis Az/Dip	T-Axis
Rumisberg	2005/05/12 01:38	25	M_L 4.1	098/63/ 172	192/83/ 027	322/13	058/24
		24	M_w 3.7	101/60/ 146	208/61/ 034	335/00	065/44
Bad Ragaz	2005/05/27 17:22	9	M_w 2.8	189/75/ 019	094/72/ 164	321/02	052/24
Vallorcine	2005/09/08 11:27	4	M_L 4.9	150/89/ 025	060/65/ 179	282/17	018/18
		8	M_w 4.5	147/88/ 006	057/84/ 178	282/03	013/06
Brugg	2005/11/12 19:31	20	M_L 4.1	206/48/-034	320/65/-133	182/50	079/10
		18	M_w 3.6	191/50/-045	314/57/-130	167/57	071/04

Table 2005.2: Focal mechanism parameters based on first-motion polarities (lines with M_L) and full-waveform inversion (lines with M_w). Azimuth and plunge of the first-motion focal mechanism for the Vallorcine event are taken from Fréchet et al. (2010); dip and rake of the nodal planes of the Vallorcine mechanism as listed here differ from the values given by Fréchet et al. (2010), because of the ambiguity that can arise when one of the nodal planes is vertical, as given by Fréchet et al. (2010).
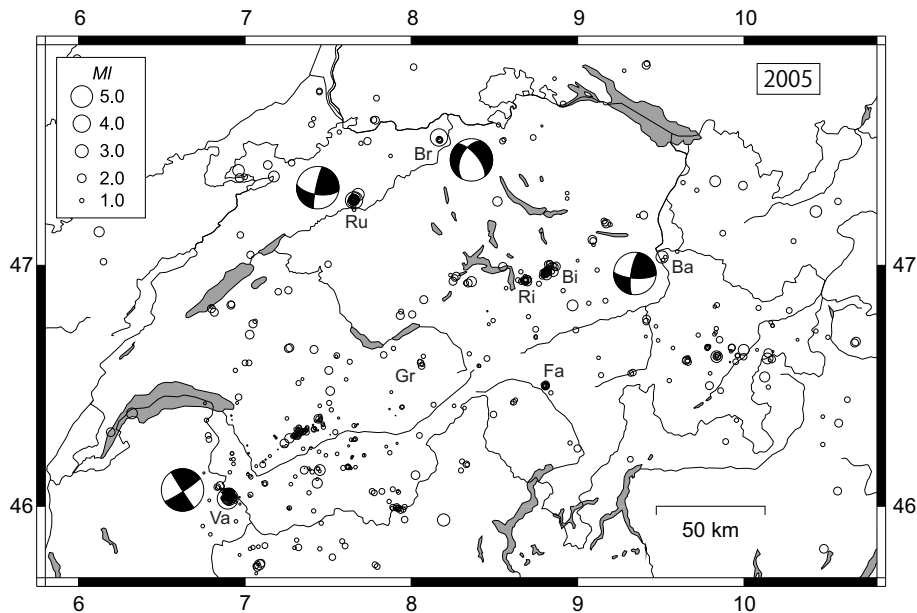
Figure 2005.1: Epicenters and focal mechanisms of earthquakes recorded by the Swiss Seismological Service during 2005. Epicenters of earthquakes mentioned in the text are Bad Ragaz (Ba), Bisistal (Bi), Brugg (Br), Faido (Fa), Grindelwald (Gr), Riemenstalden (Ri), Rumisberg (Ru), Vallorcine (Va).

Significant earthquakes of 2005

Rumisberg - Balsthal

The first of the three $M_L > 4$ events in 2005 occurred on May 12th at 03:38 local time. The epicenter was located near the town of Rumisberg on the southern edge of the Jura Mountains between the cantons Solothurn and Bern. Computed magnitudes are M_L 4.1 and M_w 3.7. The epicentral intensity I_0 reached IV (EMS98), and intensities of III and IV were reported from across most of northwestern Switzerland (Figure 2005.3). Such a large area of perceptible shaking for this event of moderate magnitude is due to its large focal depth of 25 km. This value is well-constrained by P- and S-wave arrivals at station BALST located 8 km from the epicenter and at several strong-motion stations at distances around 30 km in the Basel region. It is also confirmed by 2-D ray-tracing of Pn arrivals at several stations in eastern Switzerland.

The faultplane solution based on first-motion polarities corresponds to a strike-slip mechanism with NW-SE and NE-SW oriented P- and T-axes, typical of northwestern Switzerland. The full-waveform inversion results in a moment tensor with a stronger thrust component (Figure 2005.4). Whereas the E-W striking nodal plane of the moment tensor is similar to the one obtained from the faultplane solution, the strike and dip of the other nodal plane deviate by 16 and 22 degrees from the nodal plane compatible with the observed first-motion polarities.

The Rumisberg mainshock was preceded by a magnitude M_L 2.9 event on May 8th (Table 2005.1) and a magnitude M_L 0.9 event on May 9th. Whereas the latter was probably located in the immediate vicinity of the mainshock and
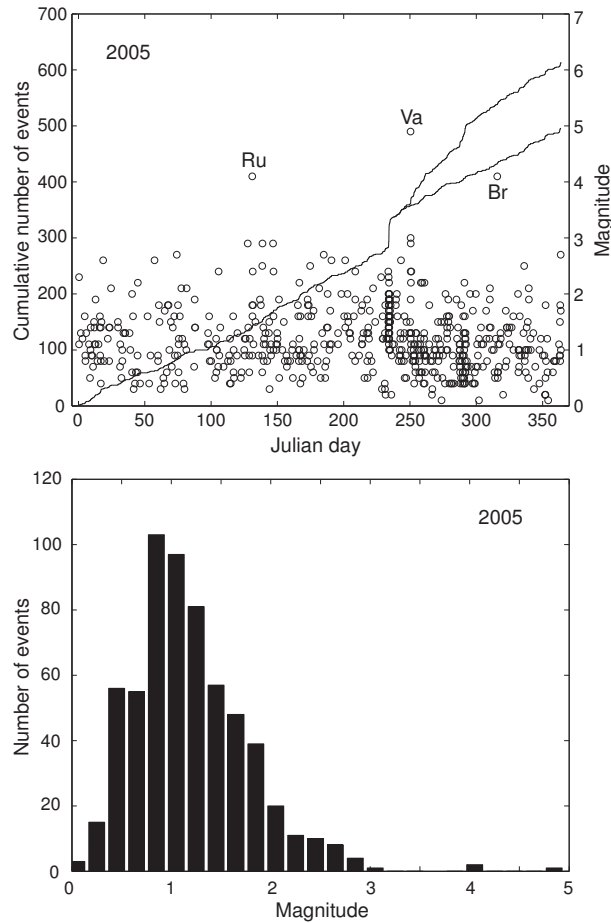
Figure 2005.2: Earthquake activity during 2005: magnitude of each event and cumulative number of events (above); histogram of magnitudes (below). The events with $M_L > 4$ are labled: Brug (Br), Rumisberg (Ru) and Vallorcine (Va). The lower curve beyond Julian day 245 in the plot of the cumulative number of events represents the evolution in time without the Vallorcine sequence. The prominent step in the cumulative number of events at Julian day 235 is the contribution of the rain-induced seismicity between August 22nd and 24th.
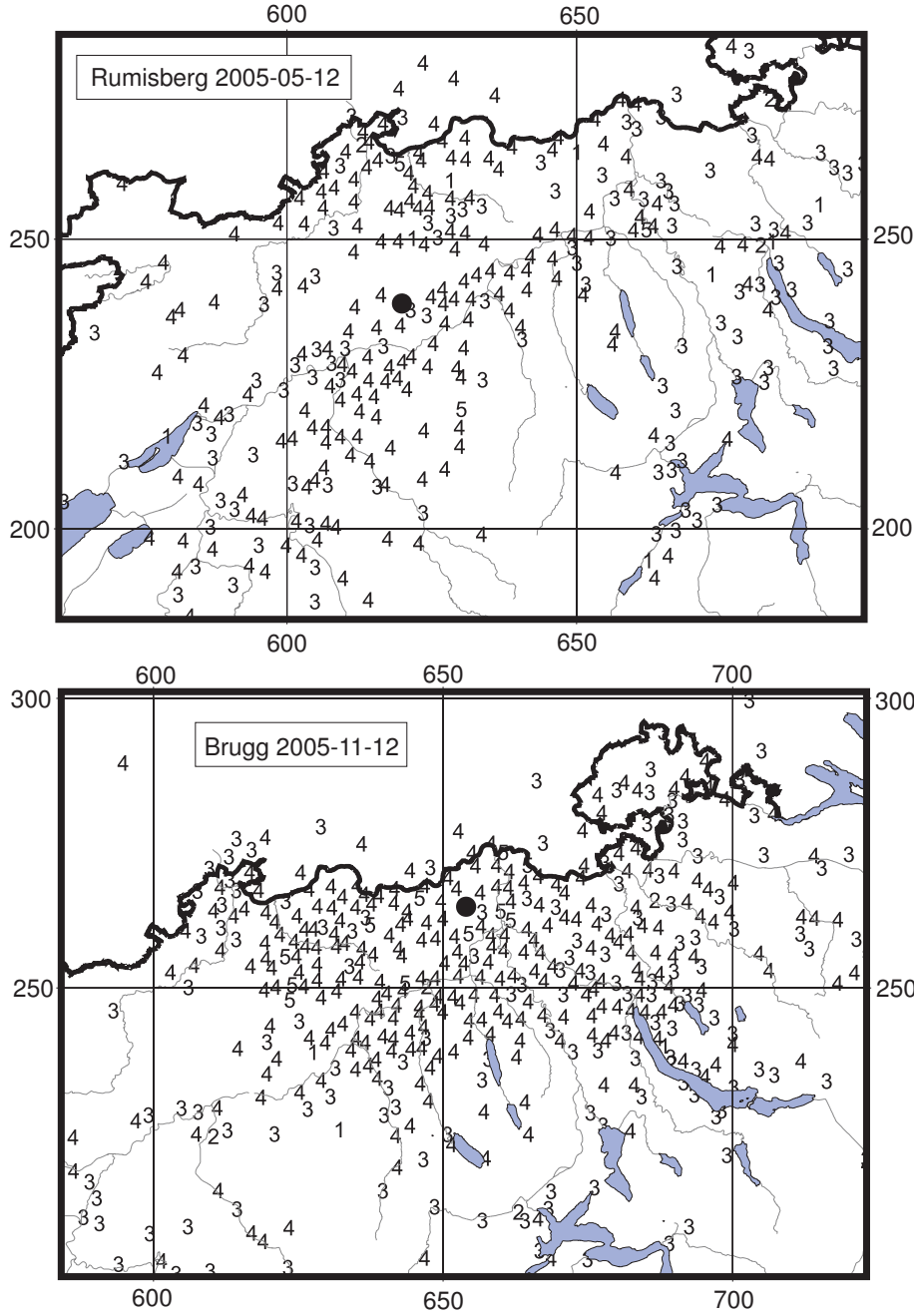
Figure 2005.3: Macroseismic observations for the events of Rumisberg (2005/05/12, 03:38 local time) and Brugg (2005/11/12, 21:31 local time). Each value represents the macroseismic intensity (EMS-98) assigned to a single postal code zone. The black dot corresponds to the instrumental epicenter. The Swiss cartesian coordinate grid is labeled in km.

Rumisberg 2006.05.12   Brugg 2005.11.12

Bad Ragaz 2006.05.27   Vallorcine 2006.09.08
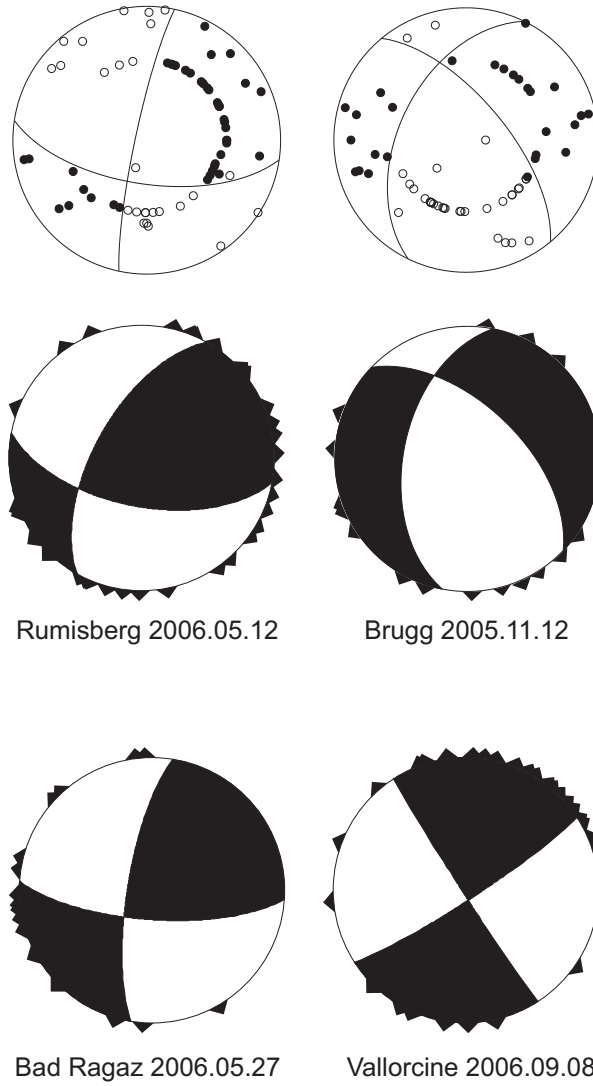
Figure 2005.4: Faultplane solutions (above) based on first-motion polarities and moment tensors (below) based on full-waveform inversion (lower hemisphere, equal area projection). In the faultplane solutions, solid circles correspond to compressive first motion (up) and empty circles to dilatational first motion (down); on the moment tensors, triangles show the station locations.

can therefore be considered a foreshock, the former was located 3-4 km further to the NE near Klus (SO), so that its relation to the mainshock is less evident. A total of 20 aftershocks were detected: after a series of 6 events with magnitudes ranging between 0.9 and 2.4 in the first 24 hours after the main event, sporadic activity, including an event of magnitude M_L 2.6 on July 21st, continued over the rest of the year (Table 2005.1).

Bad Ragaz

The M_L 2.9 event of May 27th near Bad Ragaz (Table 2005.1 and Figure 2005.1) is not very spectacular in itself. However, it is interesting, because its hypocenter coincides with that of a M_L 3.6 earthquake that occurred on February 23rd, 2000, and of another M_L 2.9 event on January 30th, 2001 (Baer et al. 2001; Deichmann et al. 2002). In fact, all three events seem to be part of a cluster that has been active off and on since the year 1998. From the broad-band signals of the event of 2005 it was possible to compute the moment tensor (Figure 2005.4). With a moment magnitude M_w 2.8 the corresponding focal mechanism is practically identical to that of the mainshock in the year 2000 (Baer et al. 2001).

Vallorcine

The strongest event of 2005 in the region covered by the map in Figure 2005.1 occurred on September 8th, 13:27 local time. The computed magnitudes are M_L 4.9 and M_w 4.5. Its epicenter was located near the village of Vallorcine, on the French side of the border along the road between Martigny and Chamonix. The cracks in the walls of several houses and the numerous rockfalls along roads in the region north of the epicenter correspond to a maximum intensity of V (EMS98). It was clearly felt also over most of western Switzerland.

To study the relation of this earthquake and its aftershocks to the known faults in the region, a temporary seismograph array was deployed in the epicentral area immediately following the mainshock (Thouvenot et al. 2006; Fréchet et al. 2006; Fréchet et al. 2010). Over 300 events were recorded during the one-month campaign, and the Swiss national network routinely detected more than 110 aftershocks until the end of the year. Only two of these aftershocks reached a magnitude $M_L > 2.5$ (Table 2005.1). The detailed analysis of the aftershock sequence shows that aftershock activity occurred in five separate clusters located at depths between 4 and 5 km. Because of the poor azimuthal station distribution, the routinely calculated focal depths of 6 and 7 km for the mainshock and the two strongest aftershocks, based on arrivals at Swiss stations alone, are poorly constrained. Therefore, in Tables 2005.1 and 2005.2, we follow Fréchet et al. 2010 and set the focal depth of the mainshock to 4 km.

The moment tensor derived from a full-waveform inversion of a large number of broad-band records corresponds to a strike-slip mechanism with NNE-SSW and WNW-ESE trending P- and T-axes (Figure 2005.4). The result is very similar to the faultplane solution based on first-motion polarities (Table 2005.2) published by Fréchet et al. (2010). From the precise relative locations of the aftershocks performed by Fréchet et al. (2010), it is clear that rupture during the Vallorcine event occurred as dextral slip on the NE striking faultplane. Several faults with similar strike, that could be related to this rupture plane, are also visible at the surface (Fréchet et al. 2010).

Brugg

The third earthquake to cause shaking felt over a large region in 2005 occurred on November 12th at 20:31 local time. Its epicenter was located near the village of Mönthal (AG), 4 km W of Brugg. Computed magnitudes are M_L 4.1 and M_w 3.6. Shaking intensity of IV (EMS98) was reported not only from the epicentral region, but also from many locations across most of northern Switzerland (Figure 2005.3). Just as in the case of the Rumisberg event, the wide area over which this event was felt is due to the relatively large focal depth. In fact, both the routinely calculated depth, which is well constrained by P- and S-arrivals at stations SULZ and ACB located at epicentral distances of 4 and 9 km, as well as the depth resulting from 2-D ray-tracing give a value of 20 km.

The source location of this earthquake coincides within the location uncertainty with the M_L 4.0 event of June 28th, 2004 (Baer et al. 2005). This is illustrated by the seismograms in Figure 2005.5(a): the identical arrival-time difference between the S- and P-onsets as well as the striking similarity of the waveforms of the S-phase imply that the hypocenters of the events of 2004 and 2005 are located at the same distance from station SULZ and that the paths between source and station are practically the same. However, the different relative amplitudes of the P- and S-phases visible on the vertical components at station SULZ shown in Figure 2005.5(b) are an indication that the focal mechanisms of the two events differ. In fact, both the faultplane solution based on first-motion polarities and the moment tensor derived from the full-waveform inversion give a normal faulting mechanism (Figure 2005.4), for which the orientation of one of the nodal planes differs significantly from the mechanism of previous year's event (Baer et al. 2005). It is also interesting to note that the P-wave onset of the event of 2005 observed at station SULZ (Figure 2005.5(c)) exhibits a small precursor phase before the onset of the main P-pulse, whereas the seismogram of the event of 2004 starts with a simple single pulse. Given the close spacing of the two hypocenters and the fact that this precursor phase is visible also at other stations situated at different azimuths relative to the source, this difference in signal character can not be due to path effects but is probably due to a more complex rupture process in 2005 than in 2004.

The mainshock in 2005 was preceded by a small foreshock (M_L 1.2) on August 2nd and was followed from November 13th to December 5th by four aftershocks with magnitudes between M_L 0.6 and 1.5.

Seismic events and rockbursts in the new Gotthard tunnel

In the Spring of 2004, a sequence of five small earthquakes (M_L 0.9 - 1.4) occurred near Faido, TI. This sequence was not recognised as being anything unusual at first. It was only in June 2005, after a magnitude M_L 1.9 earthquake at the same location that it became clear that these events were part of an ongoing sequence of small earthquakes whose time of occurrence and epicentral location correlate with some rather violent rockbursts in a section of the new Gotthard railroad tunnel, which is still under construction. In fact during the course of 2005, the national seismic network detected and located eight other events with the same epicenter and with magnitudes between M_L 0.9 and 1.6. An additional event with M_L 1.0 occurred on November 10th, 3-4 km SE of the others, and it correlates with a rockburst in a segment of the tunnel close to the epicenter. Computed focal depths, though poorly constrained, suggest a shallow source located at a depth of less than 2 km. To examine the causal relation between the earthquakes, rockbursts and observed deformation of the tunnel
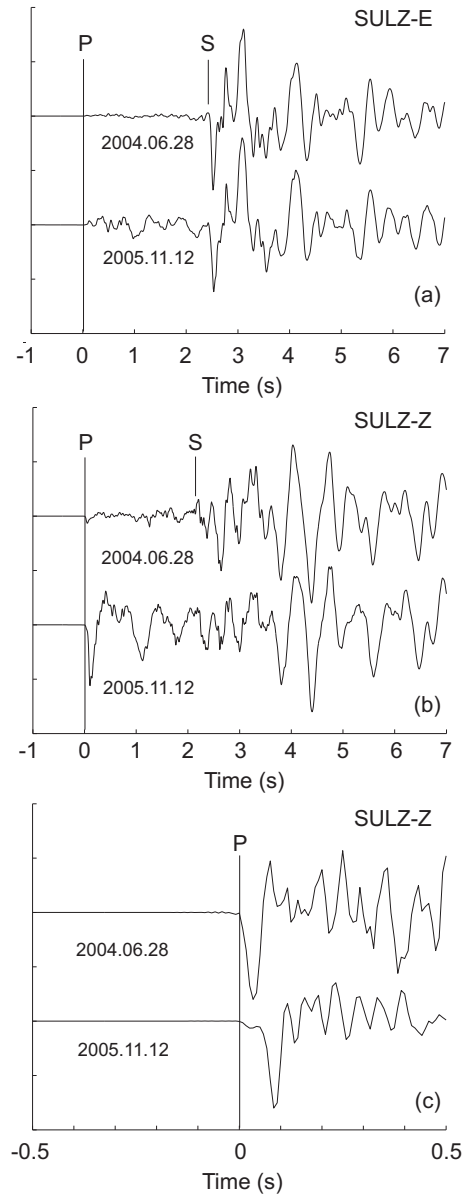
Figure 2005.5: Seismograms of the Brugg events of 2004 and 2005 recorded at station SULZ at an epicentral distance of 4 km. The traces are aligned at the arrival time of the P-wave: (a) horizontal displacement in EW direction, (b) vertical diplacement and (c)vertical velocity. Note the different time scales: (a) and (b) include both the P- and S-phases, while (c) shows an enlargement of the P-arrival alone. The identical S-P times and the similar waveforms of the S-phase seen in (a) are evidence for a similar source location. The different amplitude ratios between the P- and S-phases seen in (b) are due to differences in the focal mechanisms, and the small precursor before the P-wave onset of the event of 2005 seen in (c) is evidence for a more complex rupture process.

cross-section, an additional temporary network of seismometers was deployed in the epicentral area in the Fall of 2005, under contract from AlpTransit-Gotthard AG. First results based on records from these stations confirm the shallow focal depth as well as the correlation between these earthquakes and the observed rockbursts in the tunnel.

Rain-induced seismicity

As can be seen in Figure 2005.2, the curve of the cumulative number of events with time shows a pronounced jump at Julian day 235. This jump corresponds to an anomalous burst of activity that includes 51 events over a period of less than 48 hours that started on the afternoon of August 22nd. Of these events, 39 occurred within 12 hours between 9 PM and 9 AM of the following day. Magnitudes of these events range between 1.0 and 2.4. Single earthquake swarms that produce a large number of small earthquakes over a period of a few days are quite common. What is however unusual about this concentration of seismic activity is that it occurred simultaneously over a very large region that extends from Canton Schwyz in the northeast across the region around Stans and Alpnach, south of Lake Lucerne, all the way to Grindelwald in the Bernese Oberland. The main centers of activity were two separate clusters around Bisistal and south of Riemenstalden in Canton Schwyz (Figure 2005.1). Together these two clusters contributed more than half the total number of earthquakes observed in those two days. Although focal depths of most of these events are poorly constrained by routine location procedures, the shallow sources are confirmed at least qualitatively by both the signal character of the events (conspicuous surface waves even at short epicentral distances) and the fact that numerous events with magnitudes less than 2 were perceived by the population as loud bangs.

During this time, the region in which all of these earthquakes ocurred, suffered very intense rainfalls, which caused massive floods and numerous landslides. Given this spatial and temporal coincidence and the shallow focal depths, it is thus likely that this unusual seismic activity was induced by a sudden increase in pore pressure due to the intense precipitation. This hypothesis is furthermore supported by the fact that the two main centers of activity around Bisistal and Riemenstalden are highly permeable karst regions, where surface waters and thus fluid pressure perturbations can propagate rapidly to greater depths.

Landslides

On May 14th at 18:49 local time, a sizeable landslide came down between Gondo and Zwischbergen, south of the Simplon Pass. The corresponding seismic signals were visible over most of the national network with amplitudes equivalent to a M_L 2.1 earthquake.

Twelve days later, on May 26th at 7:16 local time, the seismograph network detected another event with similar signal character and an epicenter west of station SALAN, in the region of the Dents du Midi. Although it is higly unlikely that the recorded signals were produced by an earthquake or an explosion, it has not been possible to associate this event with a known landslide.

Seismic activity during 2006

Overview

During 2006, the Swiss Seismological Service detected and located 569 earthquakes in the region shown in Figure 2006.1. As discussed below, of these 569 events, 2 occurred in conjunction with the construction of the new Gotthard railway tunnel and 166 were induced by the stimulation of a proposed geothermal reservoir beneath the city of Basel (Figure 2006.2). Based on such criteria as the time of occurrence, the location, the signal character or on direct information, 96 additional seismic events were identified as quarry blasts and a dozen as landslides. Magnitude values of the events recorded in 2006 range from M_L 0.1 to 3.6. The events with $M_L \geq 2.5$ are listed in Table 2006.1.

In 2006, the total number of 20 events with $M_L \geq 2.5$ was below the 25 events per year observed on average over the previous 31 years in this magnitude category. The activity low of 2006 is even more significant if one considers that five of these events were artificially induced by the geothermal reservoir stimulation in Basel and would presumably not have occurred otherwise.

As in previous years, most of the other earthquakes occurred in the Valais and in Graubünden. It is also worthwhile to note that more than 10% of the naturally occurring earthquakes in 2006 were part of the aftershock activity of the M_L 4.9 earthquake that occurred on September 8th 2005 near Vallorcine, France, about halfway between Martigny and Chamonix (Figure 2006.1). These 42 aftershocks with M_L between 0.5 and 1.7 occurred at a gradually decreasing rate throughout the entire year.

Routinely calculated focal depths for all but 23 events recorded in 2006 were less than 16 km. Of these deeper events 22 are located in the lower crust beneath the Jura Mountains or the Molasse Basin of northern Switzerland with a maximum focal depth of 31 km. One exceptionally large focal depth of 45 km was calculated for a magnitude 1.9 event in the southern Alps, about 20 km E of Lecco. Lower crustal earthquakes are not uncommon in this region. However, according to Waldhauser et al. (1998) the Moho depth below the epicenter is only 41 km, so that, if the calculated focal depth is correct, this would be the first known seismic event in Switzerland and surroundings to have occurred in the upper mantle. On the other hand, the 3-D velocity model is not optimally constrained in this region, and the probability density function of the non-linear location uncertainty extends in the vertical dimension over ± 7 km, so that the calculated focal depth for this event is not sufficiently reliable to support such a conclusion.

At least six of the seismic events that occurred in Switzerland in 2006 where felt by the public. In what follows, we review these six earthquakes. For the stronger events, the traditional determination of focal mechanisms from the azimuthal distribution of first-motion polarities (faultplane solutions) has
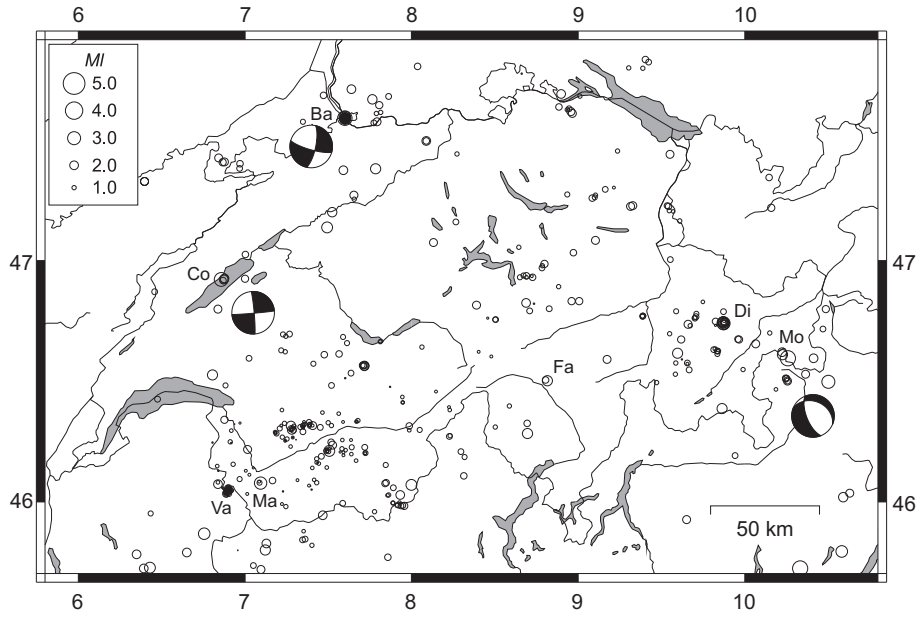
Figure 2006.1: Epicenters and focal mechanisms of earthquakes recorded by the Swiss Seismological Service during 2006. Epicenters of earthquakes mentioned in the text are Basel (Ba), Cortaillod (Co), Dischmatal (Di), Faido (Fa), Martigny (Ma), Val Mora (Mo), Vallorcine (Va).

Date & Time UTC	Lat. [°N]	Lon. [°E]	X / Y [km]	Depth [km]	Mag. [M_L]	Q	Location
2006.01.12 05:32:52	45.792	10.583	844/ 76	10	2.7	D	Valli Giudicarie, I
2006.03.18 22:49:32	46.213	7.507	605/118	3	2.6	B	Erdesson, VS
2006.03.29 09:49:45	46.923	6.858	556/197	2	3.2	A	Cortaillod, NE
2006.04.12 22:24:53	46.597	10.259	816/164	2	3.5	A	Val Mora, GR
2006.05.25 08:18:13	47.137	7.493	604/221	6	2.6	B	Brügglen, SO
2006.06.30 00:34:46	45.725	6.430	521/ 64	14	2.5	D	Ugine, F
2006.08.16 15:05:20	46.079	7.094	573/103	6	2.8	B	Martigny, VS
2006.10.17 05:41:34	46.500	10.502	835/154	8	3.1	A	Ortles, I
2006.10.20 00:11:58	45.721	10.332	825/ 67	2	3.6	B	Valli Giudicarie, I
2006.10.24 13:08:11	46.746	9.873	786/180	6	2.6	A	Dischmatal, GR
2006.10.24 20:05:29	46.743	9.873	786/180	6	3.0	A	Dischmatal, GR
2006.10.24 20:11:05	46.746	9.871	786/180	6	2.5	A	Dischmatal, GR
2006.10.31 03:08:07	46.741	9.873	786/179	5	2.8	A	Dischmatal, GR
2006.11.22 15:54:32	45.867	6.755	547/ 80	14	2.7	B	Mont Blanc, F
2006.11.24 21:31:00	46.072	8.000	643/102	9	2.5	A	Saas Almagell, VS
2006.12.08 03:06:18	47.582	7.601	612/270	5	2.6	A	Basel, BS
2006.12.08 15:46:55	47.587	7.599	612/271	5	2.7	A	Basel, BS
2006.12.08 16:48:39	47.582	7.600	612/270	5	3.4	A	Basel, BS
2006.12.08 20:19:39	47.580	7.600	612/270	5	2.5	A	Basel, BS
2006.12.14 22:39:27	47.581	7.602	612/270	4	2.5	A	Basel, BS

Table 2006.1: Earthquakes with $M_L \geq 2.5$.
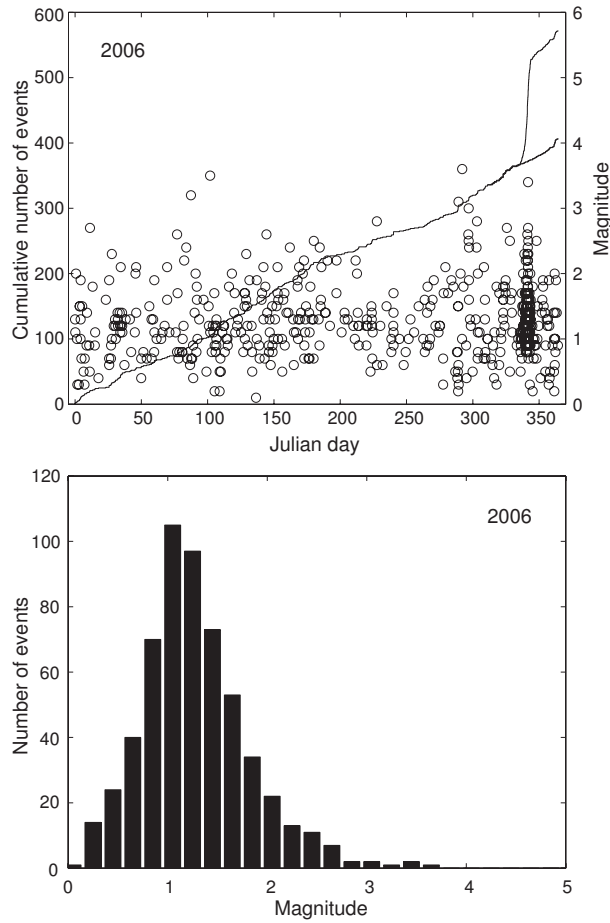
Figure 2006.2: Earthquake activity during 2006: magnitude of each event and cumulative number of events (above); histogram of magnitudes (below). The lower curve beyond Julian day 313 in the plot of the cumulative number of events represents the evolution in time without the induced seismicity of Basel.

Location	Date & Time [UTC]	Depth [km]	Mag.	Plane 1 Strike/Dip/Rake	Plane 2	P-Axis Az/Dip	T-Axis
Cortaillod	2006/03/29 09:50	2	M_L 3.2	355/86/-002	085/88/-176	310/04	220/01
		4	M_w 3.1	179/70/ 025	080/67/ 158	309/02	040/32
		5	M_w 3.0	357/80/-016	090/74/-170	313/18	044/04
Val Mora	2006/04/12 22:25	2	M_L 3.5	293/32/-130	158/66/-068	103/62	232/18
		9	M_w 3.4	280/34/-142	157/70/-062	103/56	226/20
		5	M_w 3.3	285/28/-148	166/76/-066	104/53	237/27
Basel	2006/12/08 16:49	5	M_L 3.4	012/75/-013	105/77/-165	329/20	238/02

Table 2006.2: Focal mechanism parameters based on first-motion polarities (lines with M_L) and on the two full-waveform inversion methods discussed in the text (lines with M_w; interactive above and automated below).
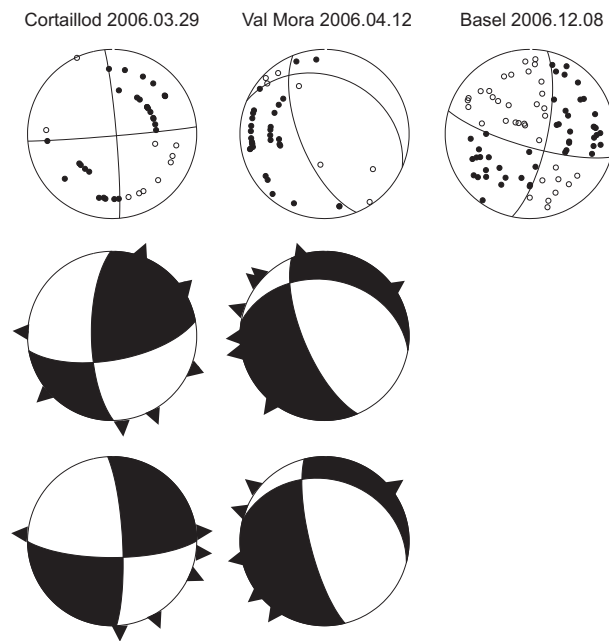
Figure 2006.3: Faultplane solutions (above) based on first-motion polarities and moment tensors (interactive in the middle and automated below) based on full-waveform inversion. All stereographs are lower hemisphere, equal area projections. In the faultplane solutions, solid circles correspond to compressive first motion (up) and empty circles to dilatational first motion (down); on the moment tensors, triangles show the station locations.
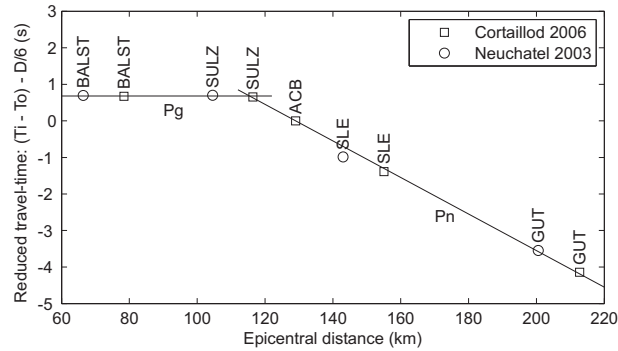
Figure 2006.4: Arrival times of the Neuchâtel event of 2003 and the Cortaillod event of 2006 observed at stations to the NE of the epicenters. The data for the two events were aligned according to the direct arrivals (Pg). The fact that the arrivals of the wave refracted at the Moho (Pn) match for the two events implies that their focal depths must be nearly identical.

been complemented by a moment tensor based on full-waveform inversion (Figure 2006.3). For these events we list in Table 2006.2 the moment magnitude (M_w) in addition to the local magnitude (M_L). Moment magnitude is calculated from the seismic moment M_0 obtained from the moment tensor inversion using the relation $M_w = (2/3) \log M_0 - 6$, where M_0 is given in N-m (Hanks & Kanamori 1979). The complete set of moment tensors calculated by the Swiss Seismological Service, including plots of all waveform fits, is available on line (http://www.seismo.ethz.ch/mt/). More comprehensive and detailed explanations of the data analysis procedures are given in previous annual reports (e.g Deichmann et al. 2004) and can be downloaded from our website (*Introduction.pdf* under *Reports* at http://www.seismo.ethz.ch).

Significant earthquakes of 2006

Cortaillod

On March 29th, shortly before noon (local time), light shaking with swaying lamps and creaking beams was perceived in several towns along the northern shore of Lake Neuchâtel. This was caused by a magnitude M_L 3.2 earthquake, whose epicenter was located about 3 km south of the town of Cortaillod. This event was followed by three aftershocks with the same epicenter and magnitudes between 1.5 and 2.0 on April 1st, May 10th and August 1st.

Although it was recorded by a sufficient number of seismic instruments with good azimuthal coverage, the closest station (TORNY) was too far away (18 km) to constrain the focal depth in a reliable way. The routinely calculated depth based on the 3D velocity model for Switzerland and using all available data gives a focal depth of 6 km; using only data from stations out ot 70 km results in depths of 9-10 km. However, the very pronounced surface waves observed at several stations suggest a much shallower hypocenter. Earthquakes with near-surface sources are known to occur in this region. One of these occurred in 2003 just 2 km north of Neuchâtel at a depth of about 2 km (Deichmann et al. 2004). The focal depth of the Neuchâtel event is well constrained by a strong-motion station situated only 2 km from the epicenter. Comparing the distance

at which the wave refracted at the Moho (P_n) begins to arrive before the direct wave (P_g) for these two events shows that their focal depths must be practically identical (Figure 2006.4). For constructing the faultplane solution, we have therefore fixed the focal depth at 2 km (Tables 2006.1 and 2006.2). With the remaining uncertainty (estimated at ±1 km) and a depth to basement of about 2 km in this area (Sommaruga, 1997), it is not possible to decide whether the source is located in the basement or in the overlying sediments. Again, given the pronounced surface waves observed at several stations, the latter possibility is very likely.

The faultplane solution based on first-motion polarities corresponds to a pure strike-slip mechanism with N-S and E-W striking nodal planes. Although station coverage to the NW is poor, the strike of the two nodal planes is well-constrained by the distribution of the other stations. Given that the mechanism is strike-slip, the result depends only marginally on the correct value of the vertical take-off angles of the rays at the source and is thus insensitive to errors in focal depth. The general nature of the focal mechanism is confirmed also by the two moment tensor solutions based on full-waveform solutions (Figure 2006.3 and Table 2006.2). Both the depth and focal mechanism are nearly identical to those of the well-documented earthquake sequences of Fribourg, located about 28 km to the ESE (Kastrup et al. 2007).

Val Mora

Shortly after midnight between April 12th and 13th, an earthquake with magnitude M_L 3.5 shook the area between the Lower Engadin, Val Müstair and Livigno. Its epicenter was located in the lower part of Val Mora, close to the border to Italy. Due to the remoteness of the source location (6 km from Pass dal Fuorn and 10 km from Livigno) and the time of occurrence, there are only a few reports of it having been felt.

To compute the source location, the records of the national broad-band network was complemented by data from two strong-motion stations at the Punt dal Gall hydroelectric dam (SPGF) and in Zernez (SZEM) as well as from stations in northern Italy (in particular station BRMO, near Bormio 16 km SSE of the epicenter). The hypocenter of this earthquake is certainly shallow. In fact, the arrival-time difference between the S- and P-wave observed at station FUORN is only 0.54 ± 0.02 seconds. Allowing for a reasonable range of V_p and V_s for the upper crust in this region, this places the source at a radial distance of 4.0 ± 0.5 km from FUORN. Considering that FUORN is situated at an altitude of 2300 m, the computed depth of 2 km relative to mean sea level, given in Tables 2006.1 and 2006.2, must be regarded as a maximum value. On the other hand, the steep angles of incidence of the rays at the surface estimated from the polarization of the P-waves observed at stations FUORN (15°) and SPGF (26°) do not allow the depth to be much less than this value. This implies that the epicenter is likely to be closer to FUORN and SPGF than the computed epicentral distances of 2.6 and 5.5 km. These inconsistencies together with large travel-time residuals observed at some stations (e.g. 0.6 s at VDL, located only 70 km from the epicenter) suggest that the 3D velocity model used for the location is not appropriate for this region.

The faultplane solution constructed from the first-motion polarities for this earthquake corresponds to an almost pure normal faulting mechanism. Although the data coverage in the NE quadrant is poor and the mentioned uncertainties of the velocity model might cast doubts on the accuracy of the vertical

take-off angles at the source, the good match with the independently computed full-waveform moment tensors indicates that this result is reliable (Figure 2006.3 and Table 2006.2). Common to all three mechanisms is a NE-SW oriented T-axis, which is typical for all focal mechanisms observed in the eastern Alps of Switzerland (e.g. Kastrup et al. 2004). Note, however, that the shallow focal depth does not seem to be resolvable by the full-waveform inversions.

Martigny

Although the magnitude reached only M_L 2.8, this event, which occurred on August 16th at 17:05 local time, was felt by several people at rest in Martigny. It was followed on the same day and on August 19th by two aftershocks of magnitude 0.9 and 1.3. Their epicenters were located near Bovernier, about 3 km SE of Martigny, so that these events are not related in any way to the earthquake sequence of 2001, which occurred 6 km to the NW of the town.

Dischmatal

In October and November a sequence of 12 events with magnitudes between M_L 1.1 and 3.0 was observed in the vicinity of Davos. The strongest event was widely felt by people at rest, who reported rattling windows, swaying lamps and creaking woodwork (intensity III-IV according to EMS98). The epicenters of these events were located in the valley of Dischma, 7 km SSE of the town. With an epicentral distance of only 4 km from station DAVOX and good azimuthal coverage by the other stations that recorded these events, the focal depth of 6 km is well constrained. This value matches also the depth of a similar earthquake sequence that occurred in the summer of 2003 in the valley of Sertig, only 3 km to the west (Deichmann et al. 2004). The number of reliable first-motion polarities is not sufficient for a faultplane solution, but the available data is compatible with a normal faulting mechanism similar to that of the Sertig events.

Seismic events and rockbursts in the new Gotthard tunnel

Starting in Spring of 2004, the national seismometer network began detecting a sequence of seismic events near Faido, TI. After a while, it became clear that the events of this sequence are correlated with some rather violent rockbursts in a section of the new Gotthard railroad tunnel, which is still under construction (Deichmann et al. 2006). The strongest event of this sequence recorded so far occurred on March 25th, 2006, at 22:42 local time. Its magnitude was only 2.4 M_L, but, due to its shallow focal depth, it was perceived as a loud bang accompanied by short but intense shaking in the town of Faido and surroundings. A second event with the same source location was detected by the nationwide network on November 6th and had a magnitude of 1.6 M_L. Several additional weaker events have also occurred, but were recorded only by sensors installed in the immediate vicinity of the epicenter. A comparison with the records of checkshots set off in the tunnel confirmed that the hypocenters of these earthquakes lie in the immediate vicinity of that part of the tunnel, where many of the rockbursts have occurred and where strong deformations of the tunnel cross-section are observed. More detailed studies of the possible causal relationship between these earthquakes and the observed rockbursts are still underway under a contract with AlpTransit-Gotthard AG.
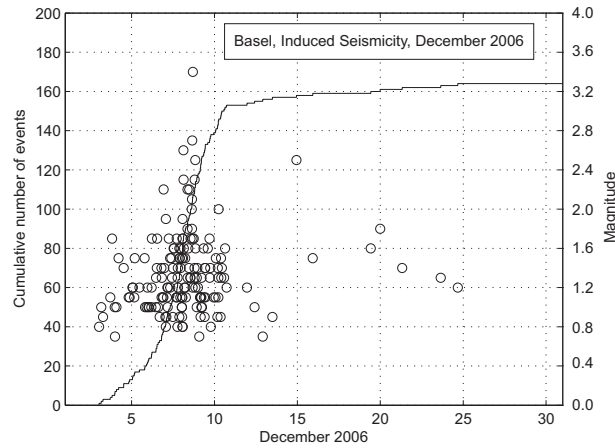
Figure 2006.5: Cumulative number of events and magnitude of the induced earthquakes in Basel, recorded by the national high-gain network of the Swiss Seismological Service during the month of December 2006.

Induced seismicity in Basel

To stimulate the reservoir for a "hot dry rock" geothermal project, that was initiated by a private/public consortium in the city of Basel, approximately 11500 m^3 of water were injected between December 2nd and 8th, 2006, at high pressures into a 5 km deep well below Kleinhüningen. A six-sensor borehole array, installed by the operators of the project at depths between 317 and 2740 meters around the well to monitor the induced seismicity, recorded more than 10500 seismic events during the injection phase (Häring et al. 2008). In the early morning hours of December 8th a magnitude M_L 2.6 event occurred within the reservoir. This exceeded the safety threshold for continued injection, so that the injection was prematurely terminated. In the afternoon and evening of the same day, two additional events of magnitude 2.7 and 3.4 occurred within the same source volume, so that the well was opened and the water allowed to flow back. In the following days about one third of the injected water volume flowed back out of the well, and the seismic activity declined rapidly thereafter (Figure 2006.5).

The vast majority of the induced seismic events were so small that they were detected only by the local borehole array. Consequently, the 165 events, with magnitudes as low as M_L 0.7, that were recorded by the national high-gain network of the Swiss Seismological Service between the beginning of the stimulation and the end of the year, represent only a small fraction of the total number of detected events. An additional event of magnitude 0.7, that was induced by the cementation of the borehole casing, had been recorded already on November 10th. Most of these stronger events were also recorded by the regional networks of France and Germany as well as by up to 30 permanent and temporary strong-motion instruments installed in the epicentral area (Deichmann & Ernst 2009; Deichmann & Giardini 2009).

Results of a more detailed analysis show that the hypocenters of the located events (about 3500 to date) are restricted to a NNW-SSE oriented lens-shaped cloud, about 1.2 km in diameter and 200 m wide, with a single offsetting branch to the ESE (Häring et al. 2008). The center of this cloud is at a depth of

about 4.5 km below ground level. In order to minimize the errors introduced by our imperfect knowledge of the velocity structure, hypocentral locations were calculated using only the P- and S-arrivals at the borehole sensors, which are all situated at radial distances between 2 and 6 km from the source. Compared to relative locations, constrained by a master event that was recorded also by a temporary sensor installed at the beginning of injection in the main borehole near the casing shoe, the absolute epicentral locations given in Table 2006.1 are shifted systematically to the ESE by 600-700 m on average (Deichmann & Giardini 2009).

Due to the large number of stations in operation at the time, the faultplane solution of the main event is exceptionally well constrained (Figure 2006.3). The focal mechanism is strike-slip with more or less NNE-SSW and ESE-WNW striking nodal planes. Moment tensors have also been calculated for this event, and the results are quite similar to the faultplane solution, but the signal-to-noise ratio of the long-period seismograms used for the inversions is so low that this must be regarded as a fortuitous good match rather than as independent evidence. Based on high-precision relative locations of this M_L mainshock with other events with similar waveforms, this event actually occurred on the WNW striking faultplane, which is optimally oriented with respect to the ambient stress field (Deichmann & Giardini 2009). Deichmann & Ernst (2009) present focal mechanisms for 19 additional events with magnitudes M_L between 1.7 and 2.7 that were induced in December 2006. Except for two events with normal faulting mechanisms and one event with a strike-slip mechanism with a strong normal faulting component, all mechanisms correspond to strike-slip rupture on mostly NS or EW oriented faultplanes. These focal mechanism are in good accord with the stress field derived from observations of natural seismicity obeserved in the past in the wider Basel region (Plenefisch & Bonjer 1997, Kastrup et al. 2004, Deichmann & Giardini 2009) and from borehole failure analyses down to 5 km in the Basel well perfomed by Valley & Evans (2009).

The main shock was felt distinctly to strongly in the urban area of Basel. People reported a short, high frequency shaking of 1-3 seconds, often accompanied by a loud bang similar to an explosion. The bang contributed significantly to the frightening effect that this event had on many witnesses. Typical macroseismic effects were creaking of woodwork and rattling of doors and windows. Effects more related to low frequency shaking, such as swinging of suspended objects and oscillations in liquid-filled containers, were mentioned less often. From the city as well as from neighbouring communities, very small non-structural damage was reported consistently for hundreds of buildings, such as hair-line cracks to the plaster or damage to the paint at building junctions. Although often difficult to verify, a significant share of the reported instances of damage is presumed to be a direct consequence of this earthquake. Consequently, macroseismic intensity in the different parts of Basel and the neighbouring municipalities ranges from IV to V according the EMS98 scale (Figure 2006.6). The radius of the intensity-IV area is about 10 km, with peaks in a SSW direction (Birsig valley, Therwil, Ettingen) and towards the East in the Rhine valley. Whereas the first peak coincides with the energy radiation pattern expected from the focal mechanism, the Rhine valley anomaly is probably due to site amplifications by poorly compacted alluvial terraces (Ripperger et al. 2009). The most distant well-established felt-reports are from the region of Sisseln/Stein/Eiken, some 30 km east of the epicentre.

Due to the premature abortion of the stimulation process, the size of the stimulated volume is insufficient for a commercially viable exploitation of
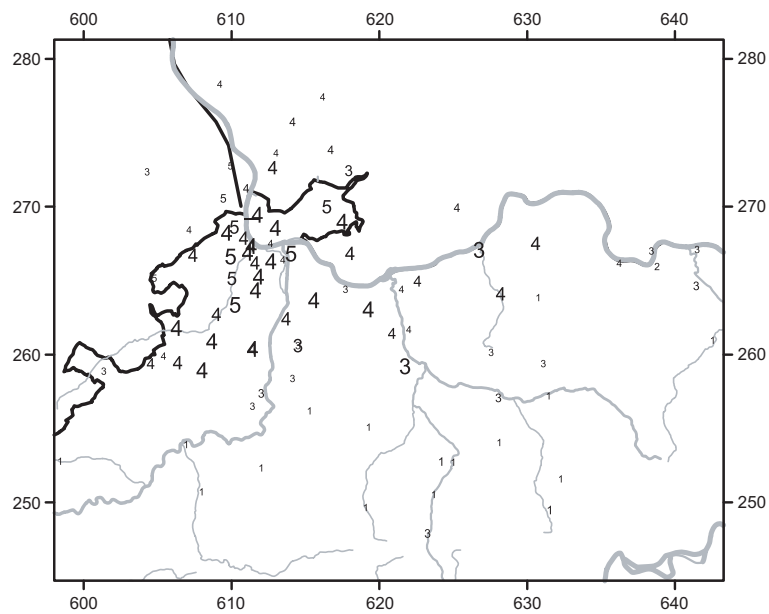
Figure 2006.6: Macroseismic intensities (EMS98) for the strongest event (M_L 3.4) induced by the geothermal reservoir stimulation in Basel (2007/12/08 17:48 local time). The map is based only on reports communicated to the Swiss Seismological Service, so it is not representative for the true shaking in Germany and France. The number size denotes the quality of the data, ranging from very poor (1-2 reports) to very good (15-60 independent reports). The Swiss cartesian coordinate grid is labeled in km.

geothermal energy. As a consequence of how the largest of these induced earthquakes was perceived by the public and of the damage that it presumably caused, the project was put on hold, pending a comprehensive assessment of the seismic risk associated with a continuation (Kraft et al. 2009).

Landslides

In the Summer of 2006, the east flank of the Eiger near Grindelwald was the site of a recurring sequence of massive rockfalls, to the extent that it became a popular tourist attraction and an enduring topic for the media. Between June and August, a dozen seismic events were recorded by the national high-gain network, which showed a similar pattern of signals at stations HASLI, LKBD and WIMIS. These signals are too emergent to identify clear arrivals and thus their source can not be located in a formal way, but given the combination of stations at which they are visible, they most probably are associated with these rockfalls. The equivalent magnitudes of these events are all well below 2.

Seismic activity during 2007

Overview

During 2007, the Swiss Seismological Service detected and located 527 earthquakes in the region shown in Figure 2007.1. As discussed below, of these 527 events, 30 are aftershocks of the stimulation of a proposed geothermal reservoir beneath the city of Basel. Based on such criteria as the time of occurrence, the location, the signal character or on direct information, 95 additional seismic events were identified as quarry blasts. Magnitude values of the events recorded in 2007 range from M_L 0 to 3.9. The events with $M_L \geq 2.5$ are listed in Tables 2007.1.

In 2007, the total number of only 20 events with $M_L \geq 2.5$ was below the 25 events per year observed on average over the previous 32 years in this magnitude category. The activity low of 2007 is even more striking if one considers that four of these events are aftershocks induced by the geothermal reservoir stimulation in Basel. Thus the general trend of lower than average activity, that started in 2005, persisted through the year 2007.

As in previous years, most of the earthquakes occurred in the Valais and in Graubünden. Routinely calculated focal depths for all but 14 events recorded in 2007 are less than 16 km. Except for two events south of the Alps in or close to the Ivrea Body, for which the routinely calculated depths are 19 and 25 km, all the deeper hypocenters are below the Molasse Basin and Jura of northern Switzerland and southern Germany.

Significant earthquakes of 2007

Landeck

With a magnitude M_L of 3.9, this earthquake, that occurred on May 19th, was the strongest event recorded in Switzerland or in its surrounding regions in 2007. The epicenter was located in Austria, near the town of Landeck. There are no reports of it having been felt in Switzerland. Given an epicentral distance of 36 km to the nearest station, the hypocentral location is uncertain. However, the shallow focal depth of 2 km (Table 2007.1) agrees with the fact that this event was not felt out to larger distances. Moreover, unusually high travel-time residuals of the location are also an indication of a shallow focal depth in a region with a complex and laterally heterogeneous crustal structure.

Muotathal

At 2:09 in the night (local time) of July 12th, the area of Muotathal was jolted by an earthquake of magnitude M_L 3.0. Despite its occurrence in the middle of the night, there are several reports of it having been clearly felt in the village of

1
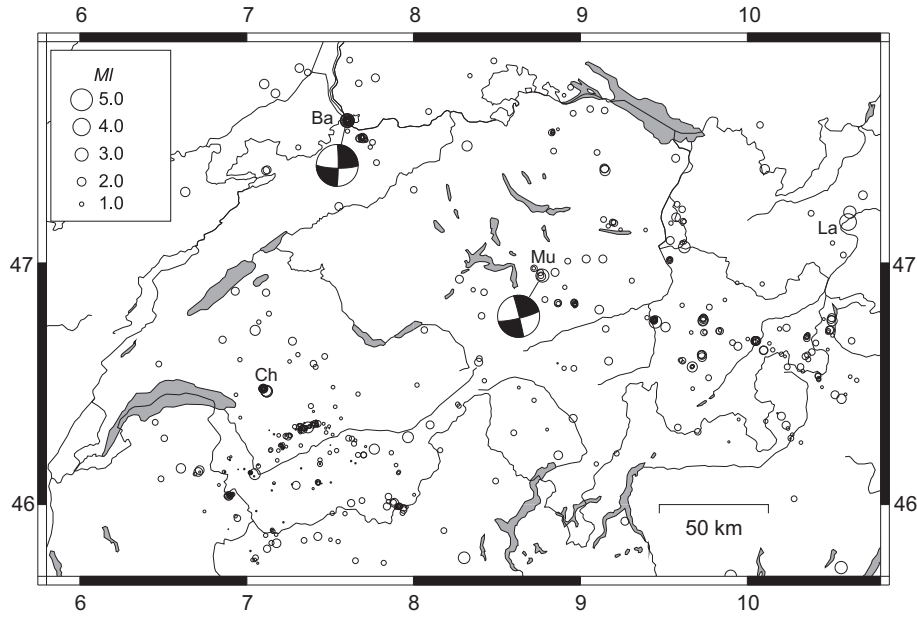
Figure 2007.1: Epicenters and focal mechanisms of earthquakes recorded by the Swiss Seismological Service during 2007. Epicenters of earthquakes mentioned in the text are Basel (Ba), Château-d'Oex (Ch), Landeck (La) and Muotathal (Mu).

Date & Time UTC	Lat. [°N]	Lon. [°E]	X / Y [km]	Depth [km]	Mag. [M_L]	Q	Location
2007.01.06 07:19:52	47.581	7.601	612/270	5	3.1	A	Basel, BS
2007.01.15 06:23:57	47.659	6.286	513/279	11	2.9	D	French Jura, F
2007.01.16 00:09:07	47.581	7.604	612/270	5	3.2	A	Basel, BS
2007.02.02 03:54:27	47.581	7.602	612/270	5	3.2	A	Basel, BS
2007.03.21 16:45:18	47.580	7.600	612/270	4	2.8	A	Basel, BS
2007.03.23 05:01:38	45.690	9.867	789/ 63	10	3.6	B	Bergamo, I
2007.03.23 05:24:19	45.702	9.901	792/ 64	10	2.7	B	Bergamo, I
2007.04.01 00:22:56	46.128	7.048	570/108	2	2.6	B	Martigny, VS
2007.04.02 09:10:33	45.778	8.303	667/ 70	25	2.7	C	Varallo, I
2007.05.19 16:19:38	47.168	10.605	840/229	2	3.9	C	Landeck, A
2007.06.28 06:32:06	45.736	10.564	843/ 70	9	2.9	B	Lago d'Idro, I
2007.07.12 00:09:32	46.949	8.771	701/200	0	3.0	B	Muotathal, SZ
2007.08.05 11:15:41	47.066	9.623	766/215	0	2.7	B	Malbun, FL
2007.08.23 21:35:00	46.758	9.449	754/180	6	2.8	B	Paspels, GR
2007.10.04 15:17:26	46.281	7.967	641/126	3	2.5	B	Glis, VS
2007.10.12 13:04:17	46.472	7.119	575/147	10	2.7	B	Château-d'Oex, VD
2007.10.15 16:25:49	47.208	10.615	841/233	5	2.9	C	Landeck, A
2007.10.24 06:14:53	46.473	7.115	575/147	10	2.6	B	Château-d'Oex, VD
2007.10.31 06:07:17	46.322	7.368	594/130	7	2.5	A	Anzere, VS
2007.12.11 16:57:39	46.471	7.120	575/147	10	2.5	B	Château-d'Oex, VD

Table 2007.1: Earthquakes with $M_L \geq 2.5$.
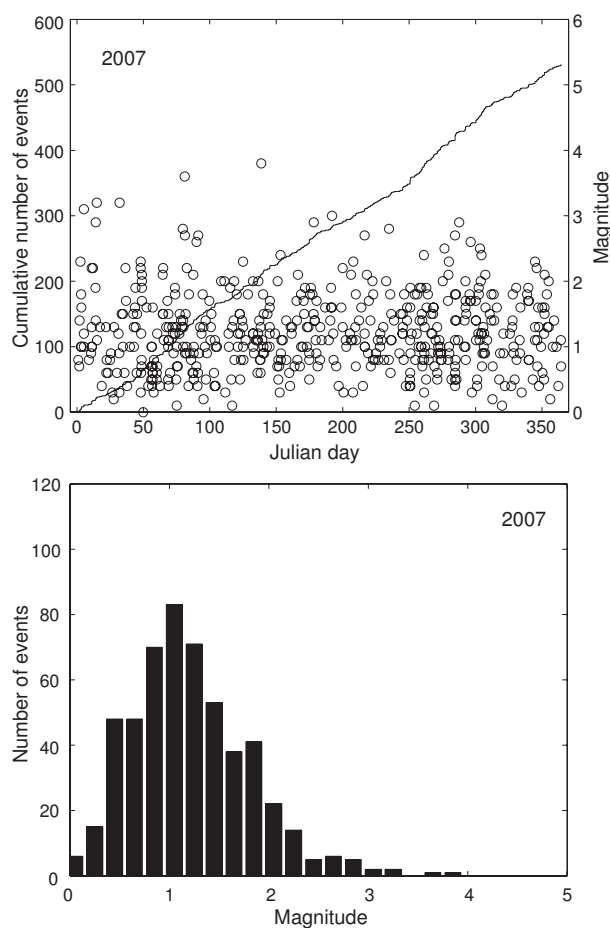
Figure 2007.2: Earthquake activity during 2007: magnitude of each event and cumulative number of events (above); histogram of magnitudes (below).

Location	Date & Time [UTC]	Depth [km]	Mag.	Plane 1	Plane 2	P-Axis	T-Axis
				Strike/Dip/Rake		Az/Dip	
Basel	2007/01/06 07:20	4	M_L 3.1	091/79/-176	360/86/-011	315/11	046/05
Muotathal	2007/07/12 00:09	2	M_L 3.0	076/82/-178	346/88/-008	301/07	031/04
		5	M_w 2.9	080/88/-160	349/70/-002	306/15	213/13

Table 2007.2: Focal mechanism parameters based on first-motion polarities (lines with M_L) and on an automated full-waveform inversion method (lines with M_w).
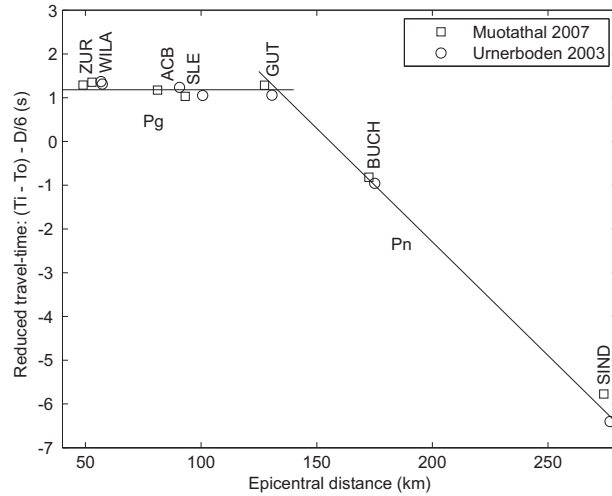
Figure 2007.3: Arrival times of the Urnerboden event of 2003 and the Muotathal event of 2007 observed at stations to the N of the epicenters. The data for the two events were aligned with respect to the arrivals of the waves refracted in the upper crust (Pg). The fact that the arrivals of the refractions at the Moho (Pn) match for the two events implies that their focal depths are very similar.

Hinterthal and some reports from scattered localities at larger distances from the epicenter.

The routinely determined location puts the hypocenter at a depth of 0 km. The closest station (MUO) is situated 10 km from the epicenter. Consequently, this focal depth is constrained only by the travel times along the rays refracted in the upper crust and in the upper mantle, and is very sensitive to the 3D velocity model used by the location algorithm. As an independent check of the focal depth, we compared the observed travel times of this earthquake with those for an event that occurred in 2003 near Urnerboden, 11 km to the east and 4 km to the south of Muotathal. The focal depth of the Urnerboden event was determined to be 3 ± 1 km by comparison with the Linthal event of 2001, that in turn is well-constrained by P- and S-arrivals observed at a strong-motion instrument 1 km from the epicenter (Deichmann et al. 2002 and 2004). As shown in Figure 2007.3, the cross-over distance of the travel-time branches of the refracted rays in the upper crust (Pg) and in the upper mantle (Pn) are practically the same for the two events. This implies that the focal depths of the two events must also be similar. The slightly later arrival of the Pn phase at station SIND in Figure 2007.3 suggests, in fact, that the Muotathal event could actually be even slightly shallower than the 3 km determined for the Urnerboden event. Thus, the hypocenter of this event was certainly located in the sediments, that are 5-6 km thick in this region (Maurer & Ansorge 1992). For the construction of the faultplane solution, we fixed the depth at 2 km and calculated the take-off angles with a 2D ray-tracing algorithm. The resulting focal mechanism is shown in Figure 2007.4 together with the optimal double-couple moment tensor derived from a full-waveform inversion of the seismograms observed at six stations located at epicentral distances between 28 and 81 km. Both solutions correspond to a strike-slip mechanism with NNW-SSE and ENE-
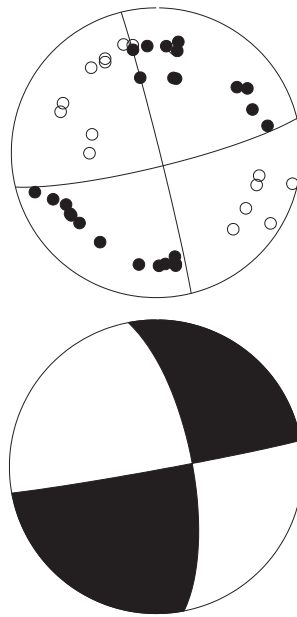
Muotathal 2007.07.12

Figure 2007.4: Faultplane solution of the M_L 3.0 Muotathal event (above) and optimal double-couple moment tensor based on a full-waveform inversion (below). The stereographs are lower hemisphere, equal area projections. Solid circles and shaded quadrants correspond to compressive first motion (up); empty circles and white quadrants correspond to dilatational first motion (down).
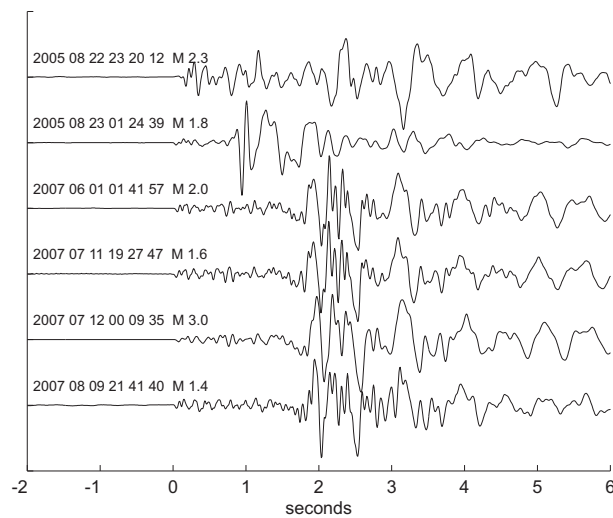

Figure 2007.5: Seismograms of two rain-induced events in the area of Bisistal and Riemenstalden during 2005 (above), and the four Muotathal events of 2007 (below), recorded at station MUO – N-S component, band-pass filtered 1-20 Hz.

WSW striking nodal planes (Table 2007.2), which is very similar to the focal mechanism of the 2003 Urnerboden event (Deichmann et al. 2004).

Judging from the almost identical seismograms (the lower four traces in Figure 2007.5), it was part of a small sequence of four events with the same source, that occurred between June 1st and August 9th. As summarized by Deichmann et al. 2006 and documented in detail by Husen et al. 2007, during the heavy rainfalls in August 2005 this region witnessed a remarkable case of precipitation-induced seismicity, with 33 events occurring within 24 hours. Contrary to what might have been expected, the sequence of 2007 does not correspond to a re-activation of the sources that were triggered by the rainfall two years earlier. This is illustrated by the two seismograms (top two traces in Figure 2007.5) that are typical for the two clusters that were active in 2005, and which differ significantly from those recorded in 2007. In fact, the epicenters of the four events recorded in 2007 lie roughly inbetween the Riemanstalden and Bisistal clusters of 2005.

Château-d'Oex

The most prolific single cluster to occur naturally in 2007 was located near the town of Château-d'Oex. It consisted of 23 events with magnitudes M_L between 0.7 and 2.7 that occurred between September 15th and December 11th. Almost half of them occurred within 26 hours, between October 12th and 13th. Judging from the striking similarity of the recorded seismograms shown in Figure 2007.6, the source and focal mechanism of all these events must have been nearly identical. However, even the records of the strongest event are not sufficient to construct a reasonably well constrained faultplane solution.

To improve the consistency of the measured arrival times across the whole sequence, we took advantage of the high signal similarity and applied a cross-correlation procedure to the P- and S- phases recorded at the four closest stations. Consequently, the calculated epicenter locations of the weaker events, that were recorded by only these four stations, form a point-like cluster in the epicenter map shown in Figure 2007.1. The systematic shift of this cluster relative to the location of the three stronger events is an artifact of the location procedure and is due to the fact that additional, more distant, arrivals were available for locating these events. In addition, given that the closest station to the epicenters is AIGLE at a distance of almost 20 km, the focal depth of about 10 km, listed in Table 2007.1 for the three $M_L \geq 2.5$ events, is only constrained by a few P_n arrivals refracted at the Moho. On the other hand, the computed focal depths of the weaker events, for which observations of P_n arrivals at large distances are lacking, put their hypocenters at the earth's surface.

Induced seismicity in Basel

To stimulate the reservoir for a "hot dry rock" geothermal project, that was initiated by a private/public consortium in the city of Basel, approximately 11500 m^3 of water were injected between December 2nd and 8th, 2006, at high pressures into a 5 km deep well below Kleinhüningen. As summarized by Baer et al. (2007) and documented in detail by Häring et al. (2008), the microseismic activity induced by this procedure increased steadily until the evening of December 8th, when a magnitude M_L 3.4 earthquake occurred within the stimulated rock volume. At that time, water injection hat already been stopped; subsequently the well was opened and the water allowed to flow back. In the following days about one third of the injected water volume escaped the well, and the seismic
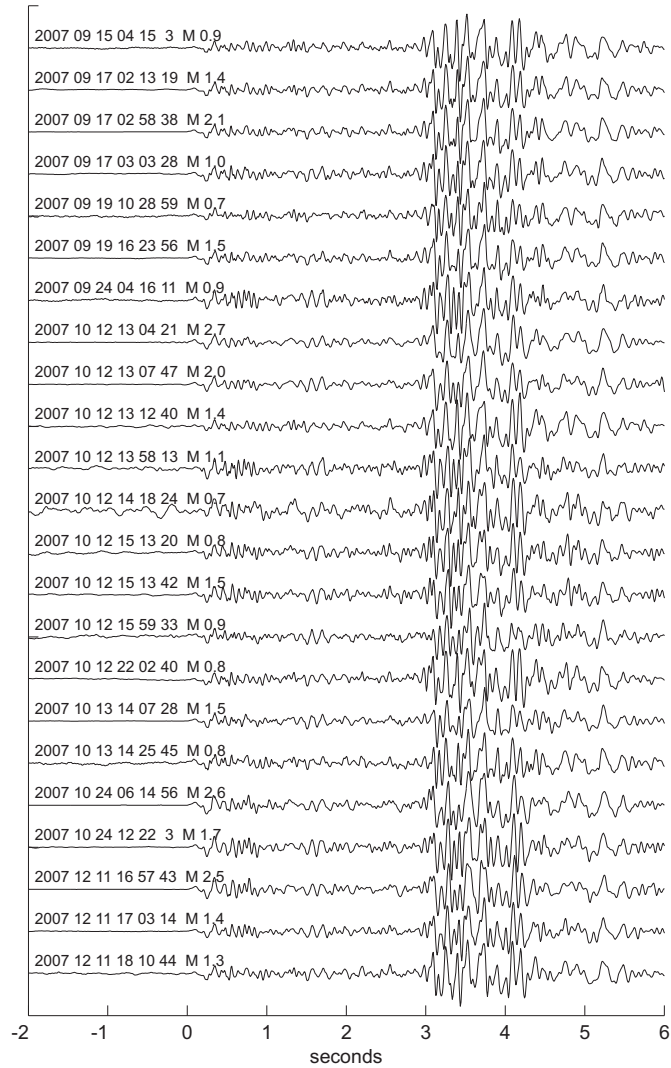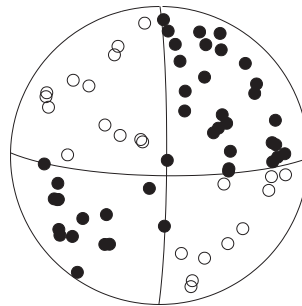
Figure 2007.6: Seismograms of the 23 events of the Château-d'Oex sequence, recorded at station AIGLE – vertical component, band-pass filtered 1-20 Hz.

Basel 2007.01.06

Figure 2007.7: Faultplane solution of the M_L 3.1 Basel event. The stereograph is a lower hemisphere, equal area projection in which solid circles correspond to compressive first motion (up) and empty circles to dilatational first motion (down).

activity declined rapidly thereafter (Häring et al. 2008). However, in the beginning of 2007 and although the water pressure at the wellhead had returned to near-normal levels, the seismic activity picked up again (Deichmann & Giardini 2009). This activity included four events with magnitudes M_L between 2.8 and 3.2, that were clearly felt by the population (Table 2007.1).

The network of high-sensitivity borehole sensors, that had been installed by the operators of the project to monitor the stimulation, detected more than 14'000 events by the end of 2006 and an additional 1046 events during 2007. The hypocenters of the more than 3500 locatable events are restricted to a NNW-SSE oriented lens-shaped cloud, about 1.2 km in diameter and 200 m wide, with a single offsetting branch to the ESE (Häring et al. 2008). The center of this cloud is at a depth of about 4.5 km below ground level.

In 2007, a total of 30 events associated with the Basel geothermal project were also recorded by the network of the Swiss Seismological Service. Their magnitudes (M_L) range between 0.8 and 3.2. The sources of all these events are located in the upper SSE corner of the hypocentral cloud (Deichmann & Giardini 2009).

A detailed documentation of the 28 focal mechanisms available to date for the Basel induced seismicity of 2006 and 2007 is presented in (Deichmann & Ernst, 2009). In Figure 2007.7 we show the faultplane solution of the first of the three events with $M_L > 3$. Given the large number of stations in the epicentral area and the good signals-to-noise ratio out to distances of almost 200 km, the solution is very well constrained. The strike-slip mechanism with N-S and E-W striking nodal planes (Table 2007.2) is in excellent agreement with the stress field derived from the natural seismicity observed in the past in the wider Basel region (Plenefisch & Bonjer 1997, Kastrup et al. 2004, Deichmann & Giardini 2009) as well as from borehole failure analyses down to 5 km in the Basel well perfomed by Valley & Evans (2009).

Seismic activity during 2008

Overview

During 2008, the Swiss Seismological Service detected and located 451 earthquakes in the region shown in Figure 2008.1. Based on such criteria as the time of occurrence, the location, the signal character or on direct communication, 75 additional seismic events were identified as quarry blasts. Magnitude values of the events recorded in 2008 range from M_L 0 to 4.0. The events with $M_L \geq 2.5$ are listed in Table 2008.1.
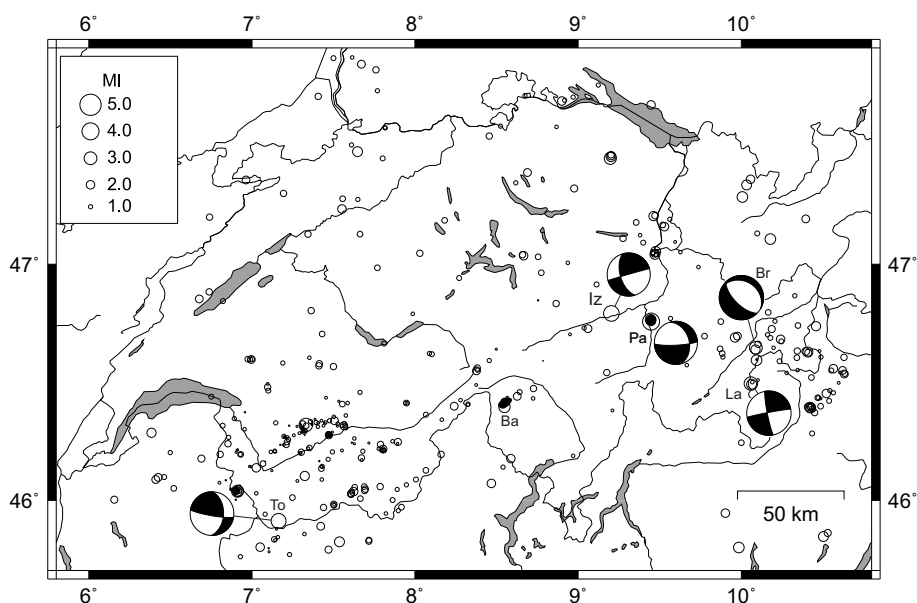

Figure 2008.1: Epicenters and focal mechanisms of earthquakes recorded by the Swiss Seismological Service during 2008. Epicenters of events mentioned in the text are Val Bavona (Ba), Brail (Br), Ilanz (Iz), La Stretta (La), Lac des Toules (To) and Paspels (Pa).

In 2008, as in previous years, most of the earthquakes, including the 6 events with $M_L > 3$, occurred in the Valais and in Graubünden. Routinely calculated focal depths for all but 10 events recorded in 2008 are less than 16 km. All the deeper hypocenters, with a maximum depth of 27 km, are below the Molasse Basin and Jura of northern Switzerland and southern Germany. Of the 451 earthquakes recorded in 2008, 29 were part of the Val Bavona sequence and 19 were part of the Paspels sequence. The seismic activity induced by the
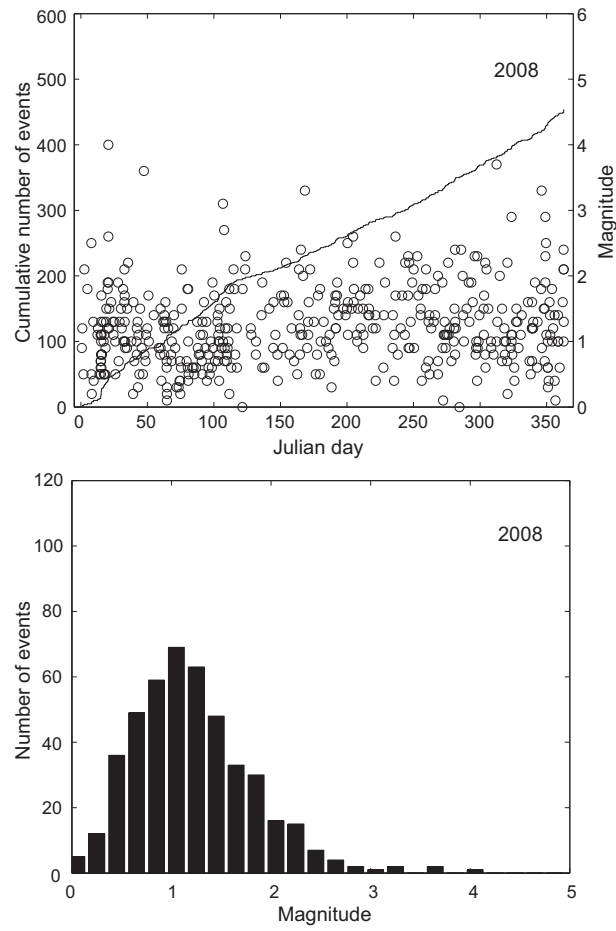
Figure 2008.2: Earthquake activity during 2008: magnitude of each event and cumulative number of events (above); histogram of magnitudes (below).

Date & Time UTC	Lat. [°N]	Lon. [°E]	X / Y [km]	Depth [km]	Mag. [M_L]	Q	Location
2008.01.08 21:41:14	46.596	10.095	803/164	7	2.5	B	Val Trupchun, GR
2008.01.21 16:40:36	46.759	9.447	753/181	8	4.0	A	Paspels, GR
2008.01.21 16:46:44	46.767	9.444	753/181	8	2.6	A	Paspels, GR
2008.02.17 12:41:31	45.920	7.171	579/ 85	7	3.6	B	Lac des Toules, VS
2008.04.17 01:07:37	46.664	10.103	804/171	7	3.2	A	Brail, GR
2008.04.17 21:42:05	46.398	8.548	685/139	7	2.7	B	Val Bavona, TI
2008.06.17 19:48:08	46.321	7.331	592/130	7	3.3	A	Glarey, VS
2008.07.19 23:30:07	47.105	10.178	808/221	3	2.5	C	Arlberg, A
2008.07.24 04:14:08	46.039	6.916	560/ 99	5	2.6	A	Vallorcine, F
2008.08.25 03:10:41	45.799	9.986	798/ 75	3	2.6	B	Endine, I
2008.11.09 07:22:31	46.793	9.204	735/184	8	3.7	A	Ilanz, GR
2008.11.20 13:20:19	46.040	6.912	559/ 99	5	2.9	A	Vallorcine, F
2008.12.13 06:02:24	46.501	10.060	801/153	2	3.2	A	La Stretta, GR
2008.12.16 00:34:33	47.443	9.197	733/256	8	2.9	B	Flawil, SG
2008.12.16 11:22:20	47.281	10.007	794/240	3	2.5	B	Schoppernau, A

Table 2008.1: Earthquakes with $M_L \geq 2.5$.

geothermal project in Basel in 2006 and 2007 (e.g. Deichmann & Ernst 2009; Deichmann & Giardini 2009) continued to decrease over the year 2008, and the events that have been recorded by the local borehole seismometers were too weak to be detected by the national broad-band network. The total number of only 15 events with $M_L \geq 2.5$ was far below the 24 to 25 events per year observed on average over the previous 33 years in this magnitude category. Thus the general trend of lower than average activity, that started in 2005, persisted through the year 2008.

Significant earthquakes of 2008

Paspels

The strongest earthquake in Switzerland and surroundings during 2008 occurred on January 21st at 17:40 local time. Its magnitude was M_L 4.0 (M_w 3.7) and its epicenter was located near the village of Paspels, 6-7 km N of Thusis (GR). Epicentral intensity reached IV-V and it was clearly felt all over southeastern Switzerland (Figure 2008.3). Three instruments of the strong-motion network situated at epicentral distances of 9 to 13 km were triggered by the quake and recorded peak horizontal ground accelerations between 0.21 and 0.34 m/s^2.

This earthquake was part of a sequence of 32 events that started in August 2007 and continued throughout the year 2008 (Figure 2008.4). Shortly after the mainshock, a temporary seismograph was installed in the immediate epicentral area. Between January 26th and 30th, this instrument recorded four aftershocks ($0.5 \geq M_L \leq 1.5$) that were detected also by the national network out to epicentral distances of 70-80 km.

With epicentral distances of about 1 km and travel-time differences between the S- and P-arrivals of about 1 s at this temporary station, the focal depths calculated for these four aftershocks vary between 8 and 9 km. This is in good agreement with the value of 7 km obtained for the mainshock from the routine
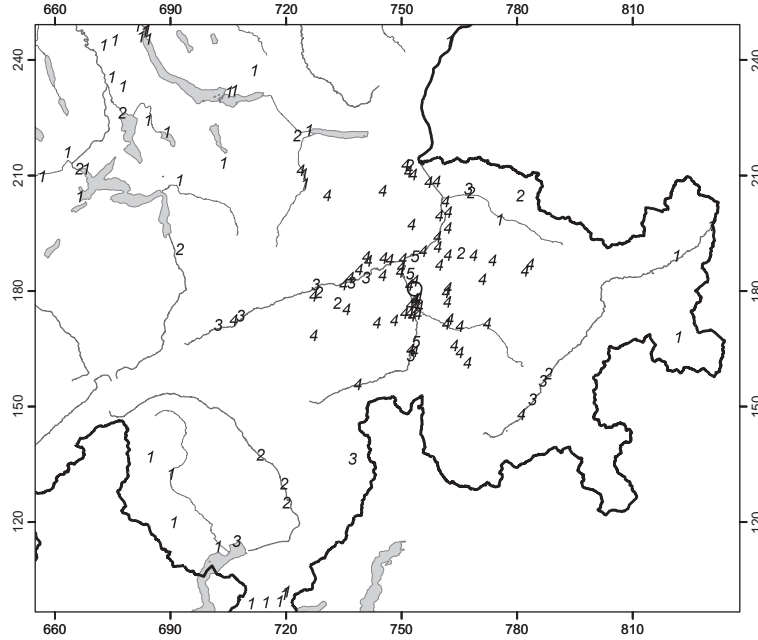
Figure 2008.3: Macroseismic intensities (EMS98) for the M_L 4.0 event near Paspels (GR). The Swiss cartesian coordinates are labeled in km.
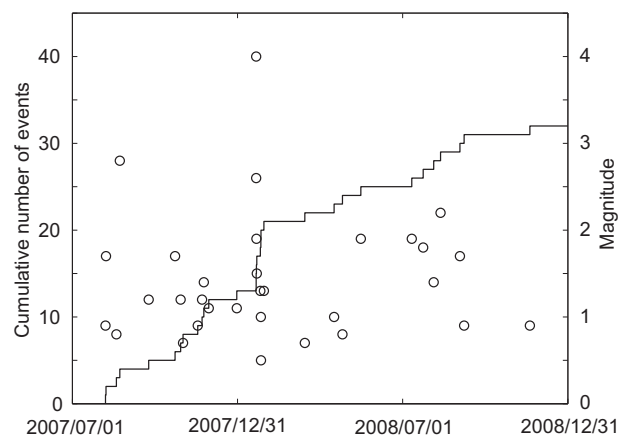

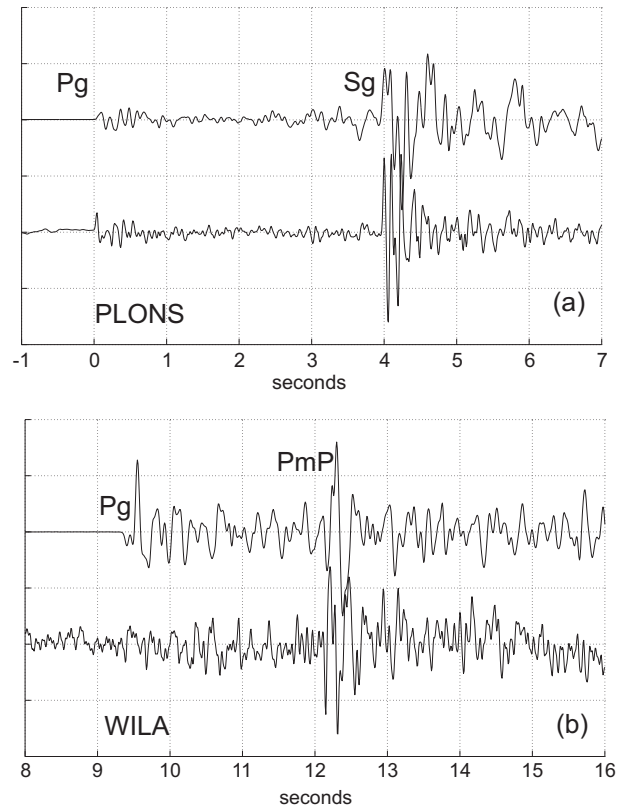Figure 2008.4: Cumulative number of events and event magnitudes of the Paspels sequence.

Figure 2008.5: (a) Seismograms of the M_L 4.0 mainshock (above) and the M_L 1.3 aftershock of 2008/01/26 06:16 (below) recorded at station PLONS (epicentral distance 33 km, azimuth 350 degrees), band-pass filtered 1-10 Hz. (b) Seismograms of the same two events recorded at station WILA (epicentral distance 84 km, azimuth 331 degrees), band-pass filtered 2-10 Hz. Both pairs of traces are aligned with respect to the Pg arrival times at station PLONS. The nearly identical travel times of the Sg phase at PLONS and of the PmP phase at WILA for the two events show that their sources must be located at similar depths.

location based on the 3D velocity model. As can be seen from the good agreement between the relative travel times of the reflections at the crust-mantle boundary (Moho) observed at station WILA (Figure 2008.5), the focal depth of the mainshock and the first of the four aftershocks recorded by the temporary station must be practically identical. To calculate the take-off angles of the rays at the source for the faultplane solution, we fixed the focal depth of the mainshock at 8 km.

The resulting focal mechanism is somewhat unusual, with one near-vertical E-W striking nodal plane and one N-S striking nodal plane dipping rather flatly to the E (Figure 2008.6). The unusual dip of the latter is well-constrained by the downward polarities of Pn refractions at the Moho observed at numerous stations in southeastern Germany. Moreover, the general type of mechanism is also matched by the result of the full-waveform moment tensor inversion, although, as listed in Table 2008.2, the orientation of the P-axes differs by 20°.

Paspels
2008.01.21

Lac des Toules
2008.02.17

Brail
2008.04.17

Ilanz
2008.11.09

La Stretta
2008.12.13
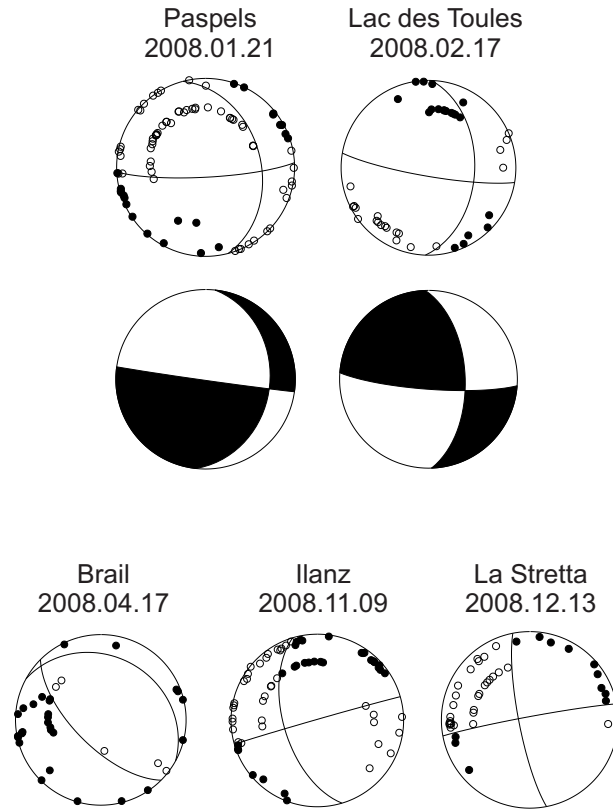
Figure 2008.6: Faultplane solutions based on first-motion polarities and, for two of the events, optimal double-couple moment tensors based on full-waveform inversion. All stereographs are lower hemisphere, equal area projections. Solid circles and shaded quadrants correspond to compressive first motion (up); empty circles and white quadrants correspond to dilatational first motion (down).

Location	Date & Time [UTC]	Depth [km]	Mag.	Plane 1	Plane 2	P-Axis	T-Axis
				Strike/Dip/Rake		Az/Dip	
Paspels	2008/01/21 16:40	8	M_L 4.0	345/38/-015	087/81/-127	322/42	205/27
		11	M_w 3.7	007/29/ 000	098/90/-119	342/38	214/38
Lac des Toules	2008/02/17 12:42	7	M_L 3.6	002/46/ 169	100/82/ 045	223/23	331/36
		5	M_w 3.4	358/56/ 169	094/81/ 034	222/16	322/30
Brail	2008/04/17 01:07	7	M_L 3.2	135/65/-083	299/26/-105	059/69	220/20
Ilanz	2008/11/09 07:22	8	M_L 3.7	163/58/-001	254/89/-148	123/23	024/21
La Stretta	2008/12/13 06:02	2	M_L 3.2	169/80/-003	260/87/-170	125/09	034/05

Table 2008.2: Focal mechanism parameters based on first-motion polarities (lines with M_L) and on an automated full-waveform inversion method (line with M_w).

Tangential   Radial   Vertical

DIX_f.05.data, VR=78.7, Max Amp=1.04e-04cm   Dist=26.6km, Az=45.3, Zcor=4

MMK_f.05.data, VR=79.3, Max Amp=4.57e-05cm   Dist=64.0km, Az=75.8, Zcor=7

AIGLE_f.05.data, VR=77.6, Max Amp=5.15e-05cm   Dist=50.4km, Az=341.4, Zcor=6

EMV_f.05.data, VR=72.2, Max Amp=6.12e-05cm   Dist=26.5km, Az=309.5, Zcor=4

SENIN_f.05.data, VR=75.6, Max Amp=6.01e-05cm   Dist=51.1km, Az=11.7, Zcor=7

TORNY_f.05.data, VR=68.4, Max Amp=5.83e-05cm   Dist=97.0km, Az=350.7, Zcor=12

Figure 2008.7: Recorded signals (continuous lines) and synthetic seismograms (dashed lines) used for the calculation of the moment tensor of the Lac des Toules event shown in Figure 2008.6.

Lac des Toules

On February 17th at 13:41 local time an earthquake with M_L 3.6 occurred in the region between Bourg Saint Pierre and the Col du Grand Saint Bernard. The epicenter was located about 3 km west of Lac des Toules. The calculated focal depth of 7 km is poorly constrained, and the distribution of travel-time residuals and a qualitative assessment of the waveform character at the closer stations suggest that it could be shallower. A shallow focal depth would also be in agreement with the relatively few reports of it having been felt beyond the immediate epicentral area and with the focal depth of 5 km obtained from the full-waveform inversion for the moment tensor (Figure 2008.7). The fault-plane solution and the best double couple moment tensor match each other to within 10° (Table 2008.2). The resulting focal mechanism corresponds either to dextral strike-slip motion on a N-S striking and flatly inclined fault or to obliquely upward directed slip on a steeply dipping, WNW-ESE striking fault. The extensional axis is inclined at more than 30° and is oriented in a NNW-SSE direction. For the Penninic domain of the Valais, which is otherwise known for its normal faulting regime with flat-lying T-axes (e.g Kastrup et al. 2004), this focal mechanism is rather unusual.

Brail

A magnitude M_L 3.2 event occurred at 02:07 local time of April 17th in the Engadine. The picenter was located in the Swiss National Park, 5 km east of Brail. It was followed two days later by an M_L 1.6 aftershock. Despite a good recording at an accelerometer in Zernez (at an epicentral distance of only 4 km), computed focal depths vary between 5 and 8 km, depending on the algorithm and number of stations used for locating the event. Ray-trace modeling of the travel times of this event observed at stations HASLI, TORNY and BRANT at an azimuth of 275° compared to the travel times of the nearby La Stretta event of December 13th, 2008, observed at the same stations shows that the Brail event must be about 5 km deeper than the La Stretta event. As discussed below, the most likely focal depth of the La Stretta event is about 2 km, so that the hypocenter of the Brail event is located at a depth of about 7 km. With this depth and with take-off angles taken from the 2D ray-trace models, the fault-plane solution results in a well-constrained normal-faulting focal mechanism with a NE-SW directed T-axis (Figure 2008.6).

Val Bavona

With a magnitude M_L 2.7, the earthquake that occurred on April 17th at the upper end of Val Bavona, in northern Ticino, was not particularly significant in itself. However it is part of a sequence of 29 events with M_L between 0.6 and 2.7 that occurred in a region which is not known for its seismic activity. About half of the events in this sequence were detected only by the local network installed in the Gotthard region and their signals were integrated into the SED data archive at a later stage. The first event of this sequence was recorded on February 4th and most of the events occurred during the months of February, March and April, but activity persisted through to December.

Ilanz

In the morning of November 9th (08:22 local time) the area around Ilanz (GR) was jolted by an earthquake with M_L 3.7. The epicenter of the earthquake, which was felt throughout northern Graubünden, Glarus and parts of Uri, was located about 2 km N of Ilanz (Figure 2008.8). Since the nearest station (LLS) is located at an epicentral distance of 16 km, the routinely calculated focal depth of 4 km is not well constrained. Lacking observations from stations close to the epicenter, calculated focal depths are constrained mainly by arrivals refracted (Pn) or reflected (PmP) at the Moho. However, the results, particularly for shallow sources, are very sensitive to the crustal velocity model and the assumed Moho topography. The Paspels earthquake of January 21st, 2008, with its epicenter only 15 km east of Ilanz and with its well-constrained focal depth, offers a unique opportunity to calibrate the velocity model and thus to determine the focal depth of the Ilanz quake relative to that of the Paspels event by means of 2D ray tracing. Ray trace models for both earthquakes were constructed based on the Moho model of Waldhauser et al. (1998) for an azimuth of 320 degrees, equivalent to a NW direction with respect to both Paspels and Ilanz. Figure 2008.9 shows the ray-tracing results for these two earthquakes, assuming a focal depth of 8 km for the Paspels event. Travel times for the Ilanz event were calculated for several focal depths between 4 and 9 km. The best match of the Pn travel times at stations FELD and KIZ, southern Germany, was obtained at the same focal depth for both events. Thus, for determining the focal mechanism
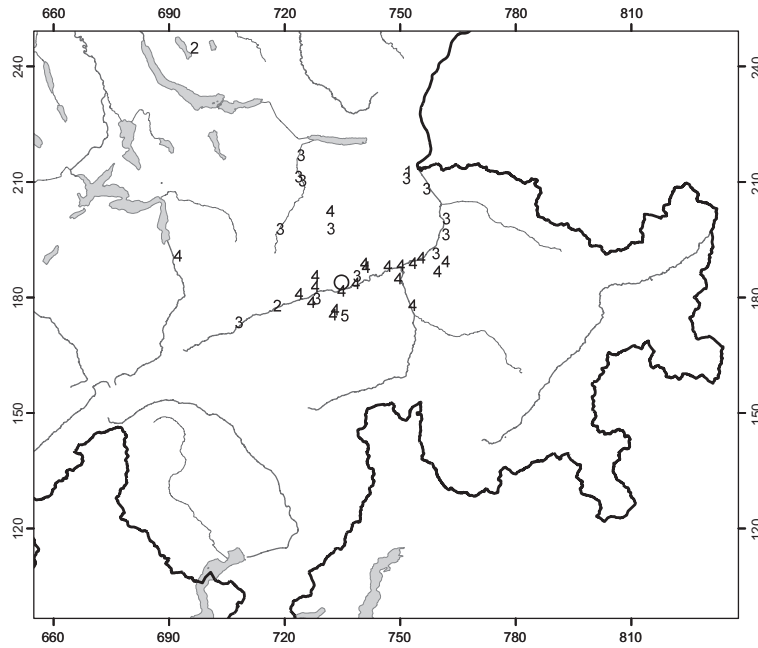
Figure 2008.8: Macroseismic intensities (EMS98) for the M_L 3.7 event near Ilanz (GR). The Swiss cartesian coordinates are labeled in km.

of the Ilanz event, the take-off angles were calculated with a source depth fixed at 8 km. Given the large number of azimuthally well-distributed stations that recorded this event, the faultplane solution is well constrained. The result is a strike-slip mechanism with NNW-SSE and ENE-WSW striking nodal planes (Figure 2008.6).

La Stretta

The last of the four M_L 3 - 4 events of the year 2008 in Graubünden occurred in the early morning of December 13th. It had a magnitude M_L of 3.2 an its epicenter was located just across the border with Italy about 8 km SSW of Livigno. It was followed by two aftershocks: the first with M_L 0.9 occurred less than five hours later, and the second with M_L 2.4 followed on December 29th. With a minimum epicentral distance of 10 km (station BERNI), the routinely computed focal depth of 0 km is constrained mainly by the Pn arrivals recorded by the distant stations in NW Switzerland. However, as shown in Figure 2008.10, a comparison of the Pg-Pn crossover distance of this event with that of the Val Mora event of 2006 shows that the focal depth of these two events must be practically the same. As documented in Baer et al. (2007), several lines of evidence lead to the conclusion that the hypocenter of the Val Mora event of 2006 was located at a depth of about 2 km. With this value for the focal depth and the same take-off angles as determined from 2D ray-trace modeling for the Val Mora event, we obtain a strike-slip focal mechanism with roughly NS and EW oriented nodal planes (Figure 2008.6). Despite the poor azimuthal coverage of the two southern quadrants, the parameters of the resulting focal mechanism are constrained to within about ±10° by the available first-motion polarities. Given the predominance of normal faulting events in this region (e.g.

Kastrup et al. 2004), this strike-slip mechanism is unusual. However the nearly NE-SW orientation of the T-axis is in good accord with the orientation of the T-axes of this year's Brail event and of the Val Mora event in 2006.
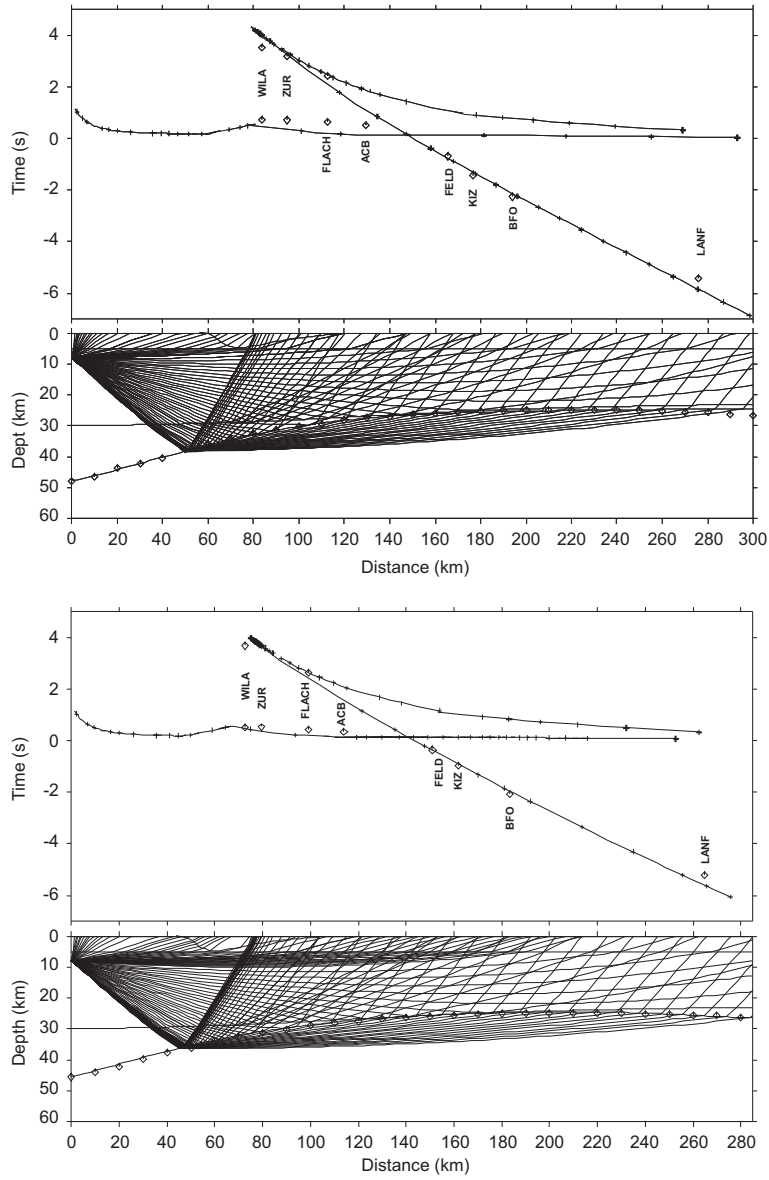
Figure 2008.9: Comparison of the 2D ray tracing models for the Paspels (above) and the Ilanz earthquakes (below), assuming a focal depth of 8 km for the Ilanz earthquake. The time axes are plotted with a reduction velocity of 6 km/s.
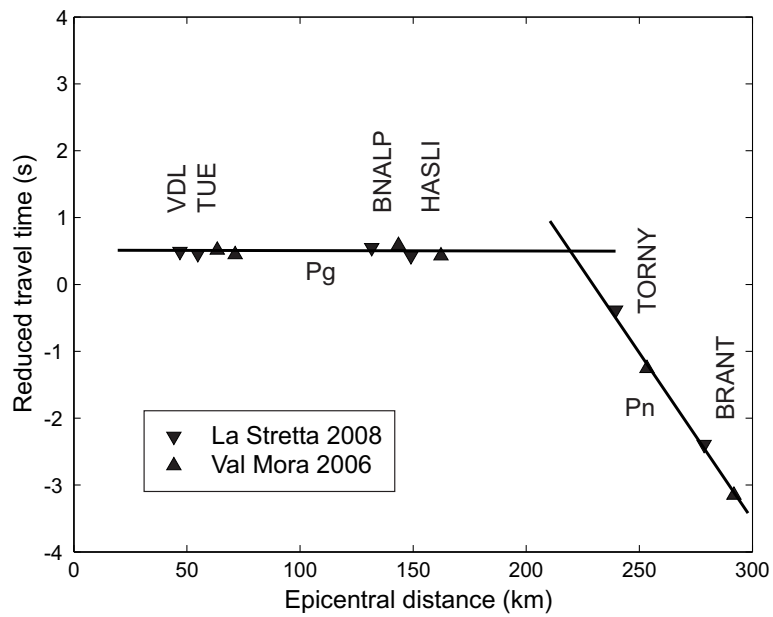
Figure 2008.10: Travel times of the 2006 Val Mora and the 2008 La Stretta events observed at six stations located WNW of the epicenters. The data points of the two events are aligned so that the Pg arrivals match. The fact that the Pn arrivals match as well means that the focal depths of the two events are practically identical.

Seismic activity during 2009

Overview

During 2009, the Swiss Seismological Service detected and located 449 earthquakes in the region shown in Figure 2009.1. Based on such criteria as the time of occurrence, the location, the signal character or on direct communication, 69 additional seismic events were identified as quarry blasts. Magnitude values of the events recorded in 2009 range from M_L 0.2 to 4.2. The events with $M_L \geq 2.5$ are listed in Table 2009.1.
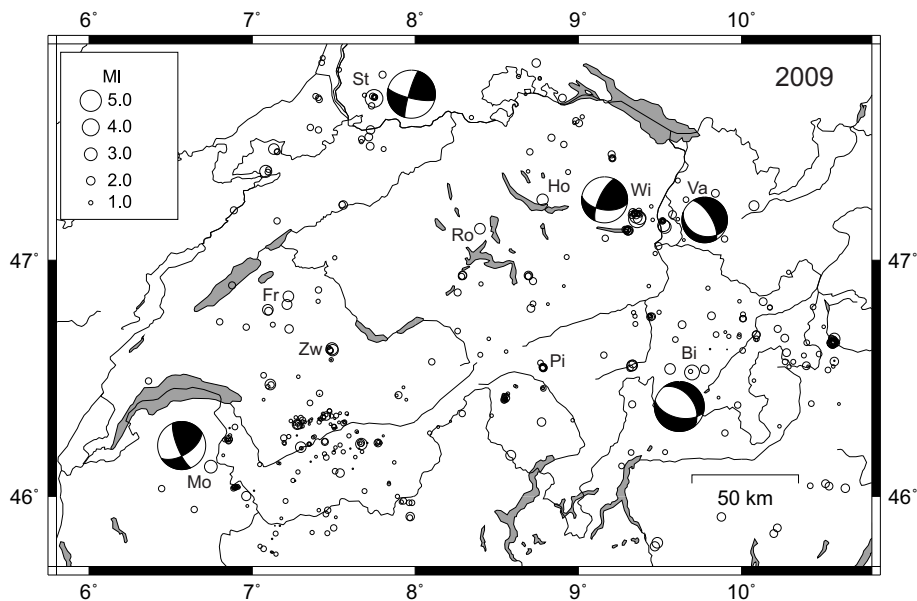
Figure 2009.1: Epicenters and focal mechanisms of earthquakes recorded by the Swiss Seismological Service during 2009. Epicenters of events mentioned in the text are Bivio (Bi), Fribourg (Fr), Hombrechtikon (Ho), Morzine (Mo), Root (Ro) Steinen (St), Vaduz (Va), Wildhaus (Wi) and Zwischenflüh (Zw).

In 2009, as in previous years, in terms of the number of events most of the earthquakes occurred in the Valais and in Graubünden. However, the two strongest events with $M_L > 4$ occurred northeast of Basel and in the Toggenburg. Routinely calculated focal depths for all but 17 events recorded in 2009 are less than 16 km. Of the deeper hypocenters, 15 are below the Molasse Basin and Jura of northern Switzerland and southern Germany; one, with a depth of 24 km, occurred in the Voralberg region (Austria) and one near Camedo, on

1

Date & Time UTC	Lat. [°N]	Lon. [°E]	X / Y [km]	Z [km]	Mag. $[M_L]$	Mag. $[M_w]$	Q	Location
2009.01.04 15:30:30	47.173	9.361	746/226	5	4.1	4.0	A	Wildhaus, SG
2009.01.04 15:48:47	47.176	9.375	747/227	5	3.1	3.1	A	Wildhaus, SG
2009.01.15 07:54:03	46.628	7.489	604/164	-2	2.8		B	Zwischenflüh, BE
2009.01.17 07:09:58	47.139	9.529	759/223	5	3.0	2.8	A	Vaduz, FL
2009.01.19 13:12:25	46.621	7.494	604/163	-2	2.7		B	Zwischenflüh, BE
2009.02.02 15:42:53	47.145	9.524	758/224	5	2.9	2.7	A	Vaduz, FL
2009.02.15 20:28:43	46.476	7.111	575/147	9	2.6	2.8	B	Château d'Oex, VD
2009.02.16 12:14:59	47.132	8.397	673/220	32	2.6	2.3	A	Root, LU
2009.03.30 01:39:54	47.464	7.134	577/257	22	2.6	2.6	A	Bonfol, JU
2009.04.02 08:54:15	47.234	6.471	527/232	7	2.7		C	Landresse, F
2009.05.05 01:39:25	47.674	7.748	623/280	12	4.2	3.7	A	Steinen, D
2009.05.09 20:54:58	46.210	7.299	589/118	7	2.5	2.5	A	Nendaz, VS
2009.05.20 13:19:09	47.372	7.083	573/247	5	2.9	2.8	B	Ocourt, JU
2009.06.18 23:03:02	46.669	10.570	840/173	10	2.7	2.6	A	Glorenza, I
2009.07.02 23:08:09	46.558	9.331	745/158	6	2.6	2.7	B	Splügen, GR
2009.07.10 01:06:47	45.802	9.485	759/ 74	13	2.6	2.6	B	Lecco, I
2009.08.12 13:52:28	47.181	9.354	745/227	4	2.9	3.0	A	Wildhaus, SG
2009.08.19 02:04:42	46.788	7.094	574/182	2	2.6	2.6	A	Matran, FR
2009.09.11 06:34:38	46.527	9.696	773/155	11	3.6	3.2	A	Bivio, GR
2009.10.12 21:56:03	46.542	9.562	763/157	7	2.5	2.3	A	Mulegns, GR
2009.10.21 16:10:59	46.128	6.747	547/109	6	3.1	3.0	A	Morzine, F
2009.11.02 12:14:35	47.253	8.780	701/234	32	2.7	2.4	A	Hombrechtikon, ZH
2009.12.12 00:17:48	46.844	7.222	584/189	2	2.6	2.7	A	Düdingen, FR
2009.12.31 10:49:36	46.224	7.669	618/119	6	2.7	2.8	B	Saint Luc, VS

Table 2009.1: Earthquakes with $M_L \geq 2.5$. The values listed under M_w are the moment magnitudes calculated from the spectral fitting method documented in Edwards et al. (2010). The focal depth of the events of Vaduz (Feb. 2nd), Matran and Düdingen have been set manually to the given values as explained in the text. In some cases, where focal depths could be constrained by comparisons with neighboring events, quality B has been changed to quality A (see text for details).

the border between the Canton Ticino and Italy. The focal depth (23 km) of the latter is poorly constrained, given the sparse station coverage in that region and the complex crustal structure in the vicinity of the Ivrea Body. The two deepest events (near Root, LU, and Hombrechtikon, ZH) were located at depths of 32 km, which puts them just above the Moho, situated at about 34 km in these two locations (Waldhauser et al. 1998). The proximity to the Moho of these two hypocenters is well constrained by the fact that the Pn phase appears as the first arrival already at epicentral distances less than 50 km. Of the 449 earthquakes recorded in 2009, 16 were part of the Wildhaus cluster and 9 were part of the Vaduz sequence. The seismic activity induced by the geothermal project in Basel in 2006 and 2007 (e.g. Deichmann & Ernst 2009; Deichmann & Giardini 2009) continued to decrease over the year 2009, and the events that have been recorded by the local borehole seismometers were too weak to be detected by the national broad-band network. The total number of 24 events with $M_L \geq 2.5$ was about equal to the yearly average over the previous 34 years
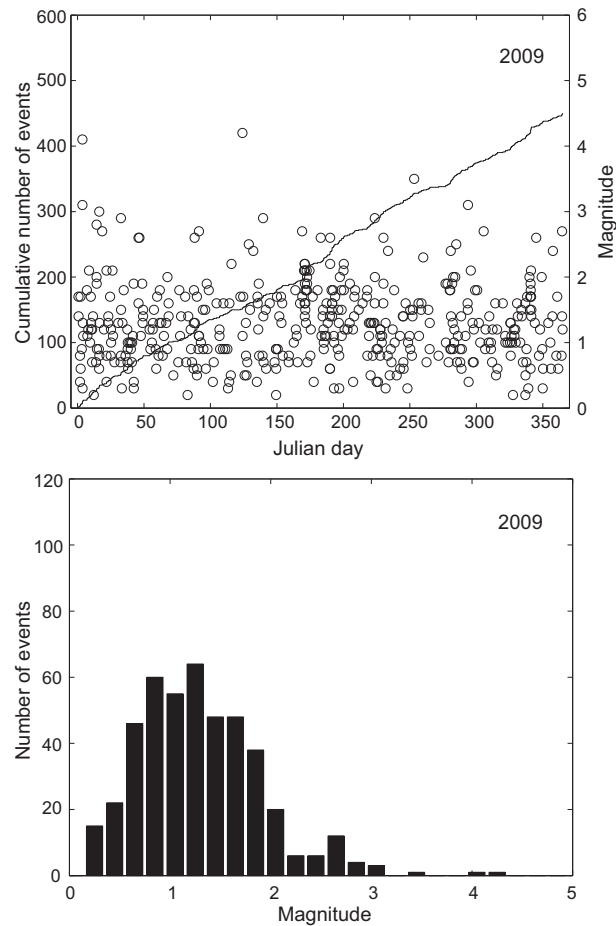
Figure 2009.2: Earthquake activity during 2009: magnitude of each event and cumulative number of events (above); histogram of magnitudes (below).

in this magnitude category.

Significant earthquakes of 2009

Wildhaus

At 16:30 local time of January 4th, the Toggenburg was jolted by an earthquake with magnitude M_L 4.1. Its epicenter was located 3 km south of Wildhaus and it produced shaking of intensities IV (EMS) in the upper Toggenburg, Appenzell, the Rheintal of Sankt Gallen and Walensee area (Figure 2009.3). Maximum measured horizontal ground motions were recorded by an accelerometer near Gams (station SGAG), at an epicentral distance of 8 km, with values of 0.66 m/s^2 PGA and 19 mm/s PGV. A value for the moment magnitude of M_w 3.7 is obtained from the full-waveform moment tensor inversion and of M_w 4.0 from the spectral fitting method.

The hypocentral location based on the Swiss 3D velocity model of Husen et al. (2003) gives a focal depth of 4.5 km. This value is constrained by small travel-time residuals of both the Pn arrivals recorded at several distant stations
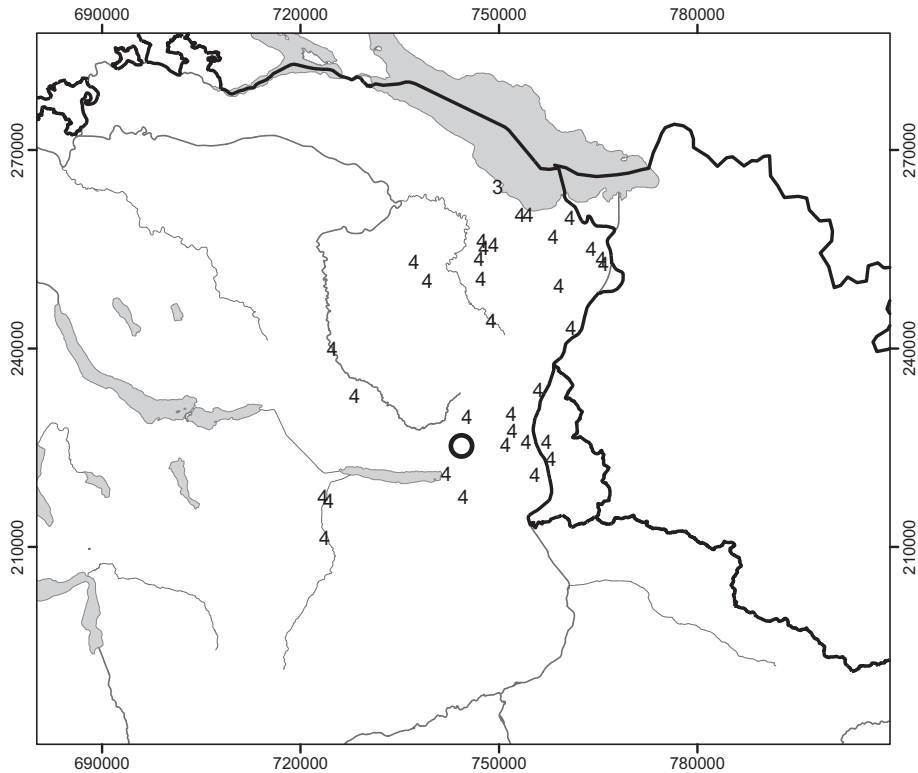
Figure 2009.3: Macroseismic intensities (EMS98) for the M_L 4.1 event near Wildhaus (SG). The Swiss cartesian coordinates are labeled in m.

and by the Pg and Sg arrivals at an accelerometer located on hard rock 6.3 km SW of the epicenter (station SBUM at Buchs-Malbun). The angle of incidence relative to vertical of the ray at this station, estimated from the polarization of the P-wave, is 52°. Assuming an average P-wave velocity $V_p = 5$ km/s and a ratio $V_p/V_s = 1.8$ for the sediments in the upper 5 km of the crust in this region, the observed S-P arrival-time difference of 1.3 s corresponds to a hypocentral distance of 8.1 km and to an epicentral distance of 6.3 km, in agreement with the result of the routine location procedure. The corresponding focal depth, assuming a straight ray path and taking into account the elevation of the station (1.4 km a.s.l), would correspond to a focal depth of 3.7 km. Even considering the uncertainties of the polarization measurement and of the assumed wave velocities, the two completely independent focal depth estimates are in very good agreement and lend confidence to the conclusion that the Wildhaus event occurred in the sedimentary cover, which in this region reaches a thickness of about 6 km (Hitz & Pfiffner 1997).

Given the relatively large magnitude of this event and the good station coverage, it was possible to construct a well-constrained faultplane solution from the observed P-wave polarities. Take-off angles of the rays at the source were calculated with a 2D ray-tracing program along profiles of different azimuths, with a focal depth set to 4.5 km. The resulting focal mechanism is strike-slip with a small thrust component. The NNW-SSE oriented P-axis is consistent with the stress field derived from the analysis of earlier earthquakes in the Helvetic
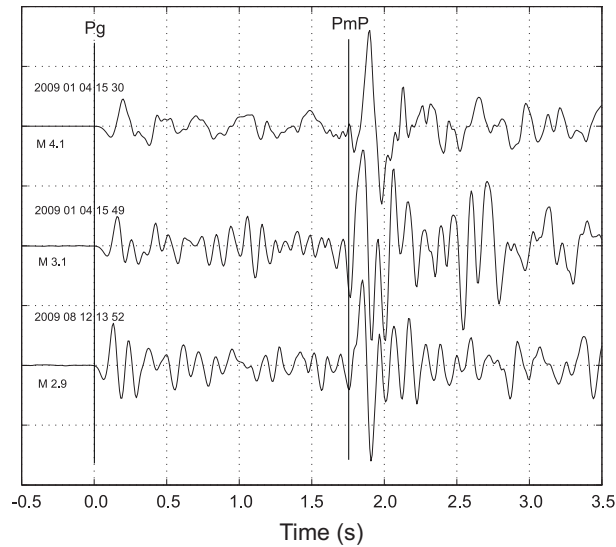
Figure 2009.4: Seismograms of the three strongest Wildhaus events recorded at station SLE (Bandpass filter 2-20 Hz) The almost identical arrival-time difference between the reflection from the Moho (PmP) and the direct wave (Pg) implies that the focal depth of the three events is also practically the same.

domain of eastern Switzerland (Kastrup et al. 2004). The horizontal orientation of the P- and T-axes of the moment tensor derived from the full-waveform inversion differs by a bit more than $10°$ from the faultplane solution, and the moment tensor has a significantly smaller thrust component (Figure 2009.5 and Table 2009.2). Given that the waveform fit is excellent (variance reduction 85%) while the double couple component of the solution (70%) is relatively small, it is conceivable that the moment tensor inversion and the faultplane solution look different because they are reflecting different aspects of the source.

Only 18 minutes later, the M_L 4.1 event was followed by an aftershock of M_L 3.1. This second event was the first of a total of 15 aftershocks recorded over the rest of the year 2009. One of these additional aftershocks, which occurred August 12th, reached a magnitude M_L 2.9; all others had magnitudes between 1.1 and 1.9. The routinely calculated hypocentral locations of the events comprising the entire sequence scatter over a relatively large volume. To a substantial extent this scatter is an artifact of the fact that the number and distribution of available stations is very different for the smaller and larger events. However, variations in the signal character among the individual events indicate that the true locations are likely to scatter as well. Preliminary results of a master-event relative location procedure, based on the manual arrival times read by the analyst, indicate that the epicenters could be distributed over an area of 2×3 km. The differences in signal character and clear polarity reversals at some key stations are evidence that the focal mechanisms of the mainshock and the two largest aftershocks are not identical either. However, the almost identical arrival-time differences between the reflection at the Moho (PmP) and the direct wave (Pg) shown in Figure 2009.4, demonstrate that, at least for the three strongest events, the focal depths are practically the same. A more detailed analysis of the hypocentral distribution and focal mechanisms of the Wildhaus

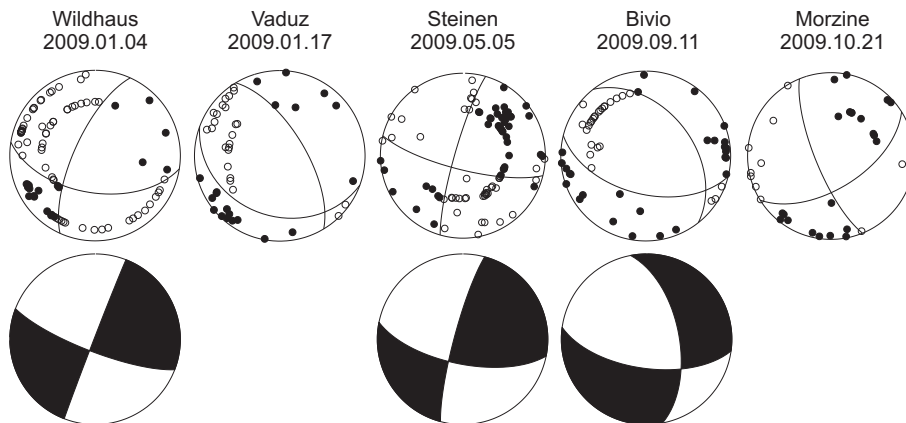| Wildhaus 2009.01.04 | Vaduz 2009.01.17 | Steinen 2009.05.05 | Bivio 2009.09.11 | Morzine 2009.10.21 |

Figure 2009.5: Faultplane solutions based on first-motion polarities (above) and optimal double-couple moment tensors based on full-waveform inversion (below). All stereographs are lower hemisphere, equal area projections. Solid circles and shaded quadrants correspond to compressive first motion (up); empty circles and white quadrants correspond to dilatational first motion (down).

sequence is still underway.

Zwischenflüh

A sequence of six events occurred between January 15th and April 3rd near Zwischenflüh (BE), with magnitudes between ML 1.0 and 2.8. The P-arrivals at most stations are rather emergent and also the S-arrivals are difficult to identify with confidence. The routine location procedure, based on the 3D velocity model, places the hypocenters of all six events at the Earth's surface. Although the location uncertainty is large, a shallow focal depth is in accord with the strong and long-lasting surface waves observed at several stations (in particular at station WIMIS at an epicentral distance of only about 12 km) and with the fact that the two events with ML 2.7 and 2.8 were clearly felt by the local population. The first event was preceded by a small foreshock that occurred 3 seconds earlier. Two additonal small events occurred in July and August about 4 km further to the south. The location algorithm puts them at a depth of 8 km. Although this value is also subject to a significant uncertainty, a larger focal depth is supported also by the higher frequency of the signals, the impulsive S-arrivals and large P-wave amplitudes on the vertical component at the closest station situated at an epicentral distance of 14 km. Thus, this doublet is not related to the earlier sequence.

Vaduz

The M_L 3.0 event, which occurred on January 17th at 8:10 in the morning local time right below the town of Vaduz, was part of a sequence of eight events that began seven hours earlier with a M_L 0.9 event. It was followed that same day by two more small events (M_L 0.8 and 1.3). For the mainshock there are 37 reports of it having been felt. After two weeks of quiescence, activity picked up again in the afternoon of February 2nd with two events with magnitudes M_L 2.9 and 1.5. Two additional small events (M_L 1.0 and 0.9) occurred February 10th and

Location	Date & Time [UTC]	Depth [km]	Mag.	Plane 1	Plane 2	P-Axis	T-Axis
				Strike/Dip/Rake		Az/Dip	
Wildhaus	2009/01/04 15:31	4	M_L 4.1	099/54/ 155	204/70/ 039	328/10	067/41
		5	M_w 3.7	111/78/ 179	201/89/ 012	335/08	067/09
Vaduz	2009/01/17 07:10	5	M_L 3.0	110/30/-125	329/66/-072	270/64	045/19
Steinen	2009/05/05 01:39	12	M_L 4.2	104/76/ 172	196/82/ 014	329/04	061/16
		8	M_w 3.6	101/66/ 171	195/82/ 024	326/11	061/23
Bivio	2009/09/11 06:35	11	M_L 3.6	104/53/-115	322/44/-061	315/70	211/05
		8	M_w 3.1	094/55/-148	345/64/-039	306/45	042/05
Morzine	2009/10/21 16:11	6	M_L 3.7	058/58/ 162	158/75/ 033	285/11	022/34

Table 2009.2: Focal mechanism parameters based on first-motion polarities (lines with M_L) and on an automated full-waveform inversion method (lines with M_w).

24th. All eight events have very similar waveforms, typical of nearly colocated events with identical focal mechanisms. The scatter in the routinely determined locations (3 km horizontally and 10 km in depth) is clearly an artifact of the different station distribution available for the location of the stronger and weaker events, and thus of the poorly constrained locations of the latter. The 4.7 km focal depth of the mainshock is based on the Swiss 3D model and relies on P- and S-arrivals recorded by an accelerometer at an epicentral distance of 5 km as well as on several Pn arrivals observed at distances between 140 and 216 km. The similarity of the focal depth of the Vaduz and Wildhaus events is confirmed by 2D ray-trace modelling of the PmP-Pg travel-time differences observed at stations TRULL and SLE (at epicentral distances between 73 and 105 km).

The faulplane solution, based on first-motion polarities, corresponds to a normal faulting mechanism with a NE-SW oriented T-axis. This mechanism is constrained to a large degree by the upward motion of the arrival at station ABSI, located in northern Italy, at a distance of 144 km ESE of the epicenter. Without this observation, the focal mechanism could also be strike-slip. For this reason, we not only checked that the seismometer was operating correctly, but, to verify that the identified first motion really corresponds to the first arrival, we also compared the observed travel time at station ABSI with the travel times at neighboring stations for the Vaduz mainshock and with the travel times observed for the M_L 4.1 Wildhaus event. As a result, we have no reason to question the reliability of the first-motion polarity observed at station ABSI, and conclude that the focal mechanism derived for the Vaduz sequence is well constrained. It is noteworthy, because it constitutes the first normal-fault mechanism observed in this region. Whereas the hypocenters of the Wildhaus earthquakes are certainly located in the Helvetic Nappes, those of the Vaduz sequence might be located in a transition zone between the Helvetic and the Austro-Alpine Nappes (Hitz & Pfiffner 1997).

Steinen

The epicenter of the earthquake that occurred at 03:39 (local time) of May 5th was located about 15 km NW of Basel, near the village of Steinen in southern
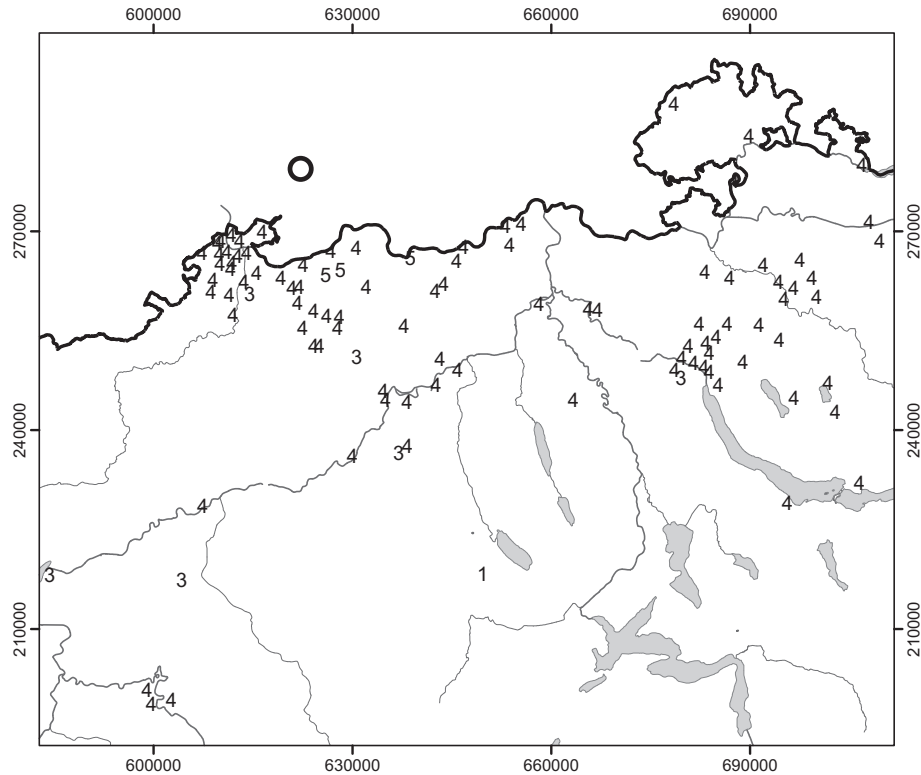
Figure 2009.6: Macroseismic intensities (EMS98) for the M_L 4.2 event near Steinen (D). The Swiss cartesian coordinates are labeled in m.

Germany. With a focal depth of 12 km and a magnitude M_L 4.2 it produced maximum intensities in Switzerland of V (EMS) and, despite its occurrence in the middle of the night, was clearly felt with intensities of IV across most of northern Switzerland (Figure 2009.6) as well as over large parts of south-western Germany and the bordering regions of France. The maximum values of measured horizontal ground motion were recorded by an accelerometer near Frenkendorf (SFRA) located at an epicentral distance of 19 km, with values of 0.54 m/s^2 (PGA) and 14 mm/s (PGV). At the site closest to the epicenter, for which records are available (station END, distance of 5 km), maximum horizontal ground motion reached 0.41 m/s^2 (PGA) and 5.6 mm/s (PGV).

With 19 stations within an epicentral distance range of 5 to 20 km and with numerous impulsive arrivals visible out to distances beyond 250 km, the hypocentral location of this event based on the Swiss 3D velocity model is very reliable. Though there are some discrepant polarities near the nodal planes, the faultplane solution is similarly well constrained and agrees closely with the results of the full-waveform inversion for the moment tensor (Figure 2009.5 and Table 2009.2). The latter features a double-couple component of 91% and a variance reduction of 83%, with a moment magnitude M_w of 3.6. Both solutions correspond to a strike-slip mechanism with NNW-SSE and ENE-WSW oriented P- and T-axes, in accord with the orientation of the known regional stress field (e.g. Kastrup et al. 2004).

In the five days following this event, the Swiss Seismological Service recorded

three aftershocks (M_L beteen 1.1 and 1.5), and a fourth aftershock (M_L 1.1) was recorded in September. An additional three events, with M_L between 1.0 and 1.6, occurred nearby in April, July and October, but at significantly larger focal depths, so that they can not be regarded as aftershocks of the May 5th event.

Bivio

The M_L 3.6 event that occurred on Sept. 11th near Bivio triggered the off-line accelerometers located in Bergün (SBET) and in Celerina (SCEM) at epicentral distances of 9 and 11 km. Peak horizontal ground motion recorded by these two instruments, which are located on hard rock, reached 0.23 m/s^2 and 0.06 m/s^2 (PGA) and 4.6 mm/s and 2.0 mm/s (PGV). There are 47 reports of it having been felt, mostly from the Engadine and central Graubünden.

Given a favourable azimuthal station coverage, the epicentral location is well constrained and insensitive to using different velocity models and different distance cut-offs for the stations used by the location algorithm. Focal depth, on the other hand, varies between 6 and 11 km, depending on whether one uses arrivals out to distances of more than 250 km or uses a distance cut-off of 72 km. The shallower focal depth is constrained by the Pn arrivals observed at larger distances and results in unusually large travel-time residuals of both P- and S-arrivals at the closest stations. Without the Pn arrivals, the calculated focal depth increases to 11 km and the residuals at the closer stations decrease to normal values. A focal depth beyond 10 km agrees also with the qualitative observation that the travel-time curve plotted through the arrival times as a function of epicentral distance is strongly curved out to distances of about 30 km. If the depth were around 6 km, the pronounced curvature of the travel-time curve would not be observed beyond about 15 km. In addition, 2D ray-tracing, using as reference the well-constrained 8 km focal depth of the M_L 4.0 Paspels event of 2008, located 31 km NW of Bivio, results in a focal depth for the Bivio event between 9 and 12 km.

Thus, the take-off angles of the rays at the source used by the faultplane solution, were calculated for a focal depth of 11 km. The result is a normal faulting mechanism with a NE-SW oriented T-axis and agrees with the moment tensor obtained from the low-frequency full-waveform inversion to within 11° (Figure 2009.5 and Table 2009.2). The moment magnitude associated with the latter is M_w 3.1. Both the type of mechanism and the orientation of the T-axis is typical for the Penninic domain of Graubünden (Roth et al. 1992, Kastrup et al. 2007).

The Bivio event was preceded on February 17th by a foreshock with M_L 1.1; two additional aftershocks occurred in 2010, with magnitudes M_L 2.0 and 1.1.

Morzine

The M_L 3.1 event that occurred October 21st, close to the town of Morzine, just across the border with France, is interesting because its epicenter is located near the events of Samoëns (2000.08.19, M_L 3.3) and Vallorcine (2005.09.08, M_L 4.9), for which detailed studies are available (Delacou et al. 2005; Fréchet et al. 2010). The epicentral location based on data from both the Swiss national network and the SISMALP stations, operated by the University of Grenoble, is reliable, and the focal depth of 6 km is well-constrained by observations at station OG03, located at an epicentral distance of only 7 km, as well as by a good azimuthal station distribution. Take-off angles for the faultplane solutions

were set equal to those of the Samoëns event, which had a similar focal depth (5 km) and for which the take-off angles were derived from 2D ray-tracing (Delacou et al. 2005). The result is a strike-slip mechanism with P- and T-axes oriented WNW-ESE and NNE-SSW, that is very similar to the mechanism of the Vallorcine event of 2005 (Fréchet et al. 2010). The mechanism of the Samoëns event is also strike-slip, but the P- and T-axes are oriented NW-SE and NE-SW.

Fribourg

The year 2009 saw four events with magnitudes M_L 1.9 - 2.6 occurring within a radius of about 6 km from the city of Fribourg. Although their magnitudes are small, they are interesting because in the years 1987, 1995 and 1999 the area of Fribourg has seen repeated sequences of earthquakes, that have reached magnitudes M_L up to 4.3 and that seem to delineate an active, several km long N-S trending fault zone east of the city (Kastrup et al. 2007). As a consequence, in 2008, the Canton of Fribourg commissioned the Swiss Seismological Service to install two additional accelerometers near Cournillens (SCOU) and near Tafers (STAF), which, as shown by the example in Figure 2009.7, have provided excellent records of these new events.
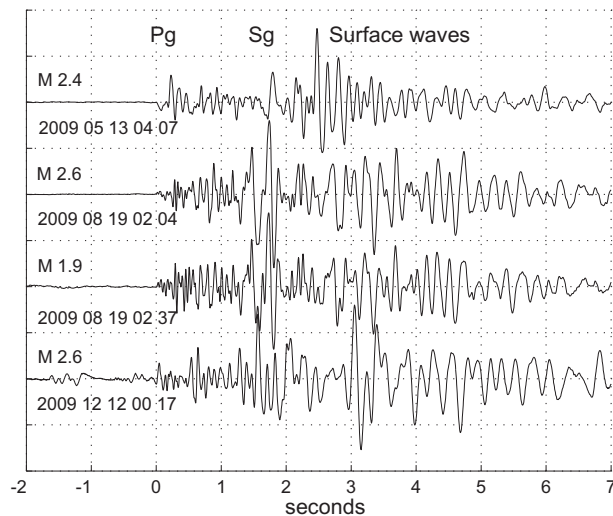
Figure 2009.7: Seismograms of the four Fribourg events recorded at station SCOU, integrated to velocity and filtered with a 2nd order band-pass filter between 1 and 20 Hz. From top to bottom, the signals correspond to the events of Tafers, Matran (2) and Düdingen. Epicentral distances vary between 7.5 and 10 km. The pronounced surface waves observed at such short epicentral distances are typical of events with hypocenters at depths of only a few km within the sedimentary layers.

Two of the four events recorded in 2009 occurred within 32 minutes from each other in the early morning hours of August 19th near the town of Matran, west of the city of Fribourg. Therefore, these two events are not in any way related to the earlier earthquake sequences east of Fribourg. The M_L 2.4 event of May 13th near Tafers and the M_L 2.6 event of December 12th near Düdingen, on the other hand, occurred along the northward continuation of the lineament
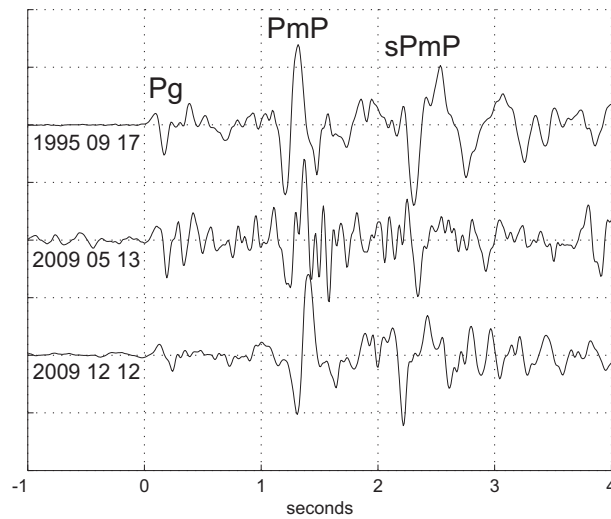
Figure 2009.8: Seismograms of one of the 1995 Fribourg events (top) and the 2009 events of Tafers (middle) and Düdingen (bottom) recorded at station ACB (epicentral distance between 114 and 119 km). The almost identical arrival-time differences between the sPmP and the PmP phases shows that the focal depth of all three events must be similar.

defined by the epicenters of the earthquake sequences of 1987, 1995 and 1999. In fact, both the routinely performed absolute locations and the results of a master-event location procedure place the epicenters of the Tafers and Düdingen events 2-2.5 km and 5.5-6 km north of the M_L 4.3 event of 1999.

The routinely determined locations were calculated with program NonLin-Loc and the Swiss 3D model (Husen et al. 2003), using the EDT option, that downweights arrivals with large residuals. In the case of the four events considered here, the downweighting applies to the S-arrivals recorded at distances between about 10 and 80 km and to the P-arrivals recorded at distances beyond about 100 km. For the Tafers and Düdingen events, the resulting focal depths are 3.5 and 4.1 km. Based on synthetic seismograms, Kastrup et al. (2007) showed that the travel-time differences between the direct reflection at the Moho (PmP) and the reflection at the Moho originating from the conversion of the S-wave at the Earth's surface (sPmP), observed for the events recorded in 1995 and 1999, could be explained best for a focal depth of about 2 km. In Figure 2009.8 we show that the PmP and the sPmP phases of the 1995 Fribourg event and the two events of Tafers and Düdingen recorded in 2009 at station ACB are very similar, and that therefore the focal depths of the 2010 events are likely to be close to 2 km as well. A shallow focal depth is also compatible with the S-P travel-time difference of only 0.7 seconds observed for the Tafers event at station STAF, located at an epicentral distance of about 1 km, as well as with the fact that the Düdingen event was felt by several people, despite its small magnitude (M_L 2.6) and its occurrence in the middle of the night.

In the case of the Matran events, the routinely calculated focal depths are nearly 6 km for the M_L 2.6 event and at the Earth's surface for the M_L 1.9 event. However, given the high similarity of the waveforms of the two Matran events (see e.g. traces 2 and 3 in Figure 2009.7) the two hypocenters must be nearly identical, and the obtained focal depth differences must be an artifact of
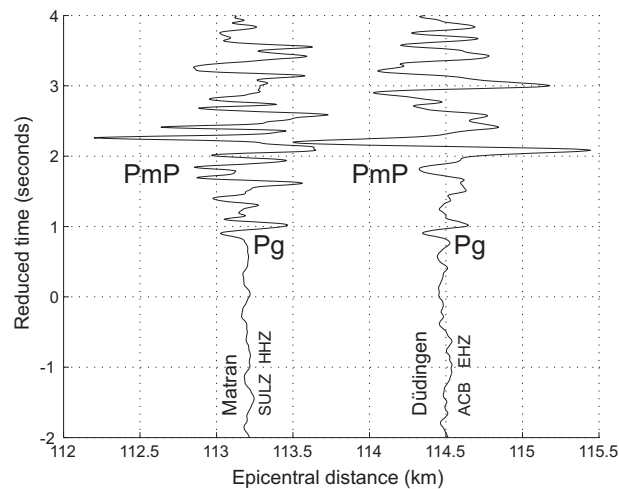
Figure 2009.9: Seismograms of the M_L 2.6 Matran event recorded at station SULZ and of the M_L 2.6 Düdingen event recorded at station ACB. Given the nearly identical epicentral distances of the two stations and a nearly horizontal Moho along the segement where the PmP reflection occurs (Waldhauser et al. 1998), the almost identical arrival-time differences between the PmP and the Pg phases shows that the focal depth of the two events must be similar.

the location procedure. In fact, the larger focal depth of the M_L 2.6 event is mainly constrained by the phase refracted at the Moho (Pn) observed at several stations in northeastern Switzerland at distances beyond about 120 km. For the weaker M_L 1.9 event these Pn arrivals are below the noise level, so that its focal depth is mathematically poorly constrained. In fact neither value is correct. A comparison of the arrival time differences between the PmP and the Pg phases observed for the stronger of the two Matran events and for the Düdingen event at almost the same epicentral distance (Figure 2009.9) shows that the most likely focal depth of the Matran events must also be around 2 km. As in the case of the Düdingen event, the first Matran event, despite its low magnitude and its occurrence in the early morning hours, was felt by several people, which again suggests that its source was shallow.

Due to the small magnitudes and the shallow focal depth of these four events, the onset of the P-phase is often emergent and does not rise clearly above the noise at larger distances. Therefore reliable first-motion polarities are too few to derive well-constrained focal machanisms. Nevertheless, the available observations are not incompatible with a strike slip mechanism, with more or less N-S and E-W oriented faultplanes (Figure 2009.10). Such a mechanism would be similar to the focal mechanisms of the 1987, 1995 and 1999 earthquake sequences (Kastrup et al. 2007) and compatible with the regional stress field (Kastrup et al. 2004).

In conclusion, the four events of 2009 near the city of Fribourg demonstrate that the seismic activity observed in the past within the near-surface sedimentary layers in this area is ongoing. Moreover, the results of the analysis of the Tafers and Düdingen events constitute evidence for a northward extension of the N-S striking fault zone, as defined by the earthquake sequences of 1987, 1995 and 1999 and postulated by Kastrup et al. (2007).
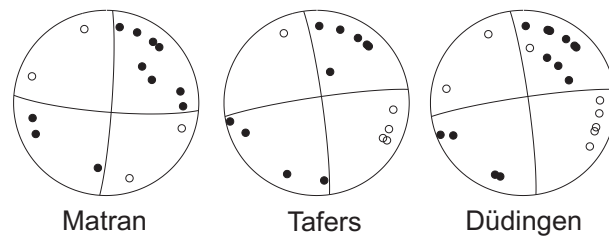
Figure 2009.10: Faultplane solutions (lower hemisphere, equal area projection) for the Tafers, Matran and Düdingen events of 2009. Take-off angles of the rays at the source are consistent with those calculated by Kastrup et al. (2007) for the Fribourg sequences of 1987, 1995 and 1999. The discrepant observation (Down) for the Düdingen event is station STAF, at an epicentral distance of only 4 km, and could therefore be due to a slight error in location and consequently in the calculated azimuth of the ray.

Piora

During 2009 the AlpTransit network recorded 51 earthquakes with local magnitudes between 0.2 and 2.0 in the Piora region. Of these 51 earthquakes, six earthquakes were strong enough to be detected by the SDSNet. Activity was spread over the entire year with a strong peak in December 2009, when 14 earthquakes occurred within three days. All earthquakes occurred north of the Piora zone in the vicinity of the Gotthard basetunnel, which was under construction at that time. Recorded waveforms show a strong similarity within different groups of events, suggesting that several fault patches ruptured repeatedly. Overall, seismicity migrated from south to north during the year, in accordance with the progression of construction work. Although some earthquakes were accompanied by rock bursts in the tunnel, no obvious correlation was observed between rock bursts and earthquake activity. Given the close temporal and spatial correlation, however, it is likely that the earthquake activity has been induced by the construction work of the Gotthard basetunnel.

Landslides

On April 19th, at 11:05, 23:35 and 23:43 (local time), the Swiss high-gain seismic network was triggered by three events with emergent and long-lasting signals, typical of large landslides (Figure 2009.11). Because of the emergent character of the signal onsets, in particular of the first two events, their source location was difficult to determine with confidence. However, the signals of the third event contain one or two more impulsive phases, that can be identified in seismograms recorded at several stations (see e.g. Figure 2009.11). Interpreting these phases as P- and S-waves gives a reasonably consistent epicenter location in the region of Pizzo Fiorera, on the border between Val Bavona (Ticino) and Val Formazza (Italy). The equivalent magnitudes of these events is 2.2, 1.7 and 2.1 M_L. Interestingly, despite its low M_L value, the first event triggered the automatic moment tensor inversion algorithm, resulting in an unusual focal mechanism, with a double-couple component that corresponds to a thrust event with more or less horizontal and vertical nodal planes. The reason that this small event triggered the full-waveform inversion is that, as is shown in Figure 2009.11, its signals are unusually large at the low frequencies normally used for such an

inversion. The corresponding equivalent moment magnitude M_w is 3.5. Such a high M_w value is not consistent with an M_L 2.2 earthquake and is further evidence for the fact that this and the other three events must be landslides. Only much later was it confirmed that these signals were caused by a massive landslide that descended that day in at least three phases from the western flanks of Pizzo Fiorera, at an altitude of about 1800 m a.s.l., and almost reached the first houses of Ponte in Val Formazza, located about 500 m lower on the floor of the valley.
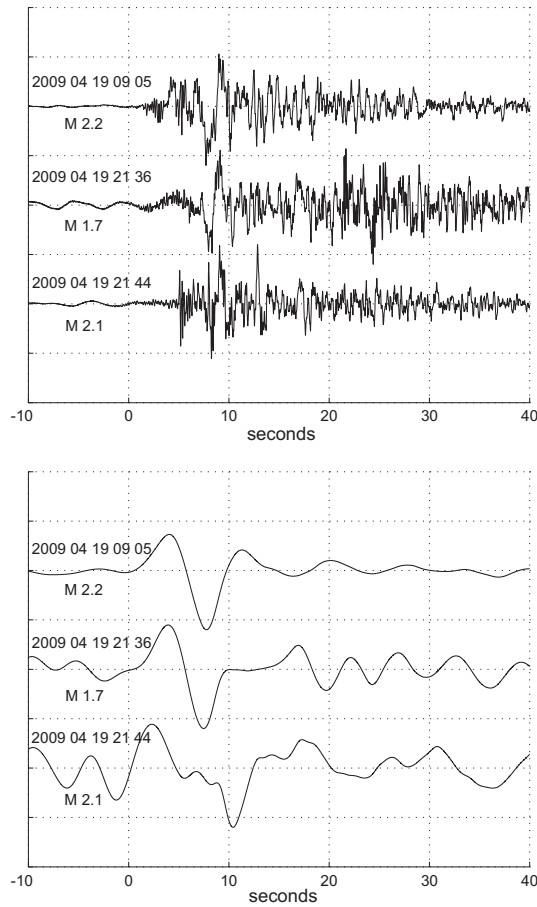
Figure 2009.11: Seismograms (vertical component, ground velocity) of the three landslides in Val Formazza recorded at station FUSIO (distance 20 km), approximately aligned at the onset of the signals (top: unfiltered; bottom: 4th order, zero-phase, band-pass filter 0.025-0.1 Hz). Note the more impulsive arrivals in the third unfiltered trace, visible at 5 and 8 seconds after the onset. In the filtered traces, the signal of the third event barely rises above the background noise, but in the seismograms of the first and second event it is clearly visible.

Seismic activity during 2010

Overview

During 2010, the Swiss Seismological Service detected and located 407 earth-quakes in the region shown in Figure 2010.1. Based on criteria such as the time of occurrence, the location, the signal character or on direct information, 85 additional seismic events were identified as quarry blasts. Magnitude values of the events recorded in 2010 range from M_L 0.1 to 3.5 (Figure 2010.2). The events with $M_L \geq 2.5$ are listed in Tables 2010.1. This table includes also the M_w values derived from the spectral fitting method of Edwards et al. (2010). Faultplane solutions based on first-motion polarities are shown in Figure 2010.3 and their parameters are listed in Table 2010.2.
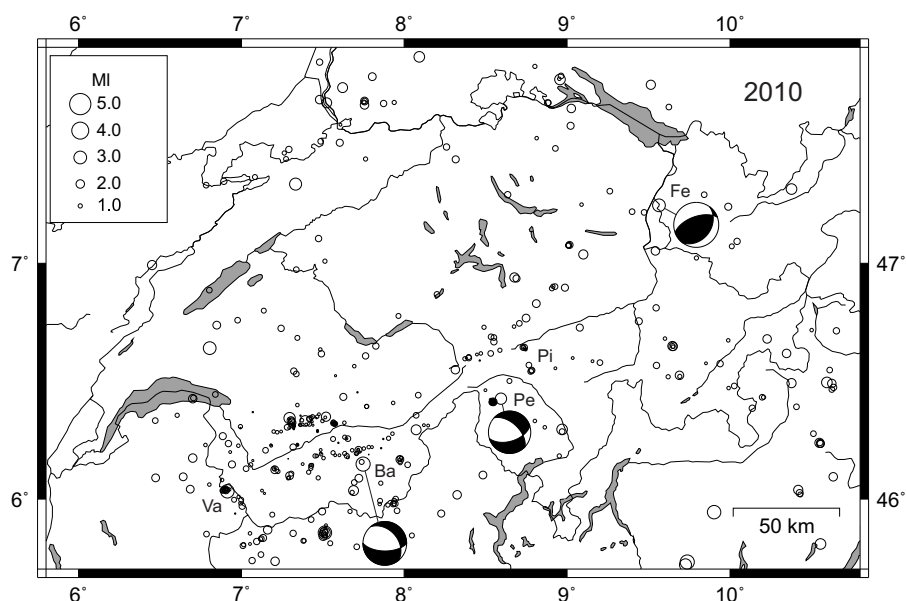
Figure 2010.1: Epicenters and focal mechanisms of earthquakes recorded by the Swiss Seismological Service during 2010. Epicenters of events mentioned in the text are Barrhorn (Ba), Feldkirch (Fe), Valle di Peccia (Pe), Piora (Pi) and Vallorcine (Va).

In 2010, a large portion of the seismic activity was concentrated in the Valais and the immediately adjacent regions, while activity in Graubünden was unusually low in comparison. Routinely calculated focal depths for all but 17 events recorded in 2010 are less than 16 km. All of the deeper hypocenters occurred

Date & Time UTC	Lat. [°N]	Lon. [°E]	X / Y [km]	Z [km]	Mag. [M_L]	Mag. [M_w]	Q	Location
2010.01.31 14:22:05	46.346	7.296	589/133	3	2.7	2.7	A	Col du Sanetsch, VS
2010.04.04 21:16:29	45.860	7.506	605/ 79	7	3.3	3.1	C	Becca de Leseney, I
2010.05.01 03:48:27	46.299	8.971	718/129	7	2.6	2.4	B	Lodrino, TI
2010.05.11 02:13:42	45.718	9.745	780/ 65	13	3.5	3.3	C	Albino, I
2010.05.14 03:35:28	45.718	9.727	778/ 65	0	2.9	2.7	D	Albino, I
2010.05.15 05:09:44	46.150	7.747	624/111	7	3.4	3.2	A	Barrhorn, VS
2010.05.24 12:32:49	47.767	8.957	714/292	11	2.6	2.6	B	Radolfzell, D
2010.06.01 03:30:06	45.856	7.512	606/ 78	7	2.5	2.5	C	Becca de Leseney, I
2010.06.07 13:19:27	46.424	8.598	689/142	7	2.7	2.4	A	Valle di Peccia, TI
2010.06.21 23:50:29	46.497	10.596	842/154	10	2.5	2.5	B	Ortles, I
2010.07.27 13:05:20	45.808	10.556	842/ 78	10	2.5	2.8	B	Lago d'Idro, I
2010.08.18 15:54:31	47.861	8.092	649/301	10	2.6	2.4	B	Feldberg, D
2010.08.22 11:14:12	46.334	7.391	596/131	6	2.5	2.6	A	Anzere (Sex Rouge), VS
2010.09.23 12:29:53	47.311	10.378	822/244	0	2.6	2.8	C	Lechtal, A
2010.10.25 20:00:31	47.243	9.564	761/235	5	3.0	2.9	A	Feldkirch, A
2010.11.12 12:42:06	46.642	6.805	551/166	8	3.0	2.9	B	Moudon, VD
2010.11.17 06:51:39	47.332	7.333	592/242	18	2.8	2.6	A	Courtételle, JU
2010.12.06 06:41:25	46.033	6.913	559/ 98	4	3.2	2.9	A	Vallorcine, F
2010.12.25 05:12:34	45.945	9.903	791/ 91	0	3.3	3.4	C	Ardesio, I

Table 2010.1: Earthquakes with $M_L \geq 2.5$. The values listed under M_w are the moment magnitudes calculated from the spectral fitting method documented in Edwards et al. (2010). The focal depth of the Feldkirch event has been set manually to the value constrained by comparison with the Vaduz events of 2009, and the quality has been changed from quality B to A (see text for details).

below the Molasse Basin and Jura of northern Switzerland and southern Germany. The deepest event was located at a depth of 31 km, northeast of the Bodensee. The seismic activity induced by the geothermal project in Basel in 2006 and 2007 (e.g. Deichmann & Ernst 2009; Deichmann & Giardini 2009) continued to decrease over the year 2010, and all events but one that have been recorded by the local borehole seismometers were too weak to be recorded by the national broad-band network. Overall, the seismic activity in and around Switzerland was low in 2010, both in terms of the number of events and in terms of the maximum event magnitude. The total number of 19 events with $M_L \geq 2.5$, of which only 7 events were actually located within Switzerland, was substantially below the yearly average of about 24 events over the previous 35 years in this magnitude range.

Significant earthquakes of 2010

Barrhorn

The strongest earthquake to have occurred within Switzerland in 2010 was the M_L 3.4 Barrhorn event of May 15th, 7:09 local time. Its epicenter was located about 5 km SW of Sankt Niklaus, VS. It was clearly felt with intensities of IV throughout the Mattertal and in the Rhone Valley as far as Brig (Figure 2010.4). A single aftershock of M_L 1.2 was recorded about seven hours later. The closest
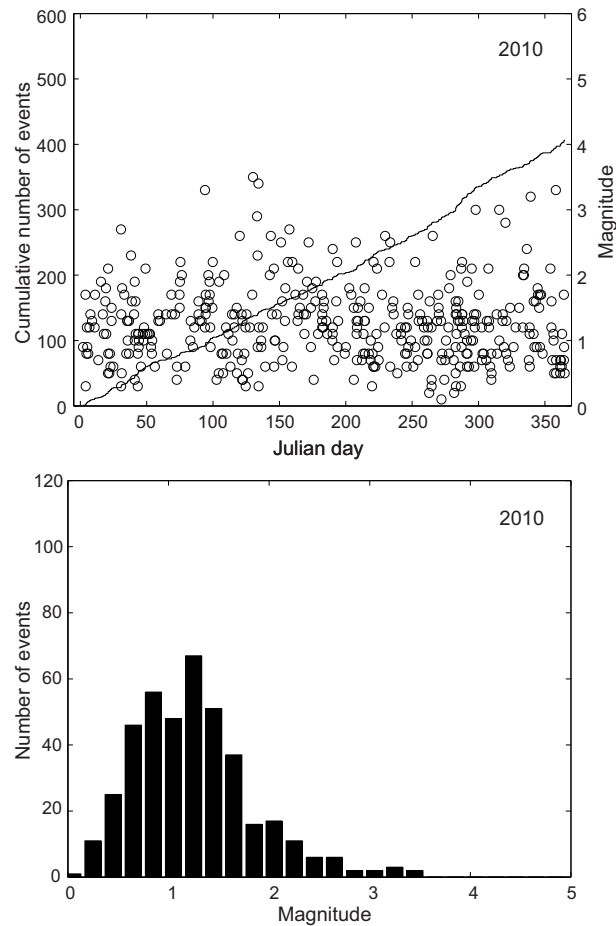
Figure 2010.2: Earthquake activity during 2010: magnitude of each event and cumulative number of events (above); histogram of magnitudes (below).

station (EMBD) is located at an epicentral distance of 10 km, so that the focal depth is constrained mainly by the more distant arrivals refracted at the Moho. The faultplane solution based on take-off angles calculated for the 3-D velocity model used in the routine location procedure gives a consistent and well-constrained normal-faulting mechanism (Figure 2010.3). This mechanism, with a NNE-SSW oriented T-axis, is typical for the earthquakes observed in the Penninic domain of the southern Valais (e.g. Kastrup et al., 2004).

Valle di Peccia

In the past, the northern part of canton Ticino was regarded as a region that is largely aseismic. However, in February 2008, an earthquake sequence became active near San Carlo in Val Bavona, a lateral valley of the upper Valle Maggia. More than 60 closely colocated events have been recorded to date and the strongest event, that occurred on April 17th, 2008, attained a magnitude M_L of 2.7 (Deichmann et al. 2009). The M_L 2.7 event that occurred in 2010 on June 7th, though located in the vicinity of this cluster, is clearly not part of this sequence. In fact its epicenter is located about 4 km ENE in the Valle di

Location	Date & Time [UTC]	Depth [km]	Mag.	Plane 1	Plane 2	P-Axis	T-Axis
				Strike/Dip/Rake		Az/Dip	
Barrhorn	2010/05/15 05:10	7	M_L 3.4	320/40/-048	090/61/-119	314/62	201/12
Peccia	2010/06/07 13:19	7	M_L 2.7	073/55/-135	313/55/ 045	283/55	193/00
Feldkirch	2010/10/25 20:00	5	M_L 3.0	250/60/ 108	037/35/ 062	327/13	198/69

Table 2010.2: Focal mechanism parameters based on first-motion polarities.
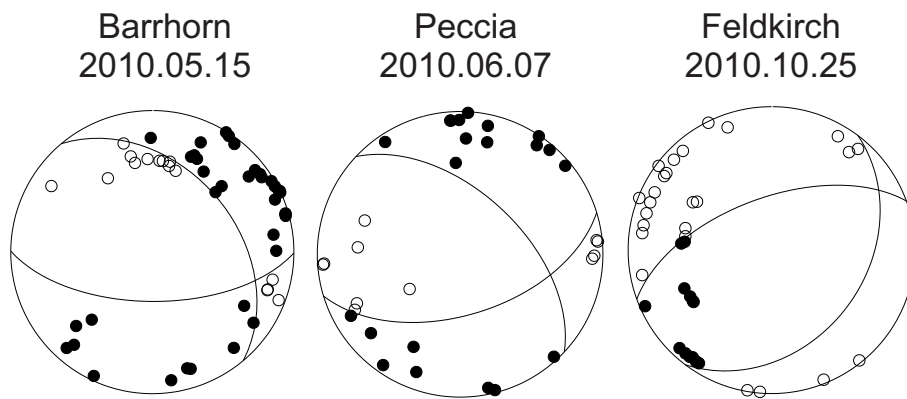
Figure 2010.3: Faultplane solutions based on first-motion polarities. All stereographs are lower hemisphere, equal area projections. Solid circles correspond to compressive first motion (up); empty circles correspond to dilatational first motion (down).
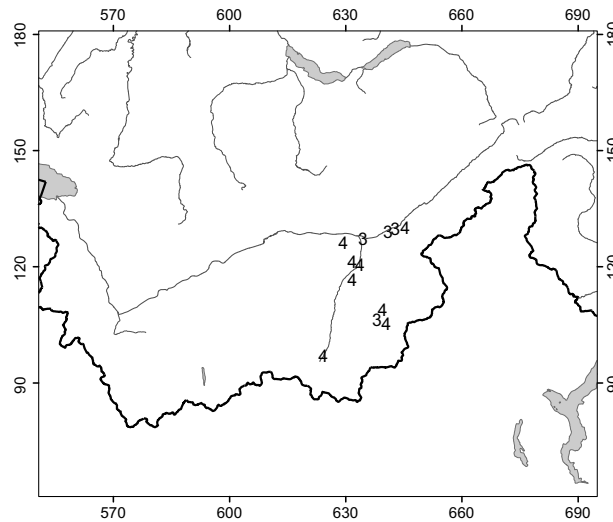
Figure 2010.4: Macroseismic intensities (EMS-98) reported for the 2010 Barrhorn event.
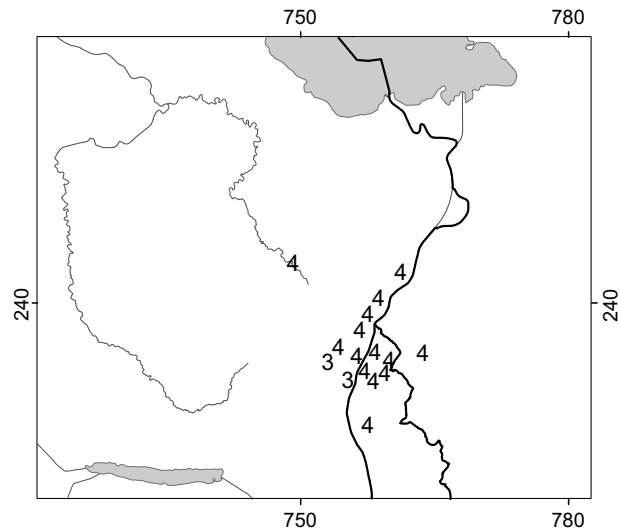
Figure 2010.5: Macroseismic intensities (EMS-98) reported for the 2010 Feldkirch event.

Peccia. The focal depth of about 7 km is constrained by P- and S-arrivals at station FUSIO situated at an epicentral distance of 6 km and by the Pn arrival recorded at station SLE in northern Switzerland. However, travel-time residuals on the order of 0.9 and 0.7 s are observed for the Pn arrivals recorded at stations BRANT and GIMEL in northwestern Switzerland. Considering that the RMS of the travel-time residuals to all other stations is 0.18 s, this points to deficiencies in the 3-D velocity model from the epicentral region in a WNW direction. The fault-plane solution obtained for this event corresponds to a normal faulting mechanism (Figure 2010.3) with a NNE-SSW trending T-axis, very similar to the focal mechanism obtained for the Barrhorn event in the Penninic domain of the Valais. Given the relatively low magnitude of this event and that consequently the number of available polarities is limited, the result is not as reliable as that of the Barrhorn event. Nevertheless, to date, it is the only focal mechanism available in this region and thus worth noting.

Feldkirch

Already in 2009, the Sanktgaller Rheintal had experienced several earthquakes (Wildhaus, M_L 4.0, 3.1 and 3.0, and Vaduz, M_L 3.0), which were clearly felt by the local population (Deichmann et al. 2010). In the evening of October 25th, the same area was again jolted by an M_L 3.0 event with epicenter near Feldkirch. It was clearly felt with intensities of IV in northern Liechtenstein and in the neighbouring areas of the Rhine Valley of Sankt Gallen (no data is available for Austria). The N-S elongation of the affected area seen in Figure 2010.5 is due to the geographical distribution of the population and should not be interpreted as source or site effects. The routinely calculated focal depth between 0 and 3 km is not well-constrained. However, a comparison of the relative arrival times between Pg and Pn phases recorded for this event at several stations in northern Switzerland with those recorded for the Vaduz event of 2009, located 10 km further south, shows that the focal depths of these two events must be identical (Figure 2010.6). Thus we fixed the focal depth to 5 km in Table 2010.1. Using
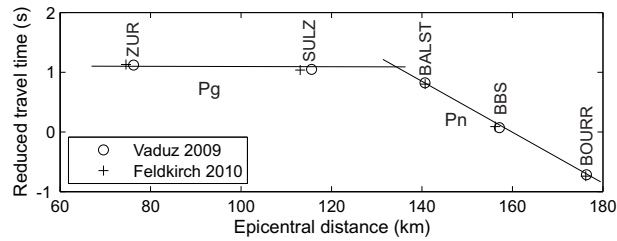
Figure 2010.6: Comparison of Pg and Pn arrival times of the 2009 Vaduz and the 2010 Feldkirch events recorded at five stations located at practically the same azimuths and distances from the two epicenters. The observations are aligned so that the Pg arrivals coincide, assuming a Pg velocity of 6 km/s. The coincidence of the Pn arrivals demonstrates that the focal depths of the two events must be identical.

the same take-off angles as those calculated for the 2009 Vaduz event, we obtain a well-constrained thrust faulting mechanism with a nearly NNW-SSE oriented P-axis. While this mechanism is substantialy different from the normal faulting mechanism of the 2009 Vaduz event (Deichmann et al. 2010), it is almost identical to that of the nearby M_L 3.6 event of Buchs, which occurred in the year 2000 (Baer et al. 2001). The most likely focal depth of all three events is between 3 and 5 km. The relative proximity of thrust and normal faulting raises some interesting questions regarding the local state of stress. Such a situation requires either substantial stress variations over a relatively small crustal volume or low levels of differential stress. The fact that earthquakes do occur would imply in the latter case that the faults that slipped must be weak. This in turn points to the likely existence of fluids at pressures above hydrostatic that reduce the effective stress and thus the strength of these faults, favouring the occurrence of earthquakes. A similar case of coexistence of thrust and normal faulting earthquakes at shallow focal depths is also observed in the region of Sarnen (Deichmann et al. 2000b).

Vallorcine

The epicenter of the M_L 3.2 event that occurred in the early morning of December 6th was located near Vallorcine, between Martigny and Chamonix, just south of the border with France. It was clearly felt in the epicentral area. Its location coincides with the aftershock zone of the M_L 4.9 event of September 8th, 2005 (Deichmann et al. 2006, Fréchet et al. 2010). It represents the second largest event in a sequence that has been active for many years. In fact, individual events belonging to this sequence can be traced back at least as far as the year 2001 (Fréchet et al. 2010), but activity really picked up in 2005, when 57 events were recorded by the network of the SED. This activity continued with varying intensity in 2006 with 33 recorded events, in 2007 with 16 events, and in 2008, 2009 and 2010 with 17 events each. Of the 17 events recorded in 2010, 13 occurred over the last four months of the year. The magnitudes of the other events in 2010 were between M_L 0.2 and 1.7. With activity still ongoing in the year 2011, an end of this seismic sequence is still not foreseeable.

Piora

During 2010, the AlpTransit network recorded 36 earthquakes with local magnitudes between 0.2 and 1.5 in the Piora region. Of these, 26 earthquakes could be located. The remaining earthquakes were too small and mostly recorded only at station PIORA, but 4 earthquakes were strong enough to be detected by the SDSNet. Their computed epicenter locations coincide to within a few hundred meters with the trace of the Gotthard base-tunnel, which was under construction at that time. Computed focal depths vary between less than 1 km and 2 km and are well constrained by arrivals recorded at station PIORA, at epicentral distances of 1 - 4 km. The true focal depths are probably even shallower, as the regional 3-D P-wave velocity model used for location may not be appropriate at this small scale.

Activity was spread more or less homogeneously over the entire year. On average, three earthquakes were recorded per month. Their waveforms show a strong similarity within different groups of events, suggesting that several fault patches ruptured repeatedly. All earthquakes occurred north of the Piora zone at distinct locations that correlate with changes in the geology, such as the Corandoni zone that represents the transition from the Piora basin to the Medelser granites. It is noteworthy that seismicity was still occurring at locations where the excavation work finished several months before. Nevertheless, given the close spatial correlation, it is likely that the earthquake activity was induced by the excavation of the Gotthard base-tunnel.

The other small cluster of earthquakes visible in Figure 2010.1 about 10 km NNW of the Piora events is not in any way related to the tunnel construction. The epicenters are located 2 km W of the trace of the tunnel and the focal depths of 7 to 9 km are well constrained by stations CUNA and CURA at epicentral distances of 2 and 9 km. All seven events occurred between the 9th and 20th of October, with local magnitudes between 0.3 and 1.6.

Landslides

In 2010, the national network detected four rockfalls at two locations. The first occurred on September 8th, 08:28 local time, when a cliff located above Almens, GR, collapsed and produced a seismic event with an equivalent M_L of 1.2. The other three occurred November 26th, 19:58, and November 27th, 03:41 and 14:27 local time, at the lower end of the Richtitobel, 1.5 km W of Muotathal, SZ. The seismic events had an equivalent M_L of 1.7-1.9, and the total volume of rock involved was estimated to be about 100'000 m^3.

Seismic activity during 2011

Overview

During 2011, the Swiss Seismological Service detected and located 522 earthquakes in the region shown in Figure 2011.1. Based on criteria such as the time of occurrence, the location, the signal character or on direct information, 92 additional seismic events were identified as quarry blasts. Magnitude values of the events recorded in 2011 range from M_L 0.1 to 3.3 (Figure 2011.2). The events with $M_L \geq 2.5$ are listed in Tables 2011.1. This table includes also the M_w values derived from the spectral fitting method of Edwards et al. (2010). Fault-plane solutions based on first-motion polarities are shown in Figure 2011.3 and their parameters are listed in Table 2011.2.
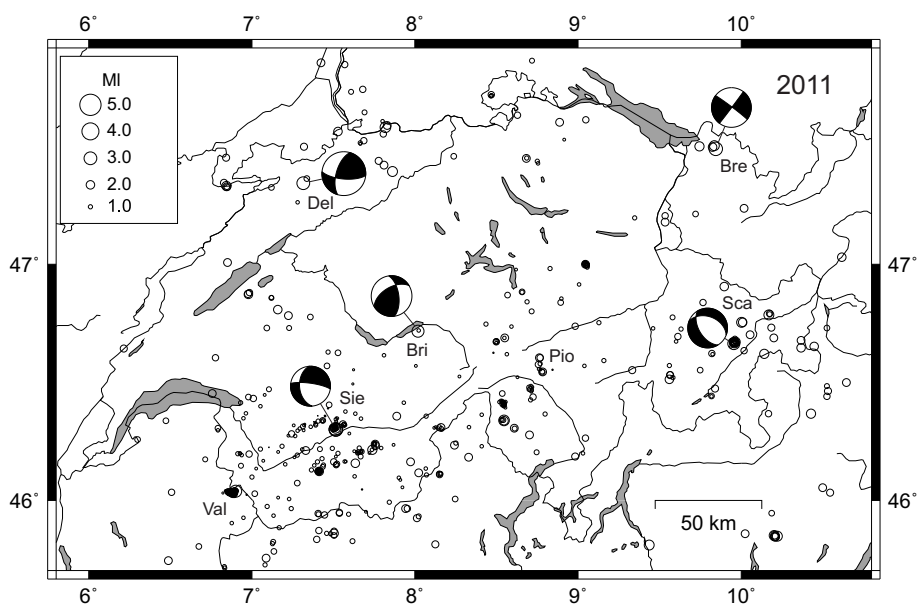
Figure 2011.1: Epicenters and focal mechanisms of earthquakes recorded by the Swiss Seismological Service during 2011. Epicenters of events mentioned in the text are Bregenz (Bre), Brienz (Bri), Delémont (Del), Piora (Pio), Scaletta Pass (Sca), Sierre, (Sie) and Vallorcine (Val).

In 2011, as in previous years, a large portion of the seismic activity was concentrated in the Valais and the immediately adjacent regions. Compared to the relative low of the year before, seismic activity in Grabünden returned to more normal levels, and the activity observed since 2008 in the region around the

1

Date & Time UTC	Lat. [°N]	Lon. [°E]	X / Y [km]	Z [km]	Mag. [M_L]	Mag. [M_w]	Q	Location
2011.01.08 20:48:17	46.304	7.516	606/128	7	3.3	3.0	A	Sierre, VS
2011.01.08 22:20:26	46.302	7.516	606/128	6	3.2	3.0	A	Sierre, VS
2011.01.08 23:32:30	46.304	7.510	605/128	7	2.8	2.7	A	Sierre, VS
2011.01.27 01:24:18	47.482	9.844	781/262	31	3.3	2.9	A	Bregenz, A
2011.03.30 13:01:12	47.572	7.818	629/269	13	2.5	2.4	A	Rheinfelden, AG
2011.04.21 11:36:39	46.719	8.019	644/174	7	2.9	2.7	A	Brienz, BE
2011.08.21 19:39:45	46.040	6.901	558/ 99	9	2.9	2.8	A	Vallorcine, F
2011.09.01 02:50:30	46.341	8.546	685/133	9	2.5	2.3	B	Bosco Gurin, TI
2011.12.03 08:32:52	46.666	9.955	792/171	9	2.8	2.8	A	Scaletta Pass, GR
2011.12.27 06:29:02	47.339	7.315	591/243	11	3.1	2.8	A	Delémont, JU

Table 2011.1: Earthquakes with $M_L \geq 2.5$. The values listed under M_w are the moment magnitudes calculated from the spectral fitting method documented in Edwards et al. (2010).

upper Valle Maggia continued with several small events. Routinely calculated focal depths for all but 12 events recorded in 2011 are less than 16 km. All of the deeper hypocenters occurred below the Molasse Basin and Jura of northern Switzerland and southern Germany. The seismic activity induced by the geothermal project in Basel in 2006 and 2007 (e.g. Deichmann & Ernst 2009; Deichmann & Giardini 2009) continued to decrease over the year 2011, and all events that have been recorded by the local borehole seismometers were too weak to be recorded by the national broad-band network. Overall, the seismic activity in and around Switzerland was low in 2011, both in terms of the number of events and in terms of the maximum event magnitude. The total number of 10 events with $M_L \geq 2.5$ is substantially below the yearly average of about 24 events over the previous 36 years in this magnitude range and is the lowest since 1975, the beginning of the Swiss instrumental earthquake catalog. The M_L 3.3 is also the lowest maximum magnitude per calender year since 1981.

Location	Date & Time [UTC]	Depth [km]	Mag.	Plane 1 Plane 2 Strike/Dip/Rake		P-Axis T-Axis Azimuth/Dip	
Sierre	2011/01/08 20:48	7	M_L 3.3	278/78/-133	175/44/-017	148/41	039/21
Sierre	2011/01/08 22:20	6	M_L 3.2	268/85/-141	174/51/-006	138/30	034/22
Bregenz	2011/01/27 01:24	31	M_L 3.3	037/89/ 003	307/87/ 179	172/01	262/03
Brienz	2011/04/21 11:36	7	M_L 2.9	352/61/ 041	239/55/ 144	114/04	208/48
Scaletta Pass	2011/12/03 08:32	9	M_L 2.8	291/42/-120	149/55/-066	114/69	222/07
Delémont	2011/12/27 06:29	11	M_L 3.1	094/70/ 150	195/62/ 023	146/05	052/35

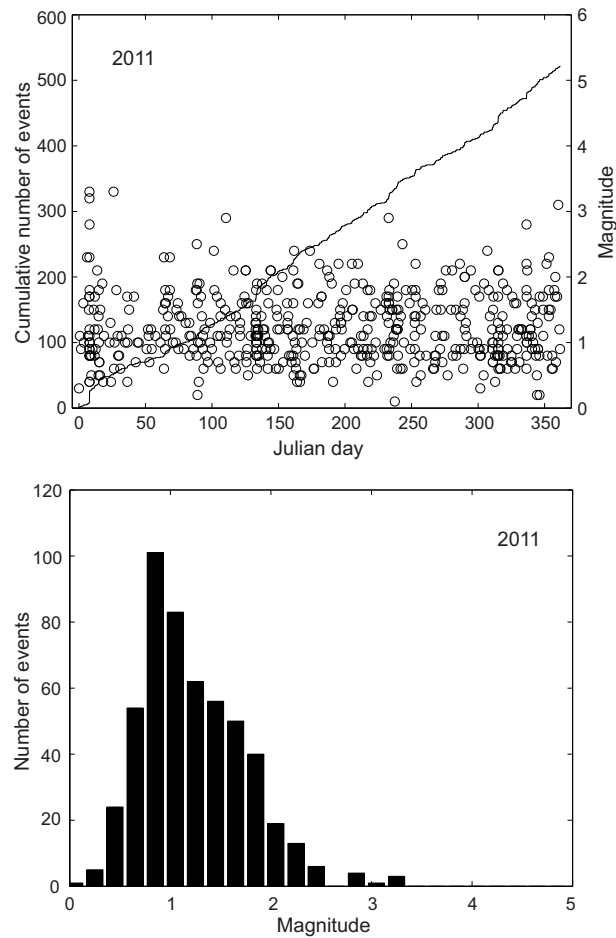Table 2011.2: Focal mechanism parameters based on first-motion polarities.

Figure 2011.2: Earthquake activity during 2011: magnitude of each event and cumulative number of events (above); histogram of magnitudes (below).

Significant earthquakes of 2011

Sierre

The earthquake sequence of Sierre represents the most significant seismic activity of 2011 in Switzerland. It comprises a total of 31 events with M_L between 0.4 and 3.3, and began January 8th at 20:28 UTC with an event of M_L 2.3. As shown in Figure 2011.4, 16 events occurred in the first five hours and included two events of M_L 3.3 and 3.2. An additional nine events occurred over the following two weeks; then the sequence continued with sporadic events until the end of the year. The epicenter of the main shock was located about 2 km NW of the town of Sierre, and the focal depth of 6-7 km is well constrained by records at two accelerographs located at epicentral distances of 3 and 8 km. This focal depth also agrees with 2-D ray-trace modeling of travel-time differences between the reflection at the Moho, PmP, the direct wave, Pg, and the refraction in the upper mantle, Pn, observed at stations in NE Switzerland.

The fault-plane solutions of the two strongest events are well constrained and are very similar to each other (Figure 2011.5 and Table 2011.2). Given that
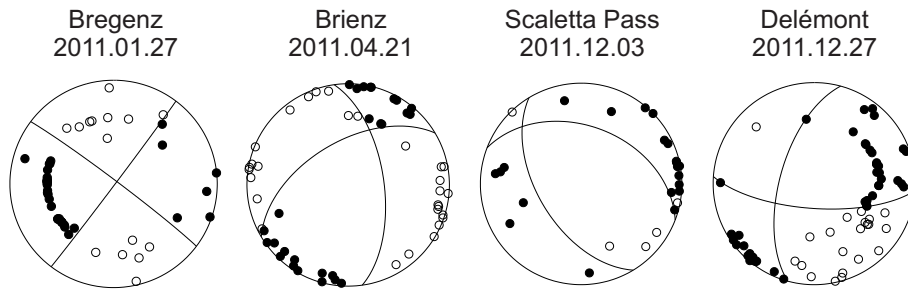
Figure 2011.3: Fault-plane solutions based on first-motion polarities. All stereographs are lower hemisphere, equal area projections. Solid circles correspond to compressive first motion (up); empty circles correspond to dilatational first motion (down).
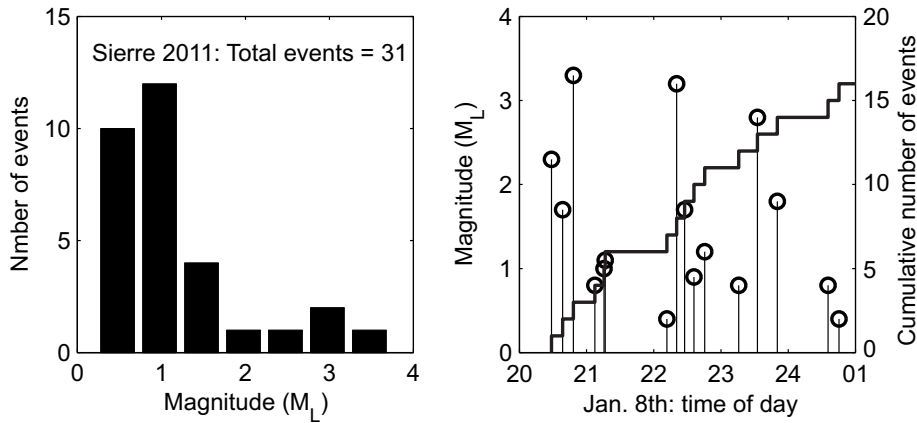

Figure 2011.4: Magnitude histogram of all events and activity as a function of time during the first five hours of the earthquake sequence of Sierre.

the signals of the individual events are very similar, it was possible to apply a time-domain cross-correlation procedure to determine high-precision arrival-time differences and thus precise hypocenter locations relative to a chosen master event. The cross-correlation procedure documented in Deichmann and Garcia-Fernandez (1992) was applied to the seismograms of the first 24 events of the sequence, recorded at six stations. It relies on a least-squares adjustment of travel-time differences computed for all possible combinations of event pairs. As master event we chose the first event of the sequence (M_L 2.3). Because of the large difference in the dominant frequency of the strongest and weakest events, which tends to impair the reliability of the cross-correlations, the correlations were performed separately, first for the master event and the three largest events and then for the master event and all the smaller events. Relative locations based on the resulting travel-time differences of five P- and four S-arrivals were computed with the method proposed by Console and DiGiovambattista (1987). For the subset of the larger events, it was possible to use also arrival-time differences of the phases reflected at the Moho (PmP) recorded at stations ZUR and CURA, which add a valuable constraint on the relative focal depths of these events. With mean relative travel-time errors of 3-6 ms, estimated from
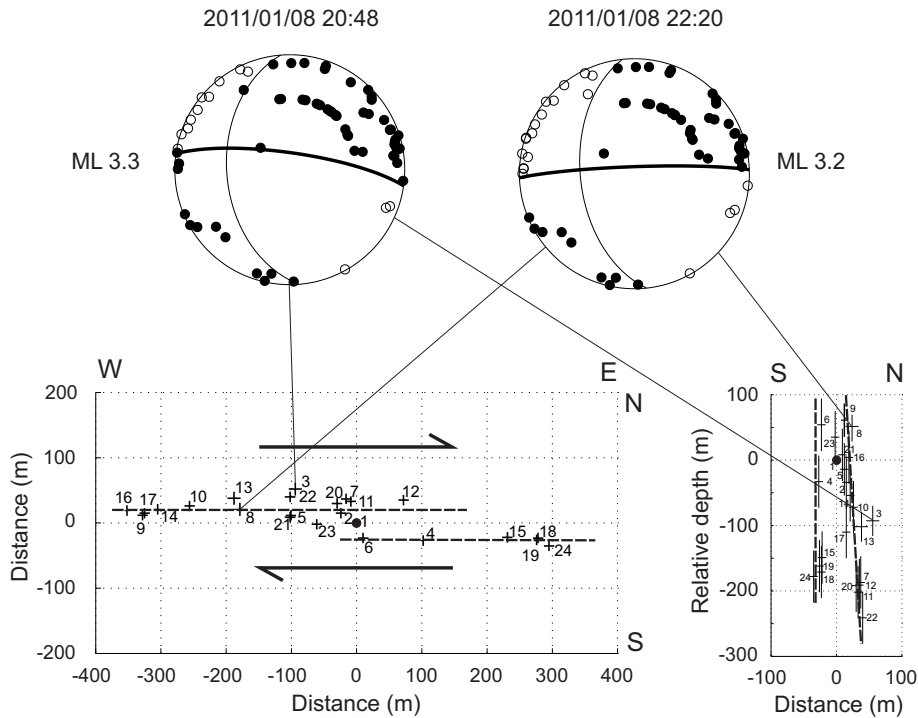
Figure 2011.5: Relative locations and fault-plane solutions of the earthquake sequence of Sierre.

the cross-correlations and mean residuals of 1-6 ms resulting from the location procedure, we obtain relative location uncertainties of 7-10 m horizontally and 22-40 m vertically (single standard deviations). As shown in Figure 2011.5, the hypocenters of the 2011 Sierre sequence delineate two separate E-W striking fault segments that are parallel to one of the nodal planes of the fault-plane solution. Thus the focal mechanism of the Sierre events corresponds to dextral strike-slip with a strong vertical component of slip along an almost vertical E-W striking fault. Noteworthy is the fact that the Sierre sequence is located at the northern edge of the Rhone Valley and is not part of the pronounced lineament further to the north that strikes WSW-ENE and that has been active for several decades. Its focal mechanism with the strong oblique component of slip is also not typical of either the strike-slip mechanisms that characterize the seismicity in the Helvetic domain of the northern Wallis nor of the normal faulting mechanisms that predominate in the Penninic nappes of the southern Wallis (Maurer et al. 1997, Kastrup et al. 2004).

The two strongest events (M_L 3.3 and 3.2) caused shaking of intensity IV (EMS-98) in the epicentral region and were felt over large parts of the Canton Wallis and in parts of the Berner Oberland (Figure 2011.6). Even the M_L 2.8 event was felt by the local population. Table 2011.3 lists peak ground velocities (PGV) and peak ground accelerations (PGA) of the two strongest events recorded at selected stations close to the epicenters. It is noteworthy that both PGV and PGA at the two closest stations (Sierre and Ayent) are higher by almost a factor of 2 for the second event than for the first, despite the fact that M_w is the same for both events and that M_L of the first one is even
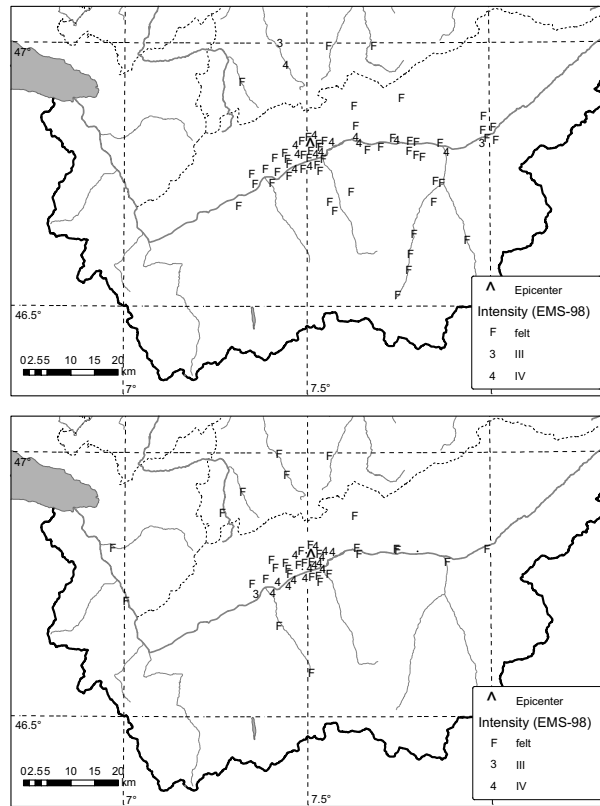
Figure 2011.6: Macroseismic intensities (EMS98) of the two strongest events of the sequence of Sierre: 2011/01/08, 21:48 local time, M_L 3.3 (left) and 23:20 local time, M_L 3.2 (right).

slightly larger than that of the second one. The difference in the measured PGV and PGA values is reflected also in the macroseismic observations: although the second event occurred later at night and the shaking at larger distance seems not to have been sufficiently strong to wake people up, the reports from people in the immediate epicentral region indicate clearly that the shaking was more intense for the second event.

Bregenz

The M_L 3.3 earthquake that occurred January 27th near Bregenz, at the north-eastern end of the Bodensee, is noteworthy because of its focal depth. The depth of 31 km is well constrained by P- and S-onsets at three stations at epicentral distances between 22 and 34 km. According to Waldhauser et al. (1998) the Moho lies at a depth of 34 to 35 km at this location. Consequently, as can be seen in Figure 2011.7, at stations located in the Alpine foreland to the west of the epicenter, the wave refracted at the Moho (Pn) appears as the first arrival already at a distance of about 70 km. Note that the time scale in Figure 2011.7 has been shifted by subtracting the epicentral distance divided by a reduction velocity of 6.4 km/s. The fact that beyond about 120 km the secondary arrivals lie on a horizontal line implies that the average P-wave velocity in the lower

2011.01.08		DIST	20:48 (M_L 3.3)			22:20 (M_L 3.2)		
STAT	LOCATION		RSH	PGV	PGA	RSH	PGV	PGA
SIES	Sierre-Solaire	3.1	.363	2.17	122.	.330	4.05	201.
SAYF	Ayent-Fortunoz	7.9	-.866	1.41	80.0	-.970	2.79	153.
VANNI	Vissoie	12.1	.393	.384	10.8	.524	.358	11.7
SIOO	Sion-Ophtalm.	13.1	-.316	.420	12.1	-.491	.412	16.2
SIOM	Sion-Mayennaz	14.7	-.353	.168	7.23	-.533	.205	9.72
SENIN	Sanetsch	17.8	-.633	.212	9.19	-.565	.211	10.1

Table 2011.3: Peak ground velocity (PGV, mm/s) and peak ground acceleration (PGA, mm/s^2) recorded at selected locations for the two strongest events of the earthquake sequence of Sierre. DIST is the epicentral distance in km and RSH is the radiation coefficient of the SH wave for each focal mechanism. PGV and PGA were determined from horizontal records rotated to maximize the absolute value of the peak amplitudes.

crust below the northern Alpine foreland is probably not higher than 6.4 km/s. Given the large focal depth and the fact that it occurred in the middle of the night, it is not surprising, that it was noticed only by very few persons. Two additional events with practically identical hypocenter locations occurred March 10th and may 25th with M_L 2.3 and 2.1.

The fault-plane solution corresponds to a strike-slip mechanism with NE-SW and NW-SE striking nodal planes. The former is well constrained by the available first-motion data, while the latter is constrained by the fact that the amplitude of the Pn phase recorded at station BFO, located at a distance of 147 km and an azimuth of 309 degrees, is so weak that the location of this station must coincide with the strike of the NW-SE nodal plane. The resulting focal mechanism and the focal depth are almost identical to those of the M_L 3.0 event that occurred April 18th, 2004, near Lindau, about 7 km to the NW of Bregenz.

Brienz

The focal depth of 7 km of the M_L 2.9 earthquake that occurred April 21st just south of Brienz is constrained by P- and S-arrivals at station HASLI, at an epicentral distance of 11 km, and by several Pn arrivals at stations in southern Germany. The fault-plane solution, shown in Figure 2011.3, corresponds to a thrust mechanism with a strong strike-slip component. The almost horizontal P-axis is oriented in a NNW-SSE direction (Table 2011.2), which is typical of the seismic deformation observed in the Helvetic domain of central Switzerland (Kastrup et al 2004). There is no evidence that this event was felt.

Vallorcine

As in previous years (e.g. Deichmann et al. 2011), the aftershock activity of the ML 4.9 earthquake that occurred in 2005 near Vallorcine, between Martigny and Chamonix, just south of the border with France (Fréchet et al. 2010), continued throughout the year 2011. A total of 48 aftershocks with magnitudes between M_L 0.4 and 2.9 were recorded in 2011.
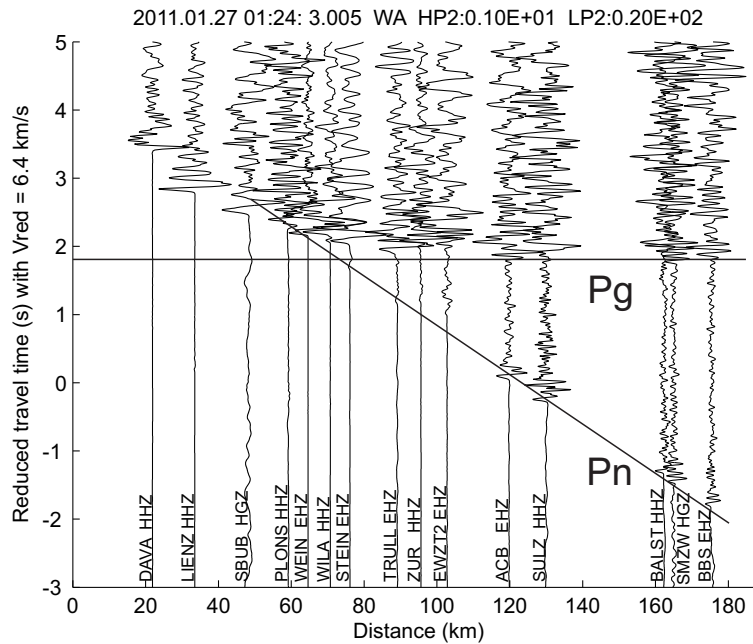
Figure 2011.7: Record section with seismograms of the Bregenz event, recorded at stations located to the west of the epicenter (within ±10°). Note that the time scale has been reduced with a velocity of 6.4 km/s.

Scaletta Pass

The M_L 2.8 event of December 3rd with epicenter located 11 km ENE of Zernez was the second event of a sequence that started November 29th. The focal depth of 9 km is constrained only by P- and S-arrivals recorded at stations SZER and DAVOX at epicentral distances of 11 and 14 km. However this focal depth is within the depth range of most well-located earthquakes in southeastern Switzerland. The normal faulting focal mechanism of this event, shown in Figure 2011.3, is very similar to that of the nearby Sertig sequence of 2005 and constitutes further evidence for the predominantly extensional deformation of this region (Marschall et al. 2012). This event was felt very mildly by a few people in the Lower Engadine.

Delémont

The earthquake that occurred December 27th at 7:29 in the morning (local time) was the fourth and last event with $M_L > 3$ of the year 2011. Its epicenter was located near the village of Courtételle, about 3 km south-west of Delémont, and the focal depth of 11 km is constrained by P- and S-arrivals at station BOURR, 9 km from the epicenter, as well as by several Pn arrivals at stations in southern Germany and south-eastern Switzerland. There are no credible reports of this earthquake having been felt.

The fault-plane solution corresponds to a strike-slip mechanism with a slight thrust component. It hinges to a very large degree on the first motion at ECH, the point on the northern edge of the nodal plane that strikes almost north-south and dips towards the west in Figure 2011.3. That the first motion at this station
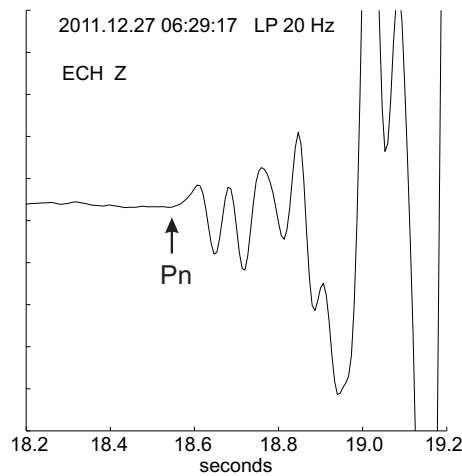
Figure 2011.8: Seismogram of the Delémont event recorded at station ECH (France): the first arrival is the phase refracted at the Moho (Pn), with upward first-motion. The signal is filtered with a 2nd order causal Butterworth low-pass filter at 20 Hz.

is unequivocally up is illustrated in Figure 2011.8. Given that ECH is located at an epicentral distance of only 98 km, it is less obvious that it is a Pn rather than a Pg phase. However, several observations support this interpretation: a) the amplitude is low compared to the subsequent phases, which is what one would expect from the Pn at distances close to the cross-over distance between Pn and Pg; b) in a plot of travel-time versus epicentral distance, its arrival-time, reduced with a velocity of 6.0 km/s, is much earlier than the Pg at station MOF at the same azimuth, and slightly earlier than the Pg observed at stations END, KIZ and FELD located in the Black Forest; c) ray-trace calculations with a simple 2D crustal model confirm that, for a focal depth of 11 km and a Moho depth that varies between 28 and 25 km, the cross-over distance is indeed around 100 km; d) and lastly, interpreting this phase with a positive polarity as a Pg results in an inconsistent fault-plane solution.

Previously in 2010, another small earthquake (M_L 2.8) occurred near the town of Courtételle, only 1-2 km ESE of the Delémont event. However, with a focal depth of 18 km, the hypocenter of the former was substantially deeper (Deichmann et al. 2011), as was verified by a comparison of the Pn/Pg crossover distances of these two events.

Piora

During 2011, the AlpTransit network recorded 46 earthquakes with magnitudes between M_L 0.2 and 1.8 in the Piora region. Of these, 33 earthquakes could be located. The remaining earthquakes were too small and mostly recorded only at station PIORA, but 9 earthquakes were strong enough to be detected by the SDSNet. Their computed epicenter locations coincide to within a few hundred meters with the trace of the Gotthard base-tunnel, which was under construction at that time. Computed focal depths vary between 1 and 2 km for the five events at minimum epicentral distances of 1-3 km (station PIORA) and between 2 and 4 km for the four events further north at minimum distances of 5 km (station

CUNA). The true focal depths are probably even shallower, as the regional 3-D P-wave velocity model used for location may not be appropriate at such a small scale. In a similar setting further south along the tunnel, near the town of Faido, routinely calculated focal depths were also found to be deeper than those determined using a velocity model that was refined based on a calibration shot (Husen et al. 2011). Compared to previous years, we observe an overall northward migration of the epicenters, in general accord with the northward extension of the ongoing tunnel excavation.

Landslides

In 2011, the national network detected 13 events that are suspected to be landslides or rock avalanches. This could be confirmed for six of these events: Bäregg near Grindelwald, Les Drus near Chamonix (four events) and Pizzo Cengalo, between Maloja and Chiavenna.

The Bäregg event occurred September 6th at 22:35 UTC. Its confirmation is based only on acoustic evidence reported by a local resident. It is possible that this event was caused by slope failure in the east flank of Eiger, similar to the events that occurred there in 2006 (Baer et al 2007).
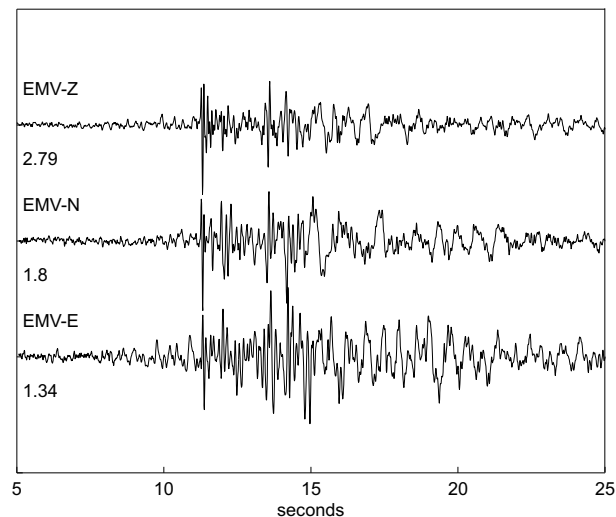

Figure 2011.9: Seismograms of the first detected rock-fall from the west face of Les Drus near Chamonix, France, recorded at station EMV (Emosson), at a distance of 15 km. The signals are filtered with a 2nd order causal Butterworth band-pass filter between 1 and 20 Hz. Note the higher-frequency signal with impulsive P- and S-arrivals embedded in the emergent and longer-lasting signal, typical for a landslide.

The four detected rock avalanches near Chamonix, France, occurred September 11th, 08:14, September 12th, 05:39 and 05:43 as well as October 30th, 06:12 UTC. These four events were caused by renewed slope failures in the west face of the Aiguille du Petit Dru. Similar events have also been detected in 1997 (Deichmann et al. 1998). Equivalent magnitudes could be computed for the first and last of these events (ML 1.5 and 1.8). As shown in Figure 2011.9, the first is particularly interesting, because, embedded in the usual emergent

wave-train, it produced highly impulsive signals that could be interpreted as P- and S-waves, resulting in an epicenter location that coincides within less than 1 km with the location of the documented rock avalanche. The impulsive signals are probably due to the impact of a large rock mass on the ground at the foot of the near-vertical west face.

The largest landslide by far occurred on December 27th, at 17:25 UTC, as part of a sequence of events associated with a massive slope failure in the north face of Pizzo Cengalo at the head of Val Bondasca, on the border with Italy. With an equivalent magnitude of M_L 2.7, it was recorded over the entire Swiss national network and was even detected by the German Regional Seismic Network. As shown in Figure 2011.10, the vibrations caused by this event lasted nearly two minutes.

In the context of a PhD project at the Department of Earth Sciences at ETH Zurich, procedures are being developed to automatically identify landslides and massive rock avalanches, and to estimate their volume based on their seismic signals. First results based on a previous master thesis have been published in Dammeier et al. (2011).
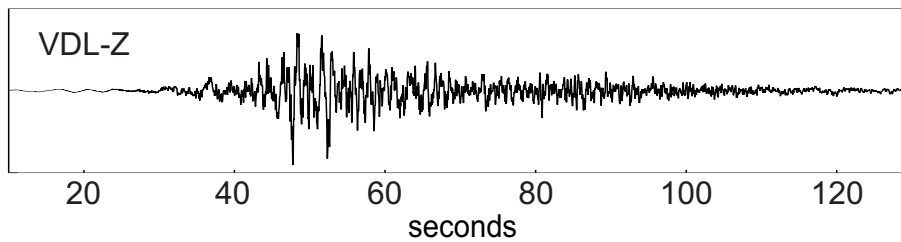

Figure 2011.10: Seismogram of the massive landslide from Pizzo Cengalo, Val Bregaglia, December 27th, 2011, recorded at station VDL (Valle di Lei), 24 km away. The signal is filtered with a 4th order zero-phase Butterworth band-pass filter between 0.2 and 20 Hz. Note the time scale: the entire seismogram is nearly 2 minutes long.

Seismic activity during 2012

Overview

During 2012, the Swiss Seismological Service detected and located 497 earthquakes in the region shown in Figure 2012.1. Based on criteria such as the time of occurrence, the location, the signal character or on direct information, 88 additional seismic events were identified as quarry blasts. Magnitude values of the events recorded in 2012 range from M_L 0.0 to 4.2 (Figure 2012.2). The events with $M_L \geq 2.5$ are listed in Tables 2012.1. This table includes also the M_w values derived from the spectral fitting method of Edwards et al. (2010). Fault-plane solutions based on first-motion polarities are shown in Figure 2012.3 and their parameters are listed in Table 2012.2.
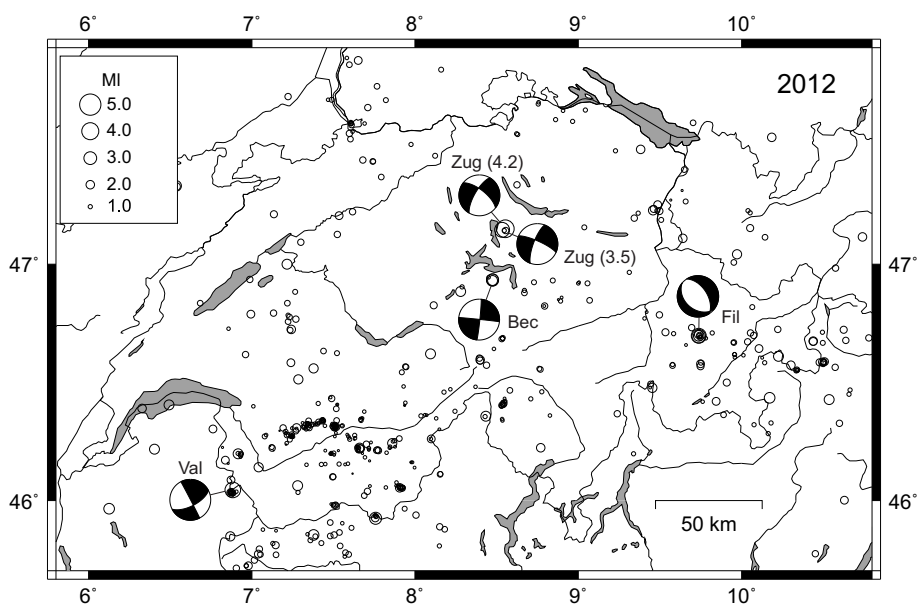

Figure 2012.1: Epicenters and focal mechanisms of earthquakes recorded by the Swiss Seismological Service during 2012. Epicenters of events mentioned in the text are Beckenried (Bec), Breithorn (Bre), Filisur (Fil), Santa Maria (SMa), Vallorcine (Val), and Zug (Zug).

In 2012, as in previous years, a large portion of the seismic activity was concentrated in the Valais and the immediately adjacent regions. Routinely calculated focal depths for all but 13 events recorded in 2012 are less than 16 km. All of the deeper hypocenters occurred below the Molasse Basin and Jura

Date & Time UTC	Lat. [°N]	Lon. [°E]	X / Y [km]	Z [km]	Mag. $[M_L]$	Mag. $[M_w]$	Q	Location
2012.01.01 15:33:50	46.698	9.737	776/174	6	3.3	3.0	A	Filisur, GR
2012.01.01 17:16:58	46.699	9.737	776/174	6	2.5	2.5	A	Filisur, GR
2012.01.02 01:42:57	46.700	9.737	776/175	6	3.5	3.2	A	Filisur, GR
2012.02.11 22:45:27	47.149	8.553	684/223	32	4.2	3.8	A	Zug, ZG
2012.02.24 00:32:30	47.144	8.534	683/222	32	3.5	3.0	A	Zug, ZG
2012.06.17 11:20:38	45.965	6.126	498/ 91	9	2.6	2.6	D	Annecy, F
2012.09.04 02:51:45	46.933	8.474	679/198	9	2.8	2.7	A	Beckenried, NW
2012.09.04 05:13:25	46.935	8.474	679/199	9	2.9	2.8	A	Beckenried, NW
2012.09.18 23:43:13	47.328	6.536	532/242	1	2.5	2.6	C	Chazot, F
2012.09.20 07:59:06	46.438	10.173	810/147	8	2.6	2.4	A	Pizzo Filone, I
2012.10.12 20:41:32	45.855	7.380	595/ 78	7	2.5	2.5	B	Valpelline, I
2012.10.25 01:10:57	46.035	6.896	558/ 98	4	3.6	3.3	A	Vallorcine, F
2012.11.28 13:32:51	45.922	7.757	625/ 86	2	2.9	2.9	B	Breithorn, I

Table 2012.1: Earthquakes with $M_L \geq 2.5$. The values listed under M_w are the moment magnitudes calculated from the spectral fitting method documented in Edwards et al. (2010).

of northern Switzerland and southern Germany, mainly between 7°E and 10°E (e.g. Deichmann 1992; Deichmann et al. 2000a). Overall, the seismic activity in and around Switzerland, in terms of the number of events, was low in 2012. The total number of 13 events with $M_L \geq 2.5$ is substantially below the yearly average of about 24 events over the previous 37 years in this magnitude range. The M_L 4.2 lower-crustal earthquake near Zug, on the other hand, had the largest magnitude since the M_L 4.9 earthquake of Vallorcine in 2005.

Location	Date & Time [UTC]	Depth [km]	Mag.	Plane 1 Strike/Dip/Rake	Plane 2	P-Axis Azimuth/Dip	T-Axis
Filisur	2012/01/02 01:42	6	M_L 3.5	327/54/-080	130/37/-103	274/78	050/08
Zug	2012/02/11 22:45	32	M_L 4.2	308/68/-160	210/72/-023	168/29	260/02
		30	M_w 3.7	308/62/-146	200/60/-033	165/43	074/01
Zug	2012/02/24 00:32	32	M_L 3.5	294/78/-164	201/74/-012	158/20	067/03
Beckenried	2012/09/04 05:13	9	M_L 2.9	006/87/ 001	276/89/ 177	321/01	231/03
Vallorcine	2012/10/25 01:10	4	M_L 3.6	063/65/-179	333/89/-025	285/18	021/17
		8	M_w 3.7	058/72/-174	326/84/-018	281/17	013/09

Table 2012.2: Focal mechanism parameters based on first-motion polarities.
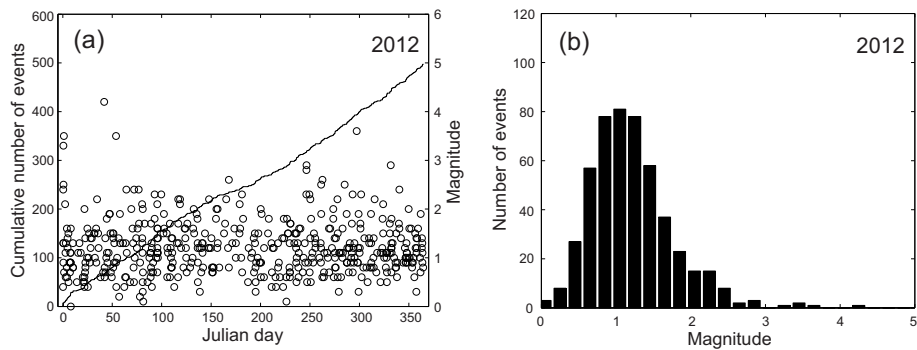
Figure 2012.2: Earthquake activity in Switzerland and surroundings during 2012: (a) magnitude of each event and cumulative number of events; (b) histogram of magnitudes.
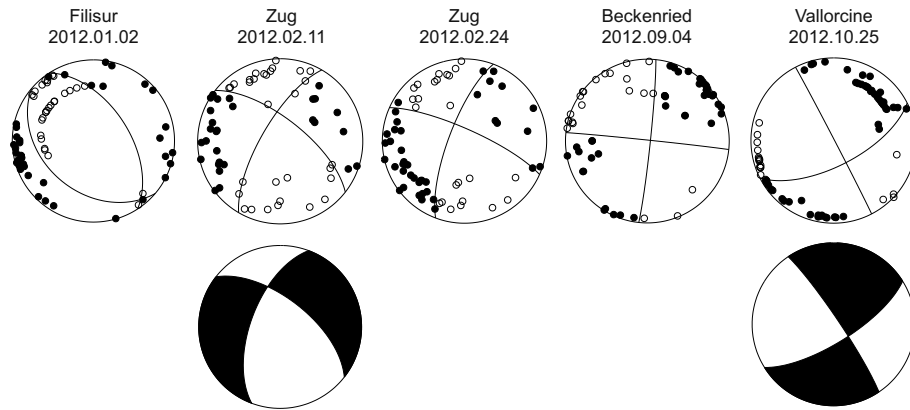

Figure 2012.3: Fault-plane solutions based on first-motion polarities. All stereographs are lower hemisphere, equal area projections. Solid circles correspond to compressive first motion (up); empty circles correspond to dilatational first motion (down).

Significant earthquakes of 2012

Filisur

On January 1st and 2nd, 2012, two moderate earthquakes with M_L 3.3 and 3.5 jolted the central parts of Kanton Graubünden. They were part of a sequence of nine events that occurred over 3 days with epicenters about 5 km east-northeast of Filisur (Marschall et al. 2013). The M_L 3.5 event was felt in the part of the Graubünden and maximum intensities of IV have been reported. With the closest station 14 km away (DAVOX), routinely computed focal depths are uncertain, and individual events scatter between 2 and 8 km, depending on the number of available arrivals. A comparison of the arrival-time differences between the reflection at the Moho (PmP) and the direct arrival (Pg) observed for the mainshock of this sequence at stations WILA and ZUR with those of one of the events of the Sertig sequence of 2003, located 8 km further to the eastnortheast, shows that the source of the Filisur sequence was slightly

shallower than the Sertig sequence (Fig. 2012.4). Since the focal depth of the Sertig sequence (7 km) is well constrained by records of a temporary station installed in the immediate vicinity of the epicenter (Deichmann et al. 2004), we conclude that the hypocenters of the Filisur sequence are located at a depth of about 6 km. This was confirmed by 2D ray-trace modeling of the Pg and PmP travel times observed at several stations in northern Switzerland.
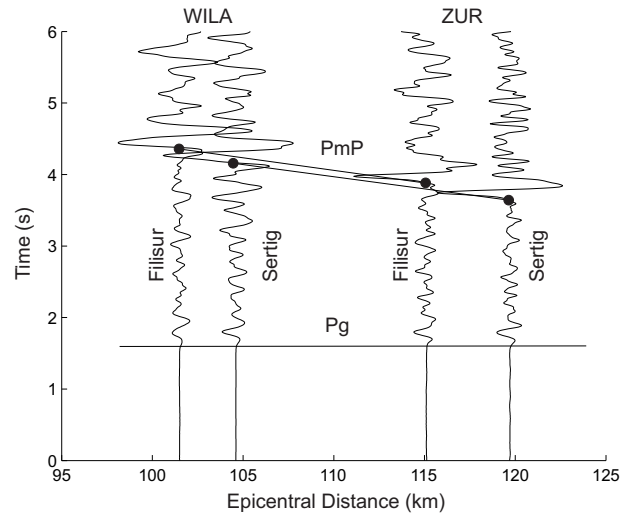

Figure 2012.4: Comparison of the PmP arrivals at stations WILA and ZUR of an event of the Sertig sequence (2003/07/18 11:01, M_L 3.9) and of the Filisur sequence (2012/01/02 01:42, M_L 3.5). The signals are integrated to displacement with a Wood-Anderson filter and filtered with a 1-20 Hz, 2nd order Butterworth band-pass filter.

The fault-plane solution computed for the M_L 3.5 event (Table 2012.2; Fig. 2012.3) is based on take-off angles derived from the 2D ray-tracing assuming a linear velocity gradient between the base of the near-surface sediments and the Moho. The result is a normal-faulting focal mechanism with a NE-SW oriented T-axis, typical for this region (e.g. Marschall et al. 2013; Kastrup et al. 2004). Judging from the high degree of similarity between the waveforms from the individual events in the sequence, the hypocenters must be closely co-located and their focal mechanisms nearly identical. To discriminate between the two nodal planes, a good constraint of the relative focal depths is essential. Given the large epicentral distance of the closest stations, this requires the inclusion of the PmP arrivals observed at stations in northern Switzerland in the cross-correlation. As a consequence, relative locations could be computed only for the three strongest events (Marschall et al. 2013). Mean travel-time residuals of the relative locations are between 2 and 3 ms, and the resulting location errors (one standard deviation) are on the order of 10 m horizontally and 23 m vertically. Within the location errors, the nodal plane dipping to the SW matches the vertical distribution of the three hypocenters best (Marschall et al. 2013).
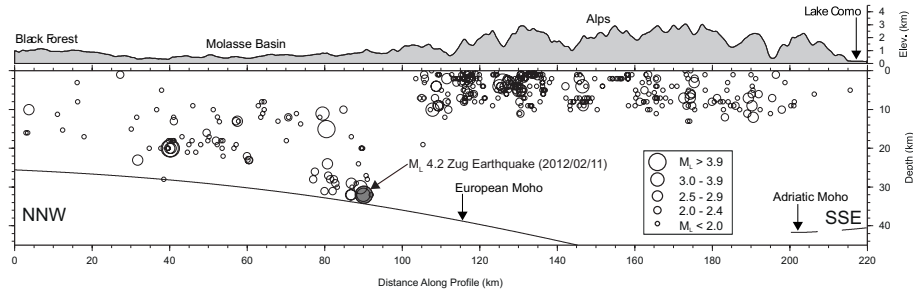
Figure 2012.5: Depth cross-section from the Black Forest to Lake Como showing the seismicity from 1984 to 2012 (circles) as recorded by the SED. The M_L 4.2 Zug mainshock of February 11, 2012 is marked as a red dot. Only earthquakes within a swath of ±30 km of the profile and with well constrained focal depths (i.e. azimuthal GAP ≤ 180°, number of observations ≥ 11, distance to closest station ≤ 30 km) are shown. These selection criteria are the same as those used for earlier compilations of focal depths (e.g. Deichmann et al. 2000a). Size of the circles is scaled by magnitude, as indicated. Crustmantle boundary (Moho) from Wagner et al. (2012) along the profile is shown as black line.
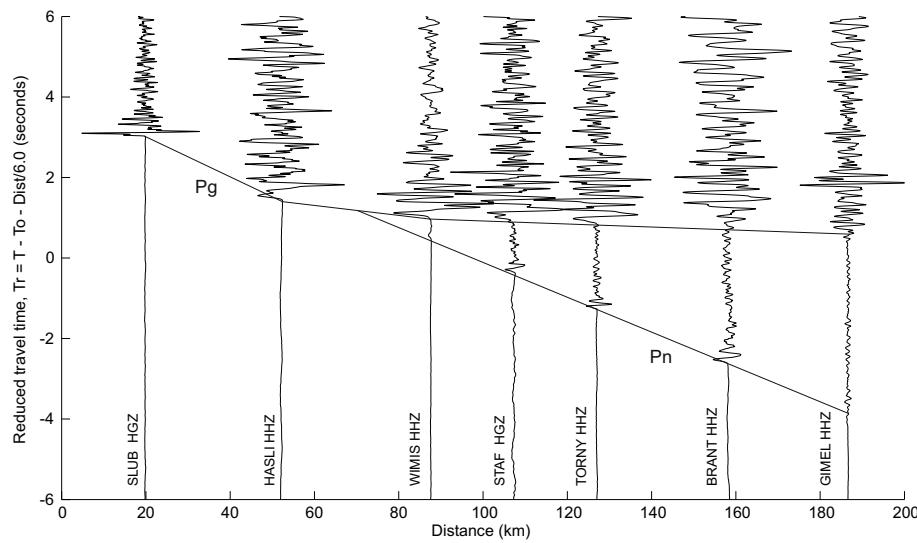

Figure 2012.6: Record section of the seismograms of the ML 3.5 Zug event of 2012/02/24 00:32 as a function of epicentral distance along a WSW trending profile. The signals are filtered with a 0.510 Hz Butterworth band-pass filter. In this direction, the apparent velocity of the Pn arrivals is 8.15 km/s and for the Pg arrivals beyond 80 km it is approximately 6.2 km/s. The unusually small PnPg cross-over distance of about 70 km is evidence for the close proximity of the hypocenter to the Moho.

Zug

The M_L 4.2 earthquake that occurred on February 11th at 11:45 pm local time (10:45 pm UTC) between Zuger- and Aegerisee, was the strongest earthquake to occur in Switzerland since the M_L 4.3 earthquake of Fribourg in 1999 and the M_L 4.9 Vallorcine earthquake in 2005, which was located just across the border with France, between Martigny and Chamonix. The hypocentral depth of 32 km is well constrained by P- and S-onsets at seven stations at epicentral distances between 20 and 40 km. According to the recently published crustal model of the Alps of Wagner et al. (2012), the Moho lies at a depth of about 34 km at this location (Fig. 2012.5). Thus, the M_L 4.2 earthquake locates close to a previously known group of lower-crustal events in the area between the lakes of Zurich and Zug discussed in previous reports (e.g. Deichmann 1992; Deichmann et al. 2000a).

Figure 2012.6 shows a record section along a WSW trending profile of an M_L 3.5 aftershock with an almost identical hypocenter location at 32 km depth. In this direction the apparent velocity of the Pn arrivals is 8.15 km/s, while for the Pg arrivals beyond 80 km it is approximately 6.2 km/s. The unusually small Pn-Pg crossover distance of about 70 km is evidence for the close proximity of the hypocenter to the Moho. The well-constrained fault-plane solution corresponds to a strike-slip mechanism with a minor component of normal-faulting (Table 2012.2; Fig. 2012.3). In agreement with other known focal mechanisms in this region, its P-axis trends towards NNW-SSE (Kastrup et al. 2004). In the two weeks following the February 11th mainshock, three aftershocks were recorded with similar locations and depths. A M_L 1.1 event occurred at 28 km depth on February 14th, followed by a M_L 1.6 event at 29 km depth on February 18th. A larger aftershock of M_L 3.5 occurred at 32 km depth on February 24th. The well-constrained fault-plane solution of this event is similar but not identical to that derived for the mainshock (Table 2012.2; Figure 2012.3).

The M_L 4.2 mainshock was felt throughout Switzerland, and was widely felt in the eastern and central Alpine foreland, spreading to the eastern extensions of the Jura to the Basel area and to the Lake of Constance (Fig. 2012.7 a). Significantly fewer reports were received from the southern and western parts of Switzerland and the Alpine area as a whole, which is even more evident in the distribution of intensities of the M_L 3.5 aftershock (Fig. 2012.7 b). The epicentral intensity on the European Macroseismic Scale (EMS) of the mainshock was IV, with a relatively flat intensity field, typical for deep events. The maximum intensity of V has been reported in a few areas, probably due to site amplification effects (Fig. 2012.7 a).

Figure 2012.8 shows the ground motion recordings of the M_L 4.2 mainshock at two stations of the Swiss National Strong Motion Network (SSMNet) installed in Lucerne about 21 km from the epicenter. Station SLUB (Bramberg) is a rock site on a hill above the city center. Station SLUW is located in the basin of Lucerne, near the main train station. The recordings at SLUB show an impulsive, unilateral signal pulse of the S-phase, with a peak displacement of 0.07 mm. The recordings at station SLUW show long-lasting reverberations due to local site effects and the peak displacement is amplified by a factor of 2 compared to the rock site.
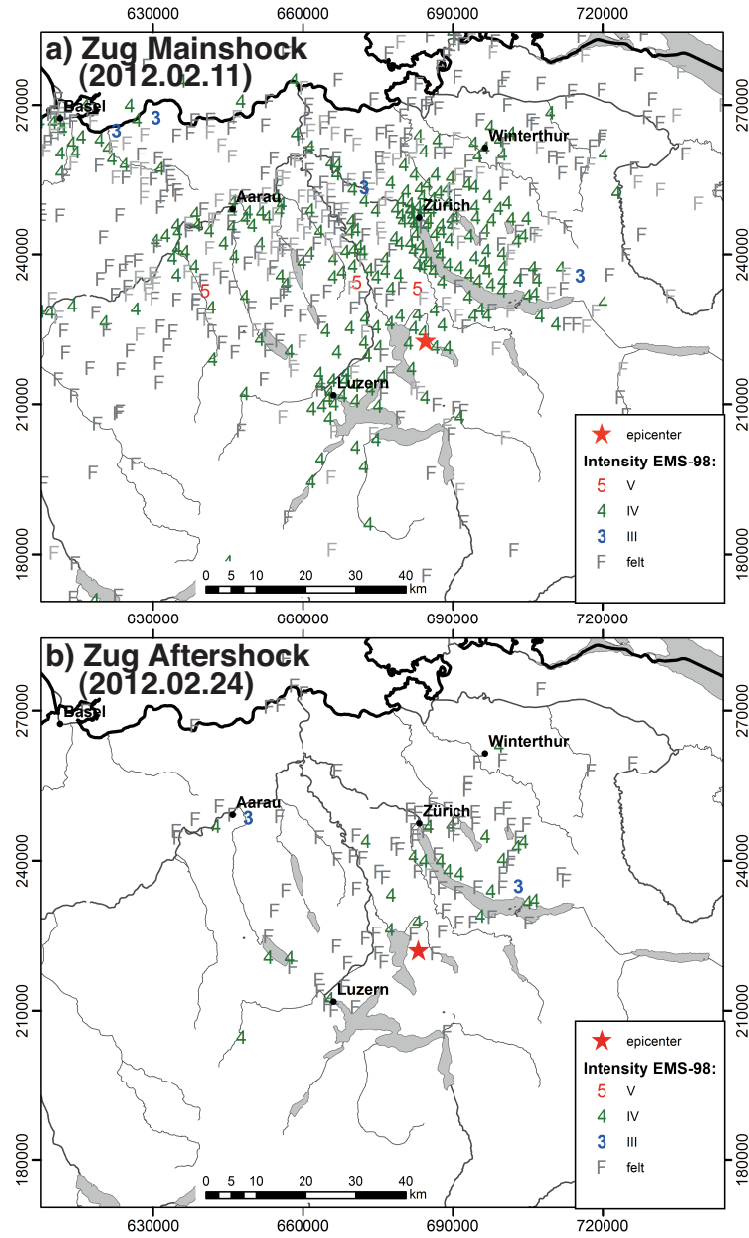
Figure 2012.7: Macroseismic intensities(EMS-98) of the M_L 4.2 Zug mainshock of February 11th (a) and the strongest aftershock with M_L 3.5 of February 24th (b).
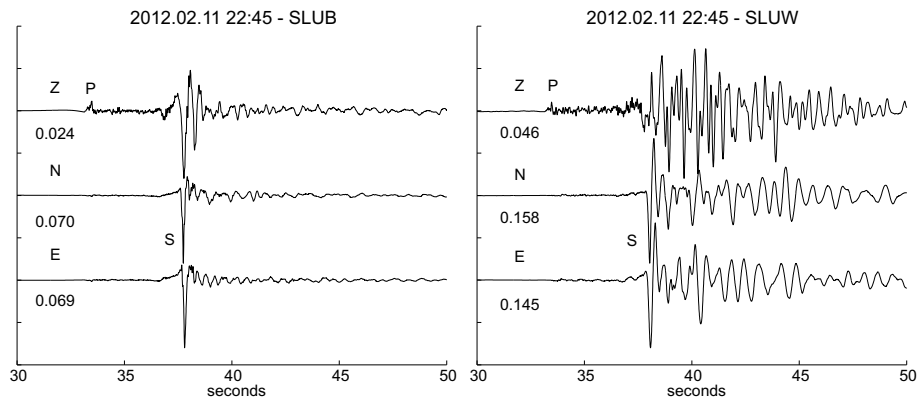
Figure 2012.8: Displacement seismograms of the M_L 4.2 earthquake of Zug recorded at two accelerographs in the city of Lucerne. Epicentral distance to both stations is about 21 km, distance between stations is about 1.6 km. To stabilize the double integration of the original accelerograms, the signals where filtered with a 0.5 Hz, 4th order, zero-phase high-pass Butterworth filter and detrended with a second order polynomial. Note the impulsive unilateral signal pulse of the S-phase on the two horizontal components at station SLUB (right), situated on hard rock, compared to the long duration reverberations of the S-phase at station SLUW (left), situated on unconsolidated sediments near the lake shore. Note also the amplification by a factor of 2 of the peak displacement (given below each trace in mm) at station SLUW compared to station SLUB.
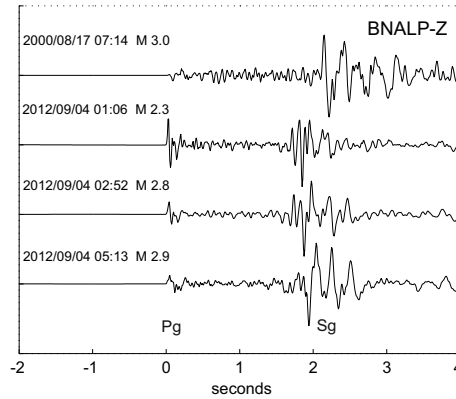
Figure 2012.9: Vertical component seismograms recorded at station BNALP of the M_L 3.0 Beckenried event of the year 2000 compared to the three Beckenried events of 2012 at epicentral distances of about 8 km. Note the larger S-P travel-time difference for the event of 2000, which is compatible with the calculated location difference between the hypocenter of this event and that of the three events of 2012. Note also the significantly larger P/S amplitude ratio of the first event of 2012 compared to that of the subsequent two events, which is indicative of a slightly different focal mechanism.
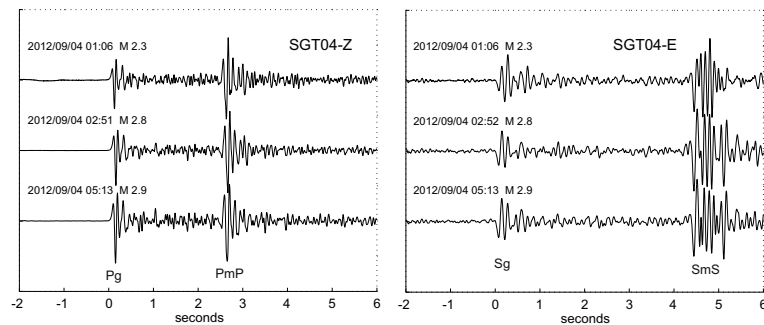

Figure 2012.10: Seismograms (ground velocity; 0.5 Hz, 4th order, zero-phase Butterworth high-pass filter) of the three Beckenried events of 2012 recorded at station SGT04 (epicentral distance 81 km). The vertical components (left panel) are aligned on the Pg arrival; the EW components (right panel) are aligned on the Sg arrival. Note the almost identical travel-time differences between the reflections at the Moho (PmP, SmS) and the direct waves (Pg, Sg) for the three events, which are indicative of an essentially identical focal depth. This is a rare example of a sequence of clear and impulsive Pg, PmP, Sg and SmS phases recorded at the same location.

Beckenried

On September 4th, three earthquakes with M_L 2.3, 2.8, and 2.9 occurred within 4 h near Beckenried on the southern shore of the Vierwaldstättersee. The events are located close to the epicenter of the M_L 3.0 earthquake of 2000 (Baer et al. 2001). The high similarity between the signals of the three events of 2012 (Figs. 2012.9 and 2012.10) suggests that the hypocenters must be co-located and their focal mechanisms must be nearly identical. The epicenter location of the 2000 event is located 2-3 km north-northeast of the others, which is in agreement with the difference in S-P times observed at station BNALP (located to the south of the epicenters) shown in Fig. 2012.9. The focal depths of the 2012 M_L 2.8 and 2.9 events are constrained by P- and S-arrivals at stations BNALP and MUO at 8 and 13 km epicentral distance as well as by several Pn arrivals (stations KIZ, GUT, UBR and BRANT). At 9-10 km depth, these events are most likely located in the basement. This differentiates them from most of the other well-located events in central Switzerland, which occurred in the overlying sedimentary units (Deichmann et al. 2000b). Assuming a constant seismic velocity ratio (Vp/Vs) for the entire crystalline crust, the observed arrival-time differences between Pg, PmP and Sg, SmS at station SGT04 (Fig. 2012.10) gives Vp/Vs = 1.73 ± 0.03.

The focal mechanism of the M_L 2.9 2012 event (Table 2012.2; Fig. 2012.3) is very similar to the one of 2000: strikeslip with more or less NS and EW trending nodal planes. The focal mechanisms of the M_L 2.9 and the M_L 2.8 events (not shown) are actually identical, as expected from the almost identical signals. The fault-plane solution of the M_L 2.3 event (not shown) is not well constrained, but it shows that the focal mechanism is not identical to that of the other events. This is also consistent with the differences in S/P amplitude ratios visible for station BNALP (less nodal) in Fig. 2012.9. The orientation of the P- and T-axes is typical for earthquakes in central Switzerland (e.g. Kastrup et al. 2004).

Vallorcine

The M_L 3.6 earthquake that occurred on October 25th close to the village of Vallorcine (France) is part of the ongoing earthquake sequence that followed the M_L 4.9 earthquake of September 2005 (Fréchet et al. 2010). The M_L 3.6 event of October 2012 was the strongest earthquake in the region since the September 2005 mainshock. The 2012 event was felt in the southwestern part of the Valais and maximum intensities of IV have been reported. The routine epicenter location of the event is within the main cluster of activity, labeled C1 in the study of Fréchet et al. (2010). The routinely computed focal depth of 11 km derived from using all available P-wave arrivals (71) is not consistent with focal depths computed for past seismicity of the Vallorcine sequence, including the M_L 4.9 2005 earthquake, despite the fact that this focal depth estimate is well constrained by the large number of Pg and Pn arrivals. Using only Pg- and Sg-wave arrivals up to 80 km distance yields a focal depth of 4 km, which is consistent with focal depths for past seismicity of the Vallorcine sequence. Due to the lack of observations at close distances and of Pn arrivals at large distances this focal depth estimate is not well constrained (uncertainty of ±3.0 km). A focal depth of 4 km yields large negative travel time residuals (> 1 s) for Pn arrivals at larger distances but smaller travel time residuals for nearby stations OGSI (RESIF) and SALAN. This suggests that a focal depth of 4 km is more consistent with observations at nearby stations but that a focal depth of 11 km
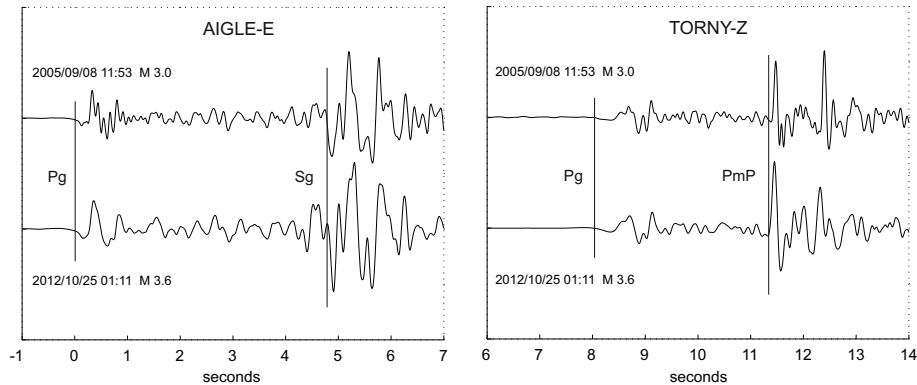
Figure 2012.11: Displacement seismograms of the Vallorcine events of 2005/09/08 (M_L 3.0) and 2012/10/25 (M_L 3.6) recorded at stations AIGLE (EW-component, 35 km epicentral distance) and TORNY (Z-component, 82 km epicentral distance). To stabilize the integration and to accentuate differences at high frequency, the signals are filtered with a 1 Hz, 4th order, zero-phase Butterworth high-pass filter and an 8 Hz, 2nd order Butterworth low-pass filter. Because the Pg onsets at TORNY are rather emergent, both sets of seismograms are aligned on the Pg arrival at station AIGLE. Note the high signal similarity as well as the almost identical SgPg arrival-time differences at AIGLE and PmPPg arrival-time differences at TORNY for the two events. These similarities are evidence of similar focal mechanisms and almost identical epicenters and focal depths.

is more consistent with distant Pn arrivals. Hypocenter locations were computed using a 3-D P-wave velocity model of Husen et al. (2003), which includes a priori information on Moho depths beneath Switzerland and surrounding regions. This model, however, shows a relatively broad velocity gradient across the Moho instead of a rather sharp velocity gradient, which would be more realistic. Consequently, Pn arrivals are traced as diving waves in the model of Husen et al. (2003), which may lead to longer ray paths when compared to those computed in a model with a sharp velocity gradient across the Moho. Longer ray paths yield larger theoretical travel times and, hence, negative travel time residuals as observed. Waveforms recorded at station AIGLE for the strongest aftershock (M_L 3.0) of the M_L 4.9, 2005 Vallorcine earthquake and the M_L 3.6, 2012 earthquake show nearly identical S-P times (Fig. 2012.11). This suggests that the M_L 3.6, 2012 earthquake occurred close to strongest aftershock of the M_L 4.9, 2005 earthquake, consistent with the obtained epicenter location. PmP arrival times of the strongest aftershock and the M_L 3.6, 2012 earthquake at station TORNY are very similar (Fig. 2012.11). This suggests that both events occurred at a similar focal depth. Given the uncertainty in computing correct Pn ray paths, as discussed above, and a focal depth of 4 km for the aftershock constrained by a densely spaced deployment in September 2005 (Fréchet et al. 2010), a focal depth of 4 km for the M_L 3.6, 2012 Vallorcine earthquake seems more plausible. The focal mechanism derived from the analysis of firstmotion polarities of the M_L 3.6 event (Table 2012.2; Fig. 2012.3) is almost identical to the mechanism of the 2005 mainshock published by Fréchet et al. (2010). The high similarity of waveforms to the 2005 aftershock and the similarity in the

focal mechanisms suggest that, as in the case of the 2005 mainshock, the plane striking N63°E was also active in the 2012 event.

Breithorn

The M_L 2.9 event of November 28th was located 10 km south of Zermatt (labeled Bre in Fig. 2012.1). The focal depth of 2 km is constrained by P and S-arrivals recorded at epicentral distances of 10 km (station SATI (INGV)) and 20 km (station MMK) and therefore uncertain. Due to the inhomogeneous distribution of first-motion observations, a focal-plane solution could not be reliably determined. The mainshock was followed by 5 aftershocks with $M_L 0.7 - 1.8$ in November and December.

Santa Maria

During 2012, a sequence of 15 earthquakes occurred in a region east of Santa Maria (Val Müstair). Based on the routine location and the high similarity of waveforms recorded at station MOSI (Bozen), seven of these events with $M_L 1.3 - 1.9$ appear to be co-located (cluster labeled SMa in Fig. 2012.1). The sequence of co-located events started on October 20th and the last event occurred on December 7th. The largest of the events on November 8th was followed by a secondary event separated by about 3 s.

Seismicity associated with the former Deep Heat Mining project in Basel

The seismic activity induced by the geothermal project in Basel in 2006 and 2007 (e.g. Deichmann and Ernst 2009; Deichmann and Giardini 2009) continued to decrease over the years 2008-2011, with only one event (M_L 0.6) being recorded by the national network in 2010. In 2012 activity seems to have picked up again: five events, with magnitudes between $M_L = 0.9 - 1.2$, were strong enough to be recorded by the national broadband network. This agrees with the assessment of Bachmann et al. (2011), according to which the seismic activity in the stimulated rock volume is expected to stay above the natural background level for several years. Master event relocation confirms that the two events of February 26th, 2010, and May 20th, 2012, as well as the three events that occurred between December 12th and 15th, 2012, are located in the same region as the hypocenters of the events which occurred towards the end of 2007 (i.e. above the casing shoe, at the southern periphery of the stimulated rock volume), whereas the event of October 3rd 2012 is located about 400 m below the casing shoe and about 400 m to the east of the main hypocentral cloud. Due to the removal of three of the borehole sensors, relative location uncertainties for the five events of 2012 are about twice as large as for the earlier events. However, with computed standard deviations of 76 m (E-W), 147 m (N-S) and 67 m (Z), the outlier location of the event of October 3rd, 2012 is well constrained.

References

Bachmann, C. E., Wiemer, S., Woessner, J., Hainzl, S. 2011: Statistical analysis of the induced Basel 2006 earthquake sequence: Introducing a probability-based monitoring approach for Enhanced Geothermal Systems. Geophysical Journal International, 186, 793807. doi:10.1111/j.1365-246X.2011.05068.x.

Badertscher, N. & Burkhard, M. 1998: Inversion alpine du graben Permo-Carbonifère de Salvan-Dorénaz et sa relation avec le chevauchement de la nappe de Morcles sus-jacente. Eclogae Geologicae Helvetiae, 91, 359-373.

Baer, M. 1990: The seismic station network of the Swiss Seismological Service. In: I. Workshop on: MEDNET, the Broad-Band Seismic Network for the Mediterranean (Ed. by E. Boschi, D. Giardini and A. Morelli). Istituto Nazionale Geofisica, Roma, 345-350.

Baer, M. & Kradolfer, U. 1987: An automatic phase picker for local and teleseismic events. Bulletin of Seismological Society of America, 77, 1437-1445.

Baer, M., Deichmann. N., Fäh, D., Kradolfer, U., Mayer-Rosa, D., Rüttener, E., Schler, T., Sellami, S., & Smit, P. 1997: Earthquakes in Switzerland and surrounding regions during 1996. Eclogae Geologicae Helvetiae, 90/3, 557-567.

Baer, M., Deichmann, N., Ballarin Dolfin, D., Bay, F., Delouis, B., Fäh, D., Giardini, D., Kastrup, U., Kind, F., Kradolfer, U., Künzle, W., Röthlisberger, S., Schler, T., Sellami, S., Smit, P., & Spühler, E. 1999: Earthquakes in Switzerland and surrounding regions during 1998. Eclogae Geologicae Helvetiae, 92/2, 265-273.

Baer, M., Deichmann, N., Braunmiller, J., Ballarin Dolfin, D., Bay, F., Bernardi, F., Delouis, B., Fäh, D., Gerstenberger, M., Giardini, D., Huber, S., Kastrup, U., Kind, F., Kradolfer, U., Maraini, S., Mattle, B., Schler, T., Salichon, J., Sellami, S., Steimen, S., Wiemer, S. 2001: Earthquakes in Switzerland and surrounding regions during 2000. Eclogae Geologicae Helvetiae, 94/2, 253-264.

Baer, M., Deichmann, N., Braunmiller, J., Bernardi, F., Cornou, C., Fäh, D., Giardini, D., Huber, S., Kästli. P., Kind, F., Kradolfer, U., Mai, M., Maraini, S., Oprsal, I., Schler, T., Schorlemmer, D., Sellami, S., Steimen, S., Wiemer, S., Wössner, J., Wyss, A. 2003: Earthquakes in Switzerland and surrounding regions during 2002. Eclogae Geologicae Helvetiae - Swiss Journal of Geosciences, 96/2, 313-324.

Baer, M., Deichmann, N., Braunmiller, J., Husen, S., Fäh, D., Giardini, D., Kästli, P., Kradolfer, U., Wiemer, S. 2005: Earthquakes in Switzerland and surrounding regions during 2004. Eclogae Geologicae Helvetiae - Swiss Journal of Geosciences, 98/3, 407-418, DOI: 10.1007/s00015-005-1168-3.

Baer, M., Deichmann, N., Braunmiller, J., Clinton, J., Husen, S., Fäh, D., Giardini, D., Kästli, P., Kradolfer, U., Wiemer, S. 2007: Earthquakes in Switzerland and surrounding regions during 2006. Swiss Journal of Geosciences, 100/3, 517-528, DOI: 10.1007/s00015-007-1242-0.

BCSF 2004: http://eost.u-strasbg.fr/bcsf/Accueil.html, publications, Les notes du BCSF, *Le séisme de Roulans (23/02/2004) – Note préliminaire.*

Bisch, P. 1996: Le séisme d'Epagny du 15 juillet 1996 – Préambule. In: Le Séisme d'Epagny (Haute-Savoie, France) du 15 Juillet 1996. Rapport de la mission AFPS. Association Française du Génie Parasismique, Paris, p 3-6.

Bouchon, M. 1982: The complete synthesis of seismic crustal phases at regional distances. Journal of Geophysical Research, 87, 1735-1741.

Braunmiller, J., Nabelek J. L., Leitner, B. & Qamar, A. 1995: The 1993 Klamath Falls, Oregon, earthquake sequence: source mechanisms from regional data. Geophysical Research Letters, 22, 105-108.

Braunmiller, J., Deichmann, N., Giardini, D., Wiemer S. and the SED Magnitude Working Group, 2005: Homogeneous moment magnitude calibration in Switzerland. Bulletin of the Seismological Society of America, 95, 1, 58-74, doi:10.1785/0120030245.

Brune, J. N. 1970: Tectonic stress and the spectra of seismic shear waves from earthquakes. Journal of Geophysical Research, 75, 4997-5010.

Brune, J. N. 1971: Correction: Tectonic stress and the spectra of seismic shear waves from earthquakes. Journal of Geophysical Research, 76, 5002.

Campus, P. & Fäh, D. 1997: Seismic monitoring of explosions: a method to extract information on the isotropic component of the seismic source. Journal of Seismology, 1, 205-218.

Cara, M., Brüstle, W., Gisler, M., Kästli, P., Sira, C., Weihermüller C. & Lambert, G. 2005: Transfrontier macroseismic observations of the Ml=5.4 earthquake of February 22, 2003 at Rambervillers, France, Journal of Seismology, 9/3, 317-328.

Clinton, J. F., Hauksson, E. & Solanki, K. 2006: An Evaluation of the SCSN Moment Tensor Solutions: Robustness of the Mw Magnitude Scale, Style of Faulting, and Automation of the Method, Bulletin of the Seismological Society of America, 96, 1689 - 1705.

Console, R. & Di Giovambattista, R. 1987: Local earthquake relative location by digital records. Physics of the Earth and Planetary Interiors, 47, 43-49.

Courboulex, F., Deichmann, N., Gariel, J.-C. 1999: Rupture complexity of a moderate intraplate earthquake in the Alps: the 1996 M 5 Epagny-Annecy Earthquake. Geophysical Journal International, 139, 152-160.

CREALP (Centre de Recherche sur lEnvironnement Alpin) 1998: Relation hydrogéologique Lac de Salanfe Source thermals de Val dIlliez. Analyse des événements séismo-hydro-géologiques de la période 1994-1996. CREALP/98.03, 37 pp.

Dammeier, F., J. R. Moore, F. Haslinger, and S. Loew (2011): Characterization of alpine rockslides using statistical analysis of seismic signals. Journal of Geophysical Research, 116, F04024, doi:10.1029/2011JF002037.

Davidovici, V. 1996: Le séisme du 15 juillet, au Nord d'Annecy. In: Le Séisme d'Epagny (Haute-Savoie, France) du 15 Juillet 1996. Rapport de la mission AFPS. Association Française du Génie Parasismique, Paris, p 99-127.

Deichmann N. 1987a: Seismizität der Nordschweiz, 1983-1986. Nagra Technischer Bericht, NTB 87-05, Nagra, Baden.

Deichmann, N. 1987b: Focal depths of earthquakes in northern Switzerland. Annales Geophysicae, 5B, 395-402.

Deichmann, N. 1990: Seismizität der Nordschweiz, 1987-1989, und Auswertung der Erdbebenserien von Günsberg, Läufelfingen und Zeglingen. Nagra Technischer Bericht, NTB 90-46, Nagra, Baden.

Deichmann, N. 1992a: Structural and rheological implications of lower-crustal earthquakes below northern Switzerland. Physics of the Earth and Planetary Interiors, 69, 270-280.

Deichmann. N. 1992b: Recent seismicity of the northern Alpine foreland of Switzerland. Eclogae Geologicae Helvetiae, 85/3, 701-705.

Deichmann, N. & Baer, M. 1990: Earthquake focal depths below the Alps and northern Alpine foreland of Switzerland. In: The European Geotraverse: Integrative Studies. (Ed. by R. Freeman, P. Giese and St. Mueller). European Science Foundation, Strasbourg, France, 277-288.

Deichmann, N. & Rybach, L. 1989: Earthquakes and temperatures in the lower crust below the northern Alpine foreland of Switzerland. In: Properties and Processes of the Lower Crust. (Ed. by R. F. Mereu, St. Mueller and D. Fountain). Am. Geophys. Union, Geophysical Monograph 51, IUGG Vol. 6, 197-213.

Deichmann, N. & Garcia-Fernandez, M. 1992: Rupture geometry from high-precision relative hypocenter locations of microearthquake clusters. Geophysical Journal International, 110, 501-517.

Deichmann. N., Baer, M., Ballarin Dolfin, D., Fäh, D., Flück, P., Kastrup, U., Kradolfer, U., Künzle, W., Mayer-Rosa, D., Röthlisberger, S., Schler, T., Sellami, S., Smit, P., & Giardini, D. 1998: Earthquakes in Switzerland and surrounding regions during 1997. Eclogae Geologicae Helvetiae, 91/2, 237-246.

Deichmann, N., Baer, M., Braunmiller, J., Ballarin Dolfin, D., Bay, F., Delouis, B., Fäh, D., Giardini, D., Kastrup, U., Kind, F., Kradolfer, U., Künzle, W., Röthlisberger, S., Schler, T., Salichon, J., Sellami, S., Spühler, E., Wiemer, S. 2000a: Earthquakes in Switzerland and surrounding regions during 1999. Eclogae Geologicae Helvetiae, 93/3, 395-406.

Deichmann, N., Ballarin Dolfin, D. & Kastrup, U. 2000b: Seismizität der Nord- und Zentralschweiz. Nagra Technischer Bericht, NTB 00-05, Nagra, Wettingen.

Deichmann, N., Baer, M., Braunmiller, J., Ballarin Dolfin, D., Bay, F., Bernardi, F., Delouis, B., Fäh, D., Gerstenberger, M., Giardini, D., Huber, S., Kradolfer, U., Maraini, S., Oprsal, I., Schibler, R., Schler, T., Sellami, S., Steimen, S., Wiemer, S., Wössner, J., Wyss, A. 2002: Earthquakes in Switzerland and surrounding regions during 2001. Eclogae Geologicae Helvetiae - Swiss Journal of Geosciences, 95/2, 249-261.

Deichmann, N., Baer, M., Braunmiller, J., Cornou, C., Fäh, D., Giardini, D., Gisler, M., Huber, S., Husen, S., Kästli, P., Kradolfer, U., Mai, M., Maraini, S., Oprsal, I., Schler, T., Schorlemmer, D., Wiemer, S., Wössner, J., Wyss, A. 2004: Earthquakes in Switzerland and surrounding regions during 2003. Eclogae Geologicae Helvetiae - Swiss Journal of Geosciences, 97/3, 447-458.

Deichmann, N., Baer, M., Braunmiller, J., Husen, S., Fäh, D., Giardini, D., Kästli, P., Kradolfer, U., Wiemer, S. 2006: Earthquakes in Switzerland and surrounding regions during 2005. Eclogae Geologicae Helvetiae - Swiss Journal of Geosciences, 99/3, 443-452, DOI:10.1007/s00015-006-1201-1.

Deichmann, N., Baer, M., Clinton, J., Husen, S., Fäh, D., Giardini, D., Kästli, P., Kradolfer, U., Wiemer, S. 2008: Earthquakes in Switzerland and surrounding regions during 2007. Swiss Journal of Geosciences, 101/3, 659-667, DOI:10.1007/s00015-008-1304-y.

Deichmann, N., Clinton, J., Husen, S., Haslinger, F., Fäh, D., Giardini, D., Kästli, P., Kradolfer, U., Marschall, I., Wiemer, S. 2009: Earthquakes in Switzerland and surrounding regions during 2008. Swiss Journal of Geosciences, 102/3, 505-514, DOI:10.1007/s00015-009-1339-8.

Deichmann, N. & Ernst, J. 2009: Earthquake focal mechanisms of the induced seismicity in 2006 and 2007 below Basel (Switzerland). Swiss Journal of Geosciences, 102/3, 457-466, DOI:10.1007/s00015-009-1336-y.

Deichmann, N. & Giardini, D. 2009: Earthquakes induced by the stimulation of an enhanced geothermal system below Basel (Switzerland). Seismological Research Letters 80/5, 784-798, doi:10.1785/gssrl.80.5.784.

Deichmann, N., Clinton, J., Husen, S., Edwards, B., Haslinger, F., Fäh, D., Giardini, D., Kästli, P., Kradolfer, U., Marschall, I., Wiemer, S. 2010: Earthquakes in Switzerland and surrounding regions during 2009. Swiss Journal of Geosciences, 103/3, 535-549, 2010, DOI:10.1007/s00015-010-0039-8.

Deichmann, N., Clinton, J., Husen, S., Edwards, B., Haslinger, F., Fäh, D., Giardini, D., Kästli, P., Kradolfer, U., Wiemer, S. 2011: Earthquakes in Switzerland and surrounding regions during 2010. Swiss Journal of Geosciences, 104/3, 537-547, DOI:10.1007/s00015-011-0084-y.

Deichmann, N., J. Clinton, S. Husen, B. Edwards, F. Haslinger, D. Fh, D. Giardini, P. Kstli, U. Kradolfer, S. Wiemer 2012: Earthquakes in Switzerland and surrounding regions during 2011. Swiss Journal of Geosciences, 105/3, 463-476, DOI:10.1007/s00015-012-0116-2.

Delacou, B., Deichmann, N., Sue, C., Thouvenot, F., Champagnac, D., Burkhard, M., 2005: Active strike-slip faulting in the Chablais area (NW Alps) from earthquake focal mechanisms and relative locations. Eclogae Geologicae Helvetiae - Swiss Journal of Geosciences, 98/2, 189-199, DOI: 10.1007/s00015-005-1159-4.

Delouis, B., Haessler, H., Cisternas, A., Rivera, L. 1993: Stress tensor determination in France and neighbouring regions. Tectonophysics, 221, 413-437.

Diehl, T., Deichmann, N., Clinton, J., Husen, S., Kraft, T., Plenkers, K., Edwards, B., Cauzzi, C., Michel, C., Kästli, P., Wiemer, S., Haslinger, F., Fäh, D., Kradolfer, U., Woessner, J., 2013: Earthquakes in Switzerland and surrounding regions during 2012. Swiss Journal of Geosciences, 106/3, 543-558, DOI:10.1007/s00015-013-0154-4.

Dreger, D. S. 2003: TDMT INV: Time Domain Seismic Moment Tensor INVersion. In W. H. K. Lee, H. Kanamori, P. C. Jennings, and C. Kisslinger (Eds.), International Handbook of Earthquake and Engineering Seismology (Part B, pp. 1627). London: Academic Press.

Edwards, B., Allmann, B., Fäh, D., Clinton, J. 2010: Automatic Computation of Moment Magnitudes for Small Earthquakes and the Scaling of Local to Moment Magnitude. Geophysical Journal International, 183/1, 407-420, DOI: 10.1111/j.1365-246X.2010.04743.x.

Edwards, B., Michel, C., Poggi, V., Fäh, D. 2013: Determination of site amplification from regional seismicity: Application to the Swiss national seismic networks. Seismological Research Letters, 84, 611621. doi:10.1785/0220120176.

Eva, E., Pastore, S. & Deichmann, N. 1998: Evidence for ongoing extensional deformation in the western Swiss Alps and thrust-faulting in the southwestern

Alpine foreland. Journal of Geodynamics 26/1, 27-43.

Faber, S., Bonjer, K.-P., Brüstle, W. & Deichmann, N. 1994: Seismicity and structural complexity of the Dinkelberg block, southern Rhinegraben. Geophysical Journal International, 116, 393-408.

Fäh, D., Giardini, D., Bay, F., Bernardi, F., Braunmiller, J., Deichmann, N., Furrer, M., Gantner, L., Gisler, M., Isenegger, D., Jimenez, M.-J., Kästli, P., Koglin, R., Masciadri, V., Rutz, M., Scheidegger, C., Schibler, R., Schorlemmer, D., Schwarz-Zanetti, G., Steimen, S., Sellami, S., Wiemer, S., Wössner, J. 2003: Earthquake catalog of Switzerland (ECOS) and the related macroseismic database. Eclogae Geologicae Helvetiae - Swiss Journal of Geosciences, 96/2, 219-236.

Fréchet, J., Thouvenot, F., Jenatton, L., Hoang-Trong, P. & Frogneux, M. 1996: Le séisme du Grand-Bornand (Haute-Savoie) du 14 décembre 1994: un coulissage dextre dans le socle subalpin. C.R. Acad. Sci. Paris, 323, IIa, 517-524.

Fréchet, J., Thouvenot, F., Frogneux, M., Deichmann, N., Cara, M. 2006: An aftershock study of the M_L 4.9 Vallorcine (French Alps) earthquake of 8 September 2005. European Geophysical Union XXIX General Assembly, Geneva, April 2006 (Abstract).

Fréchet, J., Thouvenot, F., Frogneux, M., Deichmann, N., Cara, M. 2010: The M_w 4.5 Vallorcine (French Alps) earthquake of 8 September 2005 and its complex aftershock sequence. Journal of Seismology, 15, 43-58, DOI:10.1007/s10950-010-9205-8.

Funk, M. & Bösch, H. 2001: Allalin-Gletscher. Bericht über die hydrologischen und glaziologischen Verhältnisse im Mattmarkgebiet 1999/2000, z.Hd.d. Kraftwerke Mattmark, AG. VAW Bericht Nr. 7902.52.46, ETH Zürich.

Garcia-Fernandez, M. & Mayer-Rosa, D. 1986: Improved hypocentral parameter determination using secondary regional phases. Revista de Geophysica, 42, 175-184.

Giardini, D., Wiemer, S., Fäh, D., Deichmann, N., Sellami, S., Jenni, S. and the Hazard Team of the Swiss Seismological Service 2004: Seismic Hazard Assessment 2004. Swiss Seismological Service, 81 pp.

Hanks, T. C. and H. Kanamori 1979: A moment magnitude scale. Journal of Geophysical Research, 84, B5, 2348-2350.

Häring, M. O., Schanz, U., Ladner, F., Dyer, B. C. 2008: Characterization of the Basel 1 enhanced geothermal system. Geothermics, 37, 469-495, doi:10.1016/j.geothermics.2008.06.002.

Hitz, L. & Pfiffner, O. A. 1997: Deep seismic fan-recordings and a 3D crustal model of the eastern Aar massif. In: Deep Structure of the Alps, Results of NRP20, Birkhäuser, Basel, 92-100.

Husen, S., Kissling, E., Deichmann, N., Wiemer, S., Giardini, D., Baer, M. 2003: Probabilistic earthquake location in complex three-dimensional velocity models: Application to Switzerland. Journal of Geophysical Research, 108, B2, 2077-2096.

Husen, S., Bachmann, C., Giardini, D. 2007: Locally triggered seismicity in the central Swiss Alps following the large rainfall event of August 2005. Geophysical Journal International, 171, 1126-1134 doi:10.1111/j.1365-246X.2007.03561.x

Husen, S., Kissling, E., von Deschwanden, A. (2011): Induced seismicity during the construction of the Gotthard Base Tunnel, Switzerland: hypocenter locations and source dimensions. Journal of Seismology, DOI 10.1007/s10950-011-9261-8.

INGV 2004: http://www.ingv.it/terremoti/bresciano2004/bresciano.html

Kastrup, U. 2002: Seismotectonics and stress-field variations in Switzerland. Ph.D. Thesis Nr. 14527, ETH-Zürich.

Kastrup, U., Zoback M.-L., Deichmann, N., Evans, K., Giardini, D., Michael, A. J. 2004: Stress field variations in the Swiss Alps and the northern Alpine foreland derived from inversion of fault plane solutions. Journal of Geophysical Research,109, B1, doi:10.1029/2003JB002550B01402.

Kastrup, U., Deichmann, N,, Fröhlich, A., Giardini, D. 2007: Evidence for an active fault below the northwestern Alpine foreland of Switzerland. Geophysical Journal International, 169, 1273-1288, DOI:10.1111/j.1365-264X.2007.03413.x

Keusen, H.R. 1997: Courmayeur/Brenva, éboulement du 18 janvier 1997, rapport géologique. Geotest S.A., Zollikofen, 18 pp.

Kradolfer, U. 1996: AutoDRM - The First Five Years. Seismological Research Letters, 67, 30-33.

Kradolfer, U. & Mayer-Rosa, D. 1988: Attenuation of seismic waves in Switzerland. In: Recent seismological investigations in Europe. Proceedings of the XIX General Assembly of the ESC. Moscow, October 1-6, 1984, 481-488.

Kraft, T., Mai, P. M., Wiemer, S., Deichmann, N., Ripperger, J., Kästli, P., Bachmann, C., Fäh, D., Wössner, J., and Giardini, D. 2009: Mitigating Risk for Enhanced Geothermal Systems in Urban Areas. EOS Transactions American Geophysical Union, 90/32, 273-274.

LED 2004: http://www.lgrb.uni-freiburg.de/lgrb/Fachbereiche, Erdbebendienst, Jahresbulletins, Bulletin 2004.

Lee, W. H. K. & Lahr, J. C. 1972: HYPO-71 a computer program for determining hypocenter, magnitude and first motion pattern of local earthquakes. United States Geological Survey, Open-File Report.

Lomax, A., & Curtis, A. 2001: Fast, probabilistic earthquake location in 3D models using Oct-Tree Importance sampling. Geophysical Research Abstracts, 3.

Lomax, A., Virieux J., Volant P., Thierry-Berge, C. 2000: Probabilistic earthquake location in 3D and layered models. In Advances in Seismic Event Location, edited by C.H. Thurber, and N. Rabinowitz, Kluwer Academic Publishers, Dordrecht/Boston/London, pp. 101-134.

Marschall, I., Deichmann, N., Marone, F. 2013: Earthquake focal mechanisms and stress orientations in the eastern Swiss Alps. Swiss Journal of Geosciences, 106, 79-90, DOI:10.1007/s00015-013-0129-5.

Mattle, B. 2000: Swiss National Strong Motion Network: Strong Motion Bulletin, October 1999 - November 2000. Publication Series of the Swiss Seismological Service, Nr. 113, ETH-Zürich.

Maurer, H. & Ansorge, J. 1992: Crustal structure beneath the northern margin of the Swiss Alps. Tectonophysics 207, 165-181.

Maurer H. & Deichmann, N. 1995: Microearthquake cluster detection based on waveform similarities, with an application to the western Swiss Alps. Geophysical Journal International, 123, 588-600.

Maurer, H. & Kradolfer, U. 1996: Hypocentral parameters and velocity estimation in the western Swiss Alps by simultaneous inversion of P- and S-wave data. Bulletin of the Seismological Society of America 86, 32-41.

Maurer, H., Burkhard, M., Deichmann, N., Green, A. G. 1997: Active Tectonism in the Western Swiss Alps. Terra Nova, 9, 91-94.

Müller, B., Zoback, M.-L., Fuchs, K., Mastin, L.G., Gregersen, S., Pavoni, N., Stephansson, O., Ljunggren, C. 1992: Regional patterns of tectonic stress in Europe. Journal of Geophysical Research, 89, B13, 11'517-11'526.

Nabelek, J. & Xia, G. 1995: Moment-tensor analysis using regional data: application to the 25 March, 1993, Scotts Mills, Oregon earthquake. Geophysical Research Letters, 22, 13-16.

Pavoni, N. 1977: Erdbeben im Gebiet der Schweiz. Eclogae Geologicae Helvetiae, 70/2, 351-370.

Pavoni, N. 1984: Seismotektonik Nordschweiz. Nagra Technischer Bericht, NTB 84-45, Nagra, Baden.

Pavoni, N. 1987: Zur Seismotektonik der Nordschweiz. Eclogae Geologicae Helvetiae, 80/2, 461-472.

Pavoni, N. & Roth, P. 1990: Seismicity and seismotectonics of the Swiss Alps. Results of microearthquake investigations 1983-1988. In F. Roure, P. Heitzmann and R. Polino (Eds.), Deep Structure of the Alps, Mémoire de la Societé geologique de France, Paris (Vol. 156, pp. 129-134).

Pavoni, N., Maurer, H., Roth, P., Deichmann, N. 1997: Seismicity and seismotectonics of the Swiss Alps. In: Deep structure of the Swiss Alps, results of NRP 20, Birkhäuser, Basel, 241-250.

Pfister, M. 1990: Gemeinsame Auswertung von Erdbeben-, Refraktions- und Reflexionsdaten in der Nordschweiz. Diploma thesis, Institute of Geophysics, ETH-Zürich.

Pilloud, C. 1991: Structures de déformation alpines dans le synclinal de Permo-Carbonifère de Salvan-Dorénaz (massif des Aiguilles Rouges, Valais). Mémoires de Géologie (Lausanne), No. 9, 101 pp.

Plenefisch, T. & Bonjer, K.-P. 1997: The stress field in the Rhinegraben area inferred from earthquake focal mechanisms and estimation of frictional parameters. Tectonophysics, 275, 71-97.

Poggi, V., B. Edwards and D. Fäh (2011): Derivation of a reference shear-wave velocity model from empirical site amplification. Bulletin of the Seismological Society of America 101, 258-274.

Ripperger, J., Kästli, P., Fäh, D. 2009: Ground motion and macro-seismic intensities of a seismic event related to geothermal reservoir stimulation below the city of Basel - observations and modelling. Geophysical Journal International, 179/3, 1757-1771.

Roth, P., Pavoni, N., Deichmann, N. 1992: Seismotectonics of the eastern Swiss Alps and evidence for precipitation-induced variations of seismic activity. Tectonophysics, 207, 183-197.

Rüttener, E. 1995: Earthquake hazard estimation for Switzerland. Matér. Géol. Suisse, Geophys. Nr. 29, Schweizerische Geophysikalische Kommission, ETH-Zürich, 106 pp.

Rüttener, E., Eogozcue, J., Mayer-Rosa, D. & Mueller, S. 1996: Bayesian estimation of seismic hazard for two sites in Switzerland. Natural Hazards 14, 165-178.

Sägesser, R. & Mayer-Rosa, D. 1978: Erdbebengefährdung in der Schweiz. Schweizerische Bauzeitung 78/7, 3-18.

Saikia, C. K. 1994. Modified frequency-wavenumber algorithm for regional seismograms using Filon's quadrature: Modeling of Lg waves in eastern North America. Geophysical Journal International, 118, 142-158.

Smit, P. 1997: Swiss National Strong Motion Network: Strong Motion Bulletin, October 1994 - September, 1996. Publication Series of the Swiss Seismological Service, Nr. 109, ETH-Zürich.

Smit, P. 1998a: The Swiss National Strong Motion Network - Achievements and prospects. Proceedings 11th Conference Earthquake Engineering, 6.-11. September 1998, Paris.

Smit, P. 1998b: Swiss National Strong Motion Network: Strong motion bulletin, October 1996 - May 1998. Publication Series of the Swiss Seismological Service, Nr. 111, ETH-Zürich.

Sommaruga, A. 1997: Geology of the central Jura and the Molasse basin: new insight into an evaporite-based foreland fold and thrust belt. Mémoire se la Société Neuchâteloise des Sciences Naturelles, Vol. XII, 177 pp.

Spühler, E. 1999: Swiss National Strong Motion Network: Strong motion bulletin, June 1998 - September 1999. Publication Series of the Swiss Seismological Service, Nr. 112, ETH-Zürich.

Stäuble, M, & Pfiffner, A. O. 1991: Evaluation of the seismic response of basement fold-and-thrust geometry in the Central Alps based on 2-D ray tracing. Annales Tectonicae, 5, 2-17.

Steck, A., Bigioggero, B., Dal Piaz, G. V., Escher, A., Martinotti, G., Masson, H. 1999: Carte tectonique des Alpes de Suisse occidentale et des régions avoisinantes, 1:100 000, Notice explicative par A. Steck, J. L. Epard, A. Escher, Y. Gouffon & H. Masson, 2001. Carte géologique speciale No. 123, Service hydrologique et géologique national.

Thouvenot, F. 1996: Le contexte sismologique et sismotectonique. In: Le Séisme d'Epagny (Haute-Savoie, France) du 15 Juillet 1996. Rapport de la mission AFPS. Association Française du Génie Parasismique, Paris, p 9-18.

Thouvenot, F., Fréchet, J., Tapponier, P., Thomas, J.-Ch, Lebrun, B., Ménard, G., Lacassin, R., Jenatton, L., Grasso, J.-R., Coutant, O., Paul, A. & Hatzfeld, D. 1997: The Ml-5.3 Epagny (French Alps) earthquake of 15 July 1996: a long awaited event on the Vuache fault. Geophysical Journal International, 135, 876-892, 1998.

Thouvenot, F., Fréchet, J., Frogneux, M., Deichmann, N., Cara, M. 2006: The M_L 4.9 Vallorcine (French Alps) earthquake (8 September 2005): A right-lateral strike-slip on the N60E-striking Loriaz Fault. First European Conference on Earthquake Engineering and Seismology, September 2006, (Abstract).

Valley, B. & Evans, K.F. 2009: Stress orientation to 5 km depth in the basement below Basel (Switzerland) from borehole failure analysis. Swiss Journal of Geosciences, 102/3, 467-480, DOI:10.1007/s00015-009-1335-z.

Wagner, M., Kissling, E., Husen, S. 2012: Combining controlledsource seismology and local earthquake tomography to derive a 3-D crustal model of the western Alpine region. Geophysical Journal International, 191, 789802. doi:10.1111/j.1365-246X.2012.05655.x.

Waldhauser, F. 1996: A parametrized three-dimensional Alpine crustal model and its application to teleseismic wavefront scattering. Ph.D. Thesis Nr. 11940, ETH-Zürich, 137 pp.

Waldhauser, F., Kissling, E., Ansorge, J., Mueller, St. 1998: Three-dimensional Interface Modeling with two-dimensional Seismic Data: the Alpine Crust-Mantle boundary. Geophysical Journal International, 135, 264-278.

Wiemer, S., Giardini, D., Fäh, D., Deichmann, N., Sellami, S. (2009): Probabilistic seismic hazard assessment of Switzerland: best estimates and uncertainties. Journal of Seismology, 13, 449-478, DOI: 10.1007/s10950-008-9138-7.

Wyss, A. 2002: Swiss National Strong Motion Network: Strong Motion Bulletin, December 2000 - December 2001. Publication Series of the Swiss Seismological Service, Nr. 114, ETH-Zürich.

Wyss, A. 2003: Swiss National Strong Motion Network: Strong Motion Bulletin, January 2002 - December 2002. Publication Series of the Swiss Seismological Service, Nr. 115, ETH-Zürich.

Wyss, A. 2004: Swiss National Strong Motion Network: Strong Motion Bulletin, January 2003 - December 2003. Publication Series of the Swiss Seismological Service, Nr. 116, ETH-Zürich.

Wyss, A. 2005: Swiss National Strong Motion Network: Strong Motion Bulletin, January 2004 - December 2004. Publication Series of the Swiss Seismological Service, Nr. 117, ETH-Zürich.

Yan, Q. Z., & Mechie, J. 1989: A fine structural section through the crust and lower lithosphere along the axial region of the Alps. Geophysical Journal International, 98, 465-488.

Ye, S., Ansorge, J., Kissling, E. & Mueller, S. 1995: Crustal structure beneath the eastern Swiss Alps derived from seismic refraction data. Tectonophysics 242, 199-221.